

## **INFORMATION TO USERS**

**This manuscript has been reproduced from the microfilm master. UMI films the text directly from the original or copy submitted. Thus, some thesis and dissertation copies are in typewriter face, while others may be from any type of computer printer.**

**The quality of this reproduction is dependent upon the quality of the copy submitted. Broken or indistinct print, colored or poor quality illustrations and photographs, print bleedthrough, substandard margins, and improper alignment can adversely affect reproduction.**

**In the unlikely event that the author did not send UMI a complete manuscript and there are missing pages, these will be noted. Also, if unauthorized copyright material had to be removed, a note will indicate the deletion.**

**Oversize materials (e.g., maps, drawings, charts) are reproduced by sectioning the original, beginning at the upper left-hand corner and continuing from left to right in equal sections with small overlaps.**

**Photographs included in the original manuscript have been reproduced xerographically in this copy. Higher quality 6" x 9" black and white photographic prints are available for any photographs or illustrations appearing in this copy for an additional charge. Contact UMI directly to order.**

**ProQuest Information and Learning  
300 North Zeeb Road, Ann Arbor, MI 48106-1346 USA  
800-521-0600**

**UMI<sup>®</sup>**



*Extending and Diverting the Photochemical  
Nucleophile–Olefin Combination,  
Aromatic Substitution (photo-NOCAS)  
Reaction*

by

**Bernardino Mangion  
B.Sc., M.Sc.**

**Submitted in partial fulfillment of the requirements  
for the degree of Doctor of Philosophy**

at

**Dalhousie University  
Halifax, Nova Scotia  
April 2001**

© Copyright by Dino Mangion, 2001



**National Library  
of Canada**

**Acquisitions and  
Bibliographic Services**

**395 Wellington Street  
Ottawa ON K1A 0N4  
Canada**

**Bibliothèque nationale  
du Canada**

**Acquisitions et  
services bibliographiques**

**395, rue Wellington  
Ottawa ON K1A 0N4  
Canada**

*Your file Votre référence*

*Our file Notre référence*

**The author has granted a non-exclusive licence allowing the National Library of Canada to reproduce, loan, distribute or sell copies of this thesis in microform, paper or electronic formats.**

**The author retains ownership of the copyright in this thesis. Neither the thesis nor substantial extracts from it may be printed or otherwise reproduced without the author's permission.**

**L'auteur a accordé une licence non exclusive permettant à la Bibliothèque nationale du Canada de reproduire, prêter, distribuer ou vendre des copies de cette thèse sous la forme de microfiche/film, de reproduction sur papier ou sur format électronique.**

**L'auteur conserve la propriété du droit d'auteur qui protège cette thèse. Ni la thèse ni des extraits substantiels de celle-ci ne doivent être imprimés ou autrement reproduits sans son autorisation.**

0-612-66652-2

**Canada**

**DALHOUSIE UNIVERSITY**

**FACULTY OF GRADUATE STUDIES**

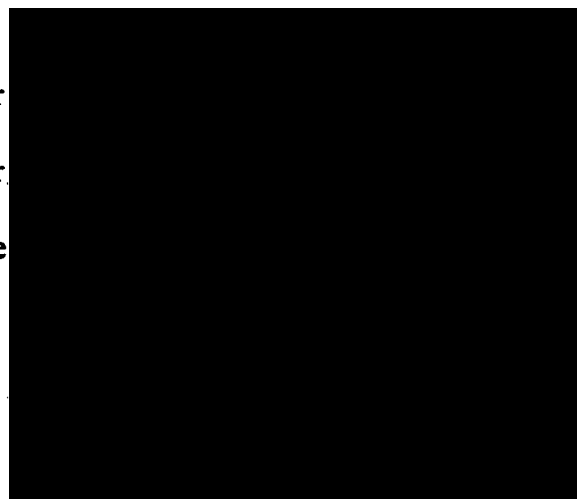
The undersigned hereby certify that they have read and recommend to the Faculty of Graduate Studies for acceptance a thesis entitled "Extending and Diverting the Photochemical Nucleophile-Olefin Combination, Aromatic Substitution (photo-NOCAS) Reaction"

by Bernardino Mangion

in partial fulfillment of the requirements for the degree of Doctor of Philosophy.

Dated: April 17, 2001

External Examiner  
Research Supervisor  
Examining Committee



DALHOUSIE UNIVERSITY

DATE: April 17, 2001

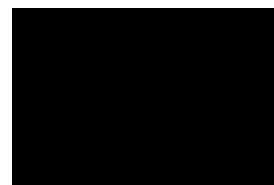
AUTHOR: Bernardino Mangion

TITLE: Extending and Diverting the Photochemical Nucleophile-Olefin  
Combination, Aromatic Substitution (photo-NOCAS) Reaction.

DEPARTMENT OR SCHOOL: Department of Chemistry

DEGREE: Ph.D. CONVOCATION: \_\_\_\_\_ YEAR: 2001

Permission is herewith granted to Dalhousie University to circulate and to have copied for non-commercial purposes, at its discretion, the above title upon the request of individuals or institutions.



Signature of Author

The author reserves other publication rights, and neither the thesis nor extensive extracts from it may be printed or otherwise reproduced without the author's written permission.

The author attests that permission has been obtained for the use of any copyrighted material appearing in this thesis (other than brief excerpts requiring only proper acknowledgement in scholarly writing), and that all such use is clearly acknowledged.

*“On the arid lands there will spring up industrial colonies without smoke and without smokestacks; forests of glass tubes will extend over the plains and glass buildings will rise everywhere; inside of these will take place the photochemical processes that hitherto have been the guarded secret of the plants, but that will have been mastered by human industry which will know how to make them bear even more abundant fruit than nature, for nature is not in a hurry and mankind is.”*

*G. Ciamician, Science, 1912, 36, 385.*

# *Table of Contents*

---

List of Tables .....	ix
Abstract .....	x
Acknowledgements .....	xi

## **1 GENERAL INTRODUCTION**

1.1 Mechanistics and Energetics of PET .....	1
1.2 The Photo-NOCAS Reaction .....	8
1.3 PET-Mediated Nucleophile Addition .....	16
1.4 Aim of the Study .....	24

## **2 EXTENDING THE PHOTO-NOCAS REACTION**

2.1 Introduction .....	26
2.2 Results .....	30
2.3 Discussion .....	48
2.4 Conclusions .....	62
2.5 Experimental .....	63
2.5.1 General information .....	63
2.5.2 X-ray crystallography .....	65
2.5.3 Materials .....	65
2.5.4 Irradiations .....	66
2.5.5 Irradiation of 1,2,4,5-tetracyanobenzene, tetramethyl- allene, and biphenyl in 3:1 acetonitrile–methanol .....	66



<b>2.5.6</b>	Irradiation of 1,2,4,5-tetracyanobenzene, 1,1-dimethylallene, and biphenyl in 3:1 acetonitrile–methanol .....	67
<b>2.5.7</b>	Irradiation of 1,4-dicyanobenzene, tetramethylallene, and biphenyl in 3:1 acetonitrile–methanol .....	68
<b>2.5.8</b>	Irradiation of 1,4-dicyanobenzene, 1,1-dimethylallene, and biphenyl in 3:1 acetonitrile–methanol .....	69
<b>2.5.9</b>	Irradiation of 1,4-dicyanonaphthalene, tetramethylallene, and biphenyl in 3:1 acetonitrile–methanol .....	70
<b>2.5.10</b>	Irradiation of 1,4-dicyanonaphthalene, 1,1-dimethylallene, and biphenyl in 3:1 acetonitrile–methanol .....	71
<b>2.5.11</b>	Irradiation of 1,4-dicyanonaphthalene and dimethylallene in 3:1 acetonitrile–methanol .....	74
<b>2.5.12</b>	Irradiation of 1,4-dicyanonaphthalene and dimethylallene in acetonitrile .....	75
<b>2.5.13</b>	Irradiation of 1,4-dicyanonaphthalene and dimethylallene in benzene .....	75

### **3 DIVERTING THE PHOTO-NOCAS REACTION**

<b>3.1</b>	Introduction .....	76
<b>3.1.1</b>	Formation and fragmentation of haloarene radical anions.....	78
<b>3.1.2</b>	Homolytic fragmentation of haloarenes .....	82
<b>3.2</b>	Results .....	86
<b>3.2.1</b>	4-Fluorobenzonitrile photochemistry .....	88
<b>3.2.2</b>	4-Chlorobenzonitrile photochemistry .....	89
<b>3.2.3</b>	4-Bromobenzonitrile photochemistry .....	93
<b>3.2.4</b>	4-Iodobenzonitrile photochemistry .....	96
<b>3.2.5</b>	4-Chloroanisole photochemistry .....	98
<b>3.2.6</b>	4-Bromoanisole and 4-iodoanisole photochemistry .....	100
<b>3.3</b>	Discussion .....	101
<b>3.3.1</b>	Direct photoaddition of methanol to 1,1-diphenylethene ...	101

3.3.2	PET addition of methanol to 1,1-diphenylethene .....	103
3.3.3	PET between haloarenes and 1,1-diphenylethene .....	105
3.3.4	PET vs direct homolytic cleavage pathways .....	109
3.4	Conclusions .....	121
3.5	Experimental .....	123
3.5.1	General information .....	123
3.5.2	Materials .....	125
3.5.3	Irradiations .....	126
3.5.4	Irradiation of 1,4-dicyanobenzene, 1,1-diphenylethene, and biphenyl in methanol .....	126
3.5.5	Irradiation of 1,1-diphenylethene in methanol .....	127
3.5.6	Irradiation of 1,4-dicyanobenzene, biphenyl, and 1-methoxy-1,1-diphenylethene in methanol .....	128
3.5.7	Irradiation of 1-methoxy-1,1-diphenylethene in methanol .....	129
3.5.8	Irradiation of 4-fluorobenzonitrile in methanol .....	129
3.5.9	Irradiation of 4-fluorobenzonitrile and 1,1-diphenylethene in methanol .....	130
3.5.10	Irradiation of 4-chlorobenzonitrile in methanol .....	130
3.5.11	Irradiation of 4-chlorobenzonitrile and 1,1-diphenylethene in methanol .....	130
3.5.12	Irradiation of 4-bromobenzonitrile in methanol .....	131
3.5.13	Irradiation of 4-bromobenzonitrile and 1,1-diphenylethene in methanol .....	132
3.5.14	Irradiation of 4-iodobenzonitrile in methanol .....	132
3.5.15	Irradiation of 4-iodobenzonitrile and 1,1-diphenylethene in methanol .....	132
3.5.16	Irradiation of 1-(4-cyanophenyl)-2,2-diphenylethene in methanol .....	134
3.5.17	Irradiation of 4-chloroanisole in methanol .....	135
3.5.18	Irradiation of 4-chloroanisole and 1,1-diphenylethene in methanol .....	135
3.5.19	Irradiation of 4-bromoanisole in methanol .....	136

<b>3.5.20</b>	Irradiation of 4-bromoanisole and 1,1-diphenylethene in methanol .....	137
<b>3.5.21</b>	Irradiation of 4-iodoanisole in methanol .....	137
<b>3.5.22</b>	Irradiation of 4-iodoanisole and 1,1-diphenylethene in methanol .....	137
<b>3.5.23</b>	Irradiation of 1-(4-methoxyphenyl)-2,2-diphenylethene and 4-iodoanisole in methanol .....	137
<b>3.5.24</b>	Thermal decomposition of 1-(4-cyanophenyl)-2-methoxy-2,2-diphenylethane and 1-methoxy-2-(4-methoxyphenyl)-1,1-diphenylethane .....	138
<b>APPENDIX</b>	.....	139
<b>REFERENCES</b>	.....	146

## List of Tables

---

Table 1	Photochemical reactions between the cyanoarenes 1–3 and the allenes 4 and 5. ....	32
Table 2	Half-wave reduction potentials ( $E_{1/2}^{\text{red}}$ ) and singlet excitation energies ( $E_{0,0}$ ) for the electron acceptors 1–3 and half-wave oxidation potentials ( $E_{1/2}^{\text{ox}}$ ) for the electron donors 4–6. ....	49
Table 3	Free energy ( $\Delta G_{\text{PET}}$ ) for the photoinduced electron transfer process between the singlet excited states of the electron acceptors 1–3 and the ground state of the electron donors 4–6. ....	50
Table 4	(a) Triplet energies of arene systems. (b) Bond dissociation of $\text{C}_6\text{H}_5\text{-X}$ . ....	85
Table 5	Photochemical reactions between the cyanoarenes (2, 22a–25a) and the alkenes (26, 29, 33a). ....	87
Table 6	Photochemical reactions between the anisoles (23b–25b) and the alkenes (26, 33b). ....	98
Table 7	Free energies, $\Delta G_{\text{PET}}$ , for the PET process between 1,1-diphenylethene (26) and the listed arenes (2, 22–25). ....	106
Table 8	Singlet ( $E_{0,0}^{\text{S}}$ ) and triplet energies ( $E_{0,0}^{\text{T}}$ ) for the haloarenes 22–25 and bond dissociation energies (BDE) for the $\text{C}_6\text{H}_5\text{-X}$ bond. ....	110

## *Abstract*

---

In the first part of this study, the electron transfer photochemistry between cyanoarene electron acceptors and aliphatic allene electron donors in the presence of methanol was investigated. In the reaction involving mononuclear arenes, such as 1,2,4,5-tetracyano- and 1,4-dicyanobenzene, a photochemical nucleophile–olefin combination, aromatic substitution (photo-NOCAS) reaction was observed. The strict regiochemistry in the isolated 1:1:1 arene–allene–methanol products, with the nucleophile attached exclusively to the central allenic carbon, confirmed the sequence of the mechanistic steps. In the case of 1,4-dicyanonaphthalene, the reaction started off along a pathway similar to the photo-NOCAS mechanism. However, the reaction eventually led to addition, rather than substitution, of the intermediate  $\beta$ -methoxyallyl radical to the cyanoarene radical anion. The resulting adduct underwent further photochemical reactions involving either an intramolecular  $[2\pi + 2\pi]$  cycloaddition or a nucleophile addition–cyclization.

The intention of the second study was to develop a photochemical mechanism complementary in its regiochemical selectivity to the photo-NOCAS reaction, by inverting the sequence of mechanistic steps. For this purpose, the electron transfer photochemistry between a series of halobenzonitriles and 1,1-diphenylethene in methanol was investigated. Halobenzonitriles generate highly unstable radical anions that undergo rapid cleavage to give cyanophenyl radicals. The olefin radical cation should thus be trapped by this reactive intermediate prior to nucleophilic attack by methanol. Although the presence of a photoinduced electron transfer pathway was confirmed, the possibility of direct homolysis of the haloarene excited state, which would also generate an aryl radical, could not be discounted. The latter mechanism found support from a series of reactions involving 4-haloanisoles that were not capable of acting as electron acceptors. The two pathways are discussed and evaluated.

## *Acknowledgements*

---

My most sincere thanks go to my supervisor, Dr. Donald R. Arnold, for his ongoing support and illuminating guidance, and for giving me this opportunity to enhance my education. I am also very grateful to Dr. James A. Pincock, Dr. Frances L. Cozens and Dr. Norman P. Schepp for many fruitful discussions on many aspects of photochemistry.

Special thanks to Dr. T. Stanley Cameron and Dr. Katherine N. Roberston, at the X-Ray Crystallography Centre at Dalhousie University, for their invaluable help – many structures encountered in this work would still be unresolved were it not for their expertise in X-ray crystallographic analysis. Similarly, thanks are due to Dr. Donald L. Hooper and Dr. Michael D. Lumsden, at the Atlantic Region Magnetic Resonance Centre at Dalhousie University, for their help with the NMR analyses. I am also grateful to Dr. Jae H. Kim, formerly at the Mass Spectroscopy Lab at Dalhousie University, for the high-resolution mass spectrometry measurements. The help from Ms. Nelaine Mora-Diez with the AM1 calculations is also thankfully acknowledged.

I am deeply indebted to my fellow colleagues and friends, who are too many to mention individually, as well as to the secretarial and technical staff at Dalhousie, for making these years so memorable.

My most heartfelt gratitude goes to my family for their persevering support and for always being there when needed, despite the ocean that separates us. Finally, my warmest thanks go to Sylvana for her unending help and interest.

The financial assistance from the Izaak Walton Killam Memorial Foundation and from Dalhousie University is gratefully acknowledged.

# *General Introduction*

---

Photoinduced electron transfer (PET) is a relatively new area of scientific study. Its beginnings can be traced back as far as the nineteenth century, but it was not until the late 1960s and early 1970s that scientists adopted a coherent and systematic approach to the topic, largely aided by the advent of spectroscopic techniques.<sup>1</sup> Although still in its infancy, PET is a rapidly growing field and has attracted the interest of scientists from various disciplines.<sup>2</sup> For the physical organic chemist it represents an easy method of generating radical ions under relatively mild conditions and allows for their subsequent investigation in a homogeneous and non-interfering environment.<sup>3</sup> In organic chemistry, interest in PET has uncovered novel synthetic pathways for the construction of organic molecules, often inaccessible by more conventional thermal methods.<sup>4</sup> Inorganic chemists and material scientists have applied PET to environmental decontamination methods using semiconductor materials.<sup>5</sup> Biochemists are investigating photosynthesis and electron transport in biological systems on the basis of simple PET models in an attempt to gain a better understanding of nature's processes, with the intention of applying them to artificial systems for solar energy storage.<sup>6</sup> Similarly, in clinical medicine, PET has recently been receiving considerable attention in connection with the photodynamic therapy of tumours.<sup>7</sup>

## **1.1 MECHANISTICS AND ENERGETICS OF PET**

The fundamental advantage for using photochemistry as a means to promote electron transfer lies in the fact that photoexcitation enhances the redox

properties of a light-absorbing molecule. This occurs because electronic excitation promotes a paired electron from the highest occupied molecular orbital (HOMO) to the lowest unoccupied molecular orbital (LUMO), a process which reduces the ionization energy (resulting in a better electron donor) and increases the electron affinity (resulting in a better electron acceptor) of the excited state with respect to the ground state. In either case, the difference in energy is equivalent to the excitation energy  $E_{0,0}$  required to promote an electron from the lowest vibrational level of the ground state to the lowest vibration level of the first excited state (Figure 1).

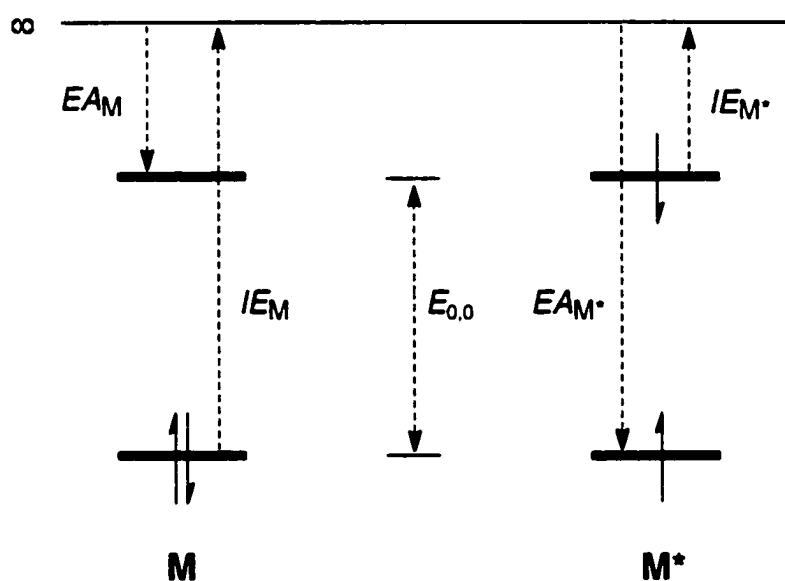


**Figure 1:** Diagrammatic representation of ionization energies ( $IE$ ) and electron affinities ( $EA$ ) for a ground state and an electronically excited state molecule  $M$ .

Whether the electronically excited molecule  $M^*$  acts as an electron donor or an electron acceptor depends on the relative energies of the frontier orbitals of  $M^*$  and of its redox partner (quencher)  $Q$  (Figure 2). If the lowest singly occupied molecular orbital (SOMO) in  $M^*$  is of lower energy than the HOMO of  $Q$ ,  $M^*$  will act as oxidizing agent, accepting an electron from  $Q$  and thereby forming a radical anion  $M^{\cdot-}$  and a radical cation  $Q^{\cdot+}$  (Figure 2a). On the other hand, if the



LUMO of Q is of lower energy than the highest SOMO of  $M^*$ , the latter will act as a reducing agent, donating an electron to Q to give a radical cation  $M^{+\cdot}$  and a radical anion  $Q^{\cdot-}$  (Figure 2b).

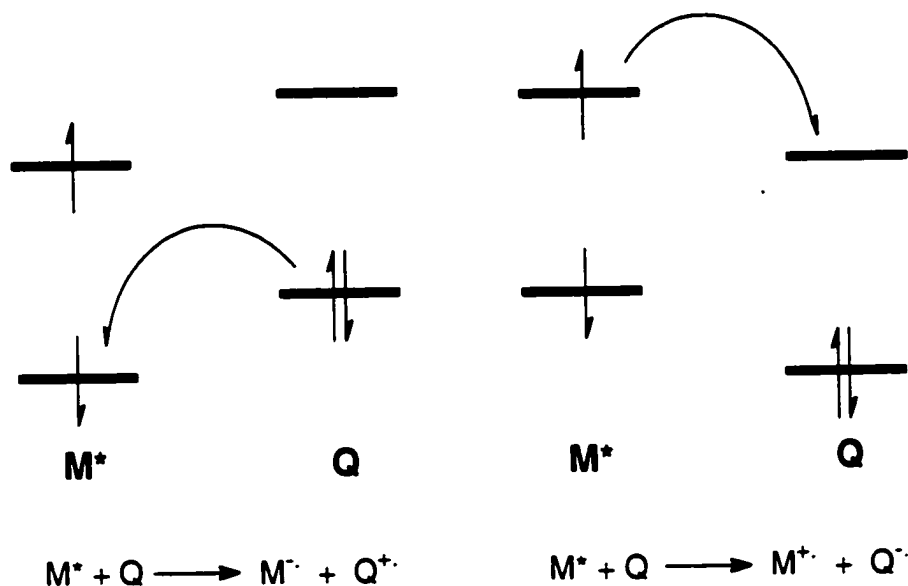


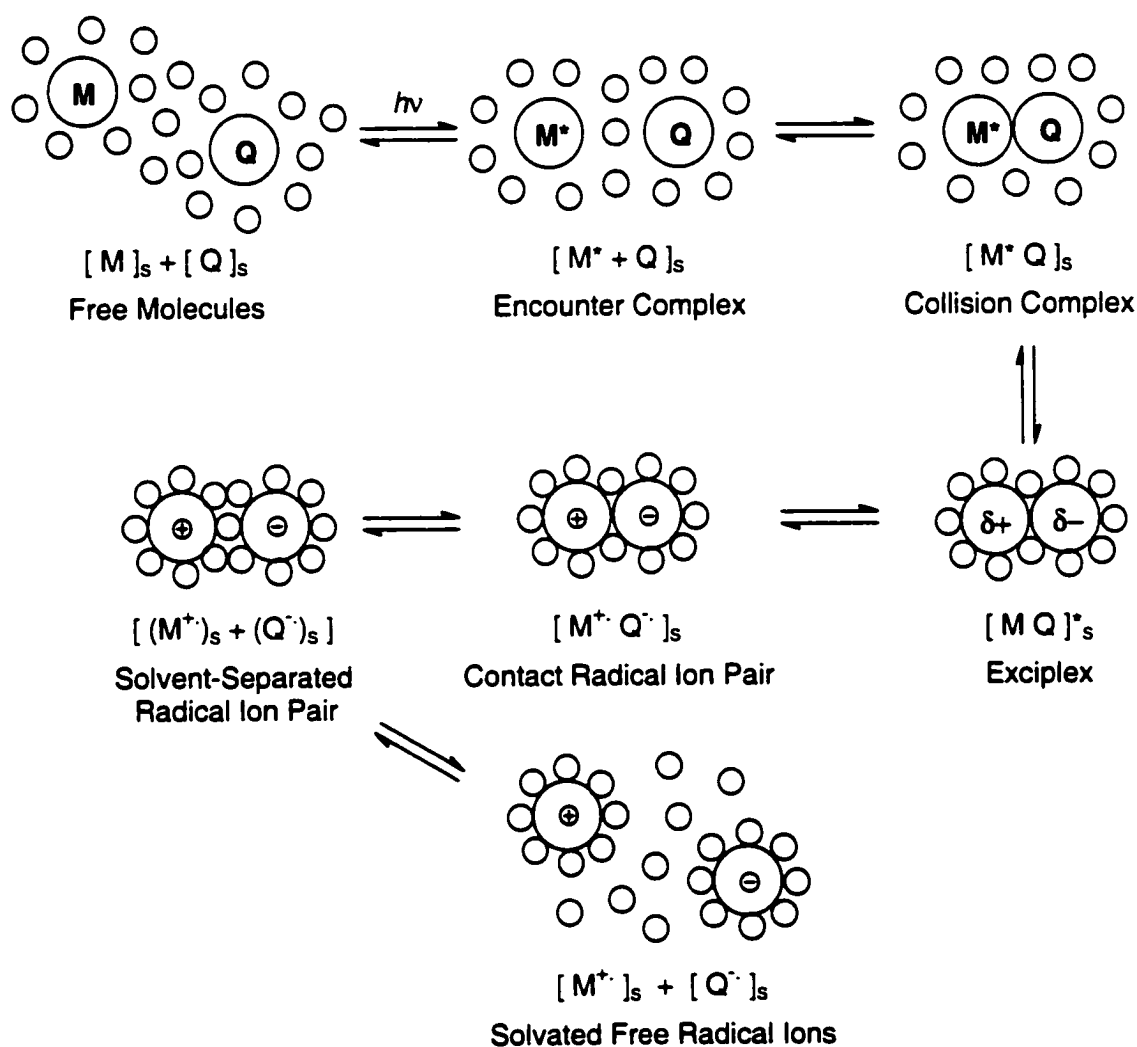
**Figure 2a**

**Figure 2b**

Depending on the degree of solvation and dissociation, different types of radical ion interactions have been postulated (Scheme 1).<sup>3b,8</sup> Which is the predominant form can, at times, be important as it determines the outcome of the PET reaction.

Upon photoexcitation of one of the components, M, an *encounter complex* is formed. This can be visualized as an intermolecular ensemble of an excited state and a ground state molecule separated by a small intermolecular distance ( $\sim 7 \text{ \AA}$ ) and surrounded by several solvent shells. This species rapidly collapses ( $10^{-9}$ – $10^{-10}$  s) to a *collision complex*, where the two components are now in direct contact. If the interaction between the collision complex pair is strong, partial charge transfer will occur to form an *exciplex*, a species characterized by a strong binding energy ( $20$ – $85 \text{ kJ mol}^{-1}$ ) and a large dipole moment that reflect the degree of charge transfer. Under the appropriate conditions, this exciplex will be

of sufficiently long lifetime to undergo light emission and is thus relatively easily detected.



**Scheme 1:** Schematic representation of the various steps involved in the formation of radical ions via PET in solution.

However, if the solvent dipoles provide sufficient stabilization, full electron transfer will occur either directly from the collision complex or from a short-lived non-emissive exciplex, resulting in a *contact radical ion pair (CRIP)*. In this species, the anion and cation are in direct contact, the whole aggregate being surrounded by solvent molecules. The next step is the formation of a *solvent-*

*separated radical ion pair (SSRIP)* where the oppositely charged radical ions are still interacting with one another but now have intact solvent shells. If these solvent-separated radical ions dissociate in the bulk of the fluid medium and become separated by a large distance, they are classified as *solvated free radical ions (FRI)*. These ionic species are completely independent of one another and can exist as distinct, randomized, solvated, and relatively long-lived moieties.

The overall free energy change of the PET step,  $\Delta G_{\text{PET}}$ , is readily predicted using the well-known Weller equation that is given as:<sup>9</sup>

$$\Delta G_{\text{PET}} = F ( E_{1/2}^{\text{ox}} - E_{1/2}^{\text{red}} - e / 4\pi\epsilon\alpha ) - E_{0,0} \quad \text{kJ mol}^{-1}$$

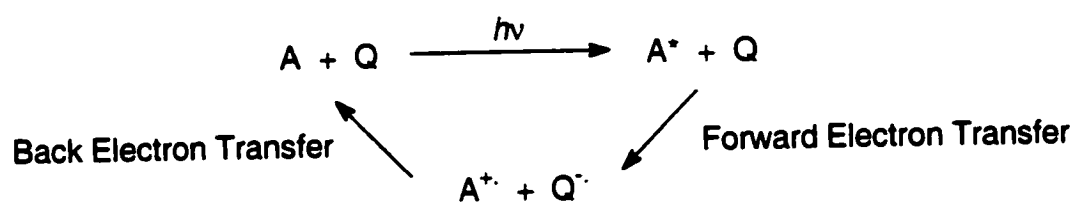
In this equation, the term in brackets represents the energy required for electron transfer in solution between ground state molecules. The half-wave oxidation ( $E_{1/2}^{\text{ox}}$ ) and reduction ( $E_{1/2}^{\text{red}}$ ) potentials take into account the ionization energy and electron affinity respectively, as well as the solvation enthalpies resulting from the stabilization of the radical ions by the action of the solvent dipoles. These redox potentials have the advantage of being easily measured experimentally using electrochemical techniques such as cyclic voltammetry. The Coulombic term ( $Fe / 4\pi\epsilon\alpha$ ) is introduced to correct for any mutual stabilization effects that arise from the formation of the radical ions at an encounter distance  $\alpha$ , in the same solvent system of dielectric constant  $\epsilon$ , and which are therefore not accounted for in the redox potentials. In methanol ( $\epsilon = 32.6 \epsilon_0$ ) this term was estimated to be  $6.1 \text{ kJ mol}^{-1}$  while in acetonitrile ( $\epsilon = 36.7 \epsilon_0$ ) it was calculated as  $5.4 \text{ kJ mol}^{-1}$ , in both cases assuming  $\alpha = 7 \text{ \AA}$ . The excitation energy term  $E_{0,0}$  is introduced to account for the fact that electron transfer occurs between an excited state molecule and a ground state molecule (Figure 1).

The equation shows that if  $E_{0,0}$  of the excited molecule is sufficiently large so as to overcome the ground state electron transfer term, then the free energy  $\Delta G_{\text{PET}}$  will be negative and the PET reaction is predicted to be spontaneous.

In his influential paper, Weller demonstrated the occurrence of a correlation of  $\Delta G_{\text{PET}}$  with the free energy of activation for PET, and hence with the rate of PET,  $k_{\text{PET}}$ .<sup>9b</sup> Both his experimental results and empirically derived relationships indicated that  $k_{\text{PET}}$  will approach the diffusion controlled limit of ca.  $1.7 \times 10^{10} \text{ M}^{-1} \text{ s}^{-1}$  when  $\Delta G_{\text{PET}}$  is  $\leq -20 \text{ kJ mol}^{-1}$ .

Although such calculations are of fundamental importance in designing PET reactions, a favourable result does not guarantee that the resulting radical ions will undergo a product-forming reaction because there are other factors that may hinder the PET step.

Primary among these is back electron transfer (BET). This involves the return of an electron from the radical anion to the radical cation, thereby regenerating the neutral molecules (Scheme 2). This process is evidently an energy-wasting step, which has to be successfully circumvented in order to attain an efficient and useful PET reaction.<sup>10</sup>



- Scheme 2 -

The free energy for BET,  $\Delta G_{\text{BET}}$ , is expressed by:

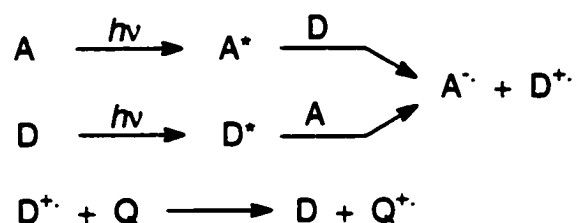
$$\Delta G_{\text{BET}} = F ( E_{\frac{1}{2}}^{\text{red}} - E_{\frac{1}{2}}^{\text{ox}} ) \quad \text{kJ mol}^{-1}$$

Clearly,  $\Delta G_{\text{BET}}$  will be highly exergonic: there is a large driving force for two radical ions to be converted back to their neutral moieties. It is often the case, however, that this process is sufficiently exergonic to fall within the Marcus inverted region where the rate of BET decreases with increasing exergonicity. For example, it has been demonstrated that the yield of free radical ions formed

when using 9,10-dicyanoanthracene as photosensitizer is 8% for hexamethylbenzene ( $\Delta G_{\text{BET}} = -240 \text{ kJ mol}^{-1}$ ) and *ca.* 83% for biphenyl ( $\Delta G_{\text{BET}} = -280 \text{ kJ mol}^{-1}$ ).<sup>10f</sup> Thus, a simple approach for maximizing the efficiency of radical ion cage escape is to use a redox pair for which PET is not exceedingly exergonic; this will result in a highly exergonic  $\Delta G_{\text{BET}}$  and consequently in a reduced rate of BET.

One of the most successful techniques for reducing BET and thus enhancing the yields of product formation is *co-sensitization*.<sup>11</sup> This involves the utilization of a third species, in addition to the fundamental donor–acceptor pair, that acts as an intermediate in the PET step.

The co-sensitizer can be either an electron acceptor or electron donor, although in most practical cases it is usually an electron donor such as an unreactive aromatic hydrocarbon (for example, biphenyl or phenanthrene). It can act as the principal light absorber or just partake in the PET step from the ground state.\* Scheme 3 illustrates a PET mechanism for a donor–acceptor (Q–A) pair mediated by a donor co-sensitizer (D).



- Scheme 3 -

Rather than occurring directly between A and Q, the primary electron transfer step takes place between the acceptor A and the co-sensitizer D (with either A or D in their excited state, A\* or D\*), generating the radical ions A<sup>•-</sup> and

---

\* There is some confusion in the literature regarding the term *co-sensitizer*, with some researchers reserving it for co-donors and co-acceptors that actually absorb the light. In the current context the term is used more freely and refers to any co-donor or co-acceptor, light absorbing or not.

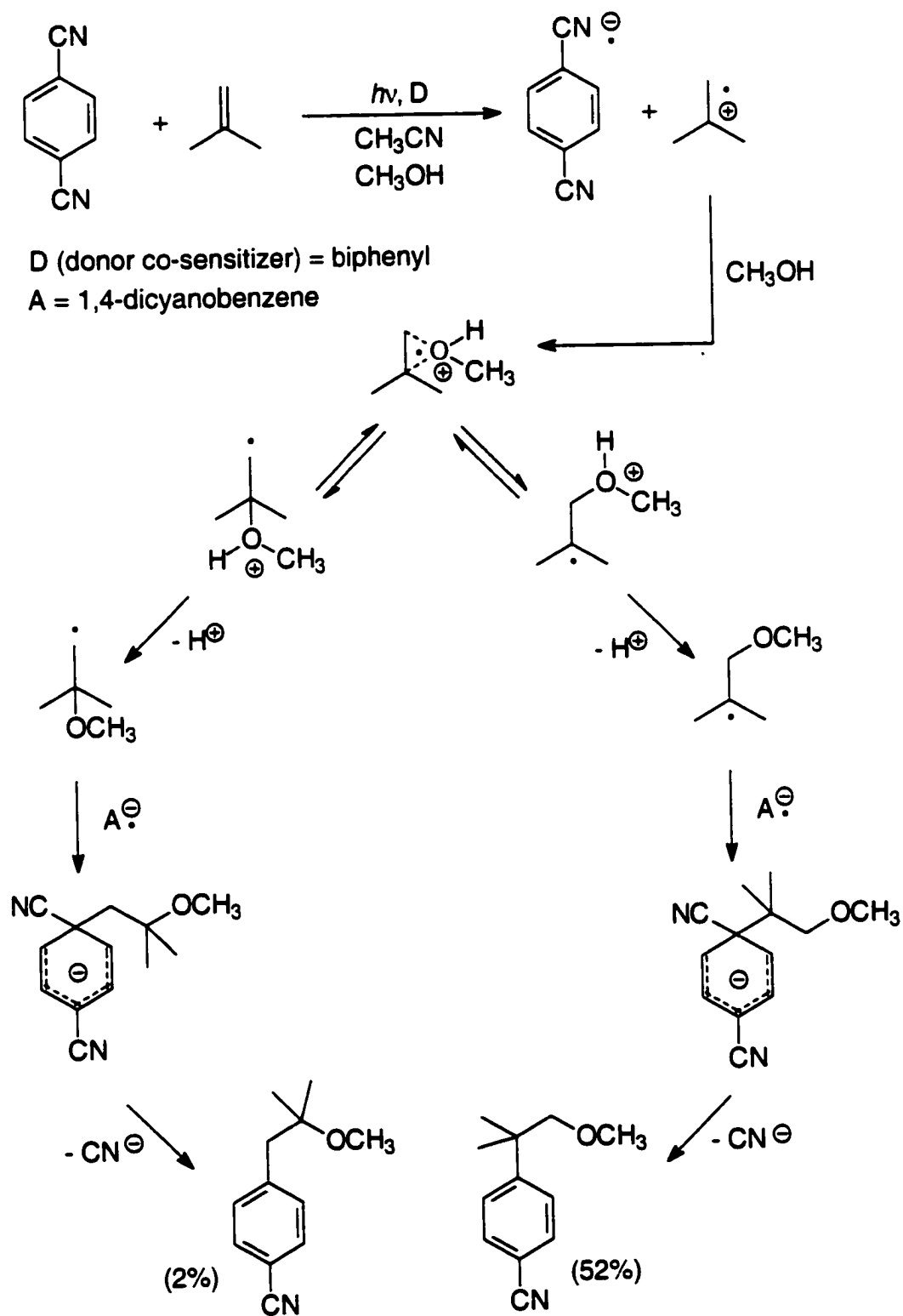
$D^{+\bullet}$  respectively. Once these diffuse apart, the co-sensitizer radical cation  $D^{+\bullet}$  can undergo a secondary electron transfer with the donor Q, regenerating the neutral co-sensitizer molecule D and the donor radical cation  $Q^{+\bullet}$ . The net result is the generation of the donor and acceptor radical ions,  $A^{\bullet-}$  and  $Q^{+\bullet}$ , in separate stages.

If the choice of co-sensitizer is appropriate, the quantum yield of formation of the radical ions in the co-sensitized mode should be increased relative to the unsensitized PET reaction. This enhancement is attributed to a slower rate of BET for the  $A^{\bullet-}-D^{+\bullet}$  pair as opposed to the  $A^{\bullet-}-Q^{+\bullet}$  pair, a phenomenon attributed to a lower reorganization energy for  $D^{+\bullet}$  going back to D.<sup>10f,10g</sup>

## 1.2 THE PHOTO-NOCAS REACTION

During the past 30 years, a considerable portion of our team's research efforts has been devoted to the study of the electron transfer photochemistry between aromatic electron acceptors and olefinic electron donors. In particular, a strong emphasis has been placed on the elucidation and development of the photochemical Nucleophile–Olefin Combination, Aromatic Substitution (photo-NOCAS) reaction. This reaction, pioneered in our laboratories in the 1980s, involves the combination of three molecules – notably an aliphatic olefin, a cyanoarene and a nucleophile – in a single synthetic step, and it exhibits interesting chemo-, regio-, and stereoselectivities. Our interests lie in its synthetic utility and potential as well as in the mechanistic information it provides on the behaviour of photogenerated radical ions.

The mechanism has been examined in detail and is well understood. This is illustrated in Scheme 4 for the archetypical example involving 1,4-dicyanobenzene as electron acceptor, 2-methylpropene as electron donor, and methanol as nucleophile.<sup>12</sup>



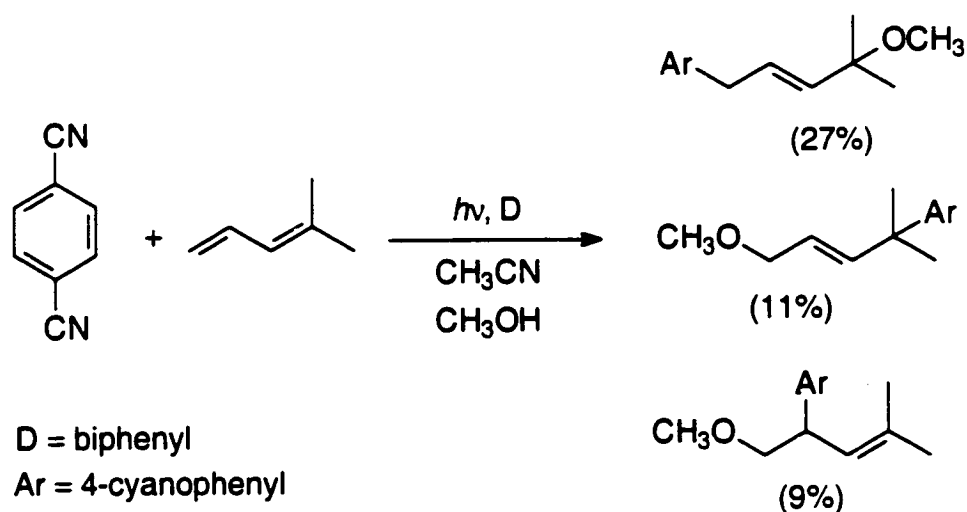
- Scheme 4 -

The first step in the mechanism involves the photochemical excitation of 1,4-dicyanobenzene to its first excited singlet state. This enhances its oxidizing properties so that it undergoes electron transfer from the olefin to give the corresponding olefin radical cation and cyanoarene radical anion. In the majority of cases, donor co-sensitization using aromatic hydrocarbons such as biphenyl has been demonstrated to have a beneficial effect. The contact radical ion pairs formed upon electron transfer may diffuse apart to give free, solvated radical ions or undergo back electron transfer to regenerate the starting materials.

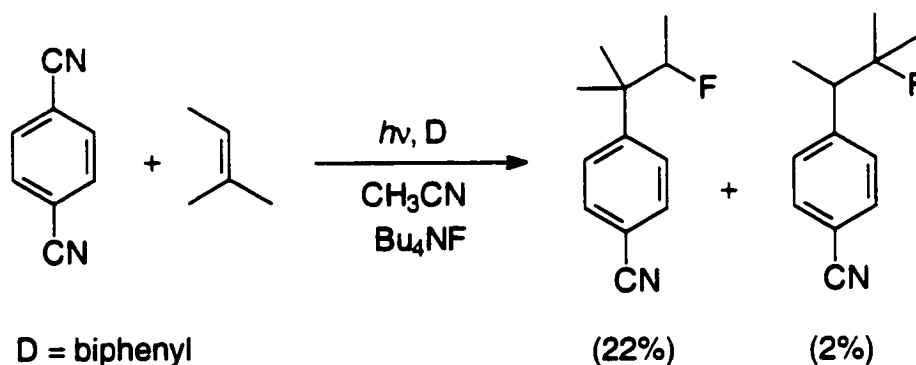
In those cases where BET is circumvented, the alkene radical cation is attacked by methanol to give a non-classical, bridged radical cation complex in equilibrium with the two possible distonic radical cations.<sup>13</sup> Subsequent deprotonation from the oxygen of the distonic radical cations, giving the corresponding  $\beta$ -methoxyalkyl radicals, determines the regiochemistry. The selectivity does not depend on kinetic factors such as steric hindrance, but rather on the stability of the radicals formed. The resulting radicals add on to the 1,4-dicyanobenzene radical anion at the *ipso* position. Rearomatization follows via expulsion of cyanide anion to give the final photo-NOCAS product.

In reactions involving methanol as nucleophile, the regiochemistry of nucleophilic addition is determined by the stability of the respective  $\beta$ -methoxyalkyl radicals. This is due to an equilibrium process via a bridged species. In cases involving charged nucleophiles (cyanide and fluoride anions), no such bridged species is possible and product ratios are not a reflection of the relative stability of the radical intermediates (Schemes 5a and 5b).<sup>14</sup> In these latter reactions, addition is kinetically controlled and the product ratio is determined before the relative stability of the resulting radicals becomes important. In such a situation, steric and polar factors dominate, so that the nucleophile adds to the less substituted side. This, however, does not necessarily give the more stable intermediate radical. In fact, the more substituted  $\beta$ -fluoroalkyl and  $\beta$ -isocyanoalkyl radicals are the *less* stable of the two possible intermediate radicals.



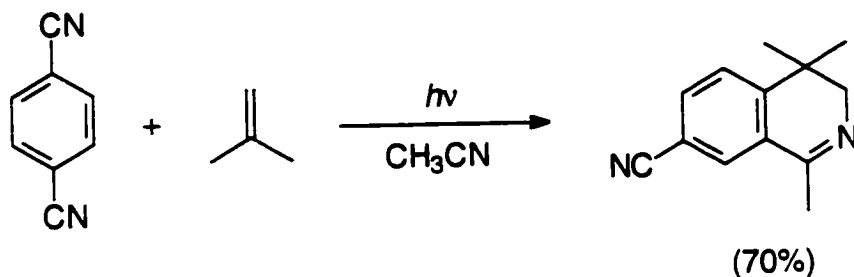


**Scheme 5a** Thermodynamic control: more heavily substituted ether is formed preferentially due to a more stable  $\beta$ -methoxyallyl radical precursor.<sup>13</sup>



**Scheme 5b** Kinetic control: less heavily substituted fluoride is formed preferentially despite a less stable  $\beta$ -fluoroalkyl radical precursor.<sup>14b</sup>

The reaction takes a different course when acetonitrile acts as the nucleophile (Scheme 6).<sup>15</sup> In this case, the distonic radical cation formed upon nucleophilic trapping of the olefin radical cation is incapable of deprotonation. Thus, addition to the arene radical anion results in the formation of a zwitterionic intermediate. This species cyclizes to eventually give the observed isoquinoline product.



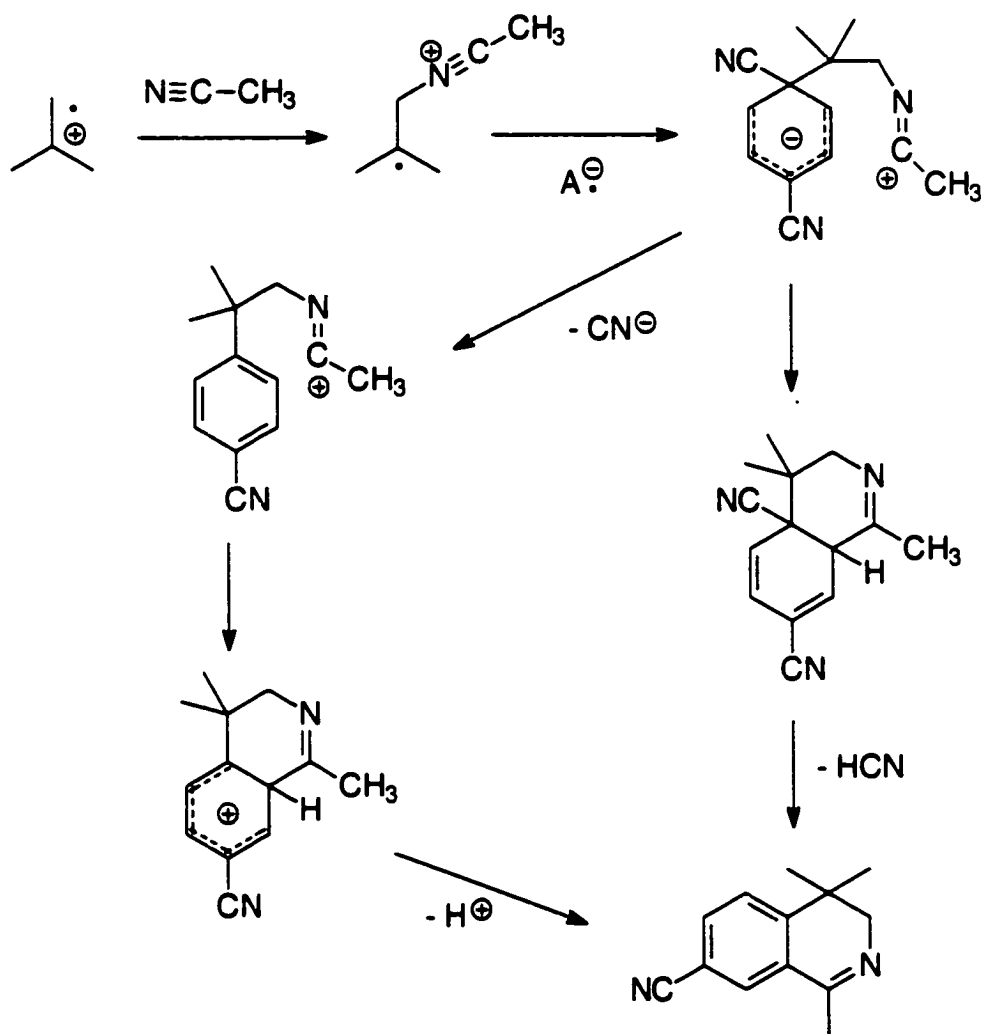
- Scheme 6 -

Two possible pathways have been proposed (Scheme 7). The zwitterionic intermediate may eliminate a cyanide anion prior to cyclization. This is followed by electrophilic attack of the cationic moiety onto the aromatic ring and subsequent deprotonation with concomitant rearomatization. Alternatively, the cyclization may occur at the cation–anion stage before the cyanide anion dissociates. This is followed by concerted loss of hydrogen cyanide.

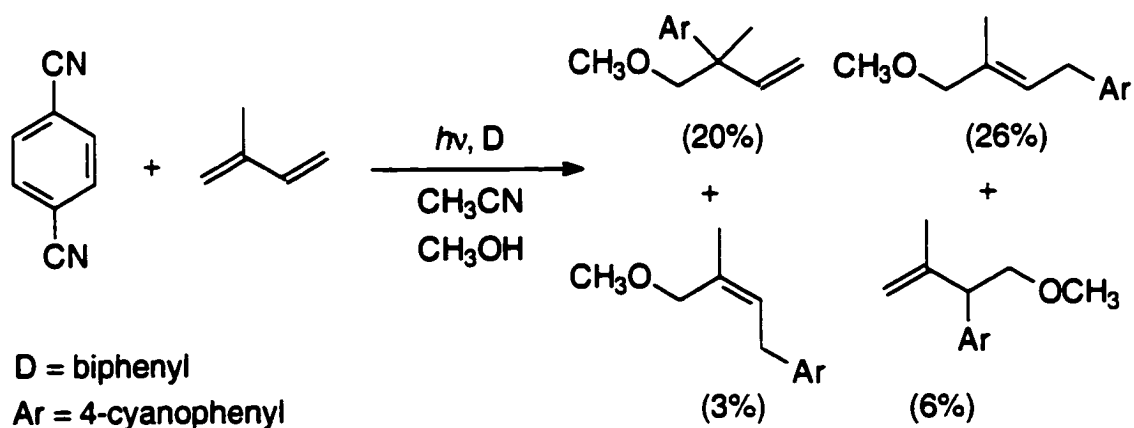
The reaction, however, was found to be limited to highly reactive alkene radical cations, having localized charge and low steric hindrance. Acetonitrile is generally too weakly nucleophilic, so that the olefin radical cations usually tend to deprotonate before they can be trapped.<sup>12a</sup>

A critical question raised in early studies on the mechanism of this and related reactions was whether the radical anion and radical cation combine before the association of the nucleophile. This dilemma was addressed in a study involving conjugated dienes as the electron donors, in which the sequence of these mechanistic steps was particularly evident from the regiochemistry of the adducts (Scheme 8).<sup>16</sup>

The results of this work indicate that the nucleophile was always attached to the terminal carbon. Subsequent coupling of the arene radical anion with the allylic radical could (and frequently did) occur at both ambident ends of the allylic radical with 1,2-addition placing the aryl group (never the nucleophile) at the 2-position. If the sequence of events were inverted, initial coupling of the radical ions would always bond the aryl group to a terminal position.



- Scheme 7 -

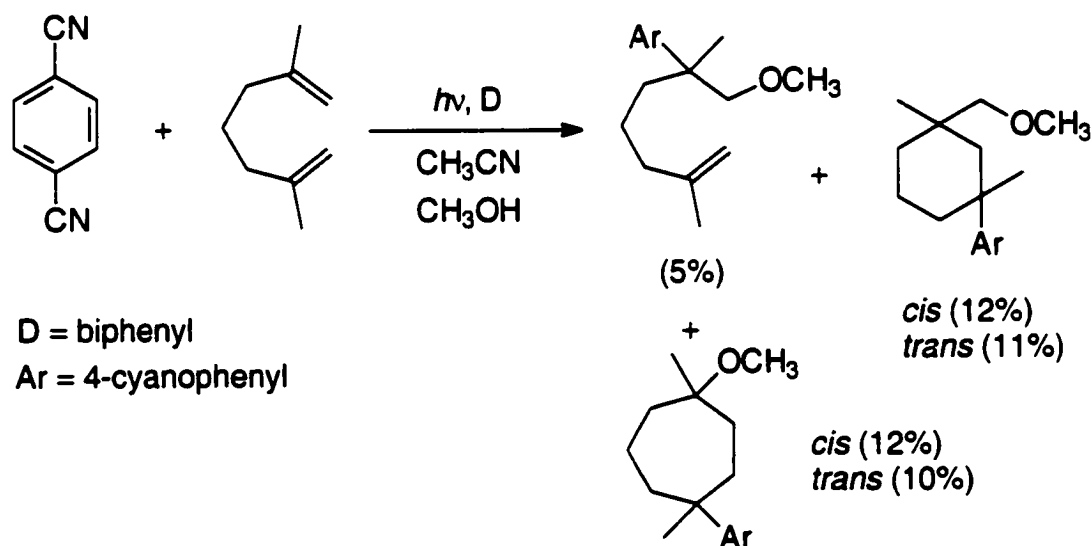


- Scheme 8 -

With non-conjugated dienes, the initially formed alkene radical cation has the option to cyclize to a 1,*n*-distonic radical cation.<sup>17</sup> For example, the radical cation of 2,6-dimethyl-1,6-heptadiene cyclizes to the 1,4-dimethyl-1,4-cycloheptyl distonic radical cation via a 1,7-*endo,endo* cyclization (Scheme 9).<sup>17b</sup>

Nucleophilic trapping of the cationic site and substitution on the arene radical anion complete the sequence.

There is, of course, another possible sequence, in which the association of the nucleophile with the alkene radical cation may precede the cyclization. This mechanism is responsible for the formation of the cyclohexane derivative in Scheme 9, and is favoured when the irradiation is performed without the addition of the donor co-sensitizer and at high concentrations of the nucleophile. Under these conditions, initial nucleophilic addition to the alkene radical cation, followed by 1,6-*endo* cyclization of the intermediate radical, gives a tertiary alkyl radical. This then substitutes on the arene radical anion to yield the cyclohexane.



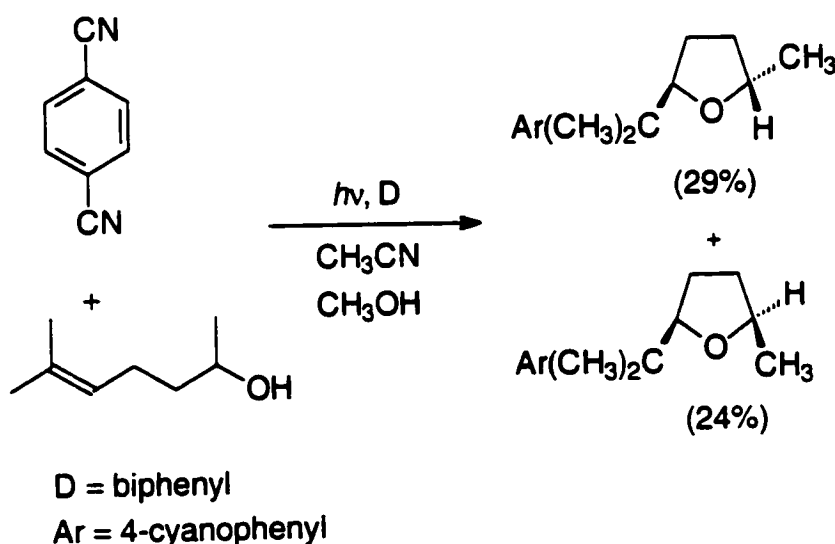
- Scheme 9 -

Involvement of the donor co-sensitizer and decreased concentration of the nucleophile (methanol) increase the lifetime of the radical cation, and cyclization to the distonic radical cation is favoured over nucleophilic trapping. The co-

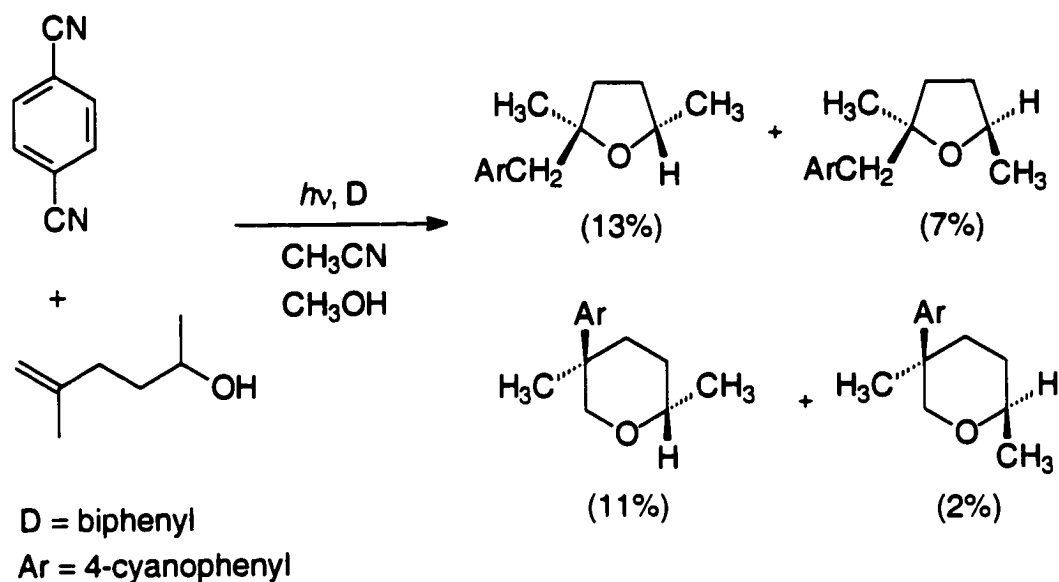
sensitizer probably complexes with the olefin radical cation, making the cationic charge less available for nucleophilic attack.

Similar cyclizations have also been achieved with alkenols serving as donors.<sup>18</sup> Here the initially formed alkene radical cation may cyclize via an intramolecular nucleophile addition of the hydroxyl terminus. These reactions exhibit a distinct preference for 1,5-*exo* over 1,6-*endo* cyclization. This selectivity can be rationalized by means of the approach vector analysis model developed by Baldwin and expanded to radical cyclization by Beckwith.<sup>19</sup>

For example, the intramolecular reaction of 6-methyl-5-hepten-2-ol cyclizes exclusively via a 1,5-*exo* mode and no products having a tetrahydropyran ring were detected. This, perhaps, is of little surprise when one considers that 1,5-*exo* cyclization leads to a tertiary radical in contrast to the secondary radical obtained from a 1,6-*endo* cyclization (Scheme 10a). The preference for 1,5-*exo* cyclization is even more evident in the reactivity of 5-methyl-5-hexen-2-ol. The normal intermolecular preference for nucleophilic attack at the primary over tertiary carbon (26:1, as observed in the reaction of 2-methylpropene, Scheme 4) is now dominated by the preference (1.5:1) for 1,5-*exo* over 1,6-*endo* cyclization (Scheme 10b).



- Scheme 10a -

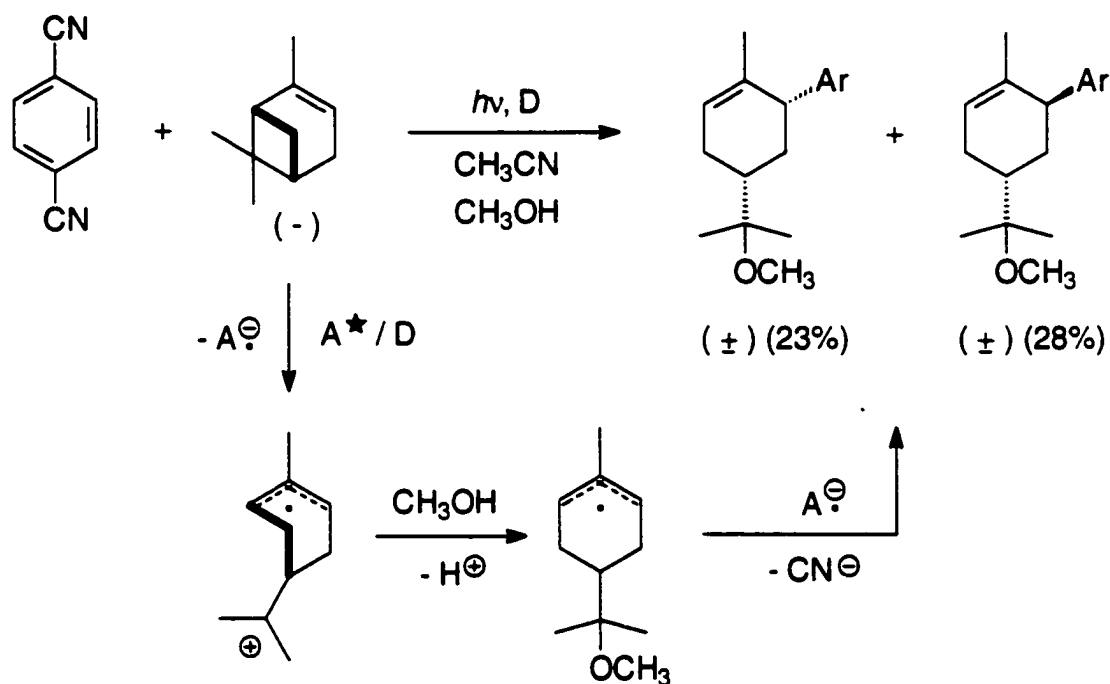


- Scheme 10b -

Another mechanistic modification takes place when the initially formed radical cation of a cyclic alkene cleaves.<sup>20</sup> An interesting example involves the cleavage of the radical cation of  $\alpha$ -pinene (Scheme 11).<sup>20a,20b</sup> Irradiation of an acetonitrile–methanol solution of 1,4-dicyanobenzene, (–)- $\alpha$ -pinene and biphenyl gave *cis* and *trans* photo-NOCAS products in good yield. The radical cation of  $\alpha$ -pinene cleaves to the achiral distonic radical cation, and the subsequent association step occurs on both the *cis* and *trans* faces giving racemic, diastereomeric adducts.

### 1.3 PET-MEDIATED NUCLEOPHILE ADDITION

Upon introduction of an aryl group onto the olefin, another mechanistic pathway becomes available.<sup>21-31</sup> After the initial PET that generates the radical ions, the olefinic radical cation is attacked by the nucleophile to generate the more stable adduct radical. Unlike its aliphatic counterpart, this radical has a sufficiently low reduction potential that enables it to undergo a second electron



A = 1,4-dicyanobenzene

D = biphenyl

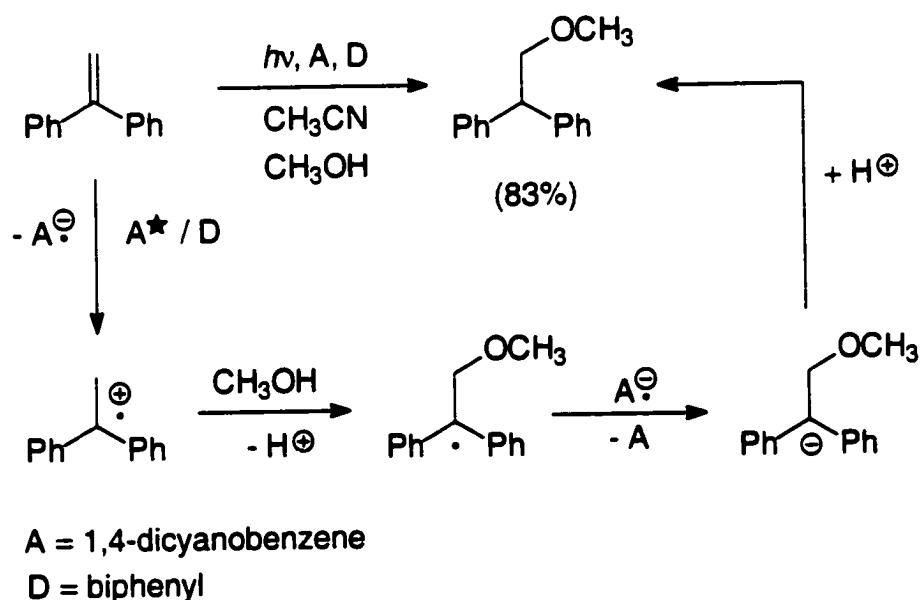
Ar = 4-cyanophenyl

- Scheme 11 -

transfer (charge-shift) with the cyanoarene radical anion. This regenerates the starting cyanoarene together with the corresponding adduct anion. This anion is subsequently protonated to form the final *anti*-Markovnikov adduct (Scheme 12). Evidence of this final step comes from the utilization of a deuterated nucleophilic agent (methanol- $O$ -d), which results in the incorporation of a deuterium atom at the  $\alpha$ -position of the alkene.<sup>22</sup> In contrast to the photo-NOCAS reaction, the cyanoaromatic electron acceptor does not get incorporated into the final product and thus behaves as a photosensitizer.

The rate of nucleophilic attack on the alkene radical cation varies from a mere  $10^4 \text{ M}^{-1} \text{ s}^{-1}$  up to the diffusion-controlled limit of  $10^{10} \text{ M}^{-1} \text{ s}^{-1}$ .<sup>23</sup> This rate depends upon both steric factors such as the bulkiness of the nucleophile and the presence of substituents on the alkene (particularly in the  $\beta$ -position), as well

as electronic effects such as the degree of charge delocalization in the alkene radical cation. This latter factor explains the reduced reactivity of 4-methoxyphenyl alkenes and the apparent inertness of 4-(dimethylamino)phenyl alkenes. Whereas 1,1-diphenylethene undergoes nucleophilic attack by methanol with a rate constant of  $10^9 \text{ M}^{-1} \text{ s}^{-1}$ , 1,1-bis(4-methoxyphenyl)ethene reacts with a rate constant of  $10^7 \text{ M}^{-1} \text{ s}^{-1}$  while 1,1-bis[4-(dimethylamino)phenyl]ethene is practically unreactive even in pure methanol.<sup>23a</sup> Arnold *et al* have carried out extensive studies on this electronic effect exerted by aryl substituents on the rate of the nucleophilic addition.<sup>24</sup>

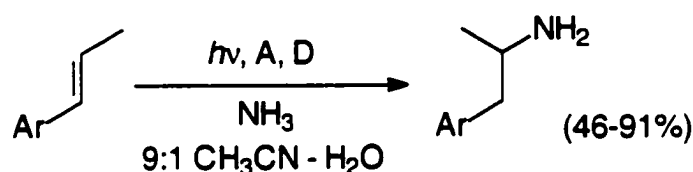


- Scheme 12 -

Since the pioneering work by Arnold and co-workers,<sup>21,22</sup> the addition of nucleophiles to aryl alkenes and related systems has been intensely investigated. It has been given considerable prominence from a synthetic viewpoint because, unlike its thermal counterpart, it proceeds in an *anti*-Markovnikov fashion.<sup>21-30</sup>



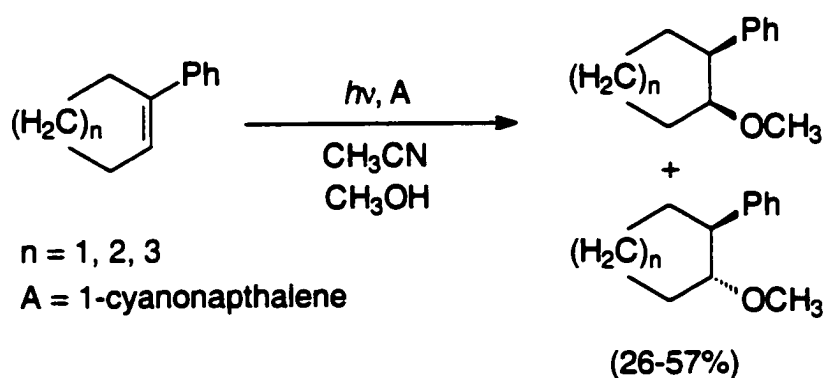
Such *anti*-Markovnikov nucleophile additions have been achieved with a wide variety of acyclic alkenes including 1,1-diarylalkenes, various styrenes and stilbenes. Successful investigations have also been carried out on cyclic alkenes including indenenes, 1-phenylcycloalkenes, 2-phenylnorbornene and certain 1,2-dihydronaphthalene derivatives. Although methanol is the most common nucleophilic agent, other alcohols have also been used successfully. These include ethanol, 2-propanol, 2-methyl-2-propanol, phenylmethanol, cyclohexanol and 2,2,2-trifluoroethanol. Furthermore, the nucleophilic addition has also been achieved with water, acetic acid, ammonia, various amines, and cyanide anion (Scheme 13).



A = 1,3- or 1,4-dicyanobenzene

D (donor co-sensitizer) = 1,2,4-triphenylbenzene

Ar = 2-methoxyphenyl, 3-methoxyphenyl, 4-methoxyphenyl,  
3,4-dimethoxyphenyl



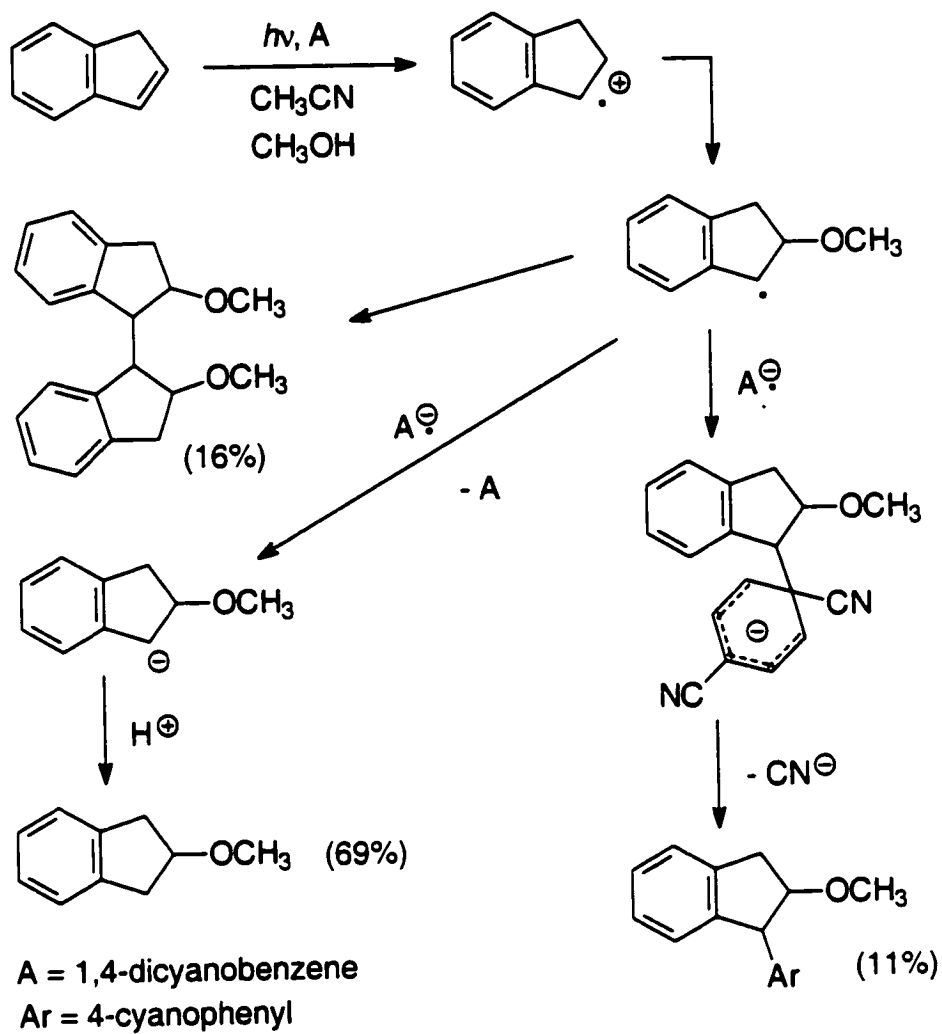
- Scheme 13 -

The use of chiral naphthalenedicarboxylates as photosensitizers results in an enantiodifferentiating nucleophile addition, exhibiting moderate enantiomeric enrichments. Chiral induction results from the formation of a diastereomeric exciplex, which is subjected to an enantiofacially selective nucleophilic attack by the alcohol. Maintaining a tight exciplex and preventing the formation of free radical ions is crucial to obtain any stereoselectivity. Consequently, conducting the reaction in non-polar solvents markedly improved the enantiomeric excess.<sup>27</sup>

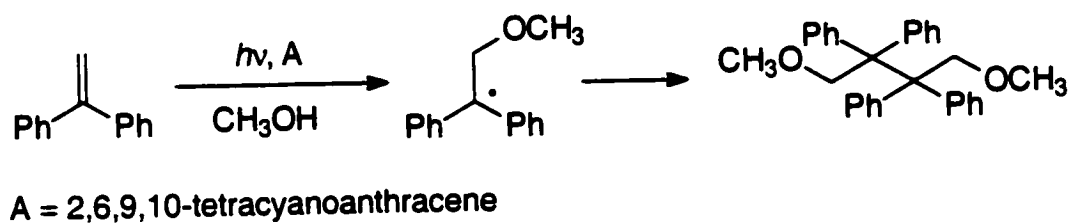
In contrast to aryl alkenes, alkyl alkenes do not give simple monomeric nucleophile adducts. The intermediate free radical cannot be reduced to the anion by the sensitizer radical anion. This is a consequence of the lower electron affinities of the intermediate allyl or alkyl radicals when compared to benzyl radicals. Instead, these radicals usually undergo radical dimerization, disproportionation, or addition to the sensitizer radical anion (*cf.* photo-NOCAS reaction).

Such alternative reactions are only observed in rare cases with aryl alkenes. Indene has a tendency to undergo radical dimerization and radical coupling with the sensitizer in addition to straightforward nucleophilic addition to the monomer (Scheme 14).<sup>28</sup>

A similar observation was made by Mattes and Farid in the 2,6,8,10-tetracyanoanthracene-sensitized methanol addition to 1,1-diphenylethene.<sup>23a</sup> Sensitization by cyanoaromatics of higher reduction potential (*e.g.*, 1,4-dicyanobenzene and 9,10-dicyanoanthracene) usually leads predominantly to the 1:1 alkene–methanol adduct. In this case, however, no 1-methoxy-2,2-diphenylethane was formed. 1,4-Dimethoxy-2,2,3,3-tetraphenylbutane, resulting from the dimerization of the radical, was formed instead (Scheme 15). This was attributed to the inability of the tetracyanoanthracene radical anion to reduce the adduct free radical to the anion.

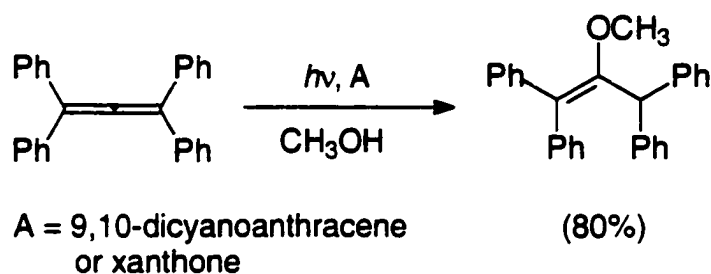


- Scheme 14 -

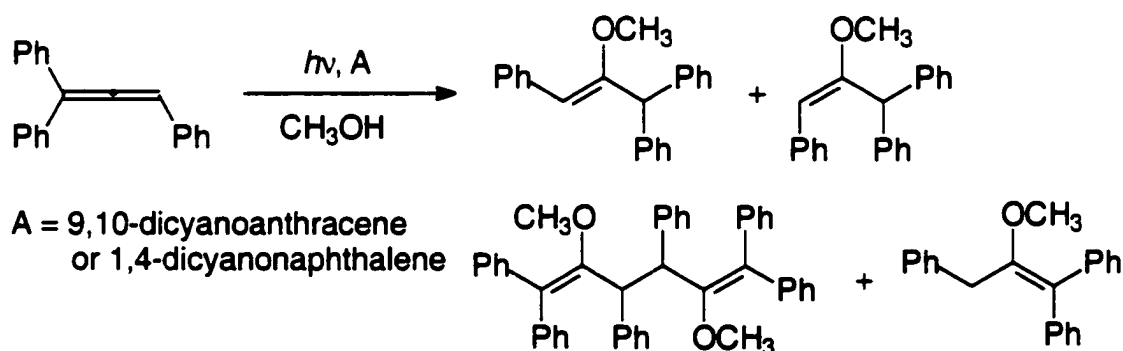


- Scheme 15 -

Phenylallenes such as tetraphenyl- and triphenylallene have also been observed to undergo *anti*-Markovnikov nucleophile addition with methanol (Schemes 16a and 16b).<sup>29</sup>



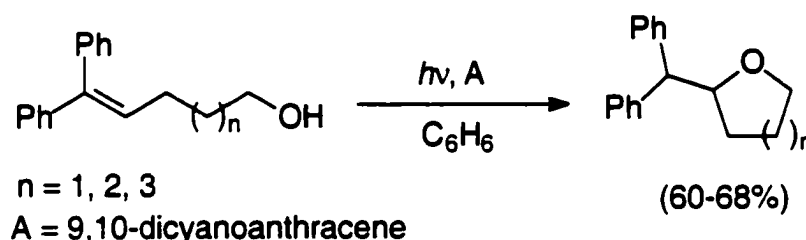
- Scheme 16a -



- Scheme 16b -

In the nucleophilic addition of triphenylallene (Scheme 16b), both monomeric and dimeric adducts are formed, depending on the reduction potential of the sensitizer. When 1,4-dicyanonaphthalene ( $E_{1/2}^{\text{red}} = -1.28$  V vs SCE) is used as sensitizer, the monomeric adducts, resulting from the intermediate methoxyallyl anion, are formed preferentially (34:1). When 9,10-dicyanoanthracene ( $E_{1/2}^{\text{red}} = -0.89$  V vs SCE) is used, the dimeric adducts, formed via coupling of the intermediate methoxyallyl radicals, are the major products (3:1). Evidently, the 1,4-dicyanonaphthalene radical anion efficiently reduces the intermediate methoxyallyl radical to the anion, whereas the more stable 9,10-dicyanoanthracene radical anion does not.

Nucleophilic additions have also been achieved intramolecularly for alkenes tethered to alcohols by means of methylene chains (Scheme 17).<sup>30</sup> The efficiency of these reactions depends on the ring size of the resulting cyclic ethers, with five- to seven-membered rings being viable while smaller and larger rings are unfavourable due to steric constraints. Mizuno has reported an enhancement of the 9,10-dicyanoanthracene-sensitized reaction in non-polar benzene solution, which suggests that an exciplex-mediated mechanism is operative.<sup>30b</sup>

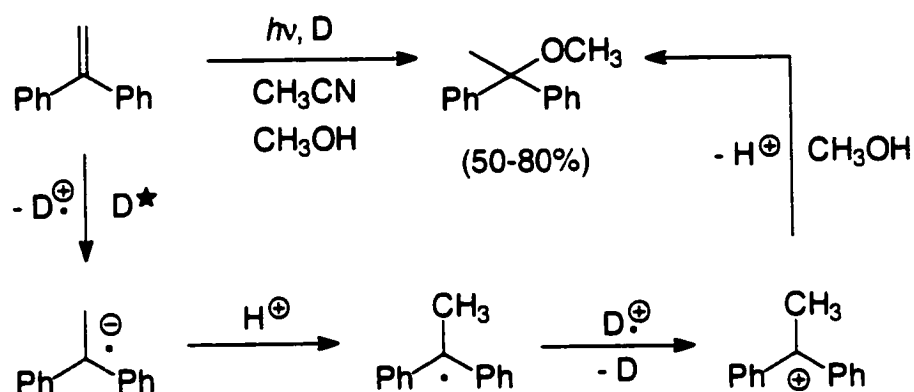


- Scheme 17 -

In all the above reactions, electron acceptors have been used to photosensitize the reaction and generate the alkene radical cation.<sup>21-30</sup> Such sensitizers include various cyanoaromatics and electron poor esters such as methyl-4-cyanobenzoate. However, if electron donating sensitizers such as 1-methoxynaphthalene, 1,4-dimethoxynaphthalene or 1-methylnaphthalene are used, the alkene radical *anion* instead of the radical *cation* will be generated (Scheme 18).<sup>21c,31</sup> Nucleophilic addition of various agents including methanol, water, cyanide ion<sup>31</sup> or 2,2,2-trifluoroethanol<sup>21c</sup> to the resulting radical anion produces the Markovnikov adduct under mild non-acidic conditions. The reversed regiochemistry is a direct consequence of the inverted sequence in the protonation and nucleophilic addition events.

Although not as synthetically useful as the PET *anti*-Markovnikov nucleophilic addition discussed earlier, this Markovnikov addition supplements the repertoire of thermal reactions that also proceed in a Markovnikov fashion,

and may become an important alternative route when "conventional" thermal pathways are unsuccessful. Even more importantly, however, it serves to highlight the flexibility of PET reactions, which by a simple change of sensitizer can result in a complete reversibility in the regioselectivity of the nucleophilic addition.



D = 1-methoxynaphthalene, 1,4-dimethoxynaphthalene  
or 1-methylnaphthalene

**- Scheme 18 -**

#### 1.4 AIM OF THE STUDY

As can be appreciated from the preceding review, the electron transfer photochemistry between electron poor aromatics, electron rich olefins and nucleophiles is a diverse area of investigation. Our research group has devoted considerable attention to these reactions and has been instrumental in developing many of the reactions, both for synthetic utility and for the mechanistic understanding they provide. In particular, we have put a great emphasis on the photo-NOCAS reaction, which we have exploited extensively as a framework towards a better understanding of the behaviour of photogenerated radical ions.

This current study consists of two main projects that are both related to our ongoing interest in the photo-NOCAS reaction and its mechanistic variations.

In the first project, we attempt to *extend* the photo-NOCAS reaction by including allenes as the olefinic electron donors. Apart from broadening the scope of the reaction from a synthetic viewpoint, the introduction of allenes provides important mechanistic information on the sequence of events in the photo-NOCAS mechanism (Scheme 4). It addresses one of the key issues in the elucidation of the mechanism – whether nucleophilic trapping of the olefinic cationic site occurs before or after association of the olefin radical cation with the arene radical anion. To date, all the work on this reaction has been performed with mononuclear systems such as 1,4-dicyanobenzene and methyl 4-cyanobenzoate as the electron acceptors.<sup>13-20</sup> In this project we also investigate the possibility of extending the photo-NOCAS reaction to dinuclear aromatic systems.

In the second project we attempt to *divert* the photo-NOCAS mechanism. With our current understanding of this class of PET reactions, we are able to modify a photochemical system in a predictable fashion. In view of this, the aim of this project is to alter the sequence of mechanistic events and thus develop a reaction that complements the photo-NOCAS reaction. In particular, we attempt this diversification by using an electron acceptor that possesses an unstable and readily cleavable radical anion.

Despite their common roots, the two projects are distinct enough to merit separate treatments. Thus, this work will be reported in separate chapters, each with its own Results, Discussion, and Experimental sections. Nevertheless, the connection between the two projects should be kept in mind.

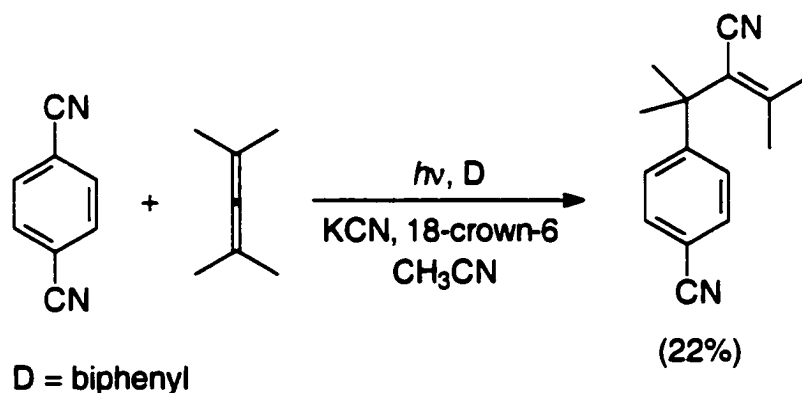
# Extending the Photo-NOCAS Reaction<sup>32</sup>

---

## 2.1 INTRODUCTION

In this study we expand our understanding of the mechanistic and synthetic aspects of the photo-NOCAS pathway by extending the reaction to aliphatic allenes as the electron donors.

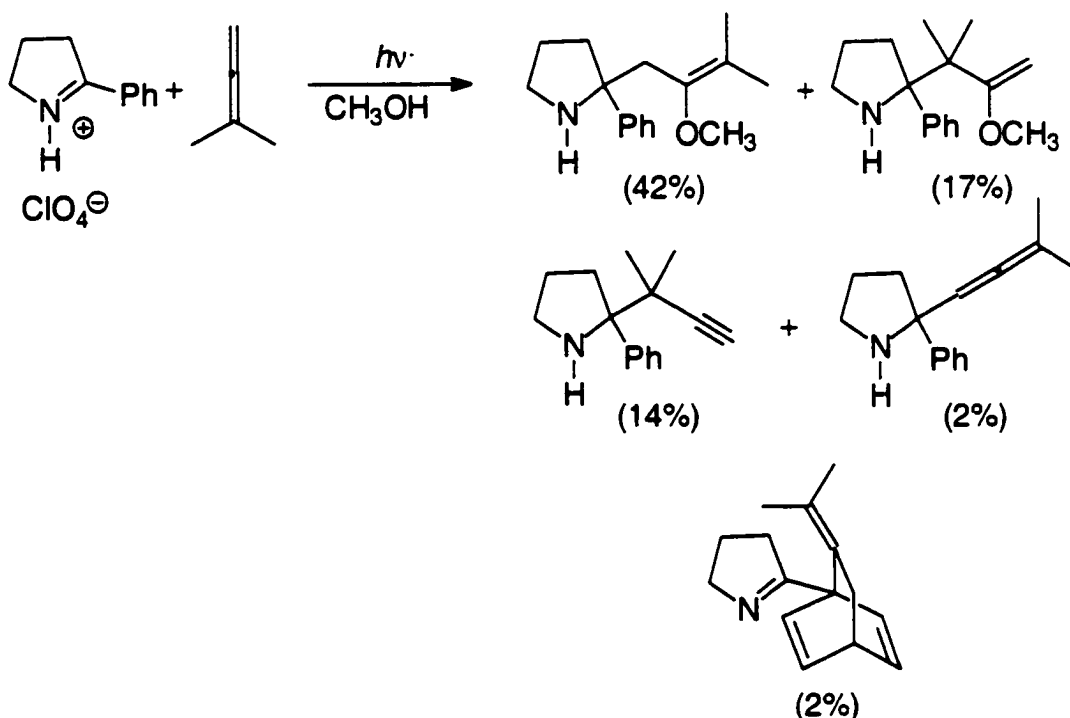
The electron transfer photochemistry of these species is relatively unexplored, and the only published studies are an earlier report from our laboratory<sup>14a</sup> and the work of Mariano.<sup>33</sup> We have previously observed that irradiation of 1,4-dicyanobenzene and tetramethylallene in the presence of cyanide anion gave the photo-NOCAS product, 4-(4-cyanophenyl)-2,4-dimethyl-2-penten-3-nitrile in 22% yield (Scheme 19).



- Scheme 19 -



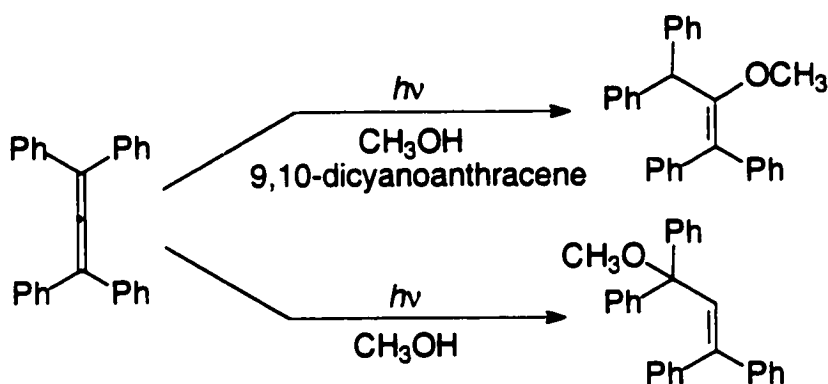
Mariano and co-workers conducted a more extensive study on a series of allenes using 2-phenyl-1-pyrrolinium perchlorate as the electron acceptor and methanol as the nucleophile. Photo-NOCAS adducts were the major products observed (Scheme 20). Deprotonation of the allene radical cation (instead of nucleophilic trapping) followed by substitution at the pyrrolinium nucleus, and cycloaddition on the phenyl ring constituted important competing side-reactions. In the absence of a nucleophile, cycloaddition became the dominant pathway.



- Scheme 20 -

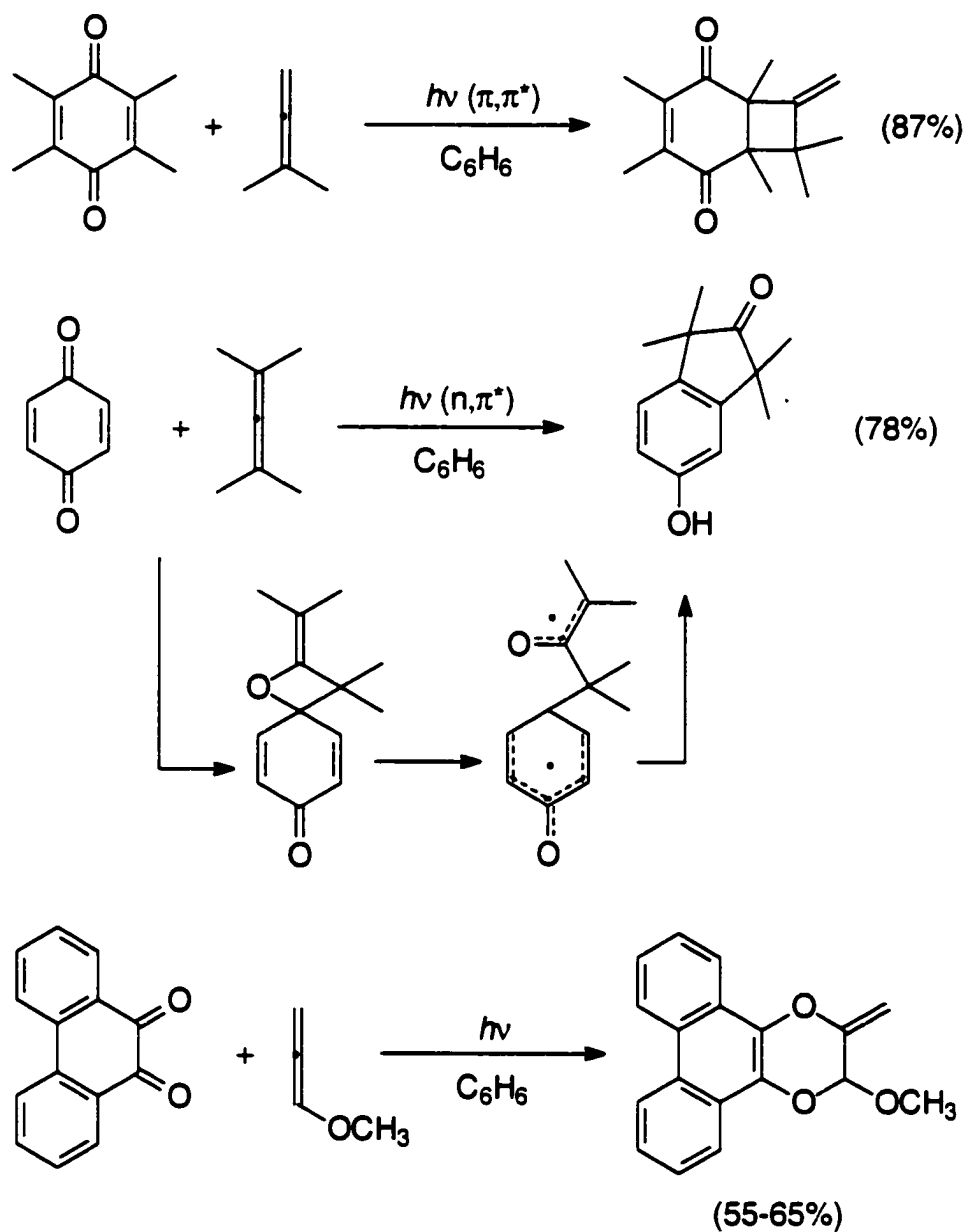
As is typical with olefins, introduction of aryl groups on the allene inhibits substitution on the electron acceptor and leads to 1:1 allene–nucleophile adducts (see Section 1.3). This is thought to be due to two reasons. First, the increased steric bulk of the intermediate allene–nucleophile adduct radical inhibits its addition to the electron acceptor radical anion. More importantly, the lower reduction potential of the radical provides an efficient alternative pathway by enabling it to undergo reduction to the anion by the electron acceptor radical

anion. Protonation of the anion yields the *anti*-Markovnikov allene–nucleophile addition product. Thus, Klett and Johnson reported that tetraphenyl- and triphenylallene undergo a photoinduced electron transfer mediated methanol addition to give a vinyl ether, in contrast to the allyl ether obtained upon direct irradiation (Scheme 21).<sup>29</sup> These results parallel studies from our laboratories with 1,1-diphenylethene and related systems.<sup>21,24,32</sup>



- Scheme 21 -

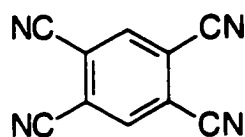
The most studied photochemical reactions of allenes are cycloadditions to ketones, cyclic enones, quinones, thiones, and related systems.<sup>34-37</sup> Although a photoinduced electron transfer mechanism has been proposed in one case,<sup>35</sup> these reactions are usually thought to proceed via a triplet state exciplex of limited charge transfer character that collapses to a 1,4-biradical.<sup>36</sup> However, in a more recent laser flash photolysis study on thione–allene photocycloadditions, no evidence for such an exciplex precursor was found and a mechanism involving direct formation of the biradical was suggested.<sup>37</sup> Whatever the operating mechanism, the reaction outcome is strongly dependent on both the structure of the reactants as well as the nature of the excited state, with  $[2\pi + 2\pi]$  cyclobutane, oxetane, and various  $[4\pi + 2\pi]$  cycloadditions reported (Scheme 22).



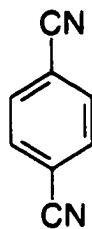
- Scheme 22 -

With a view of further defining the photochemical reactivity of allenes, we hereby present the results from our investigations of the photoinduced electron transfer reactions of the allenes tetramethylallene (2,4-dimethyl-2,3-pentadiene, **4**) and 1,1-dimethylallene (3-methyl-1,2-butadiene, **5**), with the cyanoarenes 1,2,4,5-tetracyanobenzene (**1**), 1,4-dicyanobenzene (**2**) and 1,4-dicyanonaphthalene (**3**), in the presence of methanol as nucleophile (Figure 3).

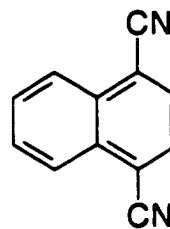
## Electron Acceptors



1

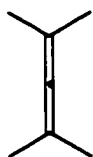


2

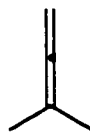


3

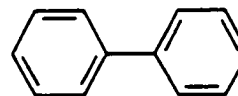
## Electron Donors



4



5



6

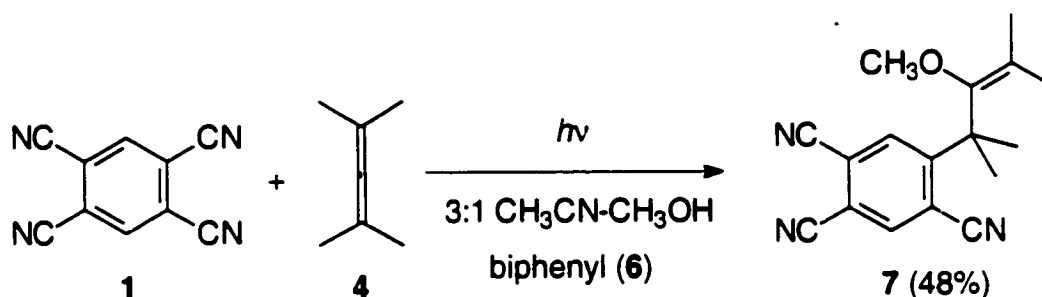
- Figure 3 -

## 2.2 RESULTS

1,2,4,5-Tetracyanobenzene (1) was irradiated in the presence of tetramethylallene (4) in 3:1 acetonitrile–methanol through a Pyrex filter ( $\lambda > 280$  nm), by means of a 1 kW medium pressure mercury lamp. Progress of the reaction was monitored by capillary column gas chromatography with a mass selective detector (GC–MS). After 45 min of irradiation, 24% of 1 was consumed (Reaction 1, Table 1). The only chromatographable product formed in detectable amounts (39%) was a crystalline 1:1:1 arene–allene–methanol adduct, identified as 4-(2,4,5-tricyanophenyl)-3-methoxy-2,4-dimethyl-2-pentene (7) by spectroscopic methods and comparison with similar products.<sup>33b</sup> In particular, the photoproduct was distinguished from another possible isomer, 3-(2,4,5-tricyanophenyl)-4-methoxy-2,4-dimethyl-2-pentene, by consideration of the allylic C-4 resonance in the  $^{13}\text{C}$  NMR spectrum. The observed signal occurred at too

high field (45.2 ppm) for it to be representative of an allylic carbon bearing a methoxy group.

The inclusion of biphenyl (**6**) as a co-donor in the photochemical mixture enhanced both the efficiency and the yield of the photoreaction boosting the rate of consumption to 50% after 45 min of irradiation and increasing the yield of photoproduct **7** to 48% (Reaction 2, Table 1; Scheme 23).



- **Scheme 23** -

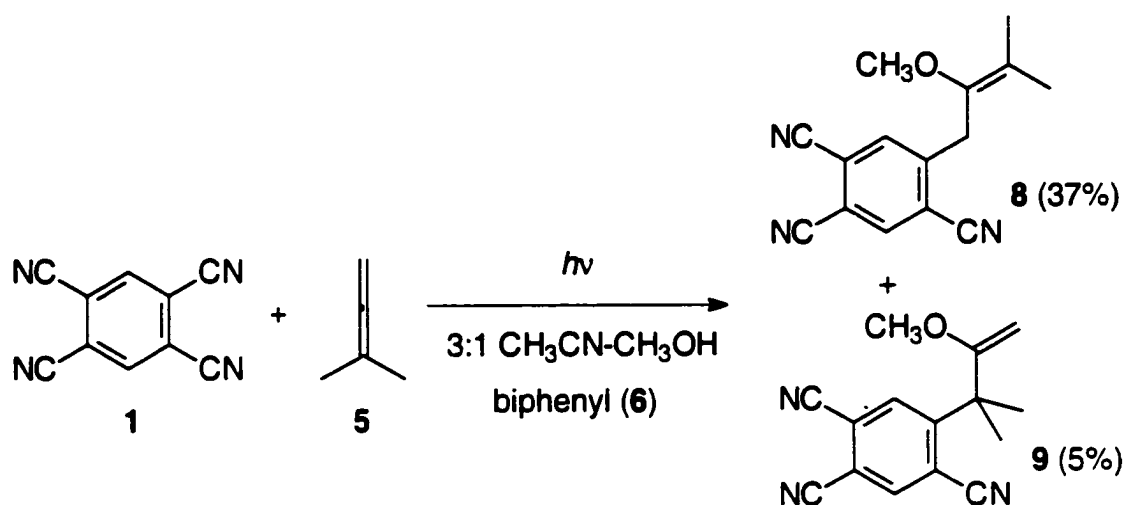
Biphenyl (**6**) also enhanced the photochemical reaction between 1,2,4,5-tetracyanobenzene (**1**) and 1,1-dimethylallene (**5**), resulting in 61% consumption of **1** after 45 min of irradiation and the formation of two isomeric 1:1:1 arene–allene–methanol adducts, 1-(2,4,5-tricyanophenyl)-2-methoxy-3-methyl-2-butene (**8**, 37%) and 3-(2,4,5-tricyanophenyl)-2-methoxy-3-methyl-1-butene (**9**, 5%) (Reaction 4, Table 1; Scheme 24). In the absence of **6**, the reaction was inefficient with only 23% consumption of **1** after 45 min of irradiation and low yields of products **8** (7%) and **9** (1%) (Reaction 3, Table 1). The two products were readily distinguished by the presence of two distinct resonances in both the <sup>1</sup>H and <sup>13</sup>C NMR spectra representing the magnetically non-equivalent methyl groups in **8**; a situation not encountered in **9**. Furthermore, **9** exhibited two doublets (<sup>2</sup>J = 3.6 Hz) at 4.28 and 4.32 ppm in the <sup>1</sup>H NMR spectrum, which are characteristic of the two geminal olefinic protons.

**Table 1** Photochemical reactions between the cyanoarenes 1–3 and the allenes 4 and 5. Reaction conditions: 1 kW medium pressure Hg lamp, Pyrex filter, 5°C, 45 min irradiation time, 3:1 acetonitrile–methanol (except where indicated otherwise).

Reaction Number	Acceptor (% consumed)	Donor	Co-donor (% recovered)	Products (% yield)
1	1 (24)	4	-	7 (39)
2	1 (50)	4	6 (94)	7 (48)
3	1 (23)	5	-	8 (7), 9 (1)
4	1 (61)	5	6 (98)	8 (37), 9 (5)
5	2 (10)	4	-	10 (7)
6	2 (46)	4	6 (98)	10 (42)
7	2 (7)	5	-	11 (21), 12 (8), 13 (8)
8	2 (43)	5	6 (95)	11 (36), 12 (4), 13 (10)
9	3 (10)	4	-	14 (11), 16 (5)
10	3 (75)	4	6 (100)	14 (54), 16 (24)
11	3 (85)	5	-	17 (8), 18 (22), 21 (26)
12	3 (95)	5	6 (94)	17 (8), 18 (18), 19 (22), 20 (20)
13 <sup>a</sup>	3 (84)	5	-	21 (38)
14 <sup>b</sup>	3 (88)	5	-	21 (42)

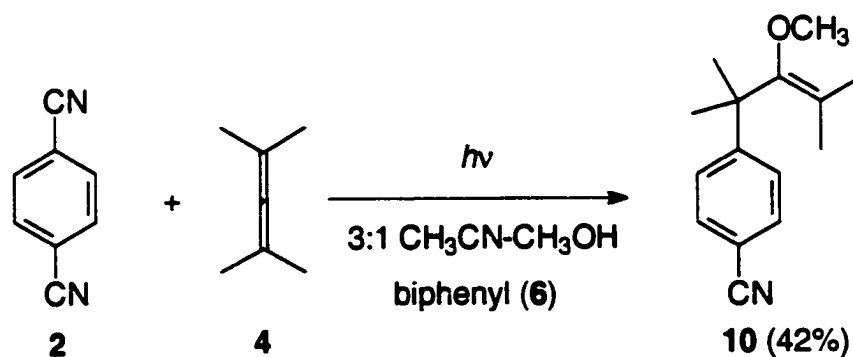
<sup>a</sup> in acetonitrile

<sup>b</sup> in benzene



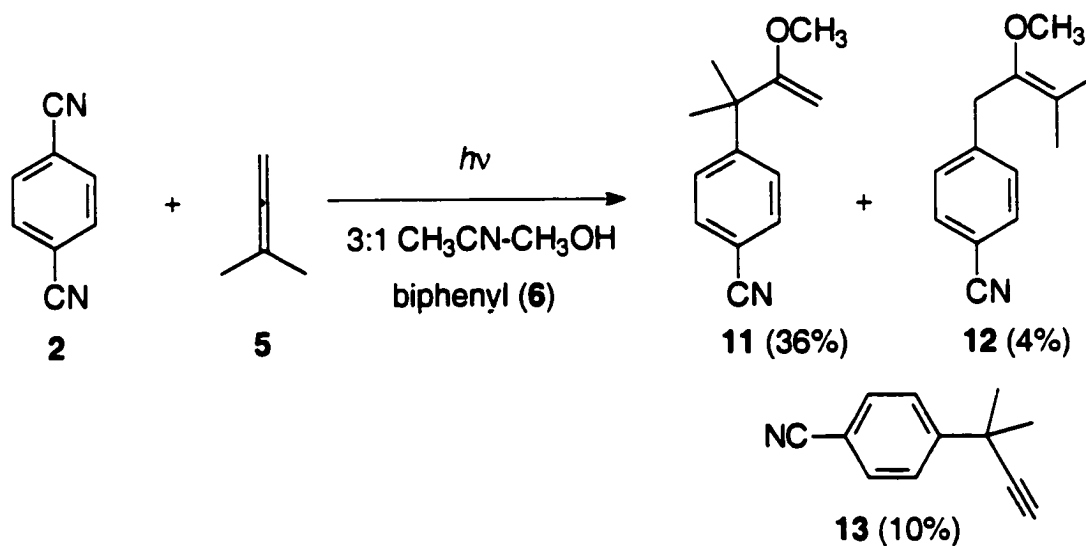
- Scheme 24 -

The irradiation of 1,4-dicyanobenzene (**2**) in the presence of tetramethylallene (**4**) in 3:1 acetonitrile–methanol led to an inefficient reaction (10% consumption after 45 min), yielding only 7% of a single 1:1:1 arene–allene–methanol adduct (Reaction 5, Table 1). This was identified as 4-(4-cyanophenyl)-3-methoxy-2,4-dimethyl-2-pentene (**10**), on the basis of its spectroscopic similarities with the analogous product (**7**) obtained when 1,2,4,5-tetracyanobenzene (**1**) is used as the electron acceptor. However, addition of biphenyl (**6**) to the reaction mixture greatly improved the reaction, resulting in 46% consumption of **1** after 45 min of irradiation and an enhanced yield of **10** of 42% (Reaction 6, Table 1; Scheme 25).



- Scheme 25 -

In analogy to the reaction between 1,2,4,5-tetracyanobenzene (**1**) and 1,1-dimethylallene (**5**), photolysis of **2** in the presence of **5** gave two 1:1:1 arene–allene–methanol adducts, arising from reaction at the non-equivalent termini of the unsymmetrical allene. In this case, however, the major product after 45 min of irradiation was 3-(4-cyanophenyl)-2-methoxy-3-methyl-1-butene (**11**), obtained in 36% yield when biphenyl (**6**) was used as co-donor (Reaction 8, Table 1; Scheme 26). The isomeric 1-(4-cyanophenyl)-2-methoxy-3-methyl-2-butene (**12**), which is the analogue of the major product in the similar reaction involving **1** (Reactions 3 and 4, Table 1), was detected only in trace amounts (4%). Its identity was tentatively though reliably established, based solely on its GC–MS characteristics; unfortunately, we were unable to isolate this compound.



- Scheme 26 -

In the absence of biphenyl (**6**), the consumption of **2** after 45 min of irradiation dropped from 43% (Reaction 8, Table 1) to 7% (Reaction 7, Table 1). The 11:12 product ratio also changed from 9.0 with **6** present to 2.6 in the absence of **6**.

This change in ratio and the contrasting regioselectivity with the equivalent reaction involving 1,2,4,5-tetracyanobenzene (**1**) led us to suspect that the switch in product ratio in this reaction might not be a consequence of alterations in the



underlying mechanism but rather a result of the adventitious consumption of **12**. However, although GC monitoring of the photoreaction did show changes in the product ratio as the reaction progressed, at no point during the reaction did the product ratio favour isomer **12**. The ratio of **11:12** varied from ca. 3.5 after 2 min to ca. 10 after 115 min of irradiation time in the biphenyl-mediated reaction (Figure 4).

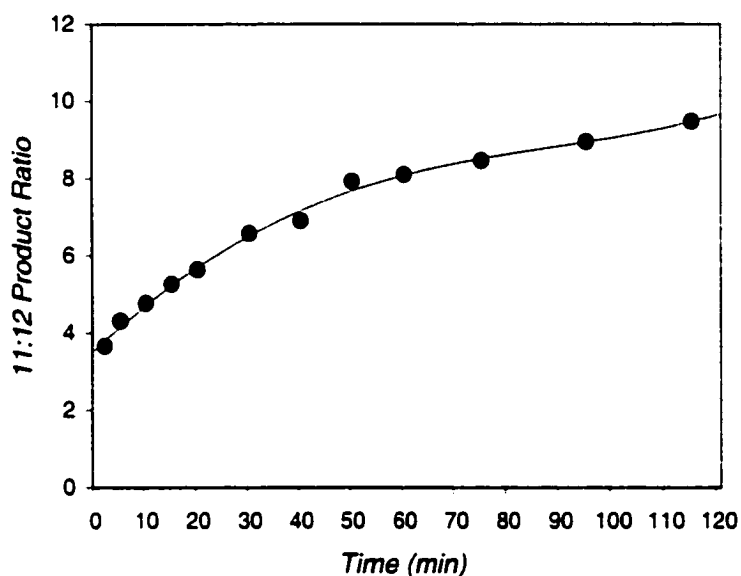
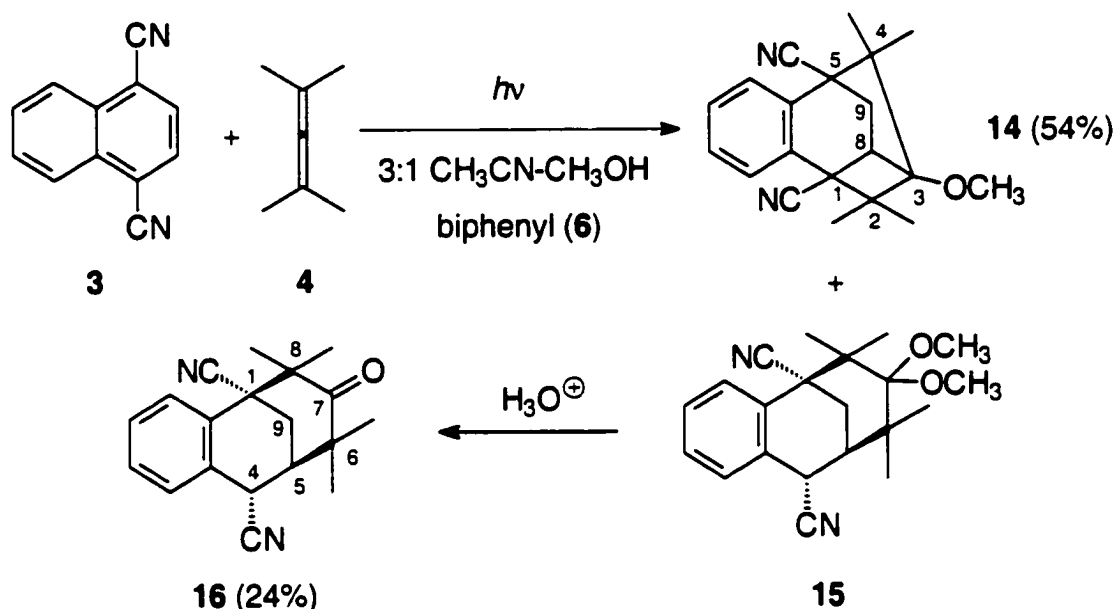


**Figure 4** Variation in product ratio **11:12** as a function of irradiation time as determined by GC analysis for the reaction between **2** and **5** in the presence of **6** in 3:1 acetonitrile–methanol.

A third product was evident in the chromatogram of the reaction between **2** and **5**, both in the absence (8%) and presence (10%) of biphenyl (**6**) (Reactions 7 and 8, Table 1). This was isolated as a colourless oil and identified spectroscopically as 3-(4-cyanophenyl)-3-methyl-1-butyne (**13**) (Scheme 26).

The photolysis of 1,4-dicyanonaphthalene (**3**) and tetramethylallene (**4**) in the presence of **6** in 3:1 acetonitrile–methanol gave two crystalline products upon chromatographic workup that were identified as 1,5-dicyano-3-methoxy-2,2,4,4-

tetramethyl-6,7-benzotricyclo[3.2.2.0<sup>3,8</sup>]nonane (**14**, 54%) and *cis*-1,4-dicyano-6,6,8,8-tetramethyl-7-oxo-2,3-benzo-*cis*-bicyclo[3.3.1]nonane (**16**, 24%) (Reaction 10, Table 1; Scheme 27). Similarly to the previous cases, removal of biphenyl (**6**) resulted in a drastic decrease in reaction efficiency, both conversion- and yield-wise (Reaction 9, Table 1).



- Scheme 27 -

The structural assignments of both products were confirmed by X-ray crystallographic analyses since spectroscopic interpretation was not conclusive (Figures 5 and 6). In particular, the absence of vicinal coupling constants in the <sup>1</sup>H NMR spectra of both products was quite misleading. In the case of **14**, only one of the two geminal C-9 protons appeared as a doublet of doublets (2.71 ppm, <sup>2</sup>J = 12.8 Hz, <sup>3</sup>J = 4.6 Hz); the other showed up as a simple doublet (1.88 ppm, <sup>2</sup>J = 12.8 Hz) and as a consequence the vicinal C-8 proton appeared as a doublet (3.45 ppm, <sup>3</sup>J = 4.6 Hz) as well. The Karplus equation predicts that a vicinal coupling constant is reduced to a minimum when the dihedral angle between the coupled protons is approximately 90°. <sup>38</sup> Crystallographic analysis of **14** suggested a value of 76° for one dihedral angle between the C-8 proton and one of the C-9 protons. The other dihedral angle is estimated as 47°. The

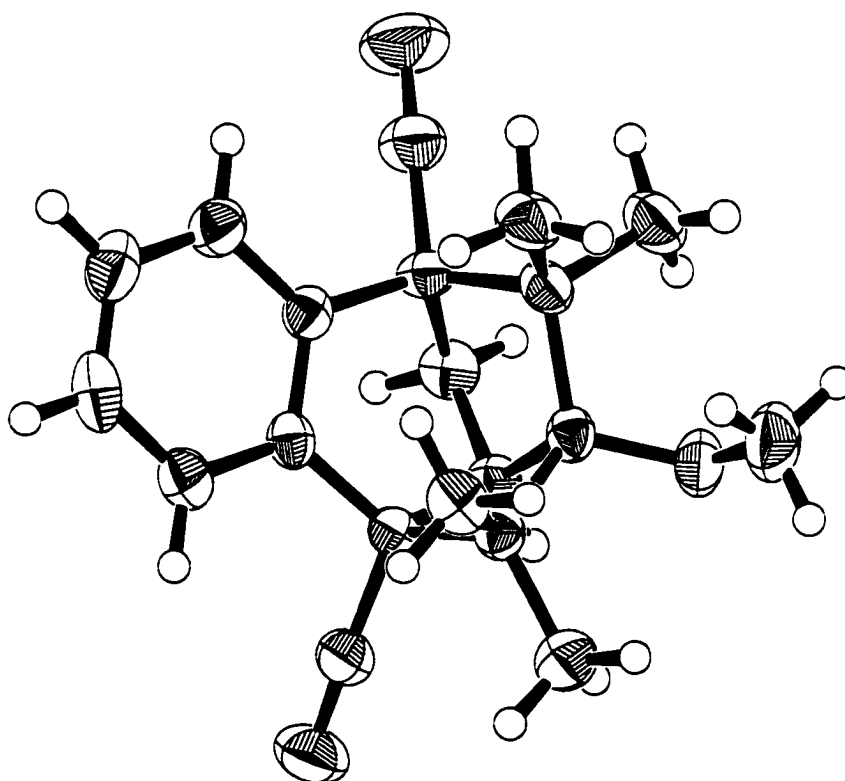


**Figure 5** Single crystal X-ray crystallographic structure of 1,5-dicyano-3-methoxy-2,2,4,4-tetramethyl-6,7-benzotricyclo[3.2.2.0<sup>3,8</sup>]nonane (**14**).

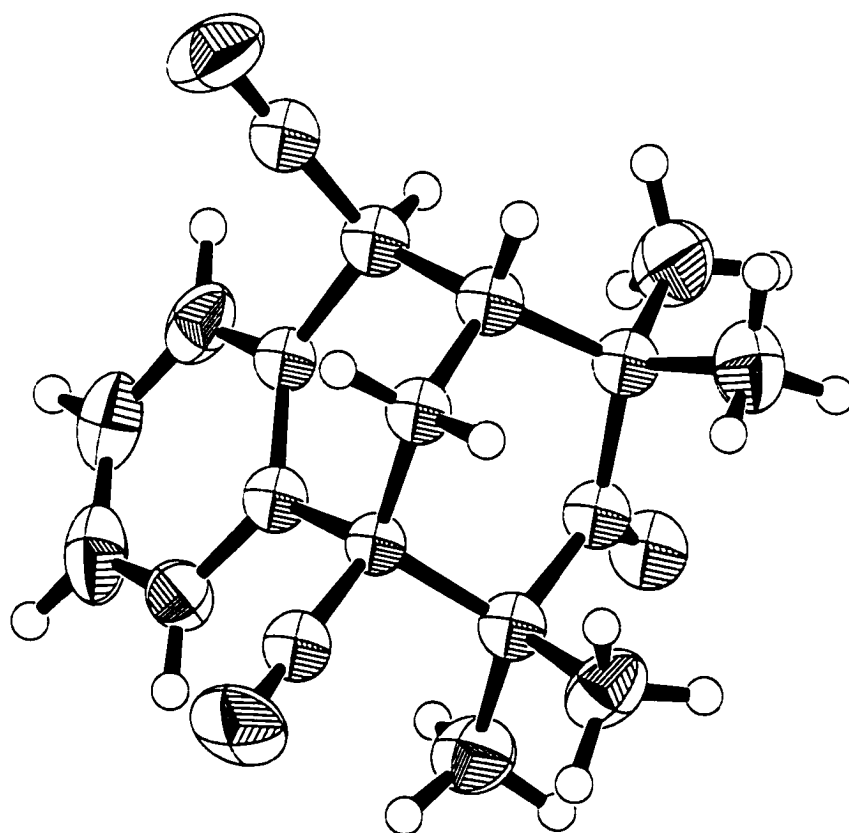
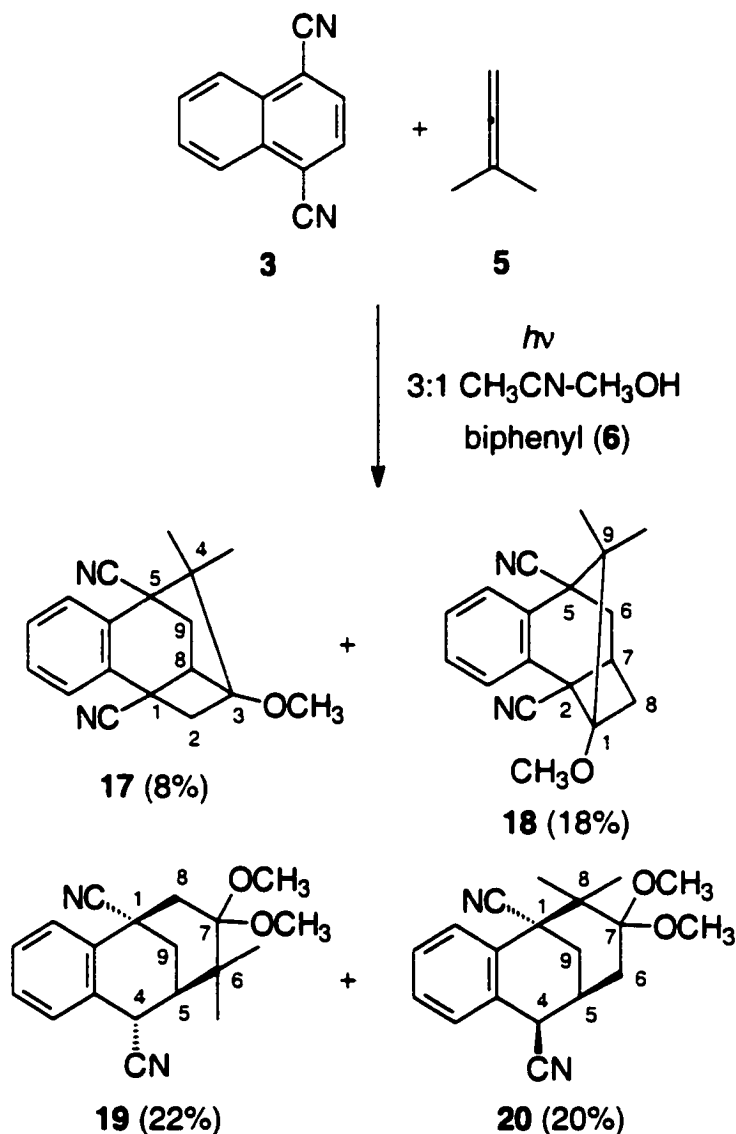


**Figure 6** Single crystal X-ray crystallographic structure of cis-1,4-dicyano-6,6,8,8-tetramethyl-7-oxo-2,3-benzo-cis-bicyclo[3.3.1]nonane (16).

observed coupling of 4.6 Hz would then represent the coupling at this 47° angle, in a situation where 0° is approximately 8 Hz. This is a reasonable value in view of the presence of electron withdrawing substituents next to the tricyclic ring protons, which may contribute to a reduction in the coupling constants.<sup>38a,39</sup>

The bicyclo-ring <sup>1</sup>H NMR resonances in **16** also displayed some peculiarities that made reliable structural elucidation difficult. One of the C-9 proton signals appeared at 3.26 ppm as a doublet of doublets of doublets, displaying a geminal coupling of 14.5 Hz to the other C-9 proton and a vicinal coupling of 4.0 Hz to the C-5 proton, as well as a long range w-coupling (<sup>4</sup>J) of 1.5 Hz to the C-4 proton. All the couplings to the C-5 proton (2.61 ppm) were either zero or small so that its resonance appeared as a broad singlet. Furthermore, the low-field C-4 proton (4.19 ppm) was a broad apparent singlet that failed to exhibit the vicinal coupling to the C-5 proton and the w-coupling to the C-9 proton at 3.26 ppm. Compound **16** is most probably the hydrolysis product of acetal **15** (*vide infra*), although we were unable to isolate **15** from the reaction mixture.

The photolysis of **3** and 1,1-dimethylallene (**5**) led to a more complex mixture of products due to the regiochemical possibilities arising from the involvement of the unsymmetrical allene. When biphenyl (**6**) was used we were able to isolate the four major products from the photochemical mixture: two 1:1:1 arene–allene–methanol tricyclic products, 1,5-dicyano-3-methoxy-4,4-dimethyl-6,7-benzotricyclo[3.2.2.0<sup>3,8</sup>]nonane (**17**, 8%) and 2,5-dicyano-1-methoxy-9,9-dimethyl-3,4-benzotricyclo[3.3.1.0<sup>2,7</sup>]nonane (**18**, 18%), and two 1:1:2 arene–allene–methanol bicyclic products, *cis*-1,4-dicyano-7,7-dimethoxy-6,6-dimethyl-2,3-benzo-*cis*-bicyclo[3.3.1]nonane (**19**, 22%) and *trans*-1,4-dicyano-7,7-dimethoxy-8,8-dimethyl-2,3-benzo-*cis*-bicyclo[3.3.1]nonane (**20**, 20%) (Reaction 12, Table 1; Scheme 28).



- Scheme 28 -

Spectroscopic identification of the products 17–20 was further complicated by the possibility of regioisomers. Therefore, the characterization of these products relied mainly on their X-ray crystallographic analyses (Figures 7–10). The <sup>1</sup>H and <sup>13</sup>C NMR spectra of the tricyclic product 17 were very similar to those of 14. In the <sup>13</sup>C NMR spectrum, the two lower field methyl carbons (26.0 and 27.0 ppm) and one of the high field quaternary carbons present in 14 were

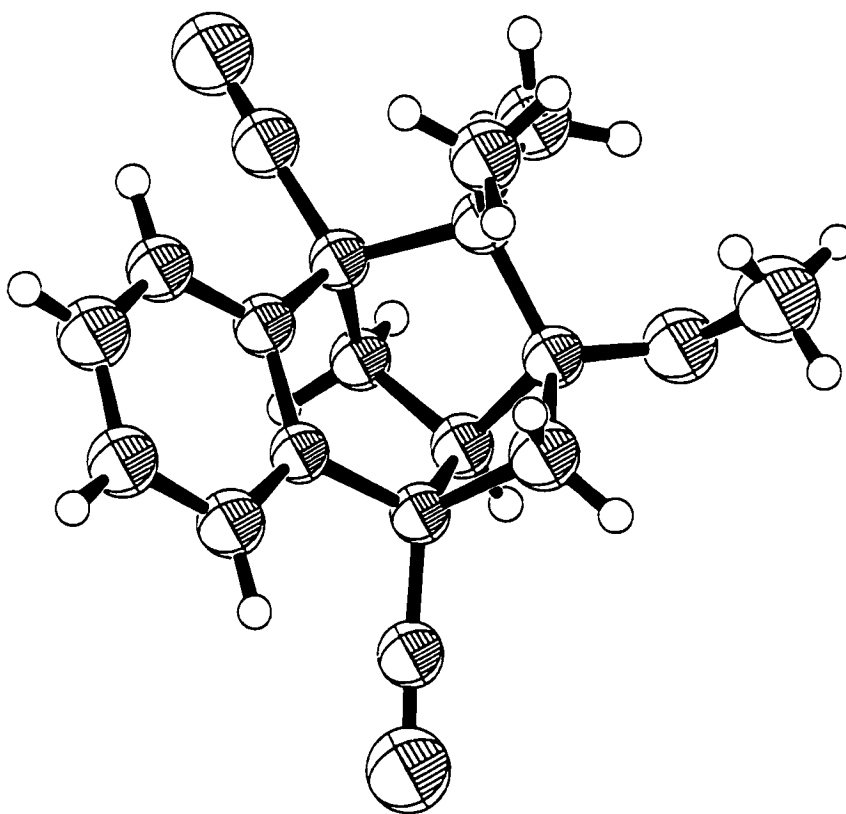


**Figure 7** Single crystal X-ray crystallographic structure of 1,5-dicyano-3-methoxy-4,4-dimethyl-6,7-benzotricyclo[3.2.2.0<sup>3,8</sup>]nonane (17).

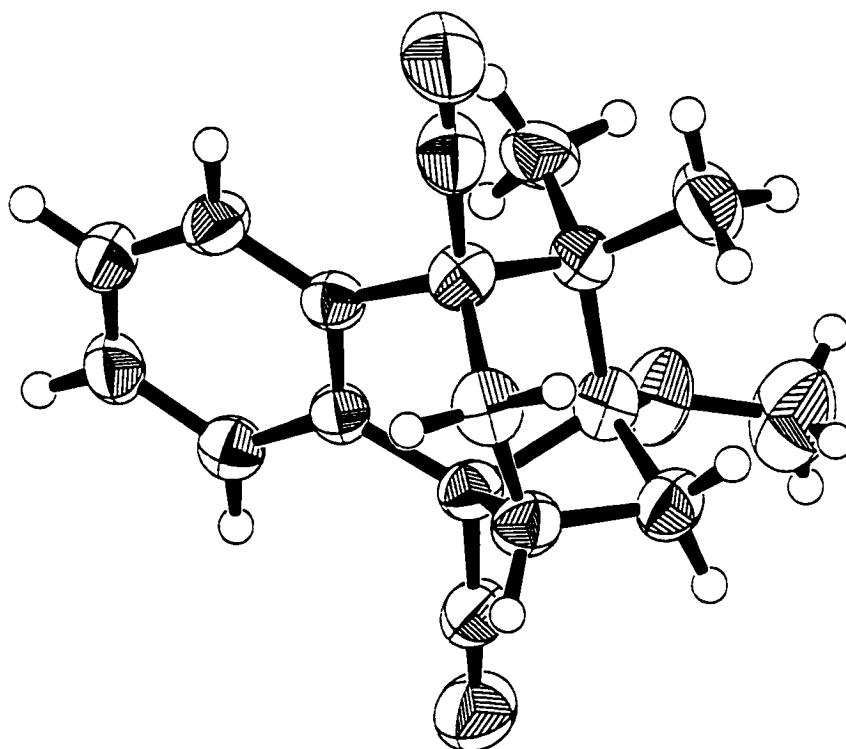


**Figure 8** Single crystal X-ray crystallographic structure of 2,5-dicyano-1-methoxy-9,9-dimethyl-3,4-benzotricyclo[3.3.1.0<sup>2,7</sup>]nonane (**18**).



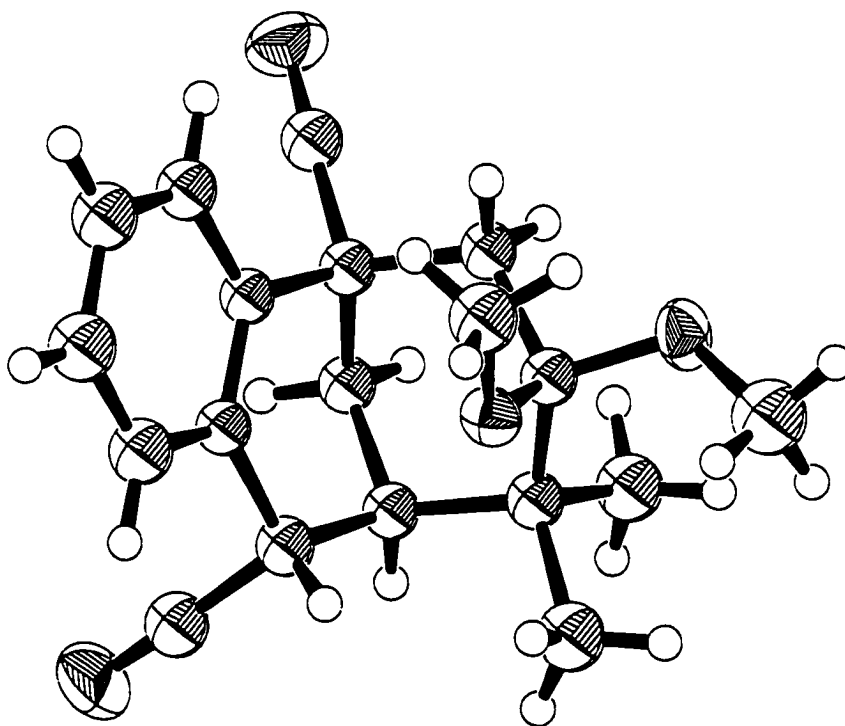


**Figure 9** Single crystal X-ray crystallographic structure of cis-1,4-dicyano-7,7-dimethoxy-6,6-dimethyl-2,3-benzo-cis-bicyclo[3.3.1]nonane (19).

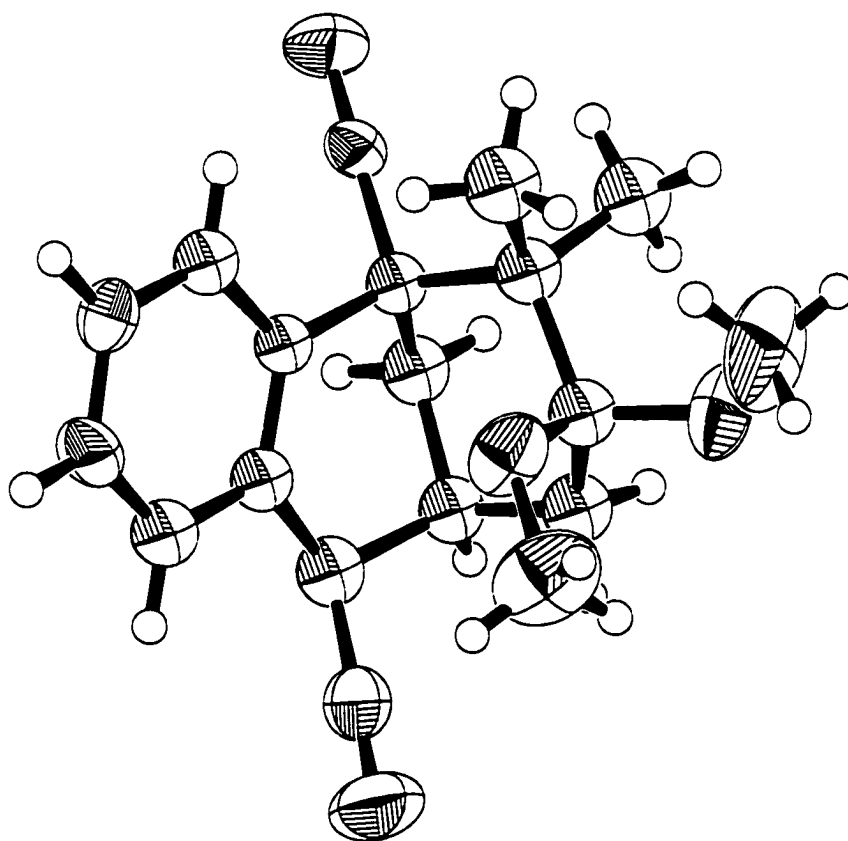


**Figure 10** Single crystal X-ray crystallographic structure of trans-1,4-dicyano-7,7-dimethoxy-8,8-dimethyl-2,3-benzo-cis-bicyclo[3.3.1]nonane (20).

replaced by a new methylene carbon resonance at 42.1 ppm in **17**. Similarly, in the  $^1\text{H}$  NMR spectrum, two methyl singlets were replaced by two coupled doublets at 2.23 ppm and 3.12 ppm ( $^2J = 12.2$  Hz) that are representative of the two geminal methylene protons.

We were confident with our assignment of the tricyclo-ring skeleton but determining the location of the *gem*-dimethyl group was more challenging. The problem was resolved by means of an X-ray crystallographic structure that, despite limited observed data and relatively high  $R$  and  $R_w$  values (isotropic refinement only), provided us with sufficiently reliable structural data to identify compound **17**.

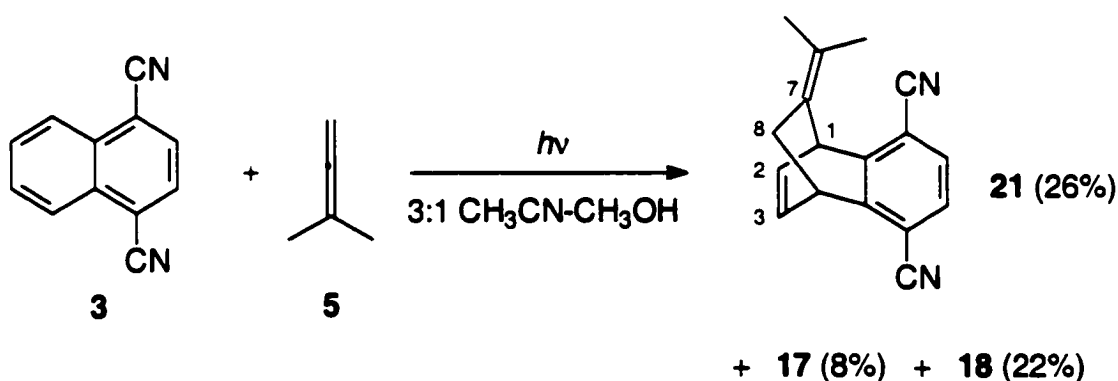
Similar to the previous products, the tricyclo product **18** exhibited some unexpected coupling patterns in its  $^1\text{H}$  NMR spectrum. A 2D  $^1\text{H}$ - $^1\text{H}$  correlation NMR experiment (COSY) confirmed that the doublet of doublets of doublets at 1.71 ppm ( $^2J = 12.8$ ,  $^3J = 7.2$ ,  $^4J = 1.2$  Hz) and the doublet at 2.50 ppm ( $^2J = 12.8$  Hz) constituted a pair of methylene protons (at C-6 or C-8). The doublet of doublets of doublets at 2.99 ppm ( $^2J = 10.7$ ,  $^3J = 7.2$ ,  $^4J = 1.2$  Hz) and the doublet at 2.20 ppm ( $^2J = 10.7$  Hz) constituted the other pair of methylene protons. The pseudo-triplet at 2.62 ppm ( $^3J = 7.2$  Hz) corresponded to the bridgehead methine proton at C-7, flanked by the two methylene groups at C-6 and C-8. These assignments imply that one of the protons in either methylene group has a vicinal coupling constant of zero with the central C-7 proton. Interestingly, the other two methylene protons exhibit a long range *w*-coupling ( $^4J = 1.2$  Hz) to one another. The *ca.*  $90^\circ$  dihedral angle ( $^3J \approx 0$  Hz) and the *w*-configuration of the two methylene protons (*w*-coupling) can be readily appreciated from a computed molecular mechanics model of the compound.

Unlike in the case of **15**, we were able to isolate the acetals **19** and **20**, which were found to be stable in the crystalline state. Nevertheless, GC-MS analysis of the two compounds indicated that the acetals decompose readily to the respective demethanolysis products ( $\text{M}^+$ ,  $m/z = 278$ ) inside the GC injector. However, when higher concentrations of the materials were injected, a second chromatographic peak representing the acetals ( $\text{M}^+$ ,  $m/z = 310$ ) largely replaced

the peak due to the decomposition products. Because of this chromatographic problem, the reported yields for these species possibly underestimate the true yields.

Just as with **16**, the C-4 proton signal in the  $^1\text{H}$  NMR spectrum (singlet, 4.30 ppm) of **19** did not exhibit any coupling to the C-5 proton. Both **16** and **19** have the two cyano groups arranged *cis* to one another. However, in acetal **20**, the cyano groups are arranged in a *trans* geometry and the C-4 proton (4.37 ppm) appears as a doublet ( $^3J = 6.1$  Hz).

Removal of biphenyl (**6**) from the reaction mixture altered the course of the photochemical reaction (Reaction 11, Table 1; Scheme 29). The major product was now a 1:1 arene–allene adduct identified as 7-isopropylidene-5,6-(2',5'-dicyanobenzo)bicyclo[2.2.2]oct-2-ene (**21**, 26%) that was absent from the reaction when **6** was used as co-donor. Also present were the tricyclo products **17** (8%) and **18** (22%), but no appreciable amounts of the acetals **19** and **20** were detected. The identity of **21** rests predominantly on an X-ray crystallographic structure analysis (Figure 11). Compound **21** was also isolated as the sole product when the reaction was carried out in pure acetonitrile or benzene (Reactions 13 and 14, Table 1).



- Scheme 29 -

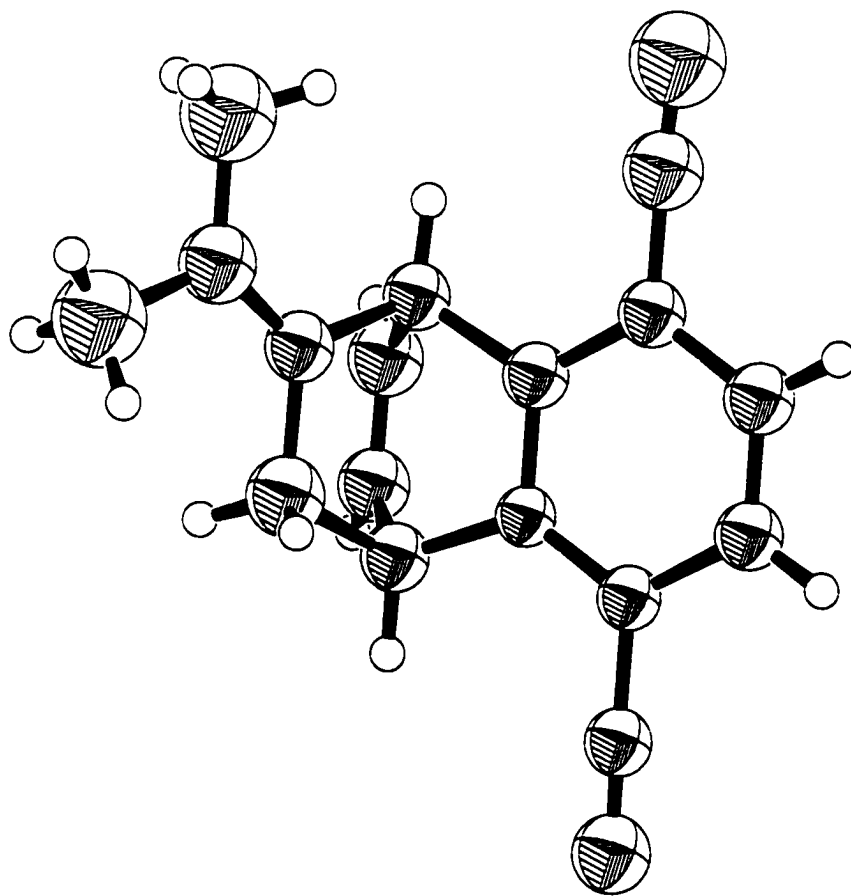


**Figure 11** Single crystal X-ray crystallographic structure of 7-isopropylidene-5,6-(2',5'-dicyanobenzo)bicyclo[2.2.2]oct-2-ene (**21**).

## 2.3 DISCUSSION

The singlet excited state of 1,2,4,5-tetracyanobenzene (**1**) possesses an exceptionally high reduction potential ( $E_{1/2}^{\text{red}}(\mathbf{1}^*) = E_{1/2}^{\text{red}}(\mathbf{1}) + E_{0,0}(\mathbf{1}) = 3.18 \text{ V}$ , Table 2), making it a very effective electron acceptor for photoinduced electron transfer (PET). The reason why **1** has not received as much attention as an electron acceptor in PET studies as other cyanoarenes, such as 1,4-dicyanobenzene (**2**) and 9,10-dicyanoanthracene, is mainly due to the pronounced stability (low reduction potential) of its radical anion. This renders it a poor photosensitizer, since its radical anion is generally incapable of being oxidized back to the neutral starting material to complete the photosensitization cycle.<sup>‡</sup> Nevertheless, it has proven to be very successful in PET reactions that do not require photosensitization but rather involve the electron acceptor as a reactant. Albini and co-workers have exploited the properties of this electron acceptor in a variety of photochemical reactions with electron donors, some of which were previously inaccessible due to their relatively high oxidation potentials.<sup>42</sup> We were thus interested in investigating how **1** would perform in a photo-NOCAS system.

To date, most of the photo-NOCAS studies in the literature have used 1,4-dicyanobenzene (**2**) almost exclusively.<sup>12-18</sup> This substrate is a well established PET electron acceptor with a singlet excited state reduction potential (2.55 V) somewhat lower than that of **1**\*

In our study, the electron donors have moderately high oxidation potentials (Table 2). As seen in Table 3, the free energy of the PET process

---

<sup>‡</sup> Typically, completion of the photosensitization cycle requires the sensitizer radical anion to reduce a radical species derived from the donor radical cation after nucleophilic trapping, deprotonation, desilylation, or some other process. The reduction potentials of most typical radicals are too high for exergonic electron transfer with  $\mathbf{1}^{\cdot-}$ .<sup>40</sup> The only cases in which photosensitization of **1** is indeed observed involve the regeneration of **1** from  $\mathbf{1}^{\cdot-}$  via an electron transfer process with a carbocationic moiety.<sup>41</sup>

**Table 2** Half-wave reduction potentials ( $E_{1/2}^{\text{red}}$ ) and singlet excitation energies ( $E_{0,0}$ ) for the electron acceptors 1–3 and half-wave oxidation potentials ( $E_{1/2}^{\text{ox}}$ ) for the electron donors 4–6. All potentials are reported vs SCE in  $\text{CH}_3\text{CN}$ .

Compound	$E_{1/2}^{\text{red}} / \text{V}^{\text{a}}$	$E_{1/2}^{\text{ox}} / \text{V}$	$E_{0,0} / \text{eV}^{\text{a}}$
1,2,4,5-Tetracyanobenzene (1)	-0.65		3.83
1,4-Dicyanobenzene (2)	-1.66		4.21
1,4-Dicyanonaphthalene (3)	-1.28		3.45
Tetramethylallene (4)		+1.93 <sup>b</sup>	
1,1-Dimethylallene (5)		+2.23 <sup>c</sup>	
Biphenyl (6)		+1.85 <sup>d</sup>	

<sup>a</sup> Ref. 4a. <sup>b</sup> Ref. 14a. <sup>c</sup> Peak Potential  $E^{\text{ox}} = 1.92 \text{ V}$  vs  $\text{Ag} / \text{Ag}^+$  in  $\text{CH}_3\text{CN}$ , cyclic voltammetry,  $100 \text{ mV s}^{-1}$  scan rate, tetraethylammonium tetrafluoroborate as supporting electrolyte.<sup>43</sup> Corrected to  $E_{1/2}^{\text{ox}}$  by subtracting  $0.03 \text{ V}$  from the peak potential;<sup>44</sup> referenced to SCE by adding  $0.34 \text{ V}$ . <sup>d</sup> Ref. 20b.

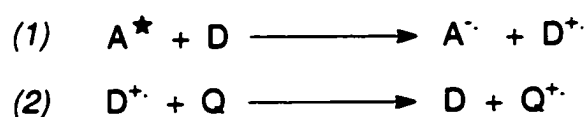
involving 1 or 2 and the electron donors is highly exergonic in all cases, and electron transfer is expected to proceed at a diffusion controlled rate. The inclusion of biphenyl (6) as a co-donor enhanced both the efficiency and the yield of all the photoreactions studied (Table 1). The role of co-donors such as 6 is not fully understood. There are numerous reports in the literature in which PET reactions are enhanced by the addition of an appropriate co-donor, generally an aromatic hydrocarbon.<sup>11</sup> Typically, the oxidation potential of the co-donor D is higher than that of the donor substrate Q but lower than the reduction potential of the excited state of the electron acceptor  $\text{A}^*$ , so that both electron transfer steps shown in Scheme 30 will be exergonic. As explained previously (Section 1.1), the reaction enhancement is usually attributed to different rates of back electron transfer for the  $\text{A}^{\cdot-} / \text{D}^{\cdot+}$  and  $\text{A}^{\cdot-} / \text{Q}^{\cdot+}$  pairs.

**Table 3** Free energy ( $\Delta G_{PET}$ ) for the photoinduced electron transfer process between the singlet excited states of the electron acceptors 1–3 and the ground state of the electron donors 4–6.

Electron Acceptor	Electron Donor	$\Delta G_{PET} / \text{kJ mol}^{-1}$ <sup>a</sup>
1	6	-134
1	4	-126
1	5	-97
2	6	-73
2	4	-65
2	5	-36
3	6	-36
3	4	-29
3	5	0

<sup>a</sup> Calculated using the Weller equation:  $\Delta G_{PET} = F (E_{1/2}^{ox} - E_{1/2}^{red} - E_{0,0} - e/4\pi\epsilon\alpha)$ .<sup>9</sup>

The Coulombic attraction term  $F/4\pi\epsilon\alpha$  was calculated as  $5.4 \text{ kJ mol}^{-1}$  by assuming an encounter distance  $\alpha$  of  $7 \text{ \AA}$ .<sup>12a</sup>



**- Scheme 30 -**

However, in many cases including the present one, the oxidation potential of the co-donor D is lower than that of the donor substrate Q, which implies that the second step in Scheme 30 is endergonic. In the current study, the free energies for the second step between the biphenyl radical cation ( $6^{+\cdot}$ ) and 4 and



5 are +8 and +37 kJ mol<sup>-1</sup> respectively.<sup>§</sup> Despite this, a marked enhancement in the photochemical reaction is observed.<sup>45</sup> The prevalent explanation put forward to account for this is that the co-donor radical cation D<sup>•+</sup> and the donor Q lie in equilibrium with a small amount of the donor radical cation Q<sup>•+</sup> and the co-donor D; consumption of Q<sup>•+</sup> drives the equilibrium forward generating more of Q<sup>•+</sup>. Alternatively, this may be viewed as the formation of a  $\pi$ -complex between D<sup>•+</sup> and Q that imparts substantial charge onto Q.<sup>†</sup> It should be kept in mind that the second electron transfer process (step 2, Scheme 30) is a charge-shift electron transfer that is quite likely to behave differently from the more common and better understood charge-separation process (step 1, Scheme 30).

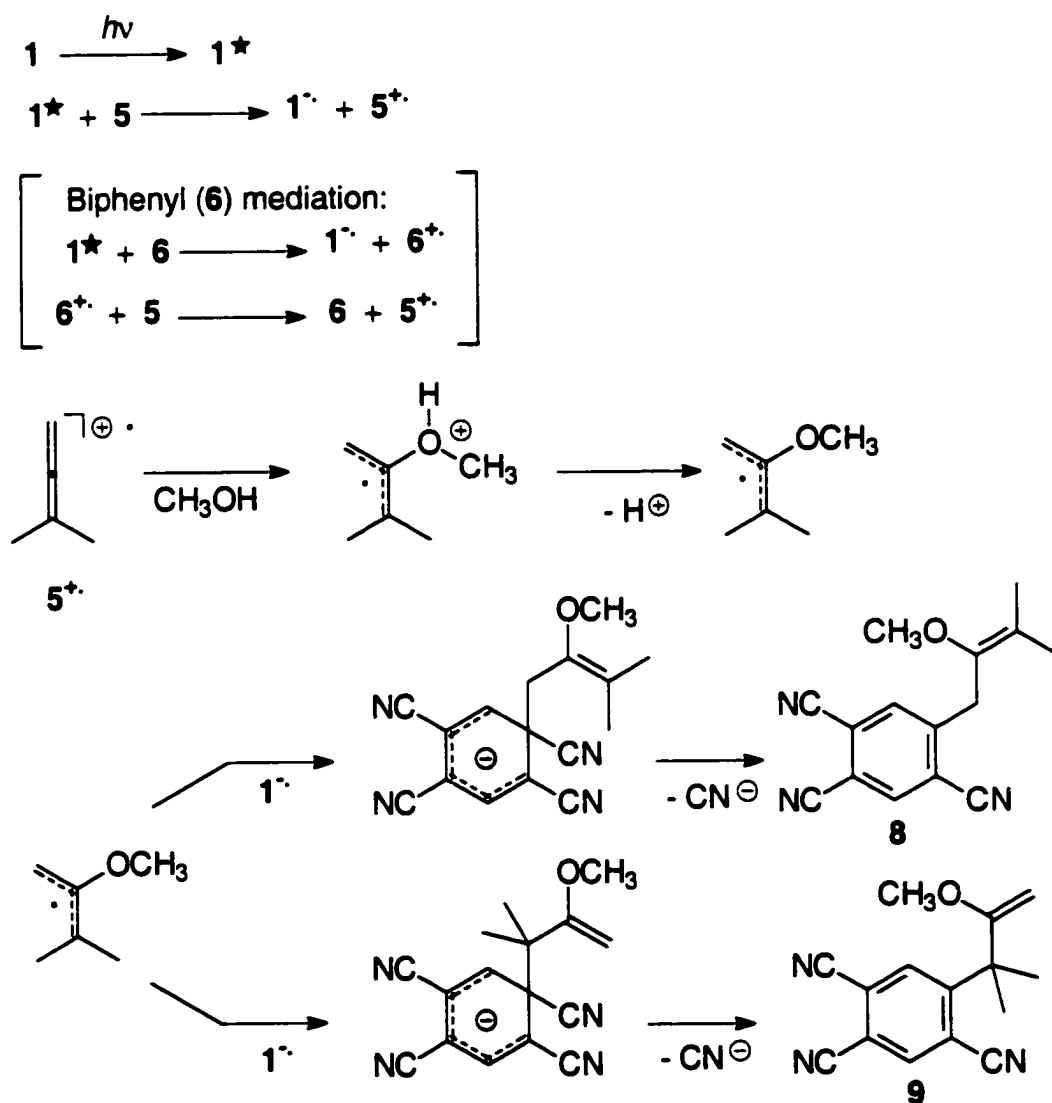
The formation of photoproducts 7–12 can be readily explained by means of a photo-NOCAS mechanism.<sup>12-18</sup> The mechanism, exemplified for 1,2,4,5-tetracyanobenzene (1) and 1,1-dimethylallene (5), is illustrated in Scheme 31. Electron transfer, either directly to the excited singlet state of 1 from the ground state of the allene 5, or mediated by biphenyl (6), leads to the formation of the cyanoarene radical anion 1<sup>•-</sup>, and the allene radical cation, 5<sup>•+</sup>. The latter adds methanol, exclusively at the central carbon, to give a  $\beta$ -methoxyallyl radical. No products arising from addition of methanol to a terminal allenyl carbon are observed. The absence of such products is clear evidence that the allene radical cation does not add to the cyanoarene radical anion via a radical coupling mechanism while still within the geminate radical ion pair, prior to nucleophilic trapping. If this mechanism was operational we would not expect to observe the

---

<sup>§</sup> Determined using:  $\Delta G_{ET} = F(E_{1/2}^{ox} - E_{1/2}^{red})$  where  $E_{1/2}^{red}$  (6<sup>•+</sup>) = 1.85 V vs SCE (CH<sub>3</sub>CN).

<sup>†</sup> Similar increases in reaction efficiency have also been reported with hydrocarbon co-donors (*e.g.*, benzene) that possess too high oxidation potentials for exergonic electron transfer with the acceptor substrate (energonic first step in Scheme 30). This is attributed to the formation of a  $\pi$ -complex between the aromatic hydrocarbon co-donor and the donor radical cation (generated in the PET step with the electron acceptor); this interaction stabilizes the donor radical cation, enhancing its diffusion out of cage with the acceptor radical anion, thus suppressing BET.<sup>46</sup>

aryl moiety attached to a terminal allenyl carbon, since this would generate a highly unstable vinyl cation. This alternative mode of reactivity was suggested in early studies on these types of photoreactions,<sup>47,48</sup> but was largely disfavoured in subsequent work<sup>49</sup> with the exception of a few special cases.<sup>50</sup> The observed reaction enhancement upon addition of biphenyl (**6**) is further proof against this alternative mechanism: generating the allene radical cation and the cyanoarene radical anion in separate stages should inhibit geminate radical ion pair reactions and increase the probability of interception of the allene radical cation by methanol prior to its addition onto the aromatic ring.



- Scheme 31 -

The final stage in the mechanism involves the addition of the  $\beta$ -methoxyallyl radical to the *ipso* position of  $1^{\cdot-}$ , which, as expected, is the site of highest spin density (Figure 11). This is followed by rearomatization of the adduct anion via expulsion of a cyanide ion to yield the final photo-NOCAS product.

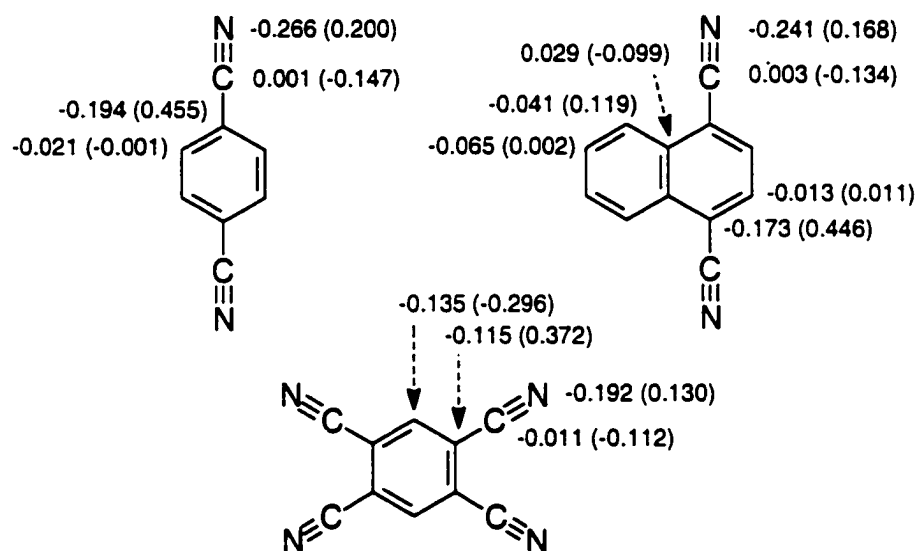


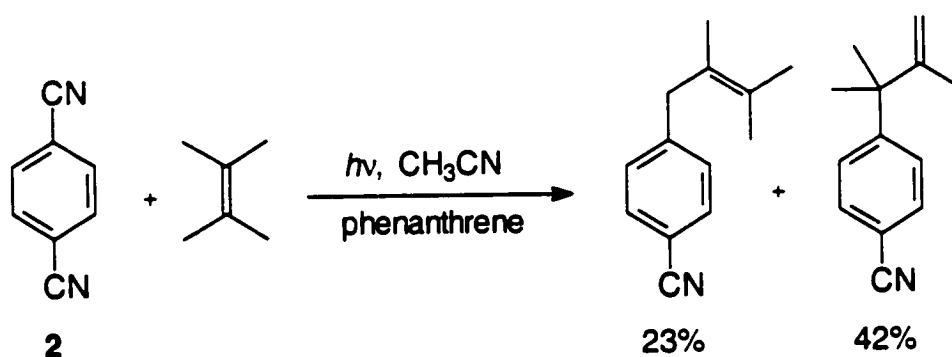
**Figure 11** Atomic charge densities with hydrogens summed into heavy atoms and total atomic spin densities (in parenthesis) for the radical anions of electron acceptors 1–3 calculated by the semi-empirical AM1 method.

The predominance of photoproduct **8** (**8:9** = 7) in the 1,2,4,5-tetracyanobenzene (**1**) reaction mixture indicates that the addition of the  $\beta$ -methoxyallyl radical to the cyanoarene radical anion is sterically controlled, with the less heavily substituted radical site being more reactive. This situation is typical of radical coupling reactions.<sup>51</sup> This observation is analogous to that reported by Mariano where reaction at the less substituted side of the  $\beta$ -methoxyallyl radical of  $5^{\cdot+}$  is favoured by a factor of 2.5 (Scheme 20).<sup>33</sup>

In the 1,4-dicyanobenzene (**1**) / 1,1-dimethylallene (**5**) reaction, the photo-NOCAS product ratio switches in favour of the product (**11**) arising from reaction

at the more sterically hindered terminus of the  $\beta$ -methoxyallyl radical. The other isomer that is equivalent to the major product in the analogous reaction involving **1** was only formed in trace amounts.

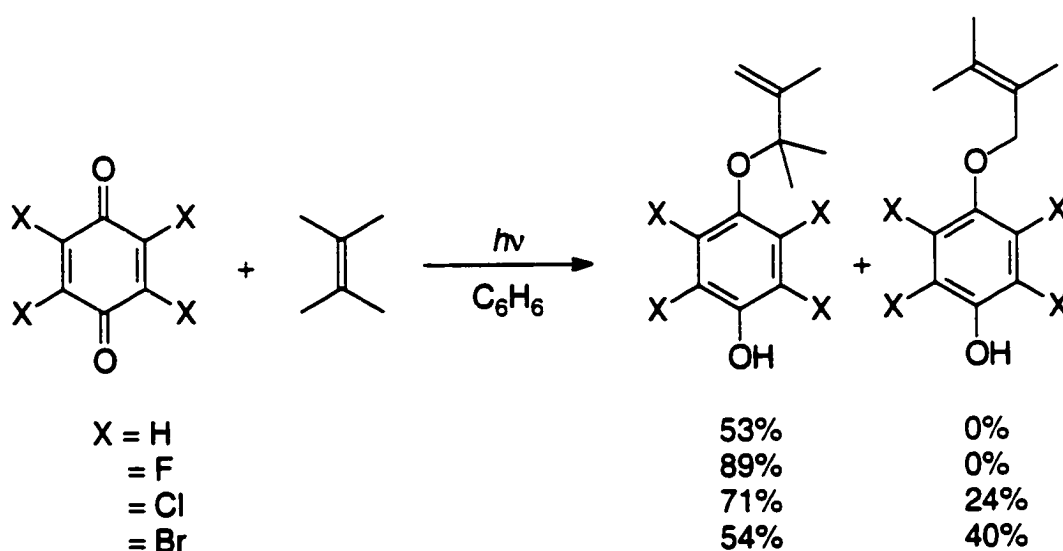
This alteration in regiochemistry has interesting implications on the behaviour of the allylic radical intermediates. It appears that, in the absence of steric crowding at the cyanoarene reaction site (as in the case of **2**), the allylic radical will react preferentially from the more highly substituted allylic terminus, which is expected to bear a greater portion of the spin density. A similar regiochemical outcome has been observed in the PET-induced substitution reaction of 2,3-dimethyl-2-butene and 1,4-dicyanobenzene (**2**), which proceeds via a very similar allylic radical, generated by deprotonation of the alkene radical cation (Scheme 32).<sup>12a,14b,16,45b</sup>



- Scheme 32 -

However, increasing the steric crowding at the *ipso*-position of the electron acceptor (as in the case of **1** or Mariano's 2-phenyl-1-pyrrolinium moiety), causes the allylic radical to react preferentially from the less substituted terminus. The fact that in these reactions both isomers are present, albeit in drastically different proportions, suggests that the two regiochemical reaction pathways must differ only slightly in their activation energy barriers. Which pathway is favoured will depend on a fine balance between various contributing factors such as steric hindrance and spin density distribution. A recent study on the PET-induced

addition of allylic radicals (formed via deprotonation of alkene radical cations) to phenoxy radicals (via proton abstraction by 1,4-benzoquinone radical anions) has shown similar trends as regards the regiochemical selectivity of non-symmetrical allylic radicals – in the absence of *ortho*-substituents on the phenoxy moiety, reaction occurred exclusively at the more highly substituted allylic terminus, but increasing the steric bulk of the *ortho*-substituents clearly favoured reaction at the less substituted allylic terminus (Scheme 33).<sup>52</sup>

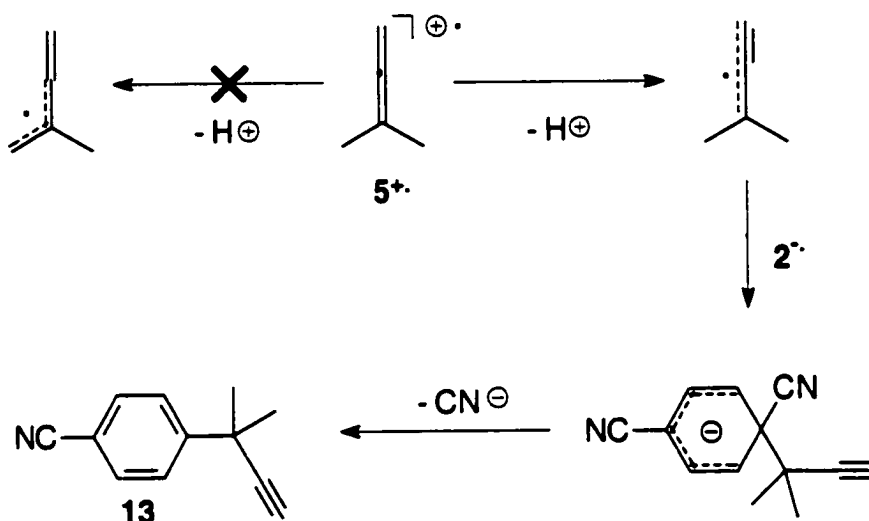


- Scheme 33 -

The third product isolated from the reaction between **2** and **5** is 3-(4-cyanophenyl)-3-methyl-1-butyne (**13**). This is thought to form via deprotonation of the allene radical cation **5<sup>•+</sup>**, according to the mechanism in Scheme 34. It is interesting to note that deprotonation in **5<sup>•+</sup>** occurs exclusively from the allenyl  $sp^2$ -carbon site rather than from the methyl  $sp^3$ -carbon centre, a phenomenon attributed to kinetic acidity.<sup>33b,53</sup>

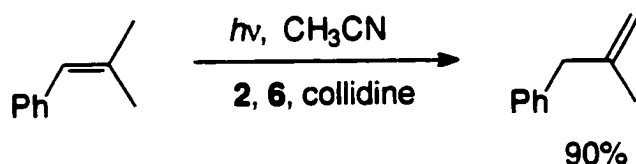
Deprotonation of alkene radical cations is commonly observed as the major reaction pathway in the absence of a nucleophile. In the case of aliphatic alkenes, the allylic radical formed upon deprotonation usually substitutes, from

either ambident end, at the *ipso*-position of the cyanoarene radical anion to give 1:1 arene-alkene products (Scheme 32).<sup>12a,14b,16,45b</sup>



- Scheme 34 -

With aromatic alkenes, the allylic radical does not substitute but instead gets reduced to the allylic anion, which can then get protonated at either end of the allylic moiety to regenerate the starting material or to give a deconjugated tautomer (Scheme 35).<sup>54</sup> This switch from substitution to reduction is typically observed on going from aliphatic to aromatic alkenes (Sections 1.2 and 1.3).



- Scheme 35 -

Alkene radical cations are generally not acidic enough for deprotonation to compete effectively with nucleophilic trapping by strong nucleophiles such as methanol.<sup>54b,54c</sup> Deprotonation only becomes competitive in the presence of weaker nucleophiles such as fluoride anion which also has substantial basic

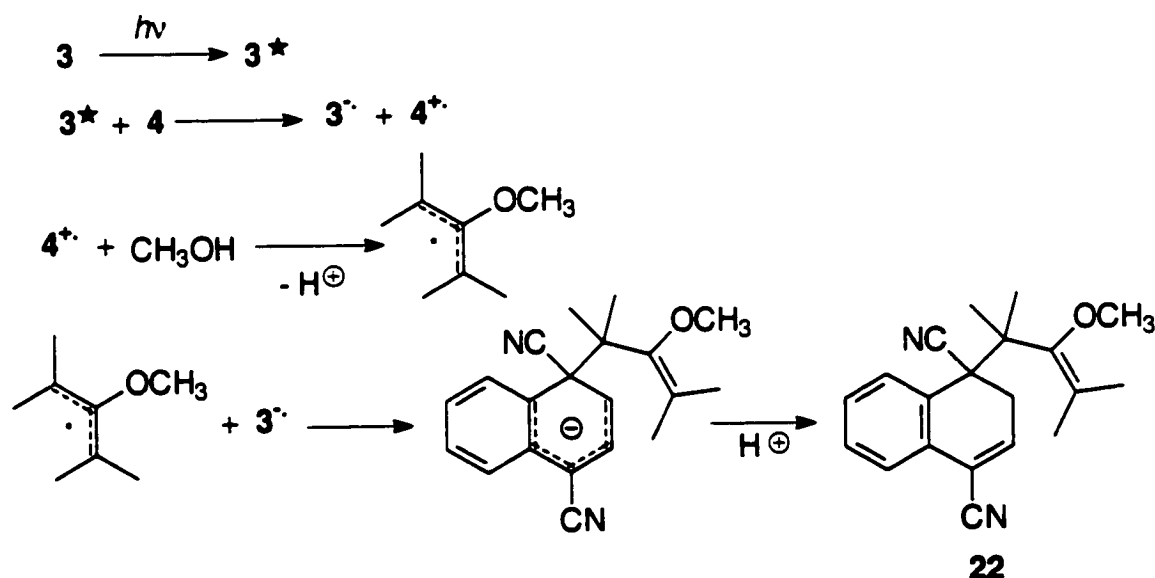
character.<sup>14b</sup> In contrast, the increased acidity of allene radical cations does allow deprotonation to compete with nucleophile addition. Further to the results obtained in this work, Mariano and co-workers also observed appreciable amounts of 1:1 products derived from deprotonation of the allene radical cation (Scheme 20). Similarly, Klett and Johnson reported the formation of a deprotonation product (1,3,3-triphenylpropyne) in their PET study on triphenylallene.<sup>29b</sup> Both of these studies were conducted in pure methanol. This increased tendency towards deprotonation is most likely attributed to the more acidic character of the  $sp^2$ -hybridized C–H bond in the allenes as opposed to the  $sp^3$ -hybridized C–H bond in the alkenes.

The photo-NOCAS reaction had never been attempted with binuclear aromatic systems. Thus, in an attempt to extend the reaction to bicyclic arenes, we investigated the photochemistry of 1,4-dicyanonaphthalene (**3**) under photo-NOCAS conditions. 1,4-Dicyanonaphthalene (**3**) possesses the lowest excited state reduction potential (2.17 V, Table 2) among the electron acceptors chosen for this study. This is mainly due to its low singlet excitation energy,  $E_{0,0}$ , itself a consequence of the extended conjugation of the  $\pi$ -system. Nevertheless, the free energies for PET are still sufficiently exergonic to ensure an efficient electron transfer process, except in the case of 1,1-dimethylallene (**5**) for which the free energy is isoergonic (Table 3).

Evidently, the products obtained from these reactions are not straightforward photo-NOCAS products (Schemes 27 and 28). The mechanism proposed to account for the observed reactions is illustrated for the reaction between 1,4-dicyanonaphthalene (**3**) and tetramethylallene (**4**) in Scheme 36. The mechanism starts along a pathway similar to that of the photo-NOCAS reaction. The 1,4-dicyanonaphthalene radical anion,  $3^{\cdot-}$ , and the alkene radical cation,  $4^{\cdot+}$ , are photochemically generated, either directly or in separate stages involving biphenyl (**6**) as co-donor. (For the sake of brevity and clarity the steps involving **6** have been omitted from Scheme 36.) The allene radical cation is intercepted by methanol to generate a  $\beta$ -methoxyallyl radical that adds onto an *ipso*-position (site of highest spin density, Figure 11) of  $3^{\cdot-}$ .

At this point the mechanism diverges from the photo-NOCAS pathway. Whereas in the photo-NOCAS reaction the adduct anion rearomatizes via expulsion of cyanide anion, in the case of **3** the anion gets protonated to give an overall addition product, **22**. This switch from substitution to addition reactions on going from a mononuclear to a binuclear aromatic system is often observed in PET reactions.<sup>48,55</sup> Presumably, this is due to the lower rearomatization energy gain in a binuclear as opposed to a mononuclear system.

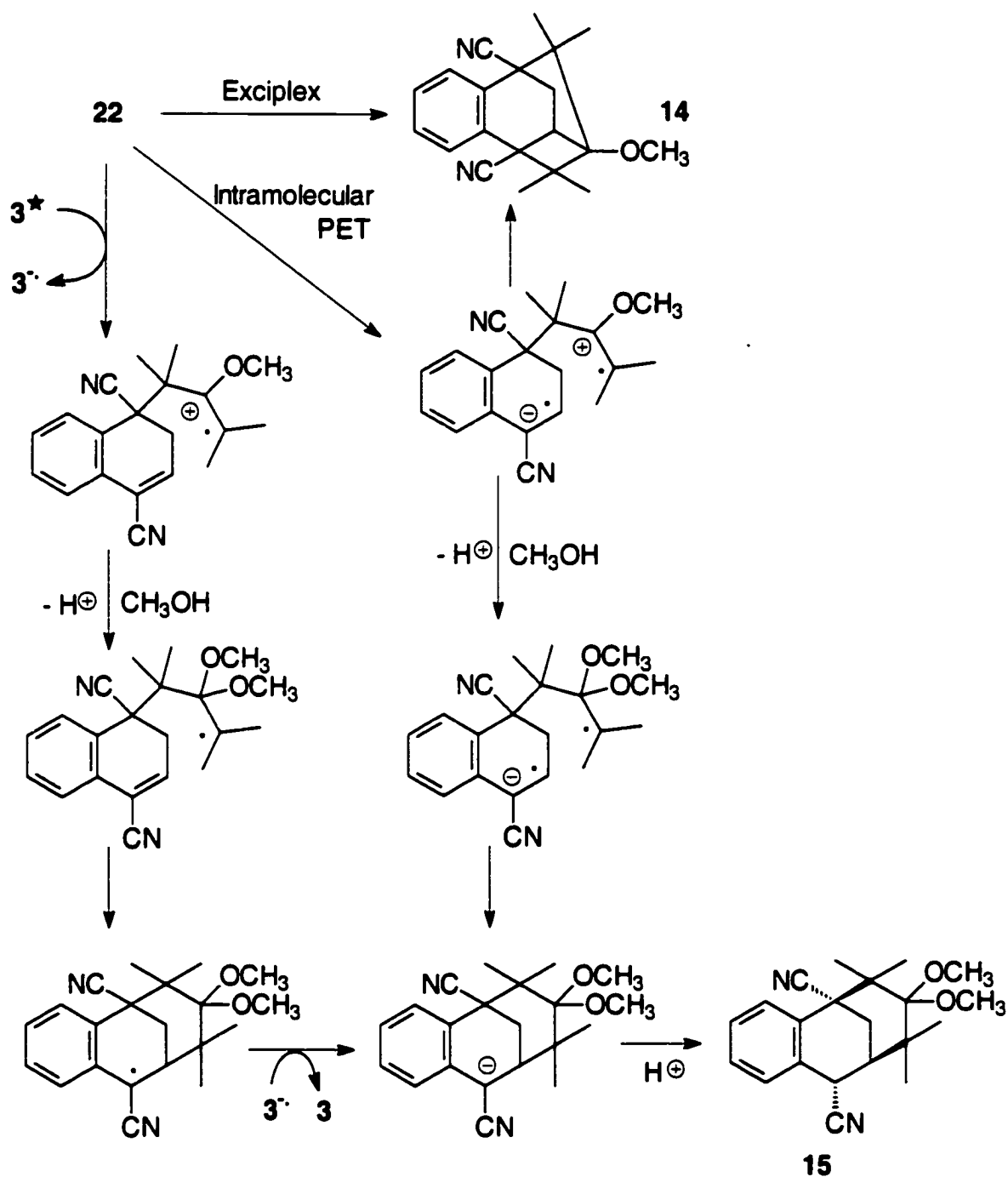
Despite an attentive search, compound **22** could not be detected in the photochemical mixture, even at low conversions. This is not very surprising when one considers that the molecule is perfectly set up to undergo further photochemical reaction. The electron rich vinyl ether (for comparison,  $E_{1/2}^{\text{ox}}$  for *Z*-2-methoxy-2-butene is ca. 1.7 V vs SCE)<sup>‡</sup> and the electron poor  $\alpha$ -cyanostyryl moiety ( $E_{1/2}^{\text{red}}$  for 2-phenylpropenenitrile is -2.20 V vs SCE)<sup>58</sup> are geometrically



- Scheme 36 -

<sup>‡</sup>  $E_{1/2}^{\text{ox}}$  was determined by means of an empirical correlation relating the peak oxidation potential ( $E^{\text{ox}}$ , solution) to the ionization potential ( $IP$ , gas phase):  $E^{\text{ox}} = (0.827 \times IP - 5.40)$  V vs Ag / Ag<sup>+</sup>;<sup>56</sup>  $E^{\text{ox}}$  was corrected to  $E_{1/2}^{\text{ox}}$  by subtracting 0.03 V,<sup>44</sup> referenced to SCE by adding 0.34 V.  $IP$  for *Z*-2-methoxy-2-butene is 8.25 eV.<sup>57</sup>





- Scheme 36 (cont) -

arranged in such a way as to allow an effective charge-transfer interaction. The tricyclo product **14** is formed via a [2π+2π] cycloaddition, either directly from the

exciplex or after intramolecular PET between the cyanostyryl and vinyl ether moieties.

Methanol trapping of the cationic vinyl ether competes with the cycloaddition reaction. Methanol adds exclusively at the  $\alpha$ -methoxy position that is expected to bear the higher positive charge density. The resulting acetal intermediate then cyclizes via a radical coupling reaction at the  $\beta$ -position of the cyanostyryl moiety to give an anionic adduct, which is subsequently protonated to yield the product **15**.

Alternatively, the radical cation of the vinyl ether moiety can be generated via an intermolecular PET with 1,4-dicyanonaphthalene (**3**), possibly aided by biphenyl (**6**). If this is the case, the radical generated upon trapping of the vinyl ether radical cation by methanol will add to the  $\alpha$ -cyanostyryl moiety to give an  $\alpha$ -cyanostyryl radical that should be readily reduced to the corresponding anion via electron transfer from **3**<sup>-</sup>. Protonation would furnish product **15**.

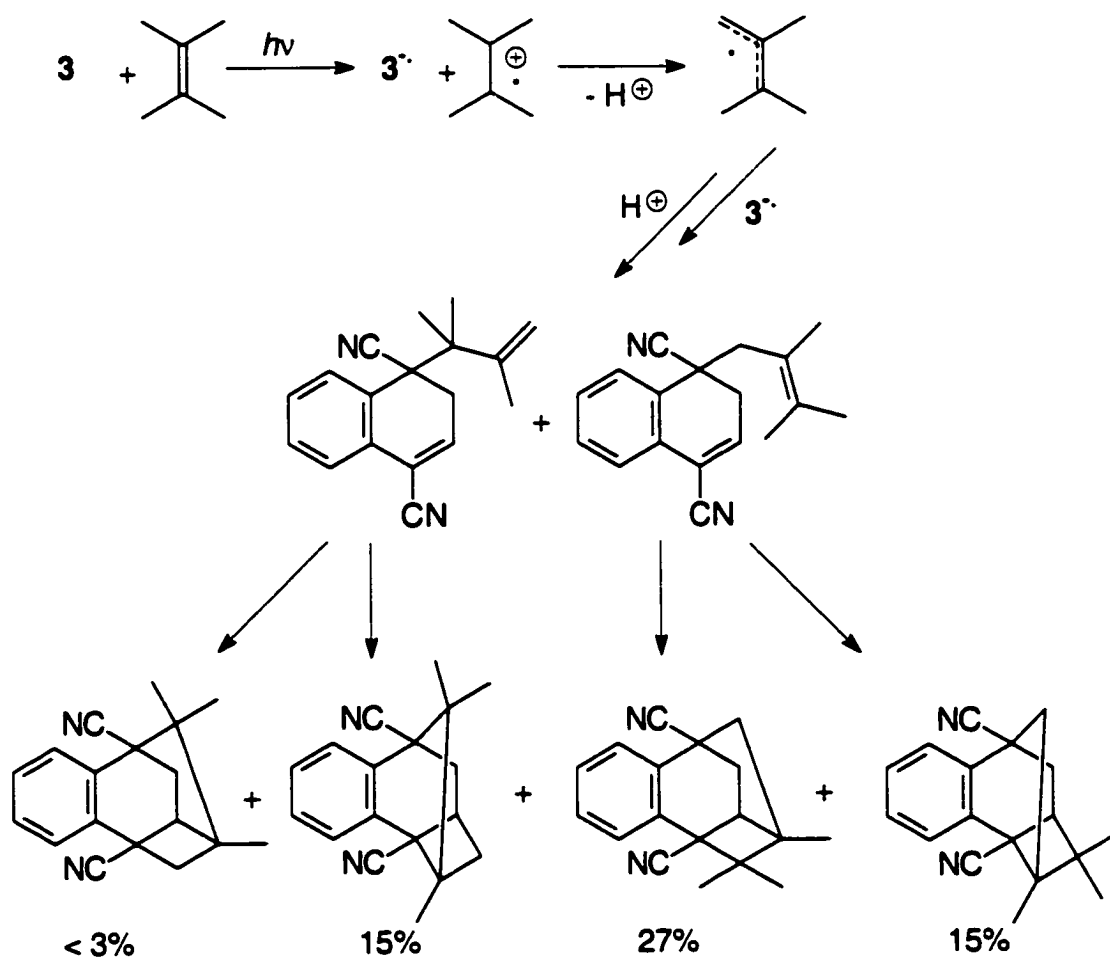
Compound **15** was not isolated in the reaction involving **4**, since it was hydrolyzed *in situ* to the corresponding ketone **16**. In the reaction involving **5**, however, the equivalent acetals **19** and **20** survived hydrolysis and were successfully isolated.

The *cis*-stereochemistry in both **16** and **19** came as a surprise since this implies that protonation occurred from what appears to be the more sterically crowded side. We were not able to detect the corresponding *trans* isomers.

Similarly to the reaction involving 1,4-dicyanobenzene (**2**), the reaction between **3** and **5** yields a predominance of products arising from reaction at the more substituted terminus of the  $\beta$ -methoxyallyl radical derived from **5**<sup>•+</sup> (**17**+**18**+**20**:**19** = 2.3). Although it is perhaps speculative to attach much significance to the absence of possible products, particularly in view of the non-quantitative yields obtained, the compounds isolated do represent the major products in the reaction.

Compounds similar to the tricyclo adducts **14**, **17**, and **18** have been observed in a previous study from our laboratory involving the photolysis of **3** and 2,3-dimethyl-2-butene in acetonitrile (Scheme 37).<sup>48</sup> Under these conditions, the

alkene radical cation generated upon PET deprotonates to give an allylic radical. From this stage onwards, the mechanistic pathway followed is very similar to the one leading to product 14 in Scheme 36. In this previous study, however, the product ratio implies that addition of the allylic radical to the *ipso*-position of the arene radical anion occurs predominantly from the less substituted end. This contrasts with our current results and lends support to the hypothesis that the regiochemical control in these reactions is very sensitive to the controlling factors and is, therefore, hard to predict reliably.



- Scheme 37 -

The effect of biphenyl (**6**) on the photochemical reaction between **3** and **5** merits some attention. As shown in Table 3, the free energy from the PET

process between **3** and **5** is isoergonic, so that electron transfer is disfavoured when no co-donor mediation is possible. The major product **21** is a  $[4\pi + 2\pi]$  photocycloadduct, formed via the addition of an allene double bond across the 5,8-position of the naphthalene ring. It is clearly a product arising directly from the exciplex and precludes the formation of separated radical ions, since a solvent-separated radical cation of **5** would invariably add methanol or alternatively undergo deprotonation prior to reaction with the arene radical anion. In fact, the formation of this cycloadduct is insensitive to solvent polarity and proceeds as efficiently in benzene as it does in methanol or acetonitrile. The fact that addition occurs across the 5,8-positions rather than across the 1,4-positions is surprising. Most of the spin and charge densities are expected to reside at the cyano-substituted ring-carbon atoms and an exciplex of substantial charge transfer character would involve the allene complexing preferentially with the cyano-substituted ring. However, exciplex formation is known to be very sensitive to steric interactions, and the unusual regiochemistry that is observed is most likely a consequence of the steric inhibitions exerted by the cyano substituents.

## 2.4 CONCLUSIONS

The photoinduced nucleophile–olefin combination, aromatic substitution (photo-NOCAS) reaction has been successfully extended to include the reactions between aliphatic allenes and cyanoarenes. Although the yields are only moderate, the reactions mentioned represent simple and straightforward one-pot synthetic methods for the products shown, which, to the best of our knowledge, are all new compounds.

More importantly, this study has provided us with further support for establishing an accurate mechanistic scheme for the photo-NOCAS reaction, which we have used in a lot of our previous work as a mechanistic framework for understanding the behaviour of photogenerated radical ions.<sup>12-18</sup> The strict

regiochemical control, involving the exclusive addition of the nucleophile to the central allenic carbon and the cyanoarene to the terminal one, supplements earlier studies from our laboratory with conjugated dienes.<sup>16</sup> It also firmly establishes the sequence of mechanistic events in the photo-NOCAS reaction, with nucleophilic trapping of the olefin radical cation occurring prior to addition to the cyanoarene radical anion.

The variations in the regiochemical selectivity observed in the reactions involving 1,1-dimethylallene (**5**) highlight the difficulty in predicting the preferred site of reactivity in non-symmetrical allylic radicals. The reaction outcome is most likely determined by a fine balance between two opposing factors: steric hindrance at the reaction site and spin density distribution in the allylic radical.

The reactions involving 1,4-dicyanonaphthalene (**3**) indicate that the photo-NOCAS reaction takes a different course with dinuclear cyanoaromatics. These reactions favour addition of the olefin-nucleophile adduct radical to the cyanoarene over substitution, most probably as a consequence of a lower rearomatization energy. In these cases, the primary photochemical products were too photoreactive to be detected. The isolated materials resulted from intramolecular  $[2\pi + 2\pi]$  cycloaddition and nucleophile addition–cyclization reactions of these elusive primary products.

## **2.5 EXPERIMENTAL**

### **2.5.1 General information**

Photochemical reactions were monitored and analyzed by gas chromatography–mass spectrometry (GC–MS) using an Hewlett-Packard 5890 gas chromatograph with an SPB-5 (Supelco) bonded 5% diphenyl / 95% dimethylsiloxane fused silica WCOT column (25 m x 0.20 mm, 0.33  $\mu\text{m}$  film thickness) and an Hewlett-Packard 5970 mass selective detector. Quantitative gas chromatographic analysis was performed on a Perkin-Elmer AutoSystem XL gas chromatograph equipped with an autosampler, flame ionization detector

(FID) and a MDN-5S (Supelco) bonded and crosslinked (5% phenyl) methylpolysiloxane fused silica WCOT column (30 m x 0.25 mm, 0.5  $\mu\text{m}$  film thickness).

Preparative separation of product mixtures was performed using flash chromatography on a 15 cm x 5 cm silica gel (Aldrich, 230–400 mesh, 60  $\text{\AA}$ ) column.<sup>59</sup> When necessary, this was followed by preparative, centrifugally accelerated, radial, thin layer chromatography of the partially purified mixtures using a Chromatotron (Harrison Research) on 4 mm, 2 mm or 1 mm silica gel (Aldrich, TLC grade 7749 with gypsum binder and fluorescent indicator) plates. The mobile phases were typically hexanes with increasing amounts of ethyl acetate. Collected fractions were analyzed by TLC using silica gel plates (Aldrich, 250  $\mu\text{m}$  plate thickness, 5–17  $\mu\text{m}$ , 60  $\text{\AA}$ , with fluorescent indicator) and/or GC–MS.

All  $^1\text{H}$  and  $^{13}\text{C}$  NMR spectra were acquired on a Bruker AC 250F spectrometer at 250.13 MHz for  $^1\text{H}$  and 62.90 MHz for  $^{13}\text{C}$ . Chemical shifts are reported in ppm relative to tetramethylsilane ( $\delta = 0$  ppm) in  $^1\text{H}$  NMR spectra and chloroform- $d$  ( $\delta = 77.0$  ppm) or acetonitrile- $d_3$  ( $\delta = 1.39$  ppm) in  $^{13}\text{C}$  NMR spectra. Coupling constants ( $J$  values) are reported in Hz. The multiplicities of the decoupled  $^{13}\text{C}$  NMR signals were determined by  $J$ -Modulated Spin-Echo ( $J$ -MOD) experiments. Infrared spectra were recorded as films on sodium chloride plates on a Nicolet 510P FT-IR spectrophotometer and are reported in wavenumbers ( $\text{cm}^{-1}$ ). Melting points were determined using a Cybron Corporation Thermolyne apparatus equipped with a digital thermocouple ( $\pm 0.1^\circ\text{C}$ ) and are corrected. Elemental analysis was carried out by Canadian Microanalytical Service Ltd., Delta, BC. High resolution mass spectrometry for exact mass determination was performed on a CEC 21-110 mass spectrometer using an electron impact energy of 70 eV.

## 2.5.2 X-ray crystallography<sup>§</sup>

Single crystal X-ray crystallographic structure determinations were performed at room temperature on a Rigaku AFC5R diffractometer equipped with a 12 kW rotating anode generator using graphite monochromated Cu K $\alpha$  (compounds **14**, **16**, and **19**) or Mo K $\alpha$  (**17**, **18**, **20**, and **21**) radiation. All data were corrected for Lorentz and polarization effects, while an empirical absorption correction ( $\psi$  scan; **14** and **17**) and/or a correction for secondary extinction (**14**, **18**, and **20**) were applied as necessary. All calculations were performed using the teXsan crystallographic software package,<sup>60</sup> except for the refinements of compounds **16** and **19** that were carried out using SHELXL-97.<sup>61</sup> Challenges with acquiring crystals of suitable size, shape and/or quality sometimes meant that not enough data could be collected for a full anisotropic refinement of the heavy atoms in a structure. In consequence, compounds **17** and **21** were refined totally isotropically; compounds **16**, **19**, and **20** were refined with some atoms anisotropic and other atoms isotropic, while compounds **14** and **18** were refined with all heavy atoms anisotropic. In all cases the reflection to parameter ratio was maintained at 5.0 or greater. Disorder was observed in only one structure (**20**) where one of the methoxy carbons was split over two positions, each with an occupancy of one half. In all structures, hydrogen atoms were placed in geometrically calculated positions and not refined.

## 2.5.3 Materials

1,4-Dicyanobenzene (98%, Aldrich) was purified by treatment with Norite in methylene chloride, followed by sublimation and recrystallization from 95% ethanol. 1,4-Dicyanonaphthalene was prepared and purified as indicated previously.<sup>62</sup> Biphenyl (99%, Aldrich) was recrystallized from methanol. 1,2,4,5-Tetracyanobenzene (Pfaltz and Bauer), tetramethylallene (97%, Aldrich), and

---

<sup>§</sup> Crystallographic data was deposited at the Cambridge Crystallographic Data Centre, Cambridge, UK. CCDC reference number 188/278. See <http://www.rsc.org/suppdata/p2/b0/b007205m/> for crystallographic files in .cif format.

1,1-dimethylallene (98%, Aldrich) were used as received. Acetonitrile was distilled twice, first from sodium hydride and then from phosphorus pentoxide. It was subsequently passed through a column of basic alumina, refluxed over calcium hydride for 24 h under a nitrogen atmosphere, fractionally distilled and stored over 3 Å molecular sieves (Aldrich). Methanol was purified by reflux and distillation over magnesium, and stored over 3 Å molecular sieves (Aldrich). Hexanes for preparative chromatography were distilled prior to use while ethyl acetate was used without further purification.

#### 2.5.4 Irradiations

Investigative irradiations were performed in 2 cm<sup>3</sup> sample volumes in 20 cm x 0.5 cm tubes using a 1 kW medium pressure mercury-arc lamp (CGE) fitted with a Quartz water-cooled jacket immersed in a bath at 5°C. Reactions used for quantitative analyses were performed in 10 cm<sup>3</sup> sample volumes in 20 cm x 1 cm tubes while large-scale preparative photochemical reactions were carried out in 60–160 cm<sup>3</sup> volumes in several 20 cm x 2 cm tubes. Tube distance from lamp axis was ca. 6 cm. All irradiations were carried out behind Pyrex ( $\lambda > 280$  nm).

Reaction details reported below are for the 10 cm<sup>3</sup> quantitative analysis samples. All yields were calibrated with respect to consumed cyanoarene. All quantitative-analysis GLC runs were done in triplicate and used an internal standard method for calibration. Pure samples of all products were isolated from large scale photoreactions (60–160 cm<sup>3</sup>) identical in composition to the reactions reported below.

#### 2.5.5 Irradiation of 1,2,4,5-tetracyanobenzene (1), tetramethylallene (4), and biphenyl (6) in 3:1 acetonitrile–methanol.

A solution of 1,2,4,5-tetracyanobenzene (1, 0.02 mol dm<sup>-3</sup>), tetramethylallene (4, 0.05 mol dm<sup>-3</sup>), and biphenyl (6, 0.05 mol dm<sup>-3</sup>) in 3:1 acetonitrile–methanol (10 cm<sup>3</sup>) was irradiated for 45 minutes. Calibrated GC–FID analysis indicated that 50% of 1 was consumed, yielding 48% of 4-(2,4,5-



tricyanophenyl)-3-methoxy-2,4-dimethyl-2-pentene (**7**). 94% of **6** was recovered after irradiation. In the absence of **6**, only 24% of **1** was consumed after 45 minutes, yielding 39% of **7**.

*4-(2,4,5-Tricyanophenyl)-3-methoxy-2,4-dimethyl-2-pentene (7).*

Colourless blocks, mp 166.9-167.6°C (from hexanes) (Found: C, 72.9; H, 5.8; N, 15.1. C<sub>17</sub>H<sub>17</sub>N<sub>3</sub>O requires C, 73.1; H, 6.1; N, 15.0%);  $\nu_{\max}$ (film; NaCl)/cm<sup>-1</sup> 3114 (m), 3042 (s), 2990 (s), 2970 (m), 2942 (s), 2916 (m), 2237 (s), 1492 (m), 1445 (m), 1371 (m), 1202 (m), 1193 (m), 1155 (m), 1131 (s), 1120 (s), 1077 (s), 936 (m) and 924 (s);  $\delta_{\text{H}}$ (250.13 MHz; CDCl<sub>3</sub>; Me<sub>4</sub>Si) 1.00 (3 H, s), 1.62 (6 H, s), 1.73 (3 H, s), 3.73 (3 H, s), 7.94 (1 H, s) and 8.03 (1 H, s);  $\delta_{\text{C}}$ (62.90 MHz; CDCl<sub>3</sub>) 18.8 (q), 19.4 (q), 28.2 (q), 45.2 (s), 61.4 (q), 113.6 (s), 113.8 (s), 114.41 (s), 114.42 (s), 117.0 (s), 119.1 (s), 119.2 (s), 130.4 (d), 139.0 (d), 153.5 (s) and 160.4 (s); *m/z* 279 (M<sup>+</sup>, 13%), 264 (100), 248 (86), 234 (81) and 194 (49).

**2.5.6 Irradiation of 1,2,4,5-tetracyanobenzene (1), 1,1-dimethylallene (5), and biphenyl (6) in 3:1 acetonitrile–methanol.**

A solution of 1,2,4,5-tetracyanobenzene (**1**, 0.02 mol dm<sup>-3</sup>), 1,1-dimethylallene (**5**, 0.05 mol dm<sup>-3</sup>), and biphenyl (**6**, 0.05 mol dm<sup>-3</sup>) in 3:1 acetonitrile–methanol (10 cm<sup>3</sup>) was irradiated for 45 minutes. Calibrated GC–FID analysis indicated that 61% of **1** was consumed, yielding 37% of 1-(2,4,5-tricyanophenyl)-2-methoxy-3-methyl-2-butene (**8**) and 5% of 3-(2,4,5-tricyanophenyl)-2-methoxy-3-methyl-1-butene (**9**). 98% of **6** was recovered after irradiation. In the absence of **6**, 23% of **1** was consumed after 45 minutes, yielding 7% of **8** and 1% of **9**.

*1-(2,4,5-Tricyanophenyl)-2-methoxy-3-methyl-2-butene (8).*

Pale yellow plates, mp 122.3-123.6°C (from hexanes);  $\nu_{\max}$ (film; NaCl)/cm<sup>-1</sup> 3111 (w), 3043 (m), 2993 (m), 2936 (s), 2831 (m), 2240 (s), 1682 (w), 1603 (m), 1489 (s), 1454 (m), 1386 (m), 1257 (m), 1196 (m), 1132 (s), 1016 (s) and 913 (m);  $\delta_{\text{H}}$ (250.13 MHz; CDCl<sub>3</sub>; Me<sub>4</sub>Si) 1.75 (3 H, s), 1.76 (3 H, s), 3.48 (3 H, s), 3.83

(2 H, s), 7.82 (1 H, s) and 8.02 (1 H, s);  $\delta_{\text{C}}$ (62.90 MHz;  $\text{CDCl}_3$ ) 17.2 (q), 19.1 (q), 32.2 (t), 57.6 (q), 113.7 (s), 114.2 (s), 114.5 (s), 114.7 (s), 117.8 (s), 119.3 (s), 121.1 (s), 134.9 (d), 136.7 (d), 144.0 (s) and 149.8 (s);  $m/z$  251 ( $\text{M}^+$ , 63%), 236 (76), 220 (100), 166 (86), 139 (61) and 85 (49) ( $\text{M}^+$ , 251.1061.  $\text{C}_{15}\text{H}_{13}\text{N}_3\text{O}$  requires  $M$ , 251.1058).

**3-(2,4,5-Tricyanophenyl)-2-methoxy-3-methyl-1-butene (9).**

Pale yellow plates, mp 129.6-130.8°C (from hexanes);  $\nu_{\text{max}}$ (film; NaCl)/ $\text{cm}^{-1}$  3108 (w), 3041 (m), 2971 (m), 2944 (w), 2239 (m), 1609 (s), 1452 (m), 1370 (m), 1295 (m), 1279 (m), 1196 (m), 1175 (m), 1166 (m), 1148 (m), 1049 (s), 928 (s) and 811 (m);  $\delta_{\text{H}}$ (250.13 MHz;  $\text{CDCl}_3$ ;  $\text{Me}_4\text{Si}$ ) 1.66 (6 H, s), 3.52 (3 H, s), 4.28 (1 H, d,  $J$  3.6), 4.32 (1 H, d,  $J$  3.6), 7.90 (1 H, s) and 8.01 (1 H, s);  $\delta_{\text{C}}$ (62.90 MHz;  $\text{CDCl}_3$ ) 27.5 (q), 45.4 (s), 55.4 (q), 83.5 (t), 113.6 (s), 114.3 (s), 114.5 (s), 115.3 (s), 116.9 (s), 119.1 (s), 132.8 (d), 138.9 (d), 156.8 (s) and 165.4 (s);  $m/z$  251 ( $\text{M}^+$ , 29%), 236 (100), 220 (30), 204 (75) and 57 (79) ( $\text{M}^+$ , 251.1076.  $\text{C}_{15}\text{H}_{13}\text{N}_3\text{O}$  requires  $M$ , 251.1058).

**2.5.7 Irradiation of 1,4-dicyanobenzene (2), tetramethylallene (4), and biphenyl (6) in 3:1 acetonitrile–methanol.**

A solution of 1,4-dicyanobenzene (**2**, 0.02 mol  $\text{dm}^{-3}$ ), tetramethylallene (**4**, 0.05 mol  $\text{dm}^{-3}$ ), and biphenyl (**6**, 0.05 mol  $\text{dm}^{-3}$ ) in 3:1 acetonitrile–methanol (10  $\text{cm}^3$ ) was irradiated for 45 minutes. Calibrated GC–FID analysis indicated that 46% of **2** was consumed, yielding 42% of 4-(4-cyanophenyl)-3-methoxy-2,4-dimethyl-2-pentene (**10**). 98% of **6** was recovered after irradiation. In the absence of **6**, only 10% of **2** was consumed after 45 minutes, yielding 7% of **10**.

**4-(4-Cyanophenyl)-3-methoxy-2,4-dimethyl-2-pentene (10).**

Colourless oil;  $\nu_{\text{max}}$ (film; NaCl)/ $\text{cm}^{-1}$  2974 (m), 2934 (m), 2838 (w), 2227 (s), 1605 (m), 1503 (m), 1465 (m), 1449 (m), 1198 (m), 1152 (m), 1127 (s), 1108 (s), 1072 (s), 1020 (m), 992 (m) and 838 (m);  $\delta_{\text{H}}$ (250.13 MHz;  $\text{CDCl}_3$ ;  $\text{Me}_4\text{Si}$ ) 1.01 (3 H, s), 1.48 (6 H, s), 1.68 (3 H, s), 3.66 (3 H, s) and 7.41-7.59 (4 H, m, AA'BB');  $\delta_{\text{C}}$ (62.90

MHz;  $\text{CDCl}_3$ ) 19.0 (q), 19.4 (q), 29.2 (q), 45.1 (s), 60.9 (q), 109.0 (s), 118.2 (s), 119.1 (s), 126.5 (d), 132.1 (d), 155.9 (q) and 156.7 (q);  $m/z$  229 ( $\text{M}^+$ , 67%), 214 (48), 197 (47), 182 (100), 116 (65) and 70 (48) ( $\text{M}^+$ , 229.1467.  $\text{C}_{15}\text{H}_{19}\text{NO}$  requires  $M$ , 229.1457).

### 2.5.8 Irradiation of 1,4-dicyanobenzene (2), 1,1-dimethylallene (5), and biphenyl (6) in 3:1 acetonitrile–methanol.

A solution of 1,4-dicyanobenzene (2, 0.02 mol  $\text{dm}^{-3}$ ), 1,1-dimethylallene (5, 0.05 mol  $\text{dm}^{-3}$ ), and biphenyl (6, 0.05 mol  $\text{dm}^{-3}$ ) in 3:1 acetonitrile–methanol (10  $\text{cm}^3$ ) was irradiated for 45 minutes. Calibrated GC–FID analysis indicated that 43% of 2 was consumed, yielding 36% of 3-(4-cyanophenyl)-2-methoxy-3-methyl-1-butene (11), 4% of 1-(4-cyanophenyl)-2-methoxy-3-methyl-2-butene (12) and 10% of 3-(4-cyanophenyl)-3-methyl-1-butyne (13). In the absence of 6, only 7% of 2 was consumed after 45 minutes, yielding 21% of 11, 8% of 12 and 8% of 13.

#### 3-(4-Cyanophenyl)-2-methoxy-3-methyl-1-butene (11).

Colourless oil;  $\nu_{\text{max}}$ (film; NaCl)/ $\text{cm}^{-1}$  2975 (s), 2926 (s), 2852 (m), 2228 (s), 1606 (s), 1505 (s), 1465 (m), 1175 (m), 1095 (m) and 840 (m);  $\delta_{\text{H}}$ (250.13 MHz;  $\text{CDCl}_3$ ;  $\text{Me}_4\text{Si}$ ) 1.46 (6 H, s), 3.47 (3 H, s), 4.09 (1 H, d,  $J$  2.8), 4.21 (1 H, d,  $J$  2.8) and 7.40–7.59 (4 H, m, AA'BB');  $\delta_{\text{C}}$ (62.90 MHz;  $\text{CDCl}_3$ ) 27.7 (q), 44.2 (s), 55.1 (q), 80.6 (t), 109.6 (s), 119.1 (s), 126.8 (d), 131.9 (d), 153.6 (s) and 168.9 (s);  $m/z$  201 ( $\text{M}^+$ , 29%), 186 (56), 169 (83), 154 (100) and 116 (87) ( $\text{M}^+$ , 201.1159.  $\text{C}_{12}\text{H}_{11}\text{N}$  requires  $M$ , 201.1154).

#### 1-(4-cyanophenyl)-2-methoxy-3-methyl-2-butene (12).

$m/z$  201 ( $\text{M}^+$ , 66%), 186 (26), 154 (55) and 116 (100).

#### 3-(4-Cyanophenyl)-3-methyl-1-butyne (13).

Colourless oil;  $\nu_{\text{max}}$ (film; NaCl)/ $\text{cm}^{-1}$  3297 (m), 2979 (s), 2933 (m), 2229 (s), 1607 (m), 1504 (m), 1457 (w), 1403 (w), 1364 (w), 1244 (w), 1096 (m), 1019 (w) and

839 (s);  $\delta_{\text{H}}$ (250.13 MHz;  $\text{CDCl}_3$ ;  $\text{Me}_4\text{Si}$ ) 1.61 (6 H, s), 2.40 (1 H, s) and 7.60-7.70 (4 H, m, AA'BB');  $\delta_{\text{C}}$ (62.90 MHz;  $\text{CDCl}_3$ ) 31.2 (q), 36.2 (s), 70.9 (d), 89.4 (s), 110.5 (s), 118.9 (s), 126.4 (d), 132.2 (d) and 151.7 (s);  $m/z$  169 ( $\text{M}^{+\cdot}$ , 5%), 154 (100) and 127 (38) ( $\text{M}^{+\cdot}$ , 169.0898.  $\text{C}_{12}\text{H}_{11}\text{N}$  requires  $M$ , 169.0891).

### 2.5.9 Irradiation of 1,4-dicyanonaphthalene (3), tetramethylallene (4), and biphenyl (6) in 3:1 acetonitrile–methanol.

A solution of 1,4-dicyanonaphthalene (**3**, 0.02 mol  $\text{dm}^{-3}$ ), tetramethylallene (**4**, 0.05 mol  $\text{dm}^{-3}$ ), and biphenyl (**6**, 0.05 mol  $\text{dm}^{-3}$ ) in 3:1 acetonitrile–methanol (10  $\text{cm}^3$ ) was irradiated for 45 minutes. Calibrated GC–FID analysis indicated that 75% of **3** was consumed, yielding 54% of 1,5-dicyano-3-methoxy-2,2,4,4-tetramethyl-6,7-benzotricyclo[3.2.2.0<sup>3,8</sup>]nonane (**14**) and 24% of *cis*-1,4-dicyano-6,6,8,8-tetramethyl-7-oxo-2,3-benzo-*cis*-bicyclo[3.3.1]nonane (**16**). 100% of **6** was recovered after irradiation. In the absence of **6**, only 10% of **3** was consumed after 45 minutes, yielding 11% of **14** and 5% of **16**.

#### *1,5-Dicyano-3-methoxy-2,2,4,4-tetramethyl-6,7-benzotricyclo[3.2.2.0<sup>3,8</sup>]nonane (14).*

Colourless plates, mp > 163°C (decomp.) (from hexanes);  $\nu_{\text{max}}$ (film; NaCl)/ $\text{cm}^{-1}$  2991 (s), 2957 (s), 2837 (w), 2236 (m), 1489 (s), 1449 (s), 1392 (m), 1378 (m), 1264 (m), 1153 (s), 1145 (s), 1121 (m), 1095 (m), 1072 (s), 1050 (m), 1018 (m) and 758 (s);  $\delta_{\text{H}}$ (250.13 MHz;  $\text{CDCl}_3$ ;  $\text{Me}_4\text{Si}$ ) 0.62 (3 H, s), 1.08 (3 H, s), 1.49 (3 H, s), 1.69 (3 H, s), 1.88 (1 H, d,  $J$  12.8), 2.71 (1 H, dd,  $J$  12.8, 4.6), 3.40 (3 H, s), 3.45 (1 H, d,  $J$  4.6) and 7.75-8.55 (4 H, m);  $\delta_{\text{C}}$ (62.90 MHz;  $\text{CDCl}_3$ ) 22.0 (q), 23.5 (q), 26.0 (q), 27.0 (q), 34.7 (t), 42.3 (s), 47.3 (d), 54.79 (s), 54.82 (s), 55.1 (q), 57.0 (s), 89.1 (s), 119.6 (s), 119.8 (s), 127.3 (d), 128.1 (d), 128.7 (d), 129.1 (d), 130.4 (s) and 135.7 (s);  $m/z$  306 ( $\text{M}^{+\cdot}$ , 0.6%), 259 (12), 238 (41), 127 (89), 95 (86) and 69 (100).

Crystal Data:  $\text{C}_{20}\text{H}_{22}\text{N}_2\text{O}$ ,  $M = 306.41$ , monoclinic,  $a = 9.927(1)$ ,  $b = 11.116(1)$ ,  $c = 15.3609(7)$  Å,  $\beta = 103.868(5)^\circ$ ,  $V = 1645.6(2)$  Å<sup>3</sup>,  $T = 296$  K, space group  $\text{P}2_1/n$  (no. 14),  $Z = 4$ ,  $\mu$  (Cu-K $\alpha$ ) = 6  $\text{cm}^{-1}$ , 3010 reflections measured, 2831 unique ( $R_{\text{int}}$

= 0.031). The final  $R$  and  $R_w$  were 0.041 and 0.039 respectively and are based on 1432 observed reflections ( $I > 3.00\sigma(I)$ ) and 209 parameters.

*cis*-1,4-Dicyano-6,6,8,8-tetramethyl-7-oxo-2,3-benzo-*cis*-bicyclo[3.3.1]nonane (16).

Colourless needles, mp 252.9-253.8°C (from methanol);  $\nu_{\max}$ (film; NaCl)/ $\text{cm}^{-1}$  2970 (m), 2964 (m), 2904 (m), 2239 (m), 1701 (vs), 1491 (m), 1477 (m), 1464 (m), 1447 (m), 1390 (m), 1371 (m), 1043 (m) and 767 (s);  $\delta_{\text{H}}$ (250.13 MHz;  $\text{CDCl}_3$ ;  $\text{Me}_4\text{Si}$ ) 1.05 (3 H, s), 1.14 (3 H, s), 1.46 (3 H, s), 1.62 (3 H, s), 2.61 (1 H, br s), 2.82 (1 H, dd,  $J$  14.5, 2.4), 3.26 (1 H, ddd,  $J$  14.5, 4.0, 1.5), 4.19 (1 H, br s) and 7.26-7.60 (4 H, m);  $\delta_{\text{C}}$ (62.90 MHz;  $\text{CDCl}_3$ ) 23.6 (q), 24.5 (q), 26.5 (q), 26.9 (t), 30.2 (q), 33.1 (d), 43.7 (d), 46.5 (s), 46.7 (s), 51.4 (s), 120.2 (s), 120.6 (s), 125.9 (s), 128.6 (d), 130.2 (d), 130.3 (d), 131.4 (d), 131.7 (s) and 213.5 (s);  $m/z$  292 ( $\text{M}^+$ , 2%), 113 (100) and 95 (25).

Crystal Data:  $\text{C}_{19}\text{H}_{20}\text{N}_2\text{O}$ ,  $M = 292.38$ , monoclinic,  $a = 6.227(1)$ ,  $b = 16.056(1)$ ,  $c = 15.917(1)$  Å,  $\beta = 92.21(1)^\circ$ ,  $V = 1590.3(3)$  Å<sup>3</sup>,  $T = 296$  K, space group Cc (no. 9),  $Z = 4$ ,  $\mu$  (Cu-K $\alpha$ ) = 6  $\text{cm}^{-1}$ , 1482 reflections measured, 1421 unique ( $R_{\text{int}} = 0.029$ ). The final  $R1$  and  $wR2$  were 0.049 and 0.168 respectively and are based on 808 observed reflections ( $I > 3.00\sigma(I)$ ) and 139 parameters.

### 2.5.10 Irradiation of 1,4-dicyanonaphthalene (3), 1,1-dimethylallene (5), and biphenyl (6) in 3:1 acetonitrile–methanol.

A solution of 1,4-dicyanonaphthalene (3, 0.02 mol  $\text{dm}^{-3}$ ), 1,1-dimethylallene (5, 0.05 mol  $\text{dm}^{-3}$ ), and biphenyl (6, 0.05 mol  $\text{dm}^{-3}$ ) in 3:1 acetonitrile–methanol (10  $\text{cm}^3$ ) was irradiated for 45 minutes. Calibrated GC–FID analysis indicated that 95% of 3 was consumed, yielding 8% of 1,5-dicyano-3-methoxy-2,2-dimethyl-6,7-benzotricyclo[3.2.2.0<sup>3,8</sup>]nonane (17), 18% of 2,5-dicyano-1-methoxy-9,9-dimethyl-3,4-benzotricyclo[3.3.1.0<sup>2,7</sup>]nonane (18), 22% of *cis*-1,4-dicyano-7,7-dimethoxy-6,6-dimethyl-2,3-benzo-*cis*-bicyclo[3.3.1]nonane (19), and 20% of *trans*-1,4-dicyano-7,7-dimethoxy-8,8-dimethyl-2,3-benzo-*cis*-bicyclo[3.3.1]nonane (20). 94% of 6 was recovered after irradiation.

**1,5-Dicyano-3-methoxy-4,4-dimethyl-6,7-benzotricyclo[3.2.2.0<sup>3,8</sup>]nonane (17).**

Colourless plates, mp 126.4-127.2°C (from hexanes-ethyl acetate);  $\nu_{\max}$ (film; NaCl)/cm<sup>-1</sup> 2981 (s), 2943 (s), 2832 (w), 2238 (m), 1489 (m), 1452 (s), 1278 (m), 1155 (s), 1115 (s), 1106 (m), 1088 (m) and 1073 (s);  $\delta_{\text{H}}$ (250.13 MHz; CDCl<sub>3</sub>; Me<sub>4</sub>Si) 0.83 (3 H, s), 1.43 (3 H, s), 1.82 (1 H, d, *J* 12.8), 2.23 (1 H, d, *J* 12.2), 2.71 (1 H, dd, *J* 12.8, 4.5), 3.12 (1 H, d, *J* 12.2), 3.27 (3 H, s), 3.51 (1 H, d, *J* 4.5) and 7.38-7.70 (4 H, m);  $\delta_{\text{C}}$ (62.90 MHz; CD<sub>3</sub>CN) 22.3 (q), 23.7 (q), 31.2 (s), 35.6 (t), 42.1 (t), 50.5 (d), 52.7 (q), 52.9 (s), 55.9 (s), 84.8 (s), 120.8 (s), 122.3 (s), 127.5 (d), 127.6 (d), 129.0 (d), 130.6 (d), 133.1 (s) and 136.7 (s); *m/z* 278 (M<sup>+</sup>, 2%), 152 (9), 99 (93) and 67 (100) (M<sup>+</sup>, 278.1416). C<sub>18</sub>H<sub>18</sub>N<sub>2</sub>O requires *M*, 278.1419).

Crystal Data: C<sub>72</sub>H<sub>72</sub>N<sub>8</sub>O<sub>4</sub> [ 4 (C<sub>18</sub>H<sub>18</sub>N<sub>2</sub>O) ], *M* = 1113.41, orthorhombic, *a* = 14.294(5), *b* = 16.505(6), *c* = 25.334(5) Å, *V* = 5977(3) Å<sup>3</sup>, *T* = 296 K, space group Pca2<sub>1</sub> (no. 29), *Z* = 4,  $\mu$  (Mo-K $\alpha$ ) = 0.78 cm<sup>-1</sup>, 6310 reflections measured. The final *R* and *R<sub>w</sub>* were 0.082 and 0.080 respectively and are based on 1679 observed reflections (*I* > 3.00 $\sigma$ (*I*)) and 336 parameters.

**2,5-Dicyano-1-methoxy-9,9-dimethyl-3,4-benzotricyclo[3.3.1.0<sup>2,7</sup>]nonane (18).**

Colourless blocks, mp 148.7-149.8°C (from hexanes);  $\nu_{\max}$ (film; NaCl)/cm<sup>-1</sup> 2976 (s), 2940 (m), 2838 (w), 2240 (m), 1486 (s), 1455 (s), 1392 (w), 1373 (w), 1276 (m), 1236 (s), 1220 (s), 1208 (m), 1151 (s), 1131 (s), 1072 (m), 1057 (s), 1026 (m) and 760 (s);  $\delta_{\text{H}}$ (250.13 MHz; CDCl<sub>3</sub>; Me<sub>4</sub>Si) 0.43 (3 H, s), 1.43 (3 H, s), 1.71 (1 H, ddd, *J* 12.8, 7.2, 1.2), 2.20 (1 H, d, *J* 10.7), 2.50 (1 H, d, *J* 12.8), 2.62 (1 H, t, *J* 7.2), 2.99 (1 H, ddd, *J* 10.7, 7.2, 1.2), 3.54 (3 H, s) and 7.27-7.65 (4 H, m);  $\delta_{\text{C}}$ (62.90 MHz; CDCl<sub>3</sub>) 21.2 (q), 21.3 (q), 32.2 (d), 34.1 (t), 34.2 (t), 42.3 (s), 48.3 (s), 49.6 (s), 54.5 (q), 84.6 (s), 118.4 (s), 119.6 (s), 123.1 (d), 125.2 (d), 128.2 (s), 128.4 (d), 128.7 (d) and 136.7 (s); *m/z* 278 (M<sup>+</sup>, 4%), 237 (11), 178 (22), 99 (80) and 67 (100).

Crystal Data: C<sub>18</sub>H<sub>18</sub>N<sub>2</sub>O, *M* = 278.35, orthorhombic, *a* = 12.214(2), *b* = 13.305(3), *c* = 9.083(2) Å, *V* = 1476.0(4) Å<sup>3</sup>, *T* = 296 K, space group P2<sub>1</sub>2<sub>1</sub>2<sub>1</sub> (no. 19), *Z* = 4,  $\mu$  (Mo-K $\alpha$ ) = 0.8 cm<sup>-1</sup>, 2481 reflections measured. The final *R* and *R<sub>w</sub>*

were 0.040 and 0.043 respectively and are based on 1071 observed reflections ( $I > 3.00\sigma(I)$ ) and 191 parameters.

*cis-1,4-Dicyano-7,7-dimethoxy-6,6-dimethyl-2,3-benzo-cis-bicyclo[3.3.1]nonane (19).*

Colourless blocks, mp 167.5-168.4°C (from methanol);  $\nu_{\max}(\text{film; NaCl})/\text{cm}^{-1}$  2990 (m), 2967 (m), 2951 (m), 2835 (m), 2237 (m), 1466 (m), 1448 (m), 1137 (s), 1125 (s), 1112 (s), 1054 (s), 1038 (m), 1030 (m), 979 (m) and 910 (m);  $\delta_{\text{H}}(250.13 \text{ MHz; CDCl}_3; \text{Me}_4\text{Si})$  1.23 (3 H, s), 1.29 (3 H, s), 2.13 (3 H, s), 2.18-2.31 (3 H, m), 2.37 (1 H, dt,  $J$  13.4, 5.2), 2.62 (1 H, ddd,  $J$  13.4, 3.7, 0.9), 3.14 (3 H, s), 4.30 (1 H, s) and 7.27-7.32 (4 H, m);  $\delta_{\text{C}}(62.90 \text{ MHz; CDCl}_3)$  23.6 (q), 25.0 (q), 29.5 (t), 31.4 (d), 37.0 (s), 37.2 (t), 42.5 (s), 46.6 (d), 47.4 (q), 50.1 (q), 100.1 (s), 122.0 (s), 122.4 (s), 127.0 (d), 127.9 (d), 128.7 (d), 129.0 (d), 130.8 (s) and 133.9 (s);  $m/z$  310 ( $\text{M}^+$ , 8%), 279 (18), 267 (15), 180 (33), 99 (77), 88 (100) and 67 (31).

Crystal Data:  $\text{C}_{19}\text{H}_{22}\text{N}_2\text{O}_2$ ,  $M = 310.39$ , monoclinic,  $a = 13.917(1)$ ,  $b = 8.5864(6)$ ,  $c = 14.304(1) \text{ \AA}$ ,  $\beta = 105.596(7)^\circ$ ,  $V = 1646.3(2) \text{ \AA}^3$ ,  $T = 296 \text{ K}$ , space group  $\text{P}2_1/\text{n}$  (no. 14),  $Z = 4$ ,  $\mu (\text{Cu-K}\alpha) = 6.5 \text{ cm}^{-1}$ , 1165 reflections measured, 989 unique ( $R_{\text{int}} = 0.024$ ). The final  $R1$  and  $wR2$  were 0.058 and 0.184 respectively and are based on 860 observed reflections ( $I > 3.00\sigma(I)$ ) and 113 parameters.

*trans-1,4-Dicyano-7,7-dimethoxy-8,8-dimethyl-2,3-benzo-cis-bicyclo[3.3.1]nonane (20).*

Colourless blocks, mp 122.9-124.6°C (from hexanes);  $\nu_{\max}(\text{film; NaCl})/\text{cm}^{-1}$  2990 (m), 2949 (m), 2834 (m), 2239 (m), 1492 (m), 1449 (m), 1171 (m), 1129 (s), 1122 (s), 1096 (m), 1073 (m), 1053 (s), 1044 (s) and 972 (m);  $\delta_{\text{H}}(250.13 \text{ MHz; CDCl}_3; \text{Me}_4\text{Si})$  1.23 (3 H, s), 1.42 (3 H, s), 1.99 (1 H, dd,  $J$  15.0, 4.9), 2.14 (1 H, ddd,  $J$  14.7, 4.0, 1.8), 2.46 (1 H, dt,  $J$  14.7, 2.0), 2.70 (3 H, s), 2.71-2.77 (2 H, m), 3.21 (3 H, s), 4.37 (1 H, d,  $J$  6.1) and 7.25-7.65 (4 H, m);  $\delta_{\text{C}}(62.90 \text{ MHz; CDCl}_3)$  20.3 (q), 24.1 (q), 29.3 (d), 31.3 (t), 32.2 (t), 37.1 (d), 47.15 (s), 47.17 (s), 49.9 (q),

50.0 (q), 100.7 (s), 120.2 (s), 122.3 (s), 126.3 (d), 127.0 (d), 128.6 (d), 129.5 (d), 131.1 (s) and 133.5 (s);  $m/z$  310 ( $M^{+}$ , 33%), 279 (100), 267 (94) and 88 (56).  
 Crystal Data:  $C_{38}H_{44}N_4O_4$  [ 2 ( $C_{19}H_{22}N_2O_2$ ) ],  $M = 620.78$ , monoclinic,  $a = 16.452(3)$ ,  $b = 9.016(2)$ ,  $c = 23.003(2)$  Å,  $\beta = 95.35(1)^\circ$ ,  $V = 3397.3(9)$  Å<sup>3</sup>,  $T = 296$  K, space group  $P2_1/a$  (no. 14),  $Z = 4$ ,  $\mu$  (Mo-K $\alpha$ ) = 0.8 cm<sup>-1</sup>, 2987 reflections measured, 2685 unique ( $R_{int} = 0.063$ ). The final  $R$  and  $R_w$  were 0.059 and 0.055 respectively and are based on 1622 observed reflections ( $I > 3.00\sigma(I)$ ) and 300 parameters.

### 2.5.11 Irradiation of 1,4-dicyanonaphthalene (3) and 1,1-dimethylallene (5) in 3:1 acetonitrile–methanol.

A solution of 1,4-dicyanonaphthalene (**3**, 0.02 mol dm<sup>-3</sup>) and 1,1-dimethylallene (**5**, 0.05 mol dm<sup>-3</sup>) in 3:1 acetonitrile–methanol (10 cm<sup>3</sup>) was irradiated for 45 minutes. Calibrated GC–FID analysis indicated that 85% of **3** was consumed, yielding 8% of 1,5-dicyano-3-methoxy-2,2-dimethyl-6,7-benzotricyclo[3.2.2.0<sup>3,8</sup>]nonane (**17**), 22% of 2,5-dicyano-1-methoxy-9,9-dimethyl-3,4-benzotricyclo[3.3.1.0<sup>2,7</sup>]nonane (**18**) and 26% of 7-isopropylidene-5,6-(2',5'-dicyanobenzo)bicyclo[2.2.2]oct-2-ene (**21**).

#### *7-Isopropylidene-5,6-(2',5'-dicyanobenzo)bicyclo[2.2.2]oct-2-ene (21).*

Colourless blocks, mp 178.1–178.9°C (from hexanes);  $\nu_{max}$ (film; NaCl)/cm<sup>-1</sup> 3081 (w), 3066 (w), 2978 (m), 2915 (s), 2855 (m), 2233 (s), 1474 (m), 1436 (m), 1400 (s), 1374 (m), 1335 (s), 1251 (m), 1175 (m), 1158 (m), 1123 (m) and 826 (s);  $\delta_H$ (250.13 MHz; CDCl<sub>3</sub>; Me<sub>4</sub>Si) 1.55 (3 H, s), 1.91 (3 H, s), 2.04 (1 H, d,  $J$  15.3), 2.30 (1 H, d,  $J$  15.3), 4.54 (1 H, m), 5.24 (1 H, dd,  $J$  5.5, 1.8), 6.61 (2 H, m) and 7.44 (2 H, s);  $\delta_C$ (62.90 MHz; CDCl<sub>3</sub>) 20.2 (q), 21.7 (q), 32.1 (t), 39.9 (d), 43.5 (d), 110.3 (s), 110.8 (s), 116.29 (s), 116.32 (s), 125.4 (s), 126.0 (s), 128.3 (d), 128.5 (d), 133.4 (d), 134.6 (d), 148.5 (s) and 149.2 (s);  $m/z$  246 ( $M^{+}$ , 82%), 231 (100), 178 (22) and 68 (72).

Crystal Data:  $C_{17}H_{14}N_2$ ,  $M = 246.31$ , orthorhombic,  $a = 13.37(1)$ ,  $b = 25.49(1)$ ,  $c = 7.920(7)$  Å,  $V = 2698(3)$  Å<sup>3</sup>,  $T = 296$  K, space group  $Pbca$  (no. 61),  $Z = 8$ ,  $\mu$



(Mo-K $\alpha$ ) = 0.7 cm<sup>-1</sup>, 2657 reflections measured. The final R and R<sub>w</sub> were 0.083 and 0.087 respectively and are based on 460 observed reflections ( $I > 3.00\sigma(I)$ ) and 77 parameters.

#### **2.5.12 Irradiation of 1,4-dicyanonaphthalene (3) and 1,1-dimethylallene (5) in acetonitrile.**

A solution of 1,4-dicyanonaphthalene (**3**, 0.02 mol dm<sup>-3</sup>) and 1,1-dimethylallene (**5**, 0.05 mol dm<sup>-3</sup> in acetonitrile (10 cm<sup>3</sup>) was irradiated for 45 minutes.

Calibrated GC–FID analysis indicated that 84% of **3** was consumed, yielding 38% of 7-isopropylidene-5,6-(2',5'-dicyanobenzo)bicyclo[2.2.2]oct-2-ene (**21**).

#### **2.5.13 Irradiation of 1,4-dicyanonaphthalene (3) and 1,1-dimethylallene (5) in benzene.**

A solution of 1,4-dicyanonaphthalene (**3**, 0.02 mol dm<sup>-3</sup>) and 1,1-dimethylallene (**5**, 0.05 mol dm<sup>-3</sup> in benzene (10 cm<sup>3</sup>) was irradiated for 45 minutes. Calibrated GC–FID analysis indicated that 88% of **3** was consumed, yielding 42% of 7-isopropylidene-5,6-(2',5'-dicyanobenzo)bicyclo[2.2.2]oct-2-ene (**21**).

# *Diverting the Photo-NOCAS Reaction*<sup>63</sup>

---

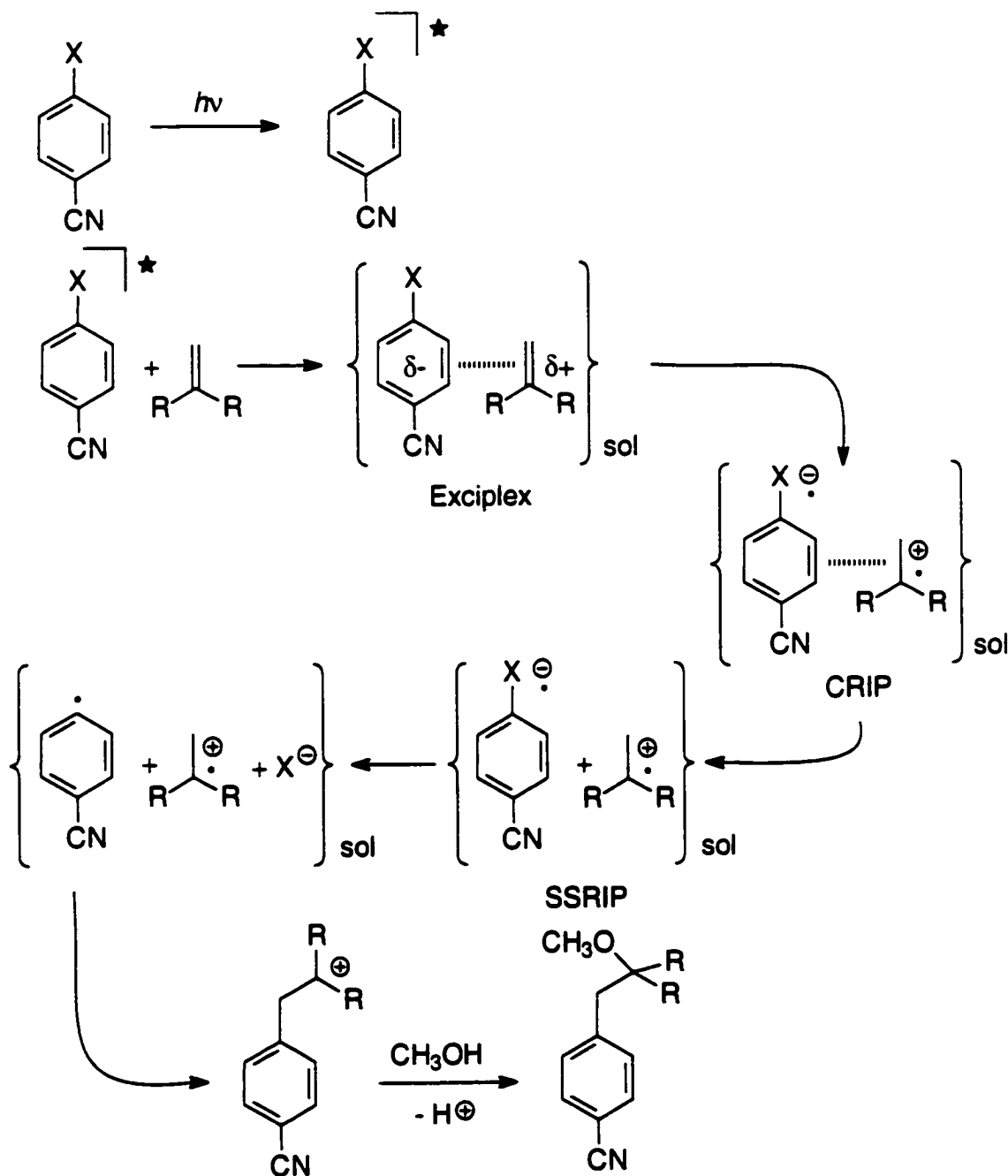
## **3.1 INTRODUCTION**

To date, investigations into the photochemical behaviour between olefinic electron donors, aromatic electron acceptors, and nucleophiles have mainly been centred on variations of the olefin and nucleophile. The electron acceptors used in these studies are invariably cyanoaromatics, commonly including 1,4-dicyanobenzene (**2**), 1,4-dicyanonaphthalene (**3**), 9,10-dicyanoanthracene, 2,6,9,10-tetracyanoanthracene, and a few others. However, not much is known on the effect of switching to different electron acceptors.

The reasons for selecting the above cyanoarenes are multifold. The cyano function is strongly electron withdrawing, imparting low reduction potentials to these compounds and thus making them good electron acceptors for the PET process. Unlike most other electron withdrawing groups (such as carbonyl, ester, and nitro functions), the cyano group has no significant excited state of its own and, therefore, it does not exhibit its own photochemistry. Furthermore, the cyanoaromatic radical anions resulting from the PET process are relatively stable and long-lived (as is evidenced by their fully reversible cyclic voltammograms) making them particularly suitable as photosensitizers. Finally, when incorporated in the product (*e.g.*, the photo-NOCAS reaction) the cyano group is a versatile function that can be readily converted into various other useful substituents.

With our current state of understanding of this class of PET reactions, we should be able to modify our photochemical system in a predictable fashion. In view of this, the aim of this study is to investigate the effect of different electron

acceptors on the outcome of the photochemical reaction. In particular, we are interested in altering the sequence of events in the mechanism by using an electron acceptor that possesses an unstable and readily cleavable radical anion. The intended mechanism is illustrated in Scheme 38, using 2-methylpropene and a benzonitrile with a cleavable group (X) as model compounds.



- Scheme 38 -

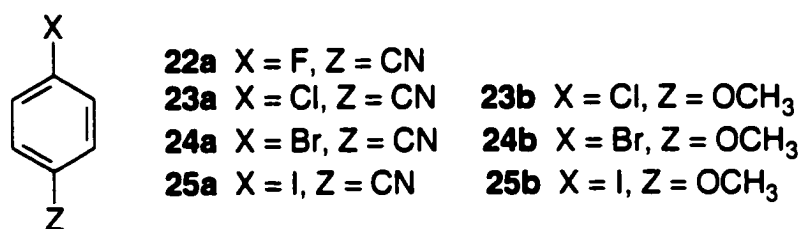
Upon excitation of one of the components, electron transfer occurs to generate the radical cation of the olefin and the radical anion of the electron acceptor. Once formed, the radical anion will cleave rapidly, probably while still in the neighbourhood of the olefin radical cation (such as in the CRIP) to give a 4-cyanophenyl radical. This very reactive intermediate will attack the alkene radical cation at the less sterically hindered end to give the more stable adduct radical. The resulting adduct is subsequently trapped by a nucleophile such as methanol to yield the final product. The regiochemistry in the proposed mechanism is reversed as compared to the photo-NOCAS reaction (Section 1.3) as a consequence of the different sequence of mechanistic events. Whereas the photo-NOCAS pathway involves the combination of the nucleophile and olefin prior to the involvement of the cyanoarene, this proposed mechanistic scheme predicts an initial combination of the olefin and the cyanoarene followed by incorporation of the nucleophile at a later stage.

### 3.1.1 Formation and fragmentation of haloarene radical anions

The compounds that have been selected for this investigation are a series of 4-halobenzonitriles, ranging from 4-fluorobenzonitrile (**22a**) to 4-iodobenzonitrile (**25a**) (Figure 12). A series of haloanisoles (**23b–25b**), which are not expected to function as electron acceptors in the PET process, were also investigated under similar conditions to provide additional insight into the mechanism. There is considerable evidence in the literature that halobenzonitrile radical anions are unstable due to fragmentation of the aryl carbon–halogen bond giving the halide anion and the corresponding aryl radical. The only possible exceptions are the fluoroarenes that possess radical anions that are thought to be stable towards fragmentation as a consequence of the high bond energy of the aryl carbon–fluorine bond.<sup>64</sup> However, this is still a contested topic.

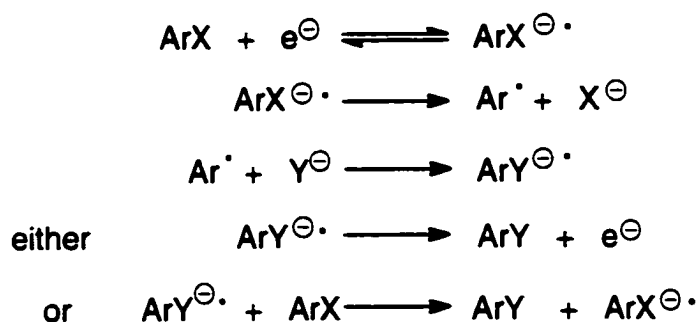
Primary evidence for the easy fragmentation of these radical anions stems from the observation that cyclic voltammetric analysis of these species gives a totally irreversible reduction wave. This indicates that the radical anion, once formed, undergoes further reaction and is not present for re-oxidation back to its

neutral form in the reverse scan. A more detailed study on the fate of halobenzonitrile radical anions under electrochemical reductive conditions has been reported in the literature.<sup>65</sup> Under these conditions, the 4-cyanophenyl radical was further reduced to the corresponding anion, which was subsequently protonated to give benzonitrile. The resulting voltammogram consisted of an irreversible wave representing the formation of the halobenzonitrile radical anion superimposed on the reversible oxidative wave of benzonitrile.



- Figure 12 -

The electrochemical formation of haloarene radical anions and their subsequent fragmentation has received considerable attention by Savéant and colleagues and has been the focus of a series of extensive studies since the early 1970s.<sup>66</sup> These researchers have been probing the mechanism in great detail, often using the unimolecular nucleophilic substitution (via a radical intermediate) reaction, S<sub>RN</sub>1, as a working model (Scheme 39).



- Scheme 39 -

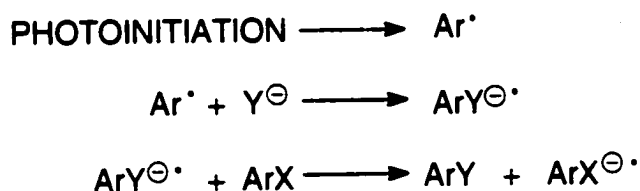
One of the aspects they have been particularly concerned with is whether the fragmentation process involves a state of concerted dissociative electron transfer or whether distinct radical anions, no matter how short lived, are formed prior to cleavage. Kinetic studies have indicated that, in the case of haloarenes, the reductive cleavage of the carbon–halogen bond involves the intermediacy of the radical anion.<sup>66j</sup> In contrast, aliphatic halides undergo a concerted dissociative electron transfer.

A number of theoretical studies using semi-empirical MNDO and AM1 theories have been conducted to model the dissociation process of haloarene radical anions.<sup>67-69</sup> The major issue these studies attempt to address is how the carbon–halogen bond, which is orthogonal to the  $\pi$ -system, cleaves when the more stable radical anion is generally of  $\pi$  nature, in accordance with the orbital symmetry of the lowest unoccupied molecular orbitals (LUMOs) of the parent neutral molecule.<sup>†</sup> Cleavage of the concerned bond necessitates the promotion of an electron to a  $\sigma$ -antibonding ( $\sigma^*$ ) orbital. It has been proposed that the halogen atom might be the reaction centre to which the electron is transferred in the first place, implying direct formation of a  $\sigma$ -radical anion.<sup>68</sup> Nevertheless, the favoured theory involves the initial formation of a  $\pi$ -radical anion that then undergoes an intramolecular electron transfer to give a  $\sigma$ -radical anion.<sup>66j,66k,69</sup> This involves stretching of the carbon–halogen bond in order to produce the electron transfer that takes place at the crossing point of the energy surfaces of the  $\pi$ - and  $\sigma$ -radical anions. The energy of the  $\pi^*$  orbital does not vary significantly when the carbon–halogen bond distance increases, whereas the energy of the  $\sigma^*$  orbital falls rapidly with distance.<sup>66j</sup> This transition is forbidden but it can occur with relative ease due to vibronic coupling. This intramolecular ET process is the rate determining step and the subsequent bond breaking is rapidly completed.

---

<sup>†</sup> In the case of iodobenzene and 2-iodopyridine, the  $\sigma$ -radical anion has been found to be the more stable species even though their LUMOs are of  $\pi$ -symmetry.<sup>69</sup>

Photochemical generation of haloarene radical anions is not as common as electrochemical generation but has received some attention, mainly with respect to the  $S_{RN}1$  mechanism (Scheme 40).<sup>70-72</sup> Nucleophiles commonly employed are anionic species such as enolates, diethylphosphite, phosphides, and cyanomethyl anion. The reaction has been performed both intermolecularly and intramolecularly.<sup>72</sup>



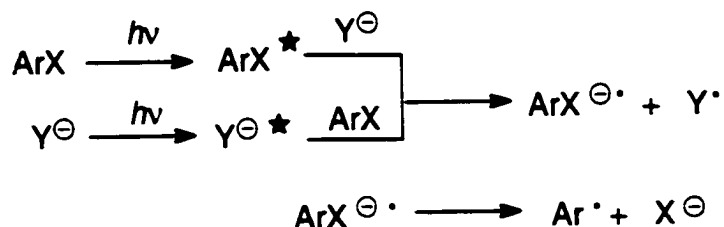
- Scheme 40 -

The mechanism of the photoinitiation step has been proposed to occur via three possible pathways:

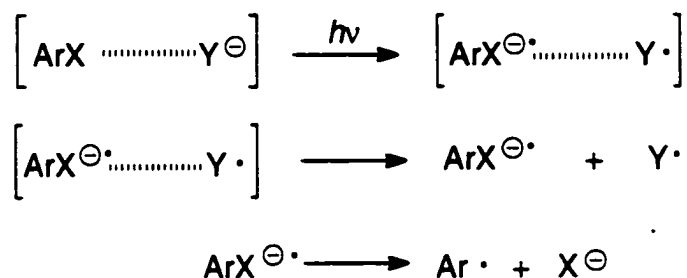
- (a) Direct homolytic cleavage of the aryl-halogen bond, producing an aryl radical.



- (b) Electron transfer from the anion to the excited state haloarene (or from the excited anion to the ground state haloarene, depending upon the relative absorption characteristics), generating a radical anion that subsequently cleaves to give an aryl radical.



- (c) Electron exchange within an excited charge-transfer complex, giving a haloarene radical anion that cleaves to give an aryl radical.



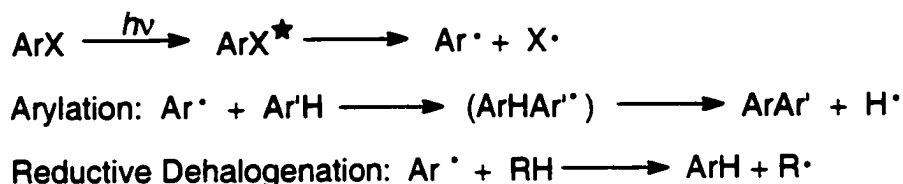
Although pathways (a) and (b) have not been discounted, the most favoured photoinitiation mode is the one involving the excited charge-transfer complex pathway (c).<sup>71</sup> This stems mainly from the straightforward observation that mixing the two moieties generally gives rise to an intensely coloured charge-transfer band, and selective irradiation of this band initiates the S<sub>RN</sub>1 reaction. Studies on the exact nature of the photoinitiation mechanism are scant, however.

### 3.1.2 Homolytic fragmentation of haloarenes

On the other hand, the direct photolysis of haloarenes has been extensively studied during the past 40 years.<sup>73-77</sup> This has often been stimulated by environmental concerns with the goal of understanding whether photolysis is an important sink for these compounds in natural waters or in the atmosphere. Many persistent pollutants are halogenated aromatic compounds and include well known toxins such as 1,1-bis(4-chlorophenyl)-2,2,2-trichloroethane (DDT), polychlorinated biphenyls (PCBs) and chlorinated dibenzo-*p*-dioxins.

Direct photolysis of haloarenes leads to the homolytic cleavage of the aryl carbon-halogen bonds, giving rise to aryl free radicals. These reactive species can either arylate a suitable aromatic reaction partner<sup>75,76</sup> or abstract hydrogen from a hydrogen atom donor<sup>77</sup> (Scheme 41). The latter process is termed reductive dehalogenation.





**- Scheme 41 -**

Lemal's initial proposition that the involvement of a  $\pi$ -haloarene intermediate in which the aryl radical is  $\pi$ -complexed with the halide atom after fragmentation,<sup>78</sup> was subsequently disproved by Arnold and co-workers.<sup>79</sup>

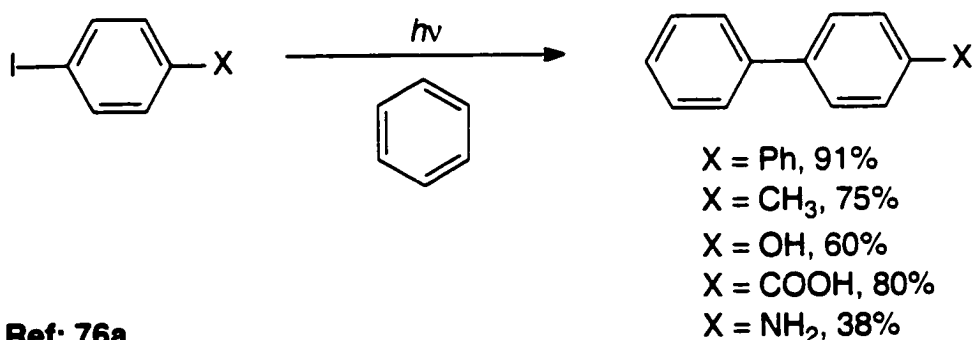
Homolysis of photoexcited iodoarenes and bromoarenes has been given considerable attention from a synthetic aspect, and has been exploited as an effective means of producing aryl radicals. Many studies have used it successfully for the synthesis of biaryls (Scheme 42a).<sup>75</sup> Another synthetic strong point of this reaction has been the use of an intramolecular arylation in the construction of polycyclic systems (Scheme 42b).<sup>76</sup> Furthermore, reductive dehalogenation has been suggested as a synthetic route to specifically deuterated aromatic compounds, by photolysis of aryl halides in solvents containing abstractable deuterium atoms.

The identification of the reactive excited state as the first excited triplet state,  $T_1$ , is unequivocal for chlorinated, brominated, and iodinated benzenes. Their quantum yields of intersystem crossing  $S_1 \Rightarrow T_1$  ( $\Phi_{ISC}$ ) are high, as are their quantum yields of dehalogenation ( $\Phi_R$ ) in hydrogen-donating solvents (*i.e.*,  $\Phi_{ISC} + \Phi_R > 1$ ).

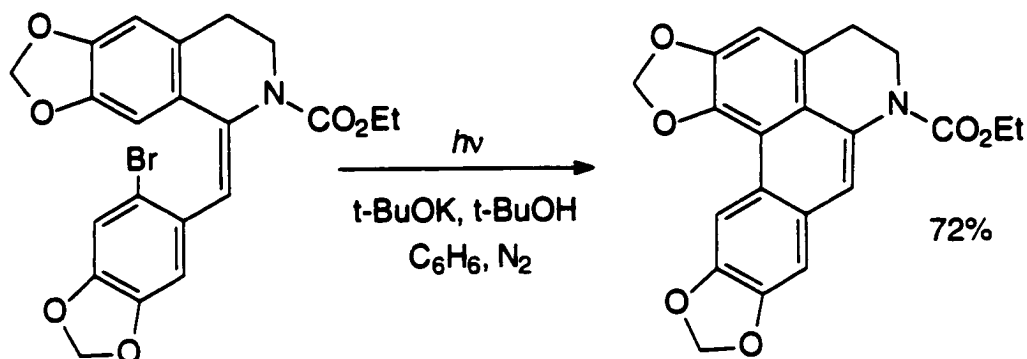
The energetics of homolysis are straightforward. Homolysis requires that the energy of the reactive excited state ( $T_1$ ) be greater than the carbon-halogen bond dissociation energy. As can be seen from the data in Tables 4a and 4b, the homolysis is exothermic for triplet iodo- and bromobenzenes, and probably also for chlorobenzenes, although the correct value of the aryl-chlorine bond dissociation energy has been subject to much controversy.<sup>74</sup> Homolysis is thermodynamically unfavourable, and generally not observed, for fluoroarenes, in

either singlet or triplet state reactions. In accordance with the data in Table 4, the haloarenes 9,10-dibromoanthracene and 1-chloropyrene are unaffected by lengthy photolysis in alkane solvents. The situation is less clear cut for substances such as 4-chlorobiphenyl and 1-chloronaphthalene. These compounds do photolyze, albeit slowly, despite unfavourable energetics. However, they probably dechlorinate mainly through the intermediacy of excimers.

**Ref: 75d**



**Ref: 76a**



**- Scheme 42 -**

Among chlorinated biphenyls, the triplet energy depends upon whether or not the molecule is *ortho*-substituted. *Ortho*-substitution raises the energy of the excited state due to partial deconjugation of the biphenyl chromophore. This, coupled with the relief of steric strain resulting from the loss of an *ortho*-chlorine,

results in biphenyls with *ortho*-chlorines having markedly larger quantum yields of homolysis than those without.

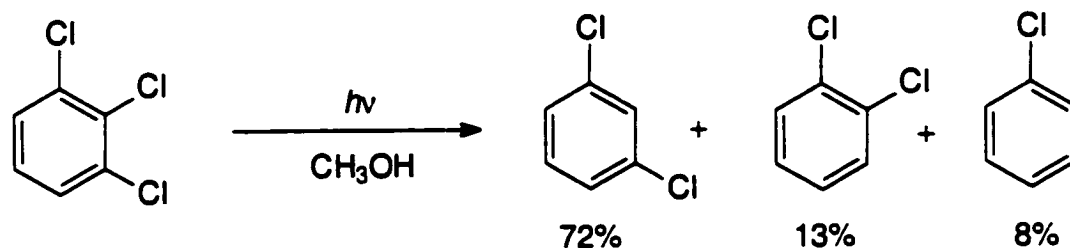
**Table 4a** Triplet energies of arene systems

Arene System	Triplet Energy (kJ mol <sup>-1</sup> )
Benzene	360
Naphthalene	255
Biphenyl (no <i>o</i> -X)	275
Biphenyl (one <i>o</i> -X)	>285
Anthracene	180
Pyrene	200

**Table 4b** Bond dissociation of C<sub>6</sub>H<sub>5</sub>-X<sup>84</sup>

X	Bond Dissociation Energy (kJ mol <sup>-1</sup> )
F	523
Cl	398
Br	313
I	268

The regiospecificity of the homolysis favours relief of steric strain.<sup>75i,77b,77c</sup>  
 For example, photolysis of 1,2,3-trichlorobenzene and 1,2,3,4-tetrachlorobenzene in hydrogen-donating media leads predominantly to the expulsion of the chlorine atom having more *ortho*-substituents (Scheme 43).<sup>77b,77c</sup>



- Scheme 43 -

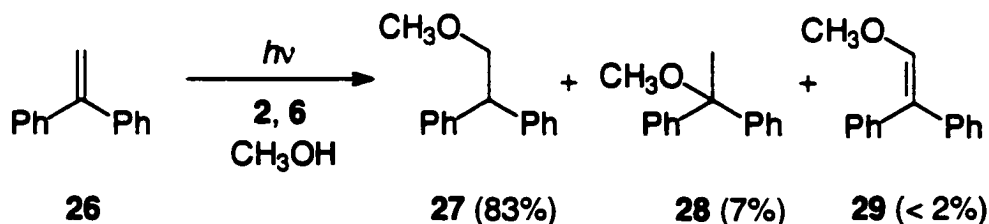
The preceding review should hopefully demonstrate the variety of photochemical reactions undergone by haloarenes. However, to our knowledge,

not much is known about the photochemistry between haloarenes and alkenes. Thus, the proposed study will fill an uninvestigated niche in the photochemistry of this class of compounds, hopefully providing both mechanistic information as well as delivering synthetic potential. It will also act as a proving ground in which to apply and test our knowledge of the behaviour of photogenerated radical ions and other reactive intermediates acquired so far in related areas of research.

### 3.2 RESULTS

The olefin 1,1-diphenylethene (**26**) was selected as the electron donor for this study. This compound is an effective electron donor, having a half-wave oxidation potential,  $E_{1/2}^{ox}$ , of 1.88 V vs SCE ( $\text{CH}_3\text{CN}$ ).<sup>80</sup> It is commonly employed in photochemical reactions so that its behaviour is relatively well understood.

As a preliminary investigation, the documented PET methanol addition to 1,1-diphenylethene (**26**) was attempted.<sup>21a</sup> This experiment constituted a useful reference for checking the performance of our systems. Whereas in the literature methyl 4-cyanobenzoate was used as sensitizer, we opted for the more popular 1,4-dicyanobenzene (**2**) in our study and the experiment produced results in close accordance with the reported one (Reaction 1, Table 5). In addition, the reaction was modified further by introducing biphenyl (**6**) as a co-donor. This led to a major enhancement in efficiency and selectivity, increasing the yield of the main product, 1-methoxy-2,2-diphenylethane (**27**), from a moderate 38% to a successful 83% (Reaction 2, Table 5; Scheme 44).



- Scheme 44 -

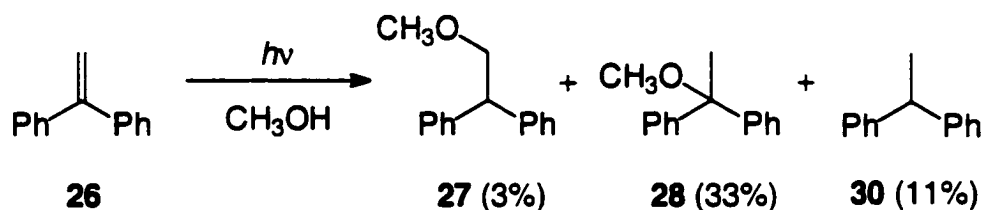
**Table 5** Photochemical reactions between the cyanoarenes (**2**, **22a–25a**) and the alkenes (**26**, **29**, **33a**). Reaction conditions: 1 kW medium pressure Hg lamp, Pyrex filter, 5°C, methanol.

Reaction Number	Acceptor (% cons.)	Donor (% cons.)	Irradiation Time (h)	Products (% yield)
1	<b>2</b> (2)	<b>26</b> (45)	6	<b>27</b> (38), <b>28</b> (7), <b>29</b> (5)
2 <sup>a</sup>	<b>2</b> (8)	<b>26</b> (100)	6	<b>27</b> (83), <b>28</b> (7), <b>29</b> (<2)
3	-	<b>26</b> (81)	300	<b>27</b> (3), <b>28</b> (33), <b>30</b> (11)
4	<b>22a</b> (0)	-	50	-
5	<b>22a</b> (0)	<b>26</b> (67)	75	<b>27</b> (21), <b>28</b> (10), <b>30</b> (2)
6	<b>23a</b> (0)	-	50	-
7	<b>23a</b> (46)	<b>26</b> (78)	75	<b>27</b> (26), <b>28</b> (2), <b>29</b> (7), <b>30</b> (<2), <b>31</b> (6), <b>32</b> (2), <b>33a</b> (3), <b>34a</b> (12), <b>35a</b> (17)
8	<b>24a</b> (100)	-	50	<b>36a</b> (71)
9	<b>24a</b> (54)	<b>26</b> (90)	75	<b>27</b> (17), <b>28</b> (2), <b>29</b> (4), <b>30</b> (<2), <b>31</b> (5), <b>32</b> (<2), <b>33a</b> (5), <b>34a</b> (8), <b>35a</b> (11), <b>36a</b> (8), <b>37a</b> (4)
10	<b>25a</b> (89)	-	50	<b>36a</b> (85)
11	<b>25a</b> (100)	<b>26</b> (88)	75	<b>27</b> (12), <b>28</b> (2), <b>29</b> (11), <b>30</b> (<2), <b>31</b> (19), <b>32</b> (<2) <b>33a</b> (38), <b>34a</b> (5), <b>35a</b> (5), <b>36a</b> (23), <b>37a</b> (21)
12	-	<b>29</b> (86)	300	<b>31</b> (40), <b>32</b> (23)
13	<b>2</b> (0)	<b>29</b> (46)	10	<b>31</b> (67), <b>32</b> (2)
14 <sup>a</sup>	<b>2</b> (0)	<b>29</b> (92)	10	<b>31</b> (85), <b>32</b> (2)
15	-	<b>33a</b> (0)	6	-
16	<b>24a</b> (0)	<b>33a</b> (0)	6	-
17	<b>25a</b> (72)	<b>33a</b> (98)	6	<b>36a</b> (80), <b>37a</b> (98)

<sup>a</sup> contains biphenyl (**6**) as co-donor.

Single ion monitoring mass spectrometry (SIM-MS) of the molecular ion of **27** revealed 96% deuterium incorporation at the bisbenzylic position (C-2) when the reaction was carried out in methanol-*O*-d. This result was corroborated by a SIM-MS measurement on the 1,1-diphenylmethyl fragment.

As a further preliminary study aimed at defining the photochemistry of 1,1-diphenylethene (**26**), the alkene was irradiated in the absence of an electron acceptor in methanol. Despite a sluggish reaction and considerable polymerization, the reaction yielded a reasonable amount of the isomeric ether, 1-methoxy-1,1-diphenylethane (**28**), together with minor amounts of 1-methoxy-2,2-diphenylethane (**27**) and 1,1-diphenylethane (**30**) (Reaction 3, Table 5; Scheme 45). These results agree with a similar study reported in the literature.<sup>81</sup> Addition of benzonitrile (**35a**) to the reaction mixture prior to irradiation did not alter the reaction outcome.

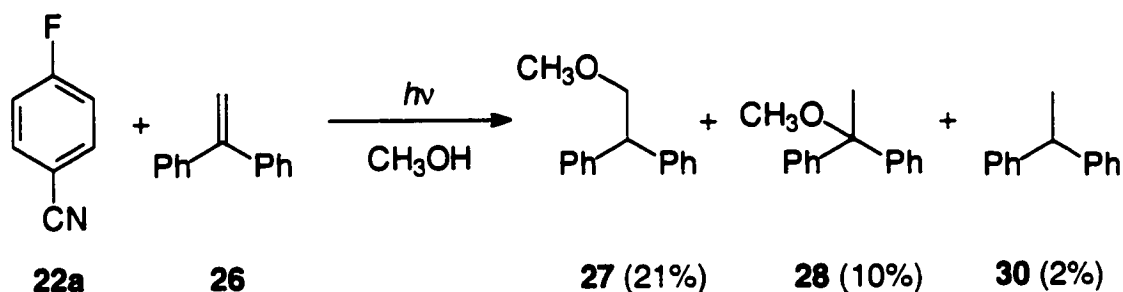


- **Scheme 45** -

### 3.2.1 4-Fluorobenzonitrile (**22a**) photochemistry

Investigations into the influence of the haloarenes were commenced using 4-fluorobenzonitrile (**22a**) as substrate. Prolonged irradiation in methanol, in the presence of the alkene **26** as well as in its absence, did not result in any consumption of the halobenzonitrile (Reactions 4 and 5, Table 5). This may be partly due to the weak absorption of the fluoroarene **22a** ( $\lambda_{\text{max}} = 272 \text{ nm}$ ,  $\epsilon = 160 \text{ dm}^3 \text{ mol}^{-1} \text{ cm}^{-1}$ ,  $\text{CH}_3\text{CN}$ ) beyond the Pyrex cut-off wavelength of 280 nm. This deficiency is accentuated when in competition with 1,1-diphenylethene (**26**) ( $\lambda_{\text{max}} = 248 \text{ nm}$ ,  $\epsilon = 11\,000 \text{ dm}^3 \text{ mol}^{-1} \text{ cm}^{-1}$ ,  $\text{CH}_3\text{CN}$ ). The only products observed in

substantial amounts were the methoxy ether isomers, **27** and **28**, resulting from the addition of methanol to the alkene (Scheme 46). No evidence of fragmentation of the fluorobenzonitrile **22a** was observed, even after irradiation for prolonged periods behind Quartz ( $\lambda > 190$  nm). When an identical reaction was performed in methanol-*O*-d, SIM-MS measurements on **27** indicated only 47% deuterium incorporation at the bisbenzylic position.



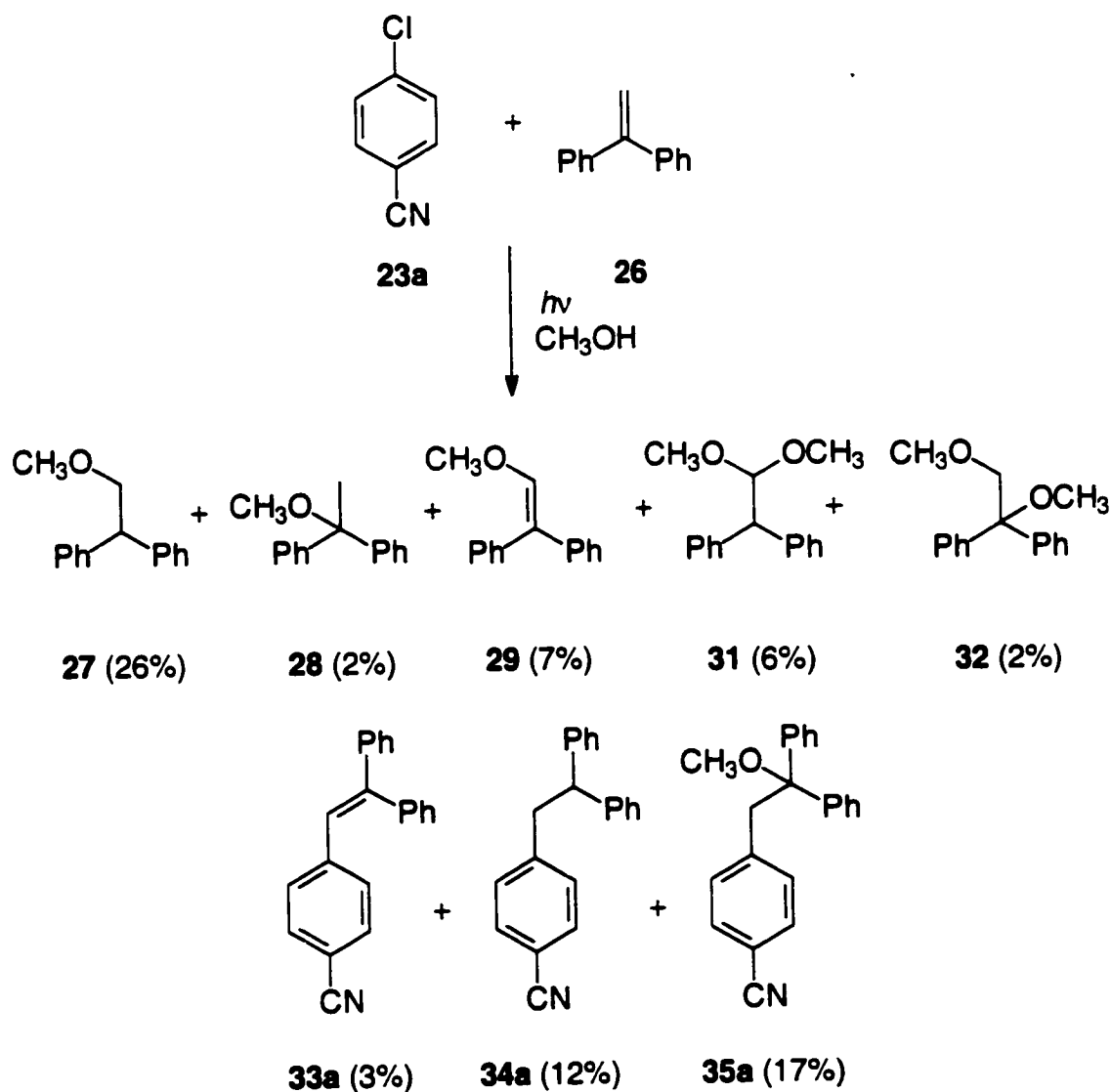
- Scheme 46 -

### 3.2.2 4-Chlorobenzonitrile (**23a**) photochemistry

4-Chlorobenzonitrile (**23a**) shows increased electronic absorption relative to its lower homologue, possessing a maximum wavelength peak at 282 nm with a molar absorptivity  $\epsilon$  of  $300 \text{ dm}^3 \text{ mol}^{-1} \text{ cm}^{-1}$ . Despite appreciable absorption beyond the Pyrex cut-off wavelength, particularly at the high concentrations employed in our studies, irradiation of **23a** in methanol in the absence of alkene **26** did not lead to any significant reaction, and GC analysis indicated 100% recovery of the starting material after prolonged photolysis (Reaction 6, Table 5). Irradiation in the presence of **26**, however, led to a notable amount of products, some of which incorporated the 4-cyanophenyl group (Reaction 7, Table 5; Scheme 47).

Characterization of all the products relied on a combination of spectroscopic ( $^{13}\text{C}$  NMR,  $^1\text{H}$  NMR and IR) and spectrometric (GC-MS) techniques. Further confirmation was obtained by comparison with reported data

from the literature for all known compounds. However, since this was rather scarce or outdated in most cases, full characterization data is reported for every product. Two of these products, notably 1-(4-cyanophenyl)-2,2-diphenylethane (**34a**) and 1-(4-cyanophenyl)-2-methoxy-2,2-diphenylethane (**35a**) are new compounds.



- Scheme 47 -

In the case of **34a**, high-resolution mass spectrometry (HRMS) confirmed the molecular formula as  $\text{C}_{21}\text{H}_{17}\text{N}$ . The routine mass spectrum was dominated



by a base peak at  $m/z = 167$ , representing the highly stabilized diphenylmethyl fragment. No molecular ion was observed due to this easy fragmentation process. The majority of structural information was obtained from  $^{13}\text{C}$  NMR spectroscopy. The fully decoupled  $^{13}\text{C}$  NMR spectrum distinguished every chemically non-equivalent carbon atom and, in conjunction with a  $J$ -MOD experiment, revealed the presence of four quaternary carbons and five sets of methine carbons at low field. The four quaternary carbons were identified as the three aromatic *ipso* carbons and the cyano carbon. Two of the methine carbon signals are roughly twice as intense as the others, identifying them as the *ortho* and *meta* carbons of the unsubstituted phenyl rings (each signal representing four chemical shift equivalent carbon atoms). The other three aromatic methine carbon signals represent the *para* carbons on the unsubstituted phenyl rings (one signal) and the *ortho* and *meta* carbons on the benzonitrile ring (two signals). The bisbenzylic and benzylic carbons resonate at relatively low field and are observed at 51.5 and 42.2 ppm respectively.

The assignment was in accordance with the information obtained from the  $^1\text{H}$  NMR spectrum, the integration of which suggested the presence of 3 aliphatic and 14 aromatic protons. The triplet at 4.19 ppm, integrating for one proton, was assigned to the bisbenzylic proton. It is coupled, with a vicinal coupling constant  $^3J$  of 7.8 Hz (typical of a freely rotating  $\text{sp}^3\text{-sp}^3$  carbon bond) to a doublet at 3.41 ppm, integrating for two protons. This latter signal was assigned to the benzylic protons. The relatively low field of these aliphatic proton signals is due to the deshielding effect of the neighbouring aromatic ring currents. The aromatic region in the  $^1\text{H}$  NMR spectrum exhibits the characteristic AA'BB' spin system of two pseudodoublets representing the aromatic protons of the 1,4-disubstituted ring, clearly distinguishable from the broad multiplet (7.16-7.25 ppm) due to the other ten protons of the unsubstituted phenyl rings.

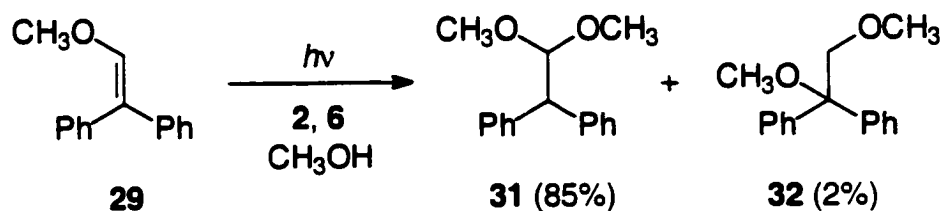
A similar method of analysis was used to identify 1-(4-cyanophenyl)-2-methoxy-2,2-diphenylethane (**35a**). Elemental analysis confirmed the molecular formula of this white crystalline material as  $\text{C}_{22}\text{H}_{19}\text{NO}$ . Routine mass spectrometry revealed the presence of a dominating base peak at  $m/z = 197$ ,

representing the highly stabilized 1-methoxy-1,1-diphenylmethyl fragment. Elimination of methanol to give the corresponding alkene radical cation resulted in another diagnostic, albeit weak, signal at  $m/z = 281$ .

The  $^{13}\text{C}$  NMR spectrum of **35a** was, as expected, quite similar to that of **34a**. The major difference, apart from the methoxy carbon signal at 51.0 ppm, was the shift of the bisbenzylic carbon to lower field (83.4 ppm) as a consequence of the added deshielding effect of the methoxy group. The  $^1\text{H}$  NMR spectrum supported the assignment, with a distinguishable AA'BB' pattern representing the 4-cyanophenyl group and a broad multiplet due to the other phenyl rings. The aliphatic region consisted of a singlet at 3.15 ppm representing the three methoxy group protons and another singlet at 3.63 ppm due to the two benzylic protons.

A SIM-MS measurement on the molecular ion of ether **27** revealed 75% deuterium incorporation at the bisbenzylic position, when methanol- $O$ -d was used as solvent. Furthermore, SIM-MS of the diphenylmethyl fragment of **34a** indicated 64% deuterium incorporation in its bisbenzylic position.

1,1-Dimethoxy-2,2-diphenylethane (**31**) and 1,2-dimethoxy-2,2-diphenylethane (**32**) are secondary photoproducts arising from the photochemical reactivity of 1-methoxy-2,2-diphenylethene (**29**), itself a product of the reaction. The alkene **29** was synthesized independently by a Wittig reaction.<sup>82</sup> It was then subjected to irradiation in the presence of 1,4-dicyanobenzene (**2**) in methanol, yielding 67% of 1,1-dimethoxy-2,2-diphenylethane (**31**) together with a trace of the other isomer **32** (Reaction 13, Table 5). Introduction of biphenyl (**6**) into the system enhanced the efficiency of the reaction and raised the yield of **31** to 85% (Reaction 14, Table 5; Scheme 48). On the other hand, direct irradiation of **29** in methanol in the absence of a sensitizer gave a mixture containing considerable amounts of both isomeric ethers (Reaction 12, Table 5).



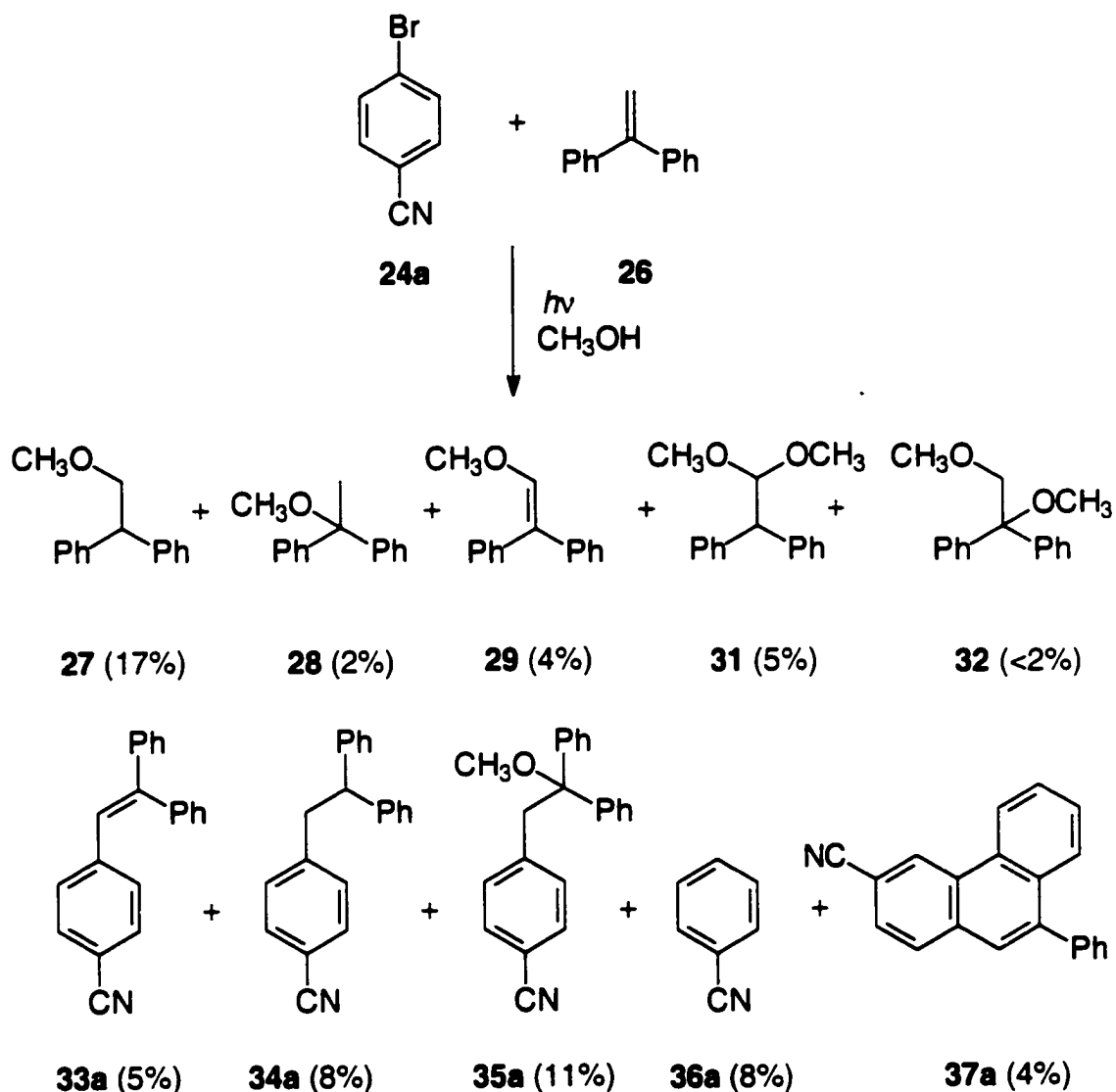
- Scheme 48 -

### 3.2.3 4-Bromobenzonitrile (24a) photochemistry

4-Bromobenzonitrile (**24a**) exhibits an absorption spectrum very similar to that of 4-chlorobenzonitrile (**23a**) with a  $\lambda_{\text{max}} = 282 \text{ nm}$ ,  $\epsilon = 370 \text{ dm}^3 \text{ mol}^{-1} \text{ cm}^{-1}$ . Irradiation in the presence of 1,1-diphenylethene (**26**) in methanol led to the formation of a series of products similar to the chlorobenzonitrile **23a** reaction, together with a substantial amount of benzonitrile (**36a**) as well as a small amount of a new compound identified as 3-cyano-9-phenylphenanthrene (**37a**) (Reaction 9, Table 5; Scheme 49).

The routine mass spectrum of **37a** is characterized by one large base peak at  $m/z = 279$  surrounded by a cluster of isotope peaks, as is characteristic of polycyclic aromatic compounds. The  $^{13}\text{C}$  NMR spectrum exhibits 19 separate signals. These include 8 due to quaternary carbons, indicating that every chemical shift non-equivalent carbon has been resolved. The  $^1\text{H}$  NMR does not provide much information, since all the aromatic protons resonate in a very narrow chemical shift window. Due to the limitations in the information provided by NMR, particularly as regards the position of the substituents on the phenanthrene ring, final confirmation of the structure was obtained by X-ray crystallography (Figure 13).

Similarly to **23a**, SIM-MS experiments on an identical reaction in methanol- $O\text{-d}$  resulted in 77% and 50% deuterium incorporation at the bisbenzyl positions of **27** and **34a** respectively.



- Scheme 49 -

In sharp contrast with the chlorobenzonitrile **23a**, irradiation of 4-bromobenzonitrile **24a** in the absence of the alkene under otherwise identical conditions led to complete consumption of the halobenzonitrile and a 71% yield of benzonitrile (**36a**) (Reaction 8, Table 5).

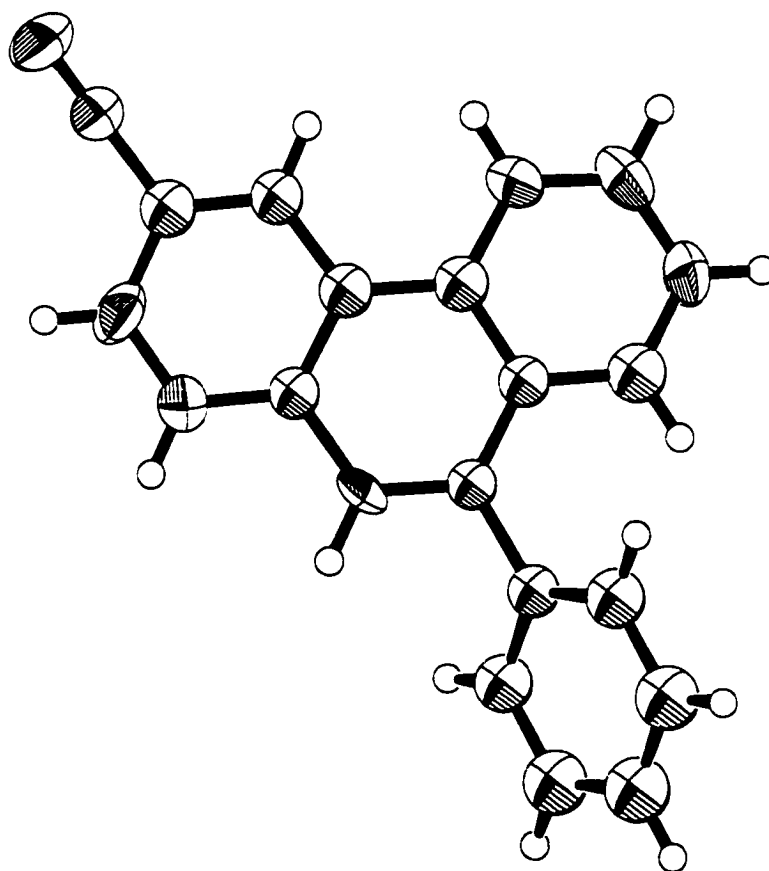
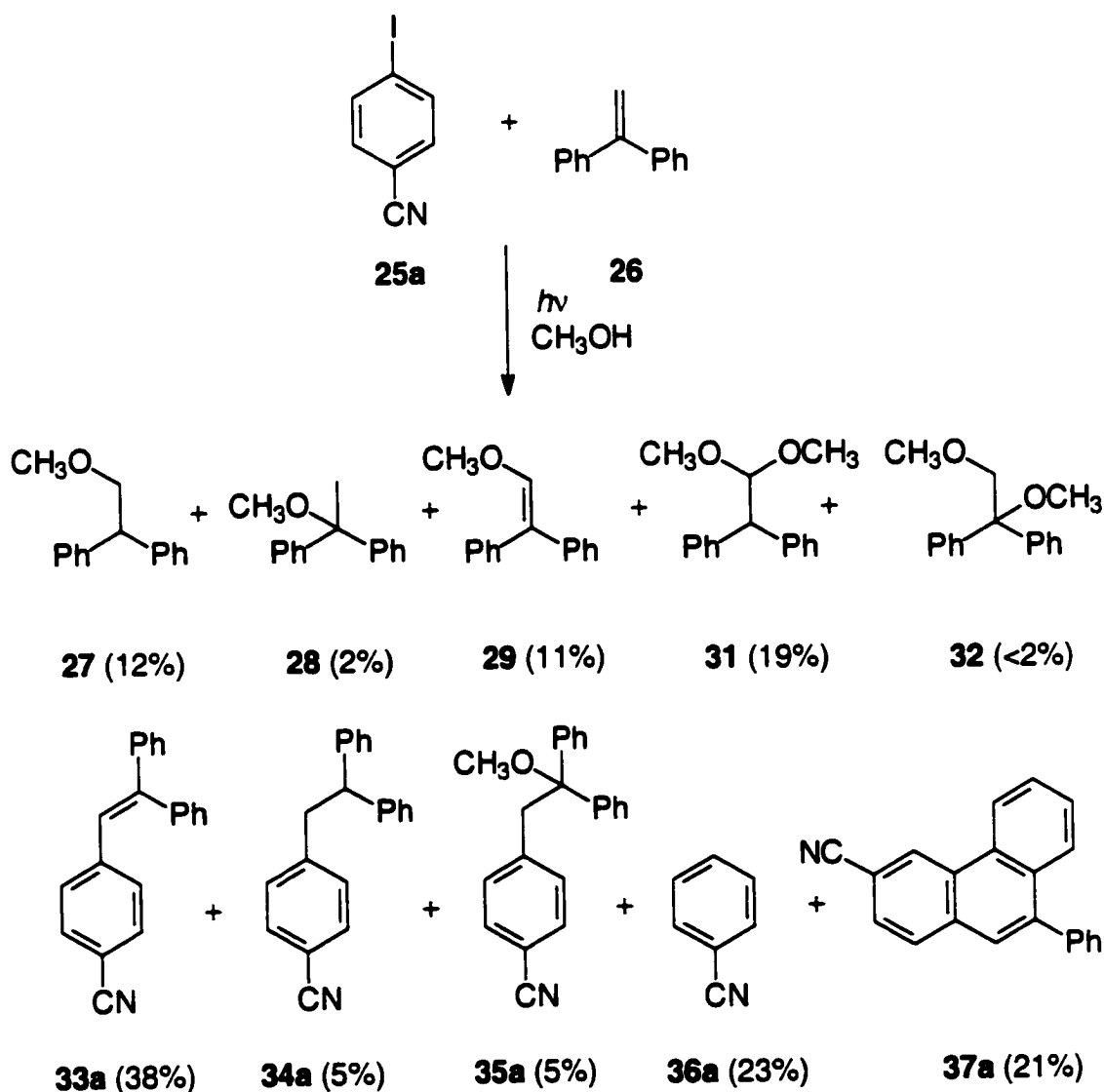


**Figure 13** : Single crystal X-ray crystallographic structure of 3-cyano-9-phenylphenanthrene (**37a**).

### 3.2.4 4-Iodobenzonitrile (25a) photochemistry

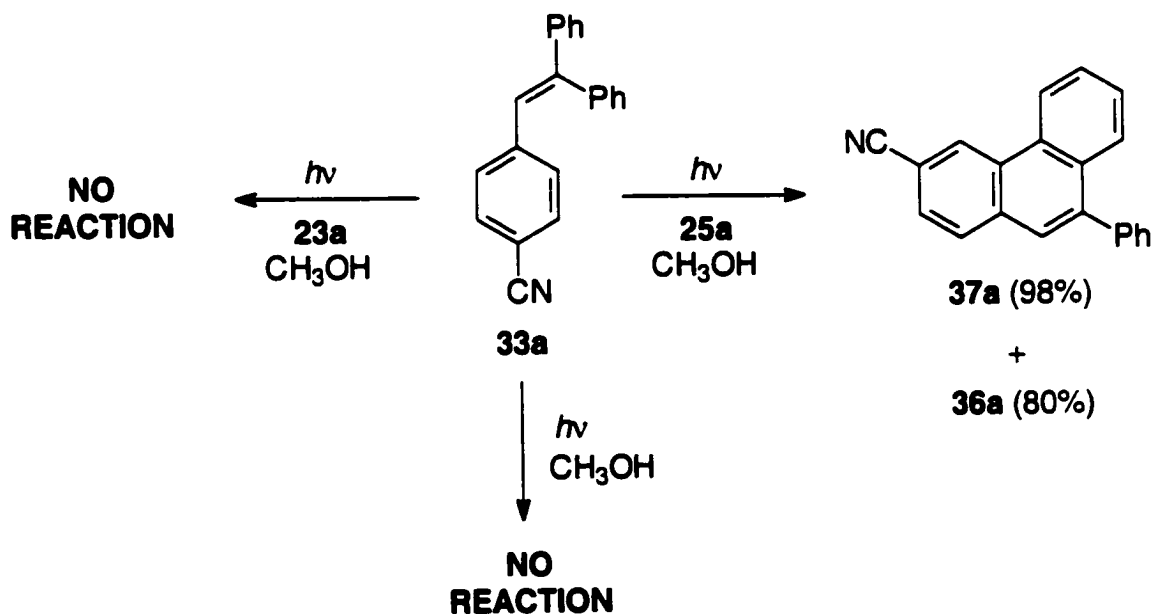
Irradiation of 4-iodobenzonitrile (**25a**) and 1,1-diphenylethene (**26**) under comparable conditions led to a similar series of products, although the distribution was appreciably different. In this case, 1-(4-cyanophenyl)-2-methoxy-2,2-diphenylethane (**35a**) was present only in minor amounts, while 1-(4-cyanophenyl)-2,2-diphenylethene (**33a**) and the phenanthrene (**37a**) were the major products at 38% and 21% yield respectively (Reaction 11, Table 5; Scheme 50).



- Scheme 50 -

SIM-MS measurements on a methanol-*O*-d reaction resulted in 86% and 41% deuterium incorporation at the bisbenzylic sites of **27** and **34a** respectively.

Careful monitoring of the photochemical reactions indicated that 3-cyano-9-phenylphenanthrene (**37a**) was produced only in the later stages of the irradiation and appeared to increase in concentration at the expense of the alkene **33a**, which was observed to diminish on prolonged irradiation. In order to confirm that the phenanthrene derivative was, in fact, a secondary product, **33a** was irradiated on its own in methanol. Surprisingly, the alkene remained unconsumed despite lengthy irradiation (Reaction 15, Table 5). In an attempt to simulate the photochemical mixture more closely, 4-iodobenzonitrile (**25a**) was introduced into the system prior to irradiation. This led to rapid consumption of the alkene **33a** and a clean conversion to 3-cyano-9-phenylphenanthrene (**37a**) (Reaction 17, Table 5; Scheme 51). This was accompanied by partial consumption of the iodobenzonitrile **25a** and the formation of benzonitrile **36a**. This experiment was repeated with 4-chlorobenzonitrile (**23a**) but no reaction was observed (Reaction 16, Table 5).



- Scheme 51 -

4-Iodobenzonitrile (**25a**) behaved similarly to its bromo analogue **24a** when irradiated in the absence of an olefin in methanol, decomposing quantitatively to benzonitrile **36a** (Reaction 10, Table 5).

### 3.2.5 4-Chloroanisole (**23b**) photochemistry

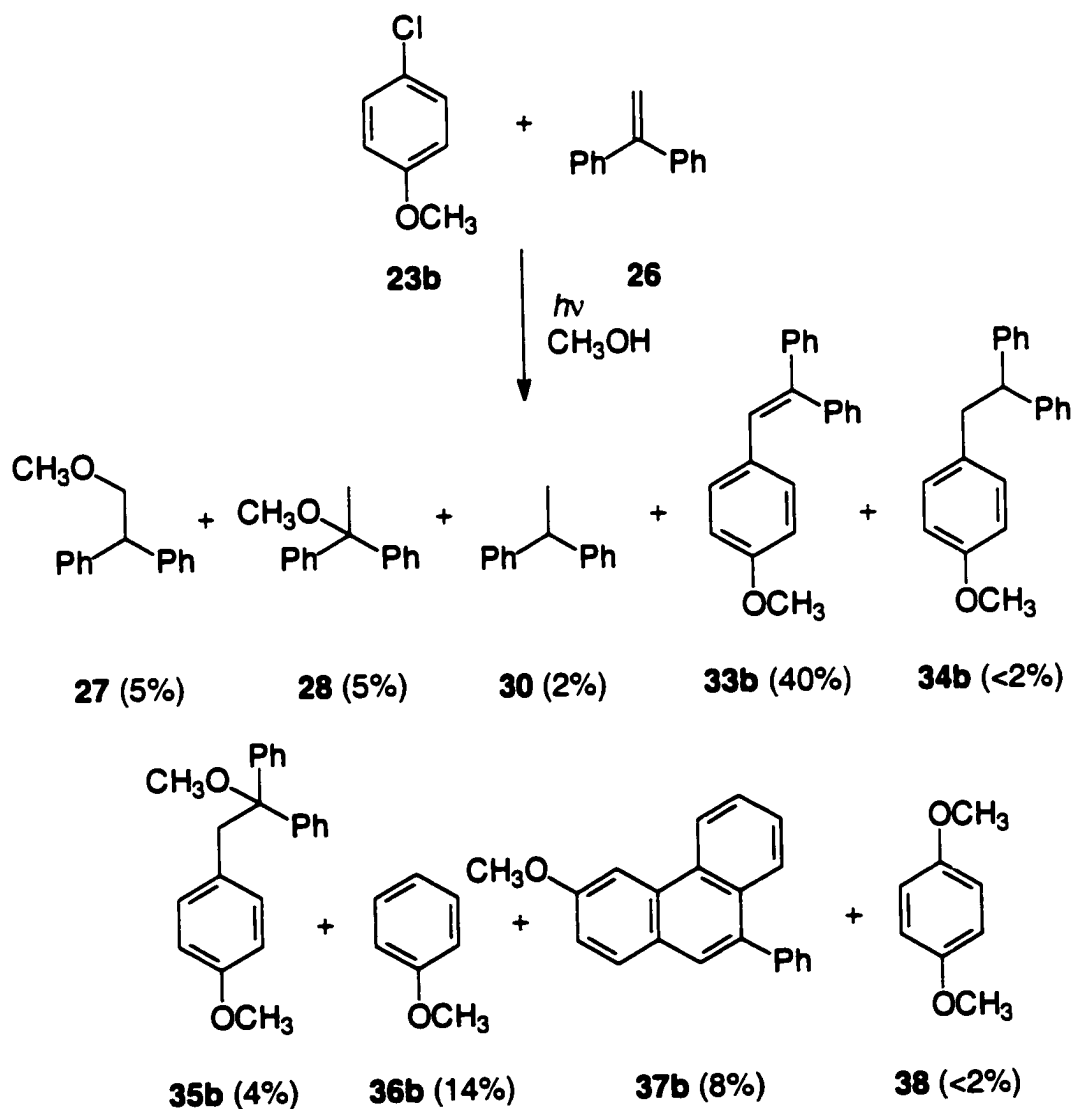
4-Chloroanisole (**23b**) was subjected to similar reaction conditions as its benzonitrile analogue **23a**. In contrast to **23a**, irradiation of anisole **23b** in methanol in the absence of an alkene led to considerable consumption of **23b**, accompanied by the formation of anisole (**36b**, 56%) and 1,4-dimethoxybenzene (**38**, 12%) (Reaction 18, Table 6). Both products were identified by comparison with authentic samples.

**Table 6** Photochemical reactions between the anisoles (**23b–25b**) and the alkenes (**26**, **33b**). Reaction conditions: 1 kW medium pressure Hg lamp, Pyrex filter, 5°C, methanol.

Reaction Number	Acceptor (% cons.)	Donor (% cons.)	Irradiation Time (h)	Products (% yield)
18	<b>23b</b> (88)	-	50	<b>36b</b> (56), <b>38</b> (12)
19	<b>23b</b> (79)	<b>26</b> (78)	75	<b>27</b> (5), <b>28</b> (5), <b>30</b> (2), <b>33b</b> (40), <b>34b</b> (<2), <b>35b</b> (4), <b>36b</b> (14), <b>37b</b> (8), <b>38</b> (<2)
20	<b>24b</b> (100)	-	50	<b>36b</b> (84)
21	<b>24b</b> (100)	<b>26</b> (69)	75	<b>27</b> (2), <b>33b</b> (30), <b>34b</b> (<2), <b>36b</b> (29), <b>37b</b> (13)
22	<b>25b</b> (64)	-	50	<b>36b</b> (87)
23	<b>25b</b> (100)	<b>26</b> (49)	75	<b>33b</b> (40), <b>34b</b> (<2), <b>36b</b> (22), <b>37b</b> (16)
24	<b>25b</b> (79)	<b>33b</b> (96)	6	<b>36b</b> (80), <b>37b</b> (94)



Irradiation of **23b** in the presence of 1,1-diphenylethene (**26**) in methanol led to a small amount of alkene–methanol adducts **27** (5%) and **28** (5%), together with a series of products incorporating the 4-methoxyphenyl moiety (Reaction 19, Table 6; Scheme 53). 1-(4-Methoxyphenyl)-2,2-diphenylethene (**33b**) was the major product (40%), but considerable amounts of anisole (**36b**, 14%), 1-(4-methoxyphenyl)-2-methoxy-2,2-diphenylethene (**35b**, 4%), and 3-methoxy-9-phenylphenanthrene (**37b**, 8%) were also formed. Only a trace of 1-(4-methoxyphenyl)-2,2-diphenylethane (**34b**) was observed. Its identification rests solely, though convincingly, on GC–MS data.



- Scheme 53 -

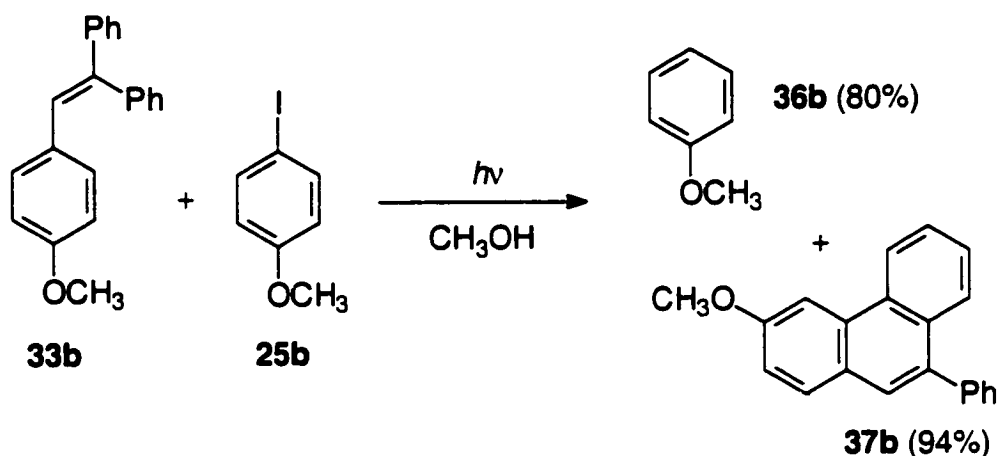
The identities of **33b** and **35b** were confirmed by comparison with samples synthesized by alternative methods (see Experimental). The spectroscopic data of these anisole derivatives matches closely with that of their benzonitrile analogues.

### 3.2.6 4-Bromoanisole (**24b**) and 4-iodoanisole (**25b**) photochemistry

4-Bromoanisole (**24b**) and 4-iodoanisole (**25b**) behaved similarly to their benzonitrile counterparts (**24a** and **25a**) when irradiated on their own in methanol. They both underwent rapid decomposition to yield anisole (**36b**) as the sole product in practically quantitative yield (Reactions 20 and 22, Table 6). In the presence of the olefin **26**, both anisoles produced a series of products similar to their chloro homologue **23b**. Unlike the corresponding benzonitriles, anisoles **24b** and **25b** did not produce any alkene–methanol adducts, but instead yielded considerable quantities of 1-(4-methoxyphenyl)-2,2-diphenylethene (**33b**), anisole (**36b**), and 3-methoxy-9-phenylphenanthrene (**37b**) (Reactions 21 and 23, Table 6).

Just like its cyano counterpart, 3-methoxy-9-phenylphenanthrene (**37b**) was shown to be a secondary photochemical product by irradiating 1-(4-methoxyphenyl)-2,2-diphenylethene (**33b**) and 4-iodoanisole (**25b**) in methanol. This led to rapid consumption of the starting materials and quantitative formation of **36b** and **37b** (Reaction 24, Table 6; Scheme 54).

In all the reactions involving the formation of the 1-aryl-2-methoxy-2,2-diphenylethanes **35a** and **35b** it was observed that the ratio of **33:35** increased as the reaction progressed. A similar trend was also noticed when the reactions were allowed to stand in the dark. In order to test this hypothesis of spontaneous degradation, two solutions of **35a** and **35b** in methanol were prepared and allowed to stand in the dark for five days. GC–MS analysis of the solutions revealed partial decomposition to **33a** and **33b** respectively. Furthermore, introduction of a trace of hydrochloric acid resulted in almost complete conversion of the ethers **35** to the corresponding alkenes **33**.



- Scheme 54 -

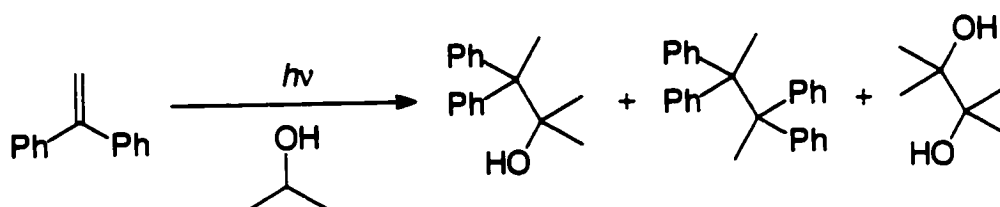
### 3.3 DISCUSSION

Before addressing the main focus of this study, which is the photochemistry of haloarenes in the presence of 1,1-diphenylethene (**26**), certain background reactions, performed to identify the photochemical behaviour of **26**, have to be investigated. Understanding these mechanisms of photochemical reaction is vital for the rationalization of the more complex situations involving the haloarenes.

#### 3.3.1 Direct photoaddition of methanol to 1,1-diphenylethene (**26**)

Interestingly, irradiation of **26** in methanol did not lead to the formation of any 2,2-diphenylpropanol, which would be expected if the alkene excited state were to abstract a hydrogen atom from methanol and subsequently couple with the resulting hydroxymethyl radical. This observation contrasts with the reported reaction between photochemically excited 1,1-diphenylethene (**26**) and 2-propanol, which yields 2-methyl-3,3-diphenyl-2-butanol, 2,2,3,3-tetraphenylbutane, and 2,3-dimethyl-2,3-butanediol, these compounds all being classical radical-derived products (Scheme 55).<sup>83</sup> The possibility of a hydrogen

abstraction occurring from the hydroxyl group in methanol is discounted upon considering the corresponding bond dissociation energies: BDE [H–CH<sub>2</sub>OH] = 393 kJ mol<sup>-1</sup>; BDE [CH<sub>3</sub>O–H] = 437 kJ mol<sup>-1</sup>.<sup>84</sup> Hence, in this case, a radical mechanism seems unlikely. This difference in reactivity on going from methanol to 2-propanol is most likely attributed to the weaker carbon–hydrogen bond in 2-propanol: BDE [H–C(CH<sub>3</sub>)<sub>2</sub>OH] = 381 kJ mol<sup>-1</sup>,<sup>84</sup> which facilitates hydrogen atom abstraction.



- Scheme 55 -

This lack of radical-derived products, a situation common to most aryl alkenes and alkynes in methanol, has been extensively investigated.<sup>85,86</sup> It is now well established that, in the case of cyclic alkenes, photoexcitation leads to a highly strained *trans* intermediate that is prone to protonation by methanol. The resulting carbocation is subsequently trapped by methanol to give the Markovnikov ether.<sup>85</sup> In the case of styrenes, protonation of the singlet excited state leads to similar products.<sup>86</sup> As expected, acid catalysis has a profound enhancement on the reaction rates in all the above studies. When considering stilbenes, protonation is no longer a key step. Laarhoven and co-workers proved that acid catalysis did not have an effect on the rate of photochemical reaction in these cases.<sup>81</sup> This was confirmed by the lack of quenching of the alkene fluorescence in an acidified medium. After a series of careful experiments, they concluded that the addition of methanol to stilbenes involves two competitive pathways: a concerted addition via either a planar or a twisted excited singlet state, and an insertion into a carbene, the latter resulting from a 1,2-hydride shift in the excited stilbene. Judging from the similarity of the products observed,

Laarhoven proposed that the photochemical addition of methanol to 1,1-diphenylethene (**26**) followed similar routes, although no specific mechanistic tests were carried out on this system.

In our hands, the photochemical reaction of **26** with methanol behaved similarly to Laarhoven's. The reaction proceeded at a somewhat sluggish rate to give 1-methoxy-1,1-diphenylethane (**28**) as major product, together with lesser amounts of its isomeric ether 1-methoxy-2,2-diphenylethane (**27**) and the photoreduction product 1,1-diphenylethane (**30**), as well as extensive polymerization (Scheme 45). However, we did not observe any products arising from a 1,2-phenyl shift, notably *E*- and *Z*-stilbene, 1-methoxy-1,2-diphenylethane and phenanthrene, as reported by Laarhoven.<sup>81</sup> These products were only present in minor amounts in Laarhoven's study, and could easily have been missed in our investigation.

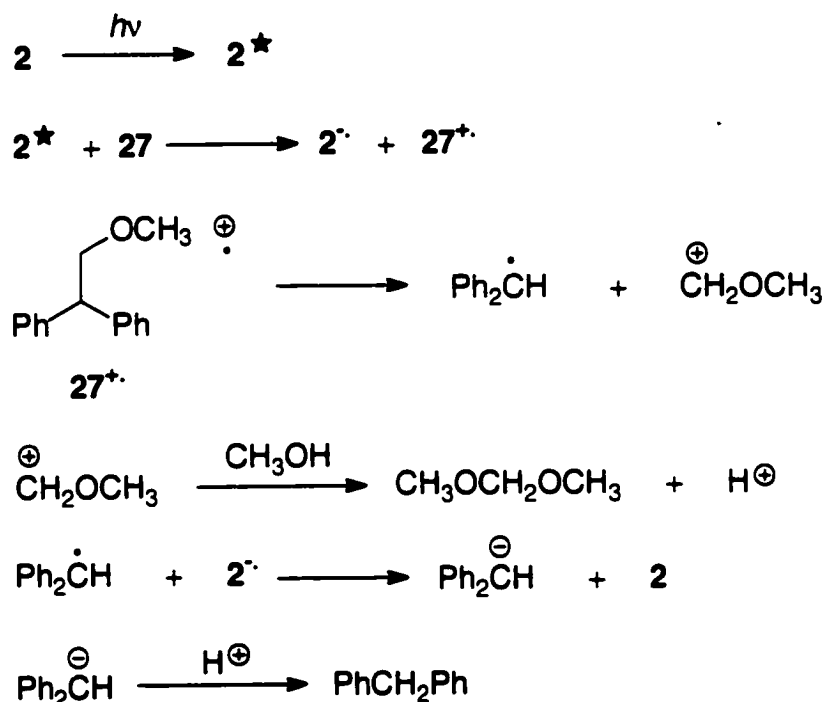
### 3.3.2 PET addition of methanol to 1,1-diphenylethene (**26**)

Introduction of an electron acceptor photosensitizer such as 1,4-dicyanobenzene (**2**) into the system radically altered the reaction outcome. In agreement with the well established mechanism for PET nucleophile addition, the reaction yielded the *anti*-Markovnikov ether 1-methoxy-2,2-diphenylethane (**27**), with only a minor amount of the Markovnikov ether **28** (Scheme 44). This closely agrees with the reported observation.<sup>21a</sup>

The introduction of biphenyl (**6**) improved the photoreaction. In this particular situation, **6** does not function solely as a straightforward donor co-sensitizer but also *selectively* co-sensitizes the reaction of interest while quenching an unwanted secondary reaction that limits the success of the primary reaction.

The presence of a second photochemical reaction involving the PET fragmentation of the ether produced from the PET nucleophilic addition is well documented (Scheme 56).<sup>24,87</sup> Generation of the radical cation of the *anti*-Markovnikov ether **27** via PET leads to its fragmentation into a diphenylmethyl radical and a methoxymethyl cation. The cationic moiety is nucleophilically

trapped to yield dimethoxymethane. The radical species is reduced by the sensitizer radical anion and subsequently protonated to give diphenylmethane. This secondary reaction has been largely responsible for the non-quantitative yields reported for this reaction.



- Scheme 56 -

Biphenyl (**6**) prevents this secondary fragmentation reaction from occurring. 1,4-Dicyanobenzene (**2**) has a reduction potential  $E_{1/2}^{\text{red}}$  of  $-1.66$  V vs SCE ( $\text{CH}_3\text{CN}$ ) and an excitation energy  $E_{0,0}$  of  $4.21$  eV ( $\text{CH}_3\text{CN}$ ),<sup>4a</sup> which implies that the free energy for the PET process will be exergonic with all electron donors having an oxidation potential  $E_{1/2}^{\text{ox}}$  lower than  $2.54$  V vs SCE. The PET methanol adduct 1-methoxy-2,2-diphenylethane (**27**) has an  $E_{1/2}^{\text{ox}}$  of  $2.15$  V vs SCE ( $\text{CH}_3\text{CN}$ ),<sup>24a</sup> and is thus expected to undergo PET with **2** at a diffusion-controlled rate. Biphenyl (**6**), however, possesses an oxidation potential  $E_{1/2}^{\text{ox}}$  of  $1.85$  V vs SCE ( $\text{CH}_3\text{CN}$ )<sup>20b</sup> that is close enough to that of **26** ( $E_{1/2}^{\text{ox}} = 1.88$  V vs SCE,  $\text{CH}_3\text{CN}$ ),<sup>80</sup> but significantly lower than that of the ether **27**. This implies that upon

introduction of **6** into the system, PET will occur preferentially with **6** as donor rather than with the ether **27**. Furthermore, whereas the secondary electron transfer between the biphenyl radical cation and 1,1-diphenylethene (**26**) is roughly isoergonic, electron transfer with the ether **27** will be prohibitively endergonic and hence non-viable. In fact, under these co-sensitizing conditions, the nucleophilic addition reaction can be driven to completion without any major degradation due to the fragmentation pathway. By means of this modification, the yield of the ether **27** has been boosted up to 83% from the previous 38%.

Ohashi and co-workers have recently reported a similar co-sensitization technique for reducing the fragmentation side reaction.<sup>25c</sup> On the other hand, Arnold and co-workers have impeded the fragmentation process by using a sensitizer that possesses a low enough singlet excited state reduction potential ( $E_{1/2}^{\text{red}^*}$ ) to render the PET step with the nucleophile adduct endergonic while selectively allowing the primary nucleophilic addition reaction to proceed unhindered.<sup>87a</sup>

### 3.3.3 PET between haloarenes (22–25) and 1,1-diphenylethene (26)

The prime requirement for an effective PET process is that the energetics for the electron transfer, as predicted by the Weller equation,<sup>9</sup> are exergonic.

Comparison of the electronic absorption spectra of the haloarenes (**22–25**) with that of 1,1-diphenylethene (**26**) indicates that these species will absorb competitively. Hence, in most cases, it is not readily established which component is the active light absorber and which excited state species is thus involved in the PET process. If both donor and acceptor reacted from their singlet excited states, then, from a straightforward energetics point-of-view, it would not really matter which constituent was actually photoexcited. The possession of similar cut-off wavelengths in the absorption spectra implies similar singlet energies. In fact, free energy calculations suggest that PET between halobenzonitriles **23a–25a** and alkene **26** will be exergonic, irrespective of which singlet excited state is involved (Table 7). On the other hand, 4-fluorobenzonitrile

**Table 7** Free energies,  $\Delta G_{\text{PET}}$ , for the PET process between 1,1-diphenylethene (**26**) and the listed arenes (**2**, **22–25**).

Arene	Excitation Energy			$\Delta G_{\text{PET}}$ (kJ mol <sup>-1</sup> ) <sup>g</sup>		
	$E_{1/2}^{\text{red}}$ (V) <sup>a</sup>	$E_{0,0}^{\text{S}}$ (eV)	$E_{0,0}^{\text{T}}$ (eV)	<sup>1</sup> A*	<sup>3</sup> A*	<sup>1</sup> D*
<b>2</b>	-1.66 <sup>b</sup>	4.21 <sup>b</sup>	3.08 <sup>e</sup>	-71	+38	-60
<b>22a</b>	<-2.5	4.44 <sup>c</sup>	3.36 <sup>c</sup>	>-12	>+92	>+21
<b>23a</b>	-2.07	4.25 <sup>c</sup>	3.20 <sup>c</sup>	-35	+66	-21
<b>23b</b>	<-2.5	4.21 <sup>d</sup>	3.39 <sup>f</sup>	>+10	>+89	>+21
<b>24a</b>	-2.02	4.30 <sup>c</sup>	3.19 <sup>c</sup>	-45	+62	-25
<b>24b</b>	<-2.5	4.21 <sup>d</sup>	3.39 <sup>f</sup>	>+10	>+89	>+21
<b>25a</b>	-1.87	4.39 <sup>d</sup>	-	-68	-	-40
<b>25b</b>	<-2.5	4.06 <sup>d</sup>	-	>+25	-	>+21

<sup>a</sup> Reduction potentials,  $E_{1/2}^{\text{red}}$ , measured by cyclic voltammetry vs SCE using 0.1 mol dm<sup>-3</sup> tetraethylammonium perchlorate as supporting electrolyte in deoxygenated acetonitrile. The cathodic waves for the haloarenes were irreversible and  $E_{1/2}^{\text{red}}$  were estimated by subtracting 0.03 V from the peak potentials obtained at a scan rate of 100 mV s<sup>-1</sup>.<sup>44</sup> Literature values for comparison: **22a** -2.48 V (SCE, CH<sub>3</sub>CN);<sup>90</sup> **23a** -2.03 V (SCE, CH<sub>3</sub>CN),<sup>66p</sup> -1.88 V (SCE, DMF);<sup>65</sup> **24a** -1.83 V (SCE, DMF);<sup>65</sup> **25a** -1.71 V (SCE, DMF).<sup>65</sup> <sup>b</sup> Ref. 4a. <sup>c</sup> Ref. 91. <sup>d</sup> Determined from the cut-off wavelength in the electronic absorption spectrum. <sup>e</sup> Ref. 92. <sup>f</sup> Ref. 93. <sup>g</sup> Calculated using the Weller equation.<sup>9</sup>  $E_{1/2}^{\text{ox}}$  (**26**) = 1.88 V (SCE, CH<sub>3</sub>CN),<sup>80</sup> Coulombic stabilization term = 6.1 kJ mol<sup>-1</sup> (CH<sub>3</sub>OH),  $E_{0,0}^{\text{S}}$  (**26**) = 4.10 eV.<sup>94</sup> <sup>1</sup>A\*: acceptor singlet excited state; <sup>3</sup>A\*: acceptor triplet excited state; <sup>1</sup>D\*: donor singlet excited state.



(22a) could lead to an exergonic free energy if its singlet excited state were involved, but its weak absorption spectrum makes it hard to absorb competitively with 26, thus rendering this possibility unlikely.

There is, however, a kinetic aspect that has to be considered as well. The lifetime of the excited state, the rate of electron transfer, and the concentration of the other constituent of the electron transfer pair (*i.e.*, the quencher) determine whether an excited state can participate in the electron transfer process. The lifetime of the excited state is inherent to that species in the particular environment, while the rate of electron transfer depends on the energetics of the process, with a  $\Delta G_{\text{PET}}$  more negative than  $-20 \text{ kJ mol}^{-1}$  usually resulting in a diffusion controlled rate ( $1.1 \times 10^{10} \text{ M}^{-1} \text{ s}^{-1}$  in  $\text{CH}_3\text{OH}^\dagger$ ).<sup>9</sup> The concentration of the quencher, on the other hand, is at the experimenter's discretion. The quencher concentration will decrease as the reaction proceeds, and this will have a further debilitating effect on the PET process.

The nature of the excited state is also important. The haloarenes, in particular the chloro, bromo, and iodo compounds, are expected to possess high quantum yields of intersystem crossing and, probably, particularly short excited singlet lifetimes. Although specific values for the compounds under investigation were not found in the literature, chlorobenzene is reported to have a quantum yield of intersystem crossing of 0.7<sup>95</sup> and a singlet lifetime of 0.74 ns.<sup>96</sup> If we borrow these values we will find that, at a quencher concentration of  $0.1 \text{ mol dm}^{-3}$ , about 50% of the singlet excited states undergo electron transfer, assuming the PET rate is at the diffusion controlled limit. Most of the unquenched excited states will intersystem cross to the triplet state. Triplets are generally longer lived

---

<sup>†</sup> The diffusion-controlled rate  $k_{\text{DIFF}}$  in methanol is calculated using the Debye equation.<sup>88</sup>

$$k_{\text{DIFF}} = 8 \times 10^3 \frac{RT}{3\eta}$$

where  $R$  is the molar gas constant ( $8.31 \text{ J mol}^{-1} \text{ K}^{-1}$ ),  $T$  is the temperature (298 K) and  $\eta$  is the viscosity of the solvent ( $0.59 \times 10^{-3} \text{ N s m}^{-2}$  for  $\text{CH}_3\text{OH}$ <sup>89</sup>).

since deactivation to the ground state, which is invariably of singlet nature, requires a second intersystem crossing. The following excited triplet lifetimes have been reported: 4-fluorobenzonitrile (**22a**) 2.05 s, 4-chlorobenzonitrile (**23a**) 0.15 s and 4-bromobenzonitrile (**24a**) 4.9 ms (ethylpropylamine glassy matrix, 77 K).<sup>91</sup> The excited triplet lifetimes are expected to be considerably long even at the reaction temperature of *ca.* 278 K. Such long lived species would allow for practically 100% quenching, but the loss in excitation energy on crossing to the triplet renders the electron transfer process prohibitively endergonic (Table 7).

The possibility of PET occurring via the singlet excited state of 1,1-diphenylethene (**26**) is disfavoured by a short excited singlet state lifetime. This was determined as *ca.* 0.3 ns in hexane by a single-photon counting experiment. Due to the weak fluorescence of **26** in methanol, a reliable lifetime in this solvent could not be measured. Alkenes are well known to possess short excited singlet state lifetimes due to rapid radiationless deactivation by the free-rotor effect. Furthermore, the excited triplet state of **26** can also be discounted as being the reactive excited state. Gorner reported that **26** has a quantum yield of intersystem crossing of  $<10^{-3}$ .<sup>94</sup> Therefore, its triplet can only be populated by triplet sensitization. Triplet state sensitization by the haloarenes or enhanced intersystem crossing due to an external heavy atom effect are possibilities. However, they are not relevant to a PET mechanism, since PET from the alkene triplet state ( $E_{0,0}^T = 2.56$  eV,<sup>94</sup> 2.64 eV<sup>97</sup>) is endergonic and hence non-viable.

The photochemistry between alkene **26** and a series of haloanisoles **23b–25b** has also been investigated in order to obtain further insight into the mechanisms involved. The haloanisoles are clearly weak electron acceptors, with reduction potentials greater than  $-2.5$  V. PET is calculated to be endergonic in all these cases, irrespective of the reacting excited state (Table 7). These haloanisoles should thus serve as good indicators for distinguishing between PET and non-PET pathways.

### 3.3.4 PET vs direct homolytic cleavage pathways

One of the major difficulties in establishing a mechanism for the observed reactivity is determining whether a photochemically excited halobenzonitrile will cleave prior to or after undergoing electron transfer. Homolytic cleavage before electron transfer will result in a phenyl radical and a halogen atom. Alternatively, if the photoexcited halobenzonitrile survives long enough to undergo electron transfer with the alkene it will generate a halobenzonitrile radical anion that subsequently cleaves to a phenyl radical and a halide anion. Both pathways eventually lead to a phenyl radical but the main difference is that the PET pathway also produces an alkene radical cation, and this has major consequences further along the mechanism. Deciding which of the two mechanisms is predominant depends on the rate of homolytic cleavage *versus* the rate of electron transfer. Here, we must recognize that PET is disadvantaged by the fact that this process is bimolecular, and is thus restricted by the rate of diffusion in the medium and by the concentration of the electron transfer partner. Its efficiency is also severely hindered by back electron transfer, which converts the radical ions back to the neutral starting materials and which thus constitutes an unproductive step. Homolytic cleavage, in its simplest form, is a unimolecular process independent of the alkene, its concentration and its rate of diffusion through the medium.

This aspect has received scarcely any attention in the literature. The most common methods used to generate haloarene radical anions avoid the formation of a haloarene excited state either by using electrochemical means for generating the radical anions or by ensuring that the other constituent of the PET pair acts as the sole light absorber.

As mentioned before, one simple method that has been used successfully to predict the likelihood of homolytic cleavage is comparing the energy of the reacting excited state with the bond dissociation energy of the bond to be cleaved. Although the bond dissociation energies of the actual haloarenes involved in this study are not available, they can be approximated to the corresponding values for the halobenzenes, as displayed in Table 8.<sup>84</sup> If we

**Table 8** Singlet ( $E_{0,0}^S$ ) and triplet energies ( $E_{0,0}^T$ ) for the haloarenes **22–25** and bond dissociation energies (BDE) for the  $C_6H_5-X$  bond.

Haloarene	$E_{0,0}^S$ (kJ mol <sup>-1</sup> )	$E_{0,0}^T$ (kJ mol <sup>-1</sup> )	BDE $C_6H_5-X$ (kJ mol <sup>-1</sup> ) <sup>d</sup>
4-fluorobenzonitrile ( <b>22a</b> )	428 <sup>a</sup>	324 <sup>a</sup>	523
4-chlorobenzonitrile ( <b>23a</b> )	410 <sup>a</sup>	309 <sup>a</sup>	398
4-chloroanisole ( <b>23b</b> )	406 <sup>b</sup>	327 <sup>c</sup>	398
4-bromobenzonitrile ( <b>24a</b> )	415 <sup>a</sup>	308 <sup>a</sup>	313
4-bromoanisole ( <b>24b</b> )	406 <sup>b</sup>	327 <sup>c</sup>	313
4-iodobenzonitrile ( <b>25a</b> )	424 <sup>b</sup>	-	268
4-iodoanisole ( <b>25b</b> )	392 <sup>b</sup>	-	268

<sup>a</sup> Ref. 91. <sup>b</sup> Determined from the cut-off wavelengths in the electronic absorption spectrum. <sup>c</sup> Ref. 93. <sup>d</sup> Ref. 84.

assume that the reacting excited state is the triplet, these values indicate that homolytic cleavage will probably be viable for the bromo and iodo derivatives but unlikely for the fluoro and chloro compounds. In the less likely situation that cleavage is rapid enough to occur from the singlet in competition with intersystem crossing, then iodo, bromo, and chloro compounds are expected to undergo homolytic cleavage. These postulates were tested by a series of experiments involving irradiation of the haloarenes in pure methanol. Whereas the bromo- (**24**) and iodoarenes (**25**) underwent extensive homolysis to give the corresponding haloarene (*i.e.*, benzonitrile or anisole), the fluoro- (**22a**) and chlorobenzonitriles (**23a**) were stable under these conditions. These observations suggest that the observed homolysis, in these cases, occurs from the excited triplet state. 4-Chloroanisole (**23b**) showed appreciable cleavage despite unfavourable energetics for the postulated pathway. Such apparently anomalous behaviour has been observed previously with compounds such as 4-

bromobiphenyl and 1-chloronaphthalene. In these cases cleavage is attributed to the involvement of excimers, which facilitate homolysis.<sup>74</sup> The inefficiency of **23b** to undergo direct, unassisted homolytic dissociation is highlighted by the formation of 1,4-dimethoxybenzene (**38**) via a photoinduced nucleophilic aromatic substitution ( $S_NAr$ ) reaction. This reaction has been observed previously, and can be taken as an indication of the stability of the carbon–chlorine bond towards direct homolytic cleavage.<sup>98</sup>

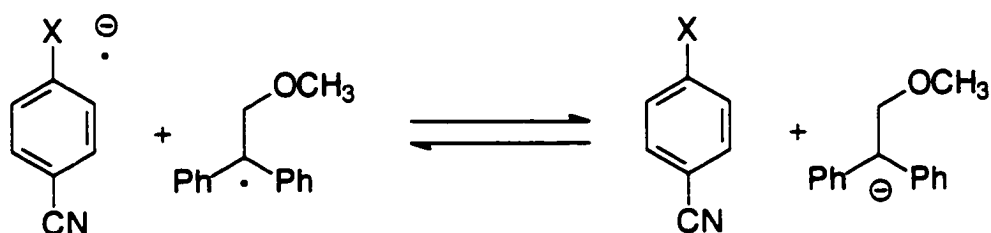
One of the strongest pieces of evidence pointing towards a PET mechanism is the observed formation of the alkene–methanol adduct, 1-methoxy-2,2-diphenylethane, **27**. The *anti*-Markovnikov regiochemistry of this compound can be best, if not solely, explained if we consider an alkene radical cation as precursor. The high deuterium incorporation (75–86%) at the bisbenzylic position when using methanol-*O*-d as solvent is a confirmation of the presence of the well known electron transfer mechanism outlined in Section 1.3. This mechanism requires a secondary electron transfer between the intermediate alkene–methanol adduct radical and the sensitizer radical anion in order to furnish the adduct anion. This anion is subsequently protonated to give the final ether **27** as product. If we approximate the half-wave reduction potential,  $E_{1/2}^{\text{red}}$ , of the 2-methoxy-1,1-diphenylethyl radical ( $\text{Ph}_2\text{C}^{\cdot}\text{CH}_2\text{OCH}_3$ ) to that of the 1,1-diphenylethyl radical ( $\text{Ph}_2\text{C}^{\cdot}\text{CH}_3$ ) that has been reported by Wayner as  $-1.34$  V vs SCE ( $\text{CH}_3\text{CN}$ ),<sup>40a</sup> we will find that the reduction of the intermediate adduct radical by the sensitizer radical anion is highly exergonic in all cases (Scheme 57).<sup>‡</sup>

This process, however, requires the halobenzonitrile radical anion to survive long enough for the secondary electron transfer to occur. This is particularly surprising since the rates of cleavage of the halobenzonitrile radical anions are extremely rapid in all cases except the fluoro, which is thought to be

---

<sup>‡</sup> Free energy for the secondary electron transfer,  $\Delta G_{\text{ET}} = F (E_{1/2}^{\text{ox}} - E_{1/2}^{\text{red}}) = F (E_{1/2}^{\text{ox}} + 1.34)$  kJ mol<sup>-1</sup>.  $\Delta G_{\text{ET}} = -31$  (X = CN, **2**);  $-112$  (F, **22a**);  $-70$  (Cl, **23a**);  $-66$  (Br, **24a**);  $-51$  (I, **25a**).

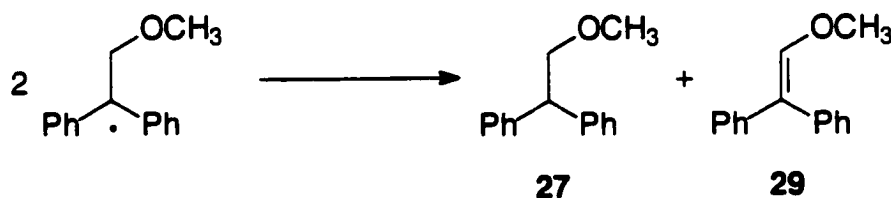
stable towards cleavage.<sup>64</sup> The rate constants have been determined by Savéant and colleagues, using electrochemical techniques, to be  $9 \times 10^8 \text{ s}^{-1}$  for **23a**,  $2 \times 10^9 \text{ s}^{-1}$  for **24a** and  $2 \times 10^{10} \text{ s}^{-1}$  for **25a**.<sup>66k</sup> The only alternative species that might possibly take part in the electron transfer process instead of the halobenzonitrile radical anions are the neutral alkene and the halide anions. However, the energetics are unfavourable in both cases. This leaves us with the halobenzonitrile radical anion as the only, though seemingly improbable, contender for the electron transfer process. There is, however, evidence in the photochemical reactions of a hindered secondary electron transfer step, presumably due to these species cleaving prior to the second electron transfer.



- Scheme 57 -

In the photoreaction involving 1,4-dicyanobenzene (**2**) and 1,1-diphenylethene (**26**) in methanol-*O*-d, the bisbenzylic position of the *anti*-Markovnikov ether product **27** exhibited 96% deuterium incorporation. This indicates that reduction of the adduct radical to the corresponding anion and its subsequent protonation is basically the only pathway leading to ether **27**. This is readily understandable from both energetic and kinetic aspects. In the halobenzonitrile reactions, however, the deuterium incorporation percentage in **27**, albeit high, is appreciably lower than in the 1,4-dicyanobenzene (**2**) case. This might reflect the unavailability of a proper reducing agent to complete the process. In such a situation, the 2-methoxy-1,1-diphenylethyl radicals would accumulate and have the option to undergo a disproportionation reaction to yield

1-methoxy-2,2-diphenylethane **27** (with no deuterium incorporation) and 1-methoxy-2,2-diphenylethene **29** (Scheme 58).



- Scheme 58 -

In fact, considerable amounts of **29** have been observed in the chloro-, bromo-, and iodobenzonitrile reactions. The compound was shown to be photochemically active, reacting similarly to 1,1-diphenylethene (**26**). It was found to undergo an efficient PET methanol addition in the presence of 1,4-dicyanobenzene (**2**) to give 1,1-dimethoxy-2,2-diphenylethane (**31**) in a moderate yield of 67%. This was boosted to a more satisfactory 85% upon introducing biphenyl (**6**) as donor co-sensitizer. Furthermore, it was shown to undergo methanol addition in the absence of any sensitizer to give the two isomeric diethers, 1,1-dimethoxy-1,1-diphenylethane (**31**) and 1,2-dimethoxy-2,2-diphenylethane (**32**). Both of these diethers are found in the photochemical reactions involving the cleavable halobenzonitriles. On the other hand, none of these products (**29**, **31**, **32**) are observed in appreciable amounts in the 1,4-dicyanobenzene (**2**) reaction.

As predicted by the energetics calculations, the haloanisoles **23–25** are too weak electron acceptors to promote PET with 1,1-diphenylethene (**26**). In fact, there is no sign of PET-induced alkene–methanol products in the haloanisole reactions (Table 6). The small amounts of alkene–methanol adducts actually detected in these reactions are most likely due to the non-PET addition of methanol to **26** (Section 3.1.1). These results are further confirmation that a PET mechanism is operational in the halobenzonitrile reactions.

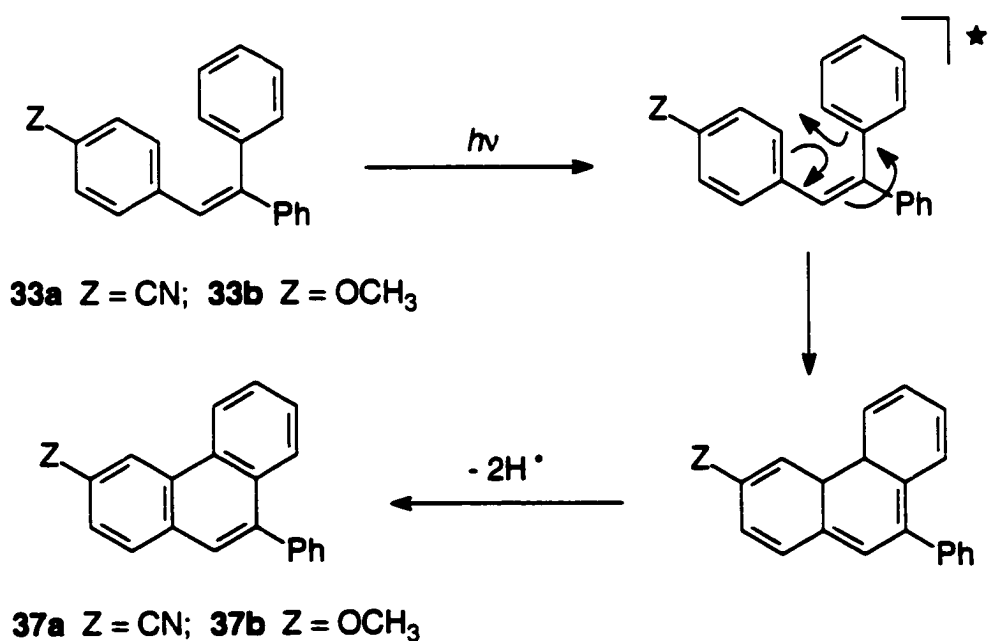
The possibility that benzonitrile (**36a**), formed via homolytic cleavage of the halobenzonitriles, might act as an electron acceptor and induce a PET mechanism was considered. Free energy calculations suggest a roughly isoergonic PET with the 1,1-diphenylethene (**26**) excited singlet state ( $E_{1/2}^{\text{red}}$  (**36a**) =  $-2.23$  V vs SCE,  $\text{CH}_3\text{CN}$ ;<sup>99</sup>  $-2.40$  V vs SCE,  $\text{DMF}$ <sup>84</sup>). However, irradiation of a mixture containing the alkene **26** and **36a** in methanol did not lead to a PET reaction. The product distribution was identical to that obtained from the photolysis of **26** on its own in methanol. This lack of PET is probably due to the short lifetime of the alkene excited singlet state, which prevents quenching by electron transfer, and to the inability of **36a** to act as the light absorber and function from *its* excited singlet state.

As highlighted in the introduction (Section 3.1), the major interest of this study is in those pathways that involve co-reactivity of the halobenzonitrile and the incorporation of the 4-cyanophenyl moiety in the final products. These products are evidently absent in the 1,4-dicyanobenzene (**2**) reaction due to the stability of its radical anion. For a similar reason, or maybe because PET is non-viable in this case, no such products are observed in the 4-fluorobenzonitrile (**22a**) reaction. Analysis of the other haloarene photoreactions reveals the presence of four products (**33–35**, **37**) resulting from the co-reaction of the alkene with the aryl fragment.

A series of separate experiments using **33a** and **33b** as starting materials established that the phenanthrene derivatives **37a** and **37b** were secondary photoproducts arising from the photoinduced cyclization of **33a** and **33b** respectively (Scheme 59). This  $6\pi$ -electrocyclization reaction is well documented.<sup>100-103</sup> Interestingly, this cyclization did not occur if **33a** or **33b** were irradiated in the absence of a haloarene. Addition of 4-chlorobenzonitrile (**23a**) to the solution also failed to induce the photocyclization and, in fact, none of this product (**37a**) was observed in the chlorobenzonitrile (**23a**) photoreactions. However, irradiation of the solution upon addition of the iodoarenes **25a** or **25b** led to a quantitative conversion of **33a,b** to the phenanthrene derivatives **37a,b**.



The difference in reactivity in the presence of the chlorobenzonitrile **23a** and iodoarenes **25a** and **25b** is intriguing. The hypothesis that the cyclization is triggered by triplet sensitization is dismissed by the fact that the chloro- and iodoarenes are expected to possess similar triplet energies and would thus not show such a marked difference in reactivity. This is confirmed in the literature where there is ample proof that the cyclization is neither initiated by triplet sensitization nor quenched by triplet quenchers.<sup>101</sup> The literature also confirms that substituents that promote intersystem crossing (such as nitro and acetyl) inhibit the reaction.<sup>102</sup> The most likely explanation lies in the fact that the  $6\pi$ -electrocyclization yields a *4a,4b*-dihydrophenanthrene derivative that has to be oxidized to the final product **37**. In the absence of a suitable oxidizing agent it will undergo a photoinduced electrocyclic ring opening back to the starting material.<sup>103</sup> The introduction of iodoarene **25a** or **25b** provides a suitable oxidizing agent in the form of an iodine atom (or molecule) derived from the homolytic cleavage of the parent iodoarene. No reactivity is observed in the presence of 4-chlorobenzonitrile (**23a**) simply because this haloarene is resistant to homolytic cleavage and thus fails to provide a suitable oxidizing agent.



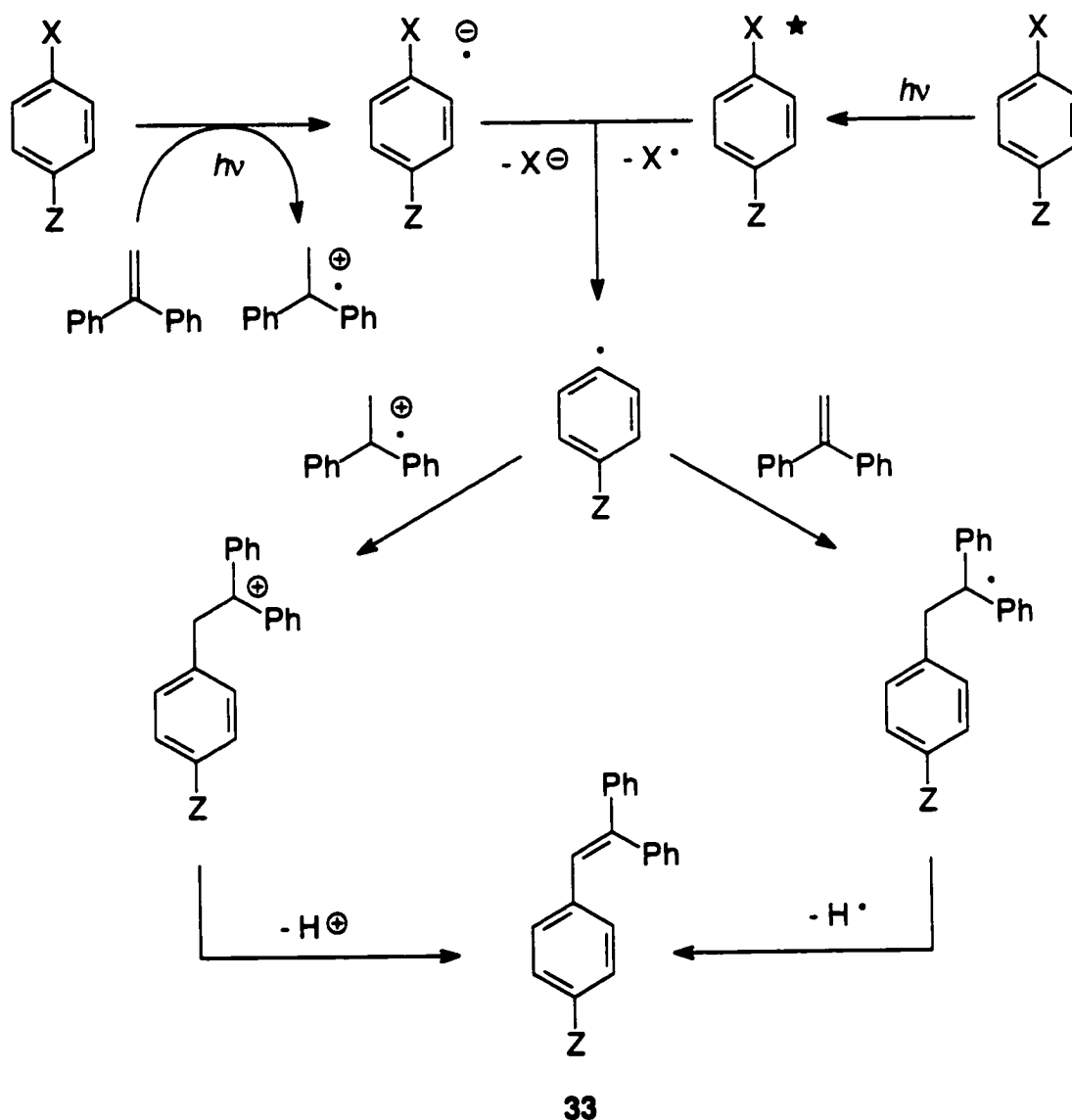
- Scheme 59 -

The formation of 1-(4-cyanophenyl)-2-methoxy-2,2-diphenylethane (**35a**) in the halobenzonitrile reactions is consistent with the PET mechanism proposed in Scheme 38. Although compound **35a** is dominant among the products incorporating the cyanophenyl group early in the course of the reaction, its relative yield tends to decrease in favour of 1-(4-cyanophenyl)-2,2-diphenylethene (**33a**) as the reaction proceeds.

Control experiments have established that **33a** and its methoxy analogue **33b** can be formed from the thermal, acid-catalyzed elimination of methanol from the corresponding ethers **35a** and **35b**, respectively. It is not clear whether this is the only route for the formation of these products. Various other photochemical pathways, both PET-induced and not, can be considered (Scheme 60). In a PET pathway, the aryl radical formed upon cleavage of the haloarene radical anion can add to the alkene radical cation to give an adduct cation that can then deprotonate to give the olefinic product **33**. Conversely, in a non-PET radical pathway, the aryl radical formed upon homolytic cleavage of the haloarene excited state can add to a neutral alkene molecule and the adduct radical can subsequently lose a hydrogen atom to give **33** or disproportionate to **33** and **34**.

Nevertheless, the thermal conversion of **35** to **33** is, quite possibly, partially responsible for the formation of **33**. It provides a rational explanation for the fact that the ratios of **33a:35a** and **33b:35b** increase as the photoreaction proceeds. The photochemical reaction generates a hydrogen halide. Hence, the acidity of the medium increases as the reaction occurs. The larger ratio of **33:35** observed on going from chloro- to iodoarene might be due to the relative acidity of these haloacids.

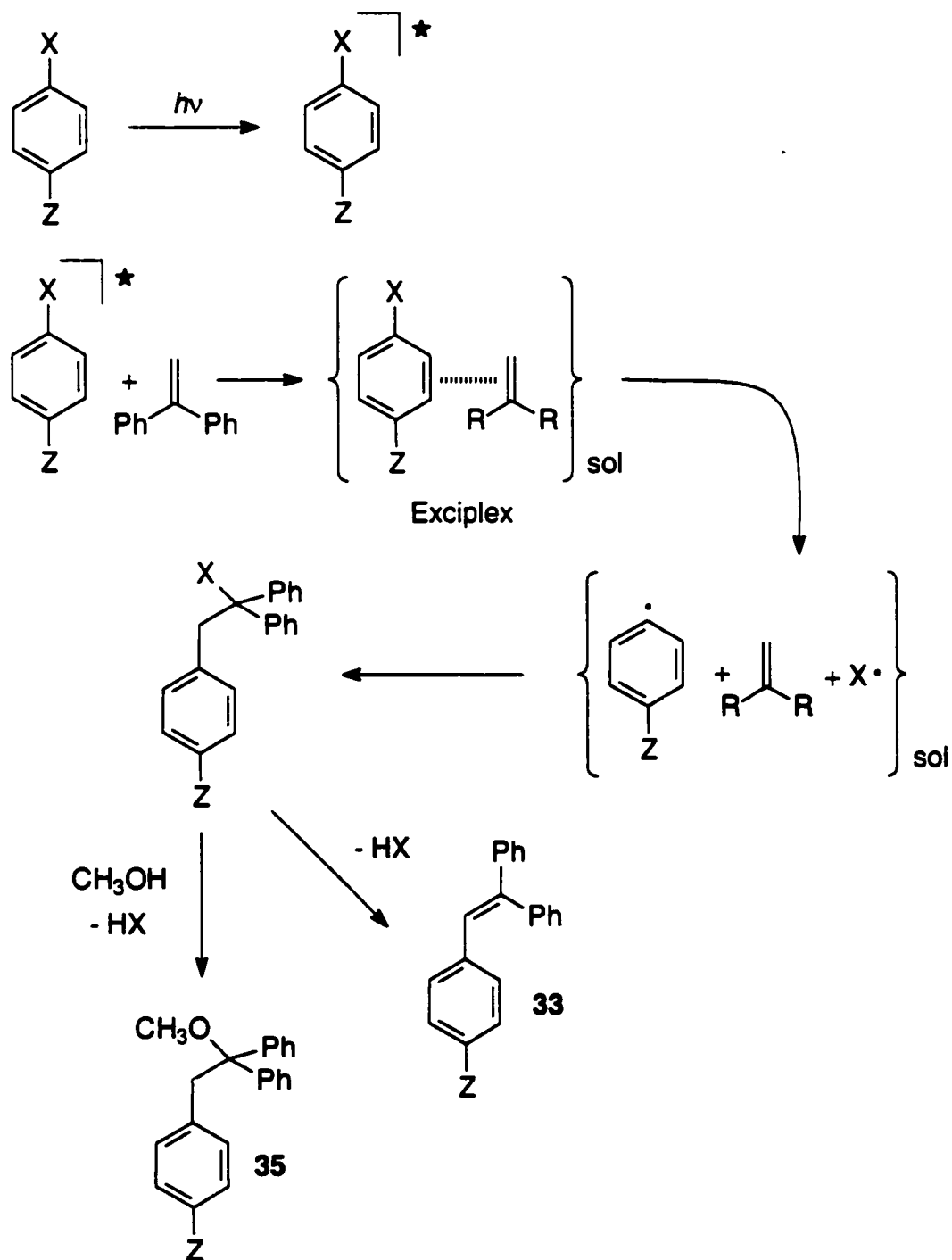
The fact that the photochemistry of the 4-haloanisoles (**23b–25b**) and 1,1-diphenylethene (**26**) leads to a series of alkene–arene products similar to that obtained from the halobenzonitriles questions the PET nature of the mechanism. The unfavourable energetics and the absence of the diagnostic *anti*-Markovnikov ether (**27**) in these reactions clearly dismiss the possibility of an underlying PET mechanism in the haloanisole photochemistry.



- Scheme 60 -

One cannot rule out, however, that the same products might be formed via different mechanisms in the halobenzonitrile and haloanisole cases. It has already been demonstrated that the formation of the alkenes **33a** and **33b** can be rationally explained using both PET-induced and direct homolysis mechanisms (Scheme 60). Similar mechanisms are plausible for the formation of 1-(4-cyanophenyl)-2-methoxy-2,2-diphenylethane (**35a**) and its 4-methoxyphenyl analogue **35b**. The PET-induced mechanism, which is potentially responsible for

the formation of **35a**, has been highlighted in Scheme 38. The alternative non-PET pathway involves the formation of an aryl radical via direct homolytic cleavage followed by addition of the aryl and halide radicals to the alkene (Scheme 61). This is basically an insertion of the alkene across the aryl carbon-

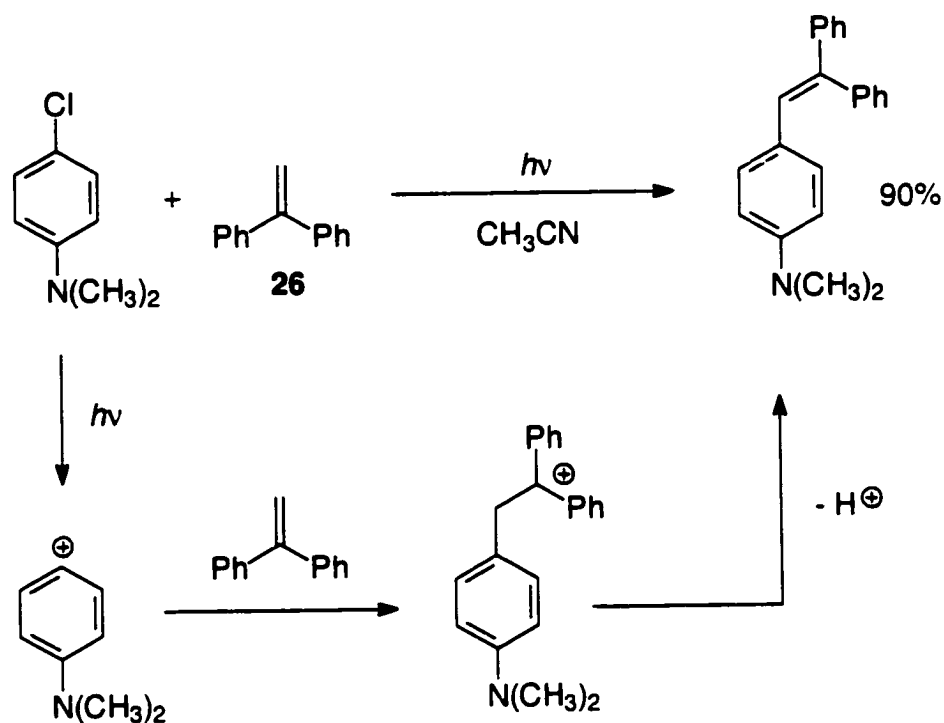


- Scheme 61 -

halogen bond. The resulting 1-aryl-2-halo-2,2-diphenylethane may subsequently undergo an  $S_N1$  reaction with methanol to furnish the observed products, ethers **35**, or it may undergo an E1 reaction to give the corresponding alkenes **33**. This key halogen-containing intermediate compound has not been observed; however, its absence is consistent with its expected high  $S_N1$  and E1 reactivities under the reaction conditions.

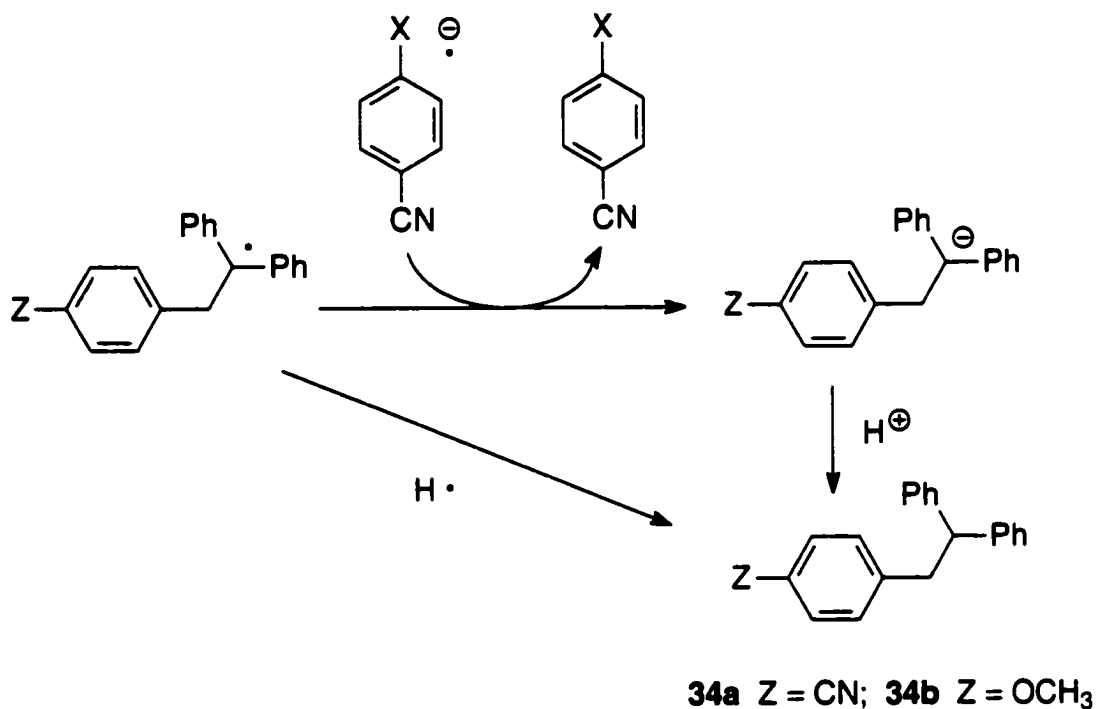
Another mechanism which might explain the haloanisole photochemistry was recently proposed by Albini and co-workers.<sup>104</sup> These researchers propose that the photochemical reaction between 4-chloro-*N,N*-dimethylaniline and a variety of alkenes including **26** in acetonitrile proceeds via an aryl cation (Scheme 62). This aryl cation is thought to form via the *heterolytic* cleavage of the aryl carbon-chlorine bond in the chloroaniline. The products obtained are very reminiscent of our reactions. Whether the 4-methoxyphenyl cation is a possible intermediate or not, is not certain at this stage. The 4-(*N,N*-dimethylamino)phenyl cation has a particular stability associated with it. Nevertheless, if the 4-methoxyphenyl cation does form, we can easily envisage a pathway similar to Scheme 62 leading to products **33b** and **35b**.

Another pair of products that we have seen in small quantities in all the reactions involving cleavable haloarenes are the 1-aryl-2,2-diphenylethanes **34a** and **34b**. Deuterium incorporation studies involving **34a** in methanol-*O*-d indicate 41–64% deuterium incorporation at the bisbenzylic position, suggesting a 2-aryl-1,1-diphenylethyl anion as precursor. The plausible route to this species is via reduction of the corresponding radical (Scheme 63). Calculations suggest that this electron transfer step is energetically viable when a halobenzonitrile radical anion acts as reducing agent. However, such a situation requires the halobenzonitrile radical anion to survive long enough for the electron transfer to occur. As previously mentioned, this is surprising in view of the short lifetimes of these species. Nevertheless, the variation in the yield of **34** in relation to the different haloarenes investigated does support this hypothesis. The 4-chlorobenzonitrile (**23a**) radical anion, which is the longest-lived anion radical



- Scheme 62 -

among all the cleavable haloarenes studied, does result in the greatest yield of **34a** (12%). This decreases in the case of the bromobenzonitrile **24a** (8%) and further in the case of the iodo derivative **25a** (5%). The haloanisoles **23b–25b** furnish only trace amounts (< 2%) of the corresponding product **34b**, although in these cases it is dubious whether the haloanisole radical anions are actually formed. This last point, as well as the incomplete deuterium incorporation in **34a** in the methanol-*O*-d reactions, requires a second reaction pathway that does not involve protonation of an anionic precursor. We suggest that this alternative route involves hydrogen atom abstraction by the 2-aryl-1,1-diphenylethyl radical (Scheme 63).



- Scheme 63 -

### 3.4 CONCLUSIONS

The involvement of a cyanoarene bearing a cleavable group has a drastic effect on the outcome of the photochemical reaction between cyanoarenes, olefins, and nucleophiles. The previously observed photo-NOCAS products are not detected.

The observed photoreactions are mechanistically quite complex. From the above discussion, it is evident that there are several plausible mechanisms that can account for the observed reactivity. It seems very probable that there are various distinct mechanisms in competition with each other, some of which can potentially lead to the same products.

The presence of the *anti*-Markovnikov ether **26** and its high bisbenzylic deuterium incorporation are clear indicators of a PET mechanism. The detection

of the enol ether **29** and its diether products **31** and **32** further support a PET mechanism in which the second electron transfer step (reduction of the alkene–methanol adduct radical) is hindered due to the poor availability of a proper reducing agent (halobenzonitrile radical anion cleaving prior to the second electron transfer). The absence of these products in the haloanisole photochemistry confirms their electron transfer nature. Whether the products incorporating the 4-cyanophenyl group are formed via a PET mechanism is uncertain. A PET pathway that rationally accounts for the formation of **33a** and **35a** has been proposed. Alternatively, a radical mechanism that involves the insertion of the alkene across the carbon–halogen bond is also possible. This mechanism is favoured when considering the observed reactivity in the haloanisole photochemistry. Another potential pathway, recently presented in the literature for similar systems,<sup>104</sup> involves heterolytic cleavage of the aryl carbon–halogen bond from the haloarene excited state and the generation of an aryl cation as reactive intermediate.

We can envisage all these pathways originating from the initial formation of an exciplex of varying degrees of charge separation, depending upon the constituents. If the charge separation is considerable, as expected in the halobenzonitrile cases, then the initial exciplex might lead to a PET mechanism as suggested initially. On the other hand, if charge separation is less favourable, as in the case of the haloanisoles, the haloarene may undergo homolytic (or possibly, heterolytic) dissociation directly from the excited state prior to electron transfer.

It is not certain whether an exciplex-mediated pathway is necessary to account for the bromo- and iodoarene photochemistry. These species were observed to cleave efficiently even in the absence of an alkene. This mechanism does find support, however, upon consideration of the 4-chlorobenzonitrile (**23a**) photochemistry. This compound is stable to irradiation on its own in methanol, but does undergo a photoreaction in the presence of **26**, clearly indicating that the latter is necessary for reaction to occur. This rules out the possibility that a straightforward, unassisted homolytic cleavage of the carbon–chlorine bond is



taking place in this case. The hypothesis of an exciplex, which activates the otherwise unreactive carbon–halogen bond towards cleavage, is a possible explanation for the observed reactivity. The role of exciplexes in similar situations involving haloarenes has been documented.<sup>105,106</sup> In particular, the enhanced homolysis of the carbon-chlorine bond as a consequence of exciplex formation between chloroarenes and dienes has been firmly established.<sup>106</sup> However, no co-reaction between the two constituents was reported in these studies; the haloarenes were observed to undergo reductive dehalogenation.

Further study is required to clarify the contributions of the various mechanisms mentioned. For this purpose it would be instructive to investigate the effect of introducing an olefinic electron donor with an extended electronic absorption spectrum. This would ensure that the olefin acts as the sole light absorber, forcing the halobenzonitrile to function as the ground state electron transfer partner. Avoiding the halobenzonitrile excited state would inhibit all pathways originating from the direct homolytic cleavage of the haloarene excited state, which would facilitate the mechanistic analysis. Once again, the haloanisoles could be used to verify whether any haloarene excited state chemistry is occurring.

An alternative strategy would be to replace the haloarene with a species that will cleave selectively after PET, but not while in its excited state. Some preliminary work was carried out with aryltrimethylammonium salts, but the reactions were not successful.

## **3.5 EXPERIMENTAL SECTION**

### **3.5.1 General information**

Photochemical reactions were monitored and analyzed by gas chromatography–mass spectrometry (GC–MS) using an Hewlett-Packard 5890 gas chromatograph with a 5% phenylmethylsilicone fused silica WCOT column (25 m x 0.20 mm, 0.33  $\mu\text{m}$  film thickness) and an Hewlett-Packard 5970 mass

selective detector. Deuterium incorporation studies were performed using single-ion monitoring mass spectrometry (SIM-MS). Quantitative gas chromatographic analysis was performed on a Perkin-Elmer AutoSystem gas chromatograph equipped with an autosampler, flame ionization detector (FID) and a DB-5 fused silica WCOT column (15 m x 0.25 mm, 1.5  $\mu\text{m}$  film thickness).

Preparative separation of product mixtures was performed using flash chromatography on a 15 cm x 5 cm silica gel (Aldrich, 230–400mesh, 60 $\text{\AA}$ ) column.<sup>59</sup> This was generally followed by preparative, centrifugally accelerated, radial, thin-layer chromatography of the partially purified mixtures using a Chromatotron (Harrison Research) on 4 mm, 2 mm or 1 mm silica gel (Aldrich, TLC grade 7749 with gypsum binder and fluorescent indicator) plates. The mobile phase was typically hexanes with increasing amounts of ethyl acetate. Collected fractions were analyzed by thin-layer chromatography using silica gel plates (Aldrich, 250  $\mu\text{m}$  plate thickness, 5–17  $\mu\text{m}$ , 60  $\text{\AA}$ , with fluorescent indicator) and/or GC–MS.

All  $^1\text{H}$  and  $^{13}\text{C}$  NMR spectra were acquired on a Bruker AC 250F spectrometer at 250.13 MHz for  $^1\text{H}$  and 62.90 MHz for  $^{13}\text{C}$ . Chemical shifts are reported in ppm relative to tetramethylsilane ( $\delta = 0$  ppm) in  $^1\text{H}$  NMR spectra and chloroform-*d* ( $\delta = 77.0$  ppm) in  $^{13}\text{C}$  NMR spectra. Coupling constants (*J* values) are reported in Hz. The multiplicities of the decoupled  $^{13}\text{C}$  NMR signals were determined by *J*-Modulated Spin-Echo (*J*-MOD) experiments. Infrared spectra were recorded as films on sodium chloride plates on a Nicolet 205 FT-IR spectrophotometer and are reported in wavenumbers ( $\text{cm}^{-1}$ ) calibrated against the 1602  $\text{cm}^{-1}$  polystyrene absorption. Ultraviolet-visible absorption spectra were recorded on a Hewlett-Packard 8452A diode-array spectrophotometer within a resolution of  $\pm 1$  nm.

Melting points were determined using a Cybron Corporation Thermolyne apparatus equipped with a digital thermocouple ( $\pm 0.1^\circ\text{C}$ ) and are corrected. Elemental analysis was carried out by Canadian Microanalytical Service Ltd., Delta, BC. High-resolution mass spectrometry for exact mass determination was performed on a CEC 21-110 mass spectrometer using an electron-impact energy

of 70 eV. X-ray crystallographic analysis was performed at room temperature on a Rigaku AFC5R diffractometer with graphite monochromated Cu K $\alpha$  radiation and a 12 kW rotating anode generator.

The cyclic voltammetry was performed on an EG&G PARC Potentiostat Model 173 and an EG&G PARC Universal Programmer Model 175. The measurements were done in a three-electrode electrochemical cell (5 cm<sup>3</sup> volume) equipped with a spherical platinum working electrode, a platinum coil counter electrode and a saturated calomel reference electrode (SCE). The acetonitrile solutions were deoxygenated by bubbling argon (presaturated with solvent) for 15 minutes prior to measurement. Tetraethylammonium perchlorate (0.1 mol dm<sup>-3</sup>) was used as supporting electrolyte. The voltammograms were scanned at 100 mV s<sup>-1</sup> and calibrated against the 1,4-dicyanobenzene reduction wave at -1.66 V.<sup>17b</sup> In all cases the electron transfer was irreversible and the half-wave potential was taken at 0.03 V before the peak potential.<sup>44</sup>

### 3.5.2 Materials

1,4-Dicyanobenzene (98%, Aldrich) was purified by treatment with Norite in methylene chloride, followed by sublimation and recrystallization from 95% ethanol. 4-Iodobenzonitrile (Acros) and 4-bromobenzonitrile (98%, Aldrich) were recrystallized from hexanes while 4-chlorobenzonitrile (99%, Aldrich) was recrystallized from an ethanol-water mixture. Biphenyl (99%, Aldrich) was recrystallized from methanol. 4-Fluorobenzonitrile (99%, Aldrich), 4-chloroanisole (99%, Aldrich), 4-bromoanisole (99%, Aldrich), 4-iodoanisole (99%, Aldrich), and 1,1-diphenylethene (97%, Aldrich) were used as received.

Methanol was purified by reflux and fractional distillation over magnesium and stored over 3 Å molecular sieves (Aldrich). Hexanes for preparative chromatography were fractionally distilled prior to use while ethyl acetate was used without further purification. Acetonitrile (anhydrous, Aldrich) for electrochemistry was used as received and transferred under nitrogen by cannula.

### 3.5.3 Irradiations

Investigative irradiations were performed in 2 cm<sup>3</sup> sample volumes in 20 cm x 0.5 cm tubes using a 1 kW medium pressure mercury-arc lamp (CGE) fitted with a Quartz water-cooled jacket immersed in a bath at 5°C. Reactions used for quantitative analyses were performed in 10 cm<sup>3</sup> sample volumes in 20 cm x 1 cm tubes while large-scale preparative photochemical reactions were carried out in 20 cm<sup>3</sup> volumes in 20 cm x 2 cm tubes. All large-scale and quantitative-analysis reactions were deoxygenated by nitrogen ebullition for 15 minutes prior to irradiation. Tube distance from lamp axis was ca. 6 cm. Unless otherwise stated, all irradiations were carried out behind Pyrex ( $\lambda > 280\text{nm}$ ).

Dark control experiments were prepared for all major photochemical reaction mixtures. These consisted of solutions identical in composition to the ones being irradiated but stored in the dark. These controls were monitored after a time interval equal to that of the irradiated solutions and in no case was any reactivity observed, except where specifically mentioned.

Reaction details reported below are for the 10 cm<sup>3</sup> quantitative-analysis samples unless otherwise stated. All yields were calibrated with respect to consumed starting material, *i.e.*, the haloarene or 1,1-diphenylethene, depending on whether the product incorporates the 4-cyanophenyl/4-methoxyphenyl group or not. All quantitative-analysis GC runs were done in triplicate and used an internal standard method for calibration. Wherever relevant, isolated yields are also reported.

### 3.5.4 Irradiation of 1,4-dicyanobenzene (2), biphenyl (6), and 1,1-diphenylethene (26) in methanol.

A solution of 1,4-dicyanobenzene (**2**, 0.02 mol dm<sup>-3</sup>), biphenyl (**6**, 0.05 mol dm<sup>-3</sup>), and 1,1-diphenylethene (**26**, 0.05 mol dm<sup>-3</sup>) in methanol (10 cm<sup>3</sup>) was irradiated for 6 h. Calibrated GC-FID analysis indicated 100% alkene consumption together with a 92% recovery of **2** and an 84% recovery of **6**. Products resulting from the photoreaction include 1-methoxy-2,2-diphenylethane (**27**, 83%), 1-methoxy-1,1-diphenylethane (**28**, 7%), and 1-methoxy-2,2-

diphenylethene (**29**, 2%). A pure sample of **27** was obtained from a large-scale photoreaction (30 cm<sup>3</sup>) identical in composition to the above, while **28** was obtained from an alternative photoreaction (*vide infra*).

SIM-MS of an identical photoreaction in methanol-*O*-d indicated 96% deuterium incorporation at the bisbenzylic position (C-2) of **27**.

#### *1-Methoxy-2,2-diphenylethane (27)*

Isolated yield: 81%, colourless oil;  $\nu_{\max}$ (film; NaCl)/cm<sup>-1</sup> 3087, 3061, 3027, 2982, 2922, 2874, 1601, 1495, 1451, 1121 and 699; <sup>1</sup>H NMR spectrum in accordance with published data:<sup>107</sup>  $\delta_{\text{H}}$ (250.13 MHz; CDCl<sub>3</sub>; Me<sub>4</sub>Si) 3.36 (3 H, s), 3.92 (2 H, d, *J* 7.3), 4.29 (1 H, t, *J* 7.3) and 7.16-7.29 (10 H, m);  $\delta_{\text{C}}$ (62.90 MHz; CDCl<sub>3</sub>) 51.0 (d), 58.9 (q), 76.0 (t), 126.5 (d), 128.2 (d), 128.4 (d) and 142.1 (s); *m/z* 212 (M<sup>+</sup>, 4%), 167 (100), 165 (36), 152 (19) and 77 (7).

Compound **29** was positively identified and characterized by alternative synthesis via a Wittig reaction from benzophenone and methoxymethyltriphenylphosphonium bromide, using a literature procedure with minor modifications.<sup>108</sup>

#### *1-Methoxy-2,2-diphenylethane (29)*

Colourless oil;  $\nu_{\max}$ (film; NaCl)/cm<sup>-1</sup> 3055, 3029, 2932, 2836, 1634, 1496, 1447, 1231, 1108, 764 and 698;  $\delta_{\text{H}}$ (250.13 MHz; CDCl<sub>3</sub>; Me<sub>4</sub>Si) 3.76 (3 H, s), 6.45 (1 H, s) and 7.18-7.40 (10 H, m);  $\delta_{\text{C}}$ (62.90 MHz; CDCl<sub>3</sub>) 60.6 (q), 120.5 (s), 126.4 (d), 126.6 (d), 127.6 (d), 128.0 (d), 128.2 (d), 128.3 (d), 129.8 (d), 137.6 (s), 140.4 (s) and 146.4 (d); *m/z* 210 (M<sup>+</sup>, 100%), 167(98) and 165(78).

### **3.5.5 Irradiation of 1,1-diphenylethane (26) in methanol.**

A solution of 1,1-diphenylethane (**26**, 0.05 mol dm<sup>-3</sup>) in methanol (10 cm<sup>3</sup>) was irradiated for 300 h. Calibrated GC-FID analysis indicated that 81% of **26** was consumed, yielding 1-methoxy-2,2-diphenylethane (**27**, 3%), 1-methoxy-1,1-diphenylethane (**28**, 33%), and 1,1-diphenylethane (**30**, 11%). Appreciable

polymerization was also noticed. Pure samples of **28** and **30** were isolated from a large-scale photoreaction (100 cm<sup>3</sup>) identical in composition to the above.

**1-Methoxy-1,1-diphenylethane (28).**

Isolated yield: 22%, colourless oil;  $\nu_{\max}$ (film; NaCl)/cm<sup>-1</sup> 3089, 3059, 3025, 2981, 2935, 2825, 1492, 1446, 1104, 755 and 699; <sup>1</sup>H NMR spectrum in accordance with published data.<sup>81</sup>  $\delta_{\text{H}}$ (250.13 MHz; CDCl<sub>3</sub>; Me<sub>4</sub>Si) 1.56 (3 H, s), 3.16 (3 H, s), 7.22-7.38 (10 H, m);  $\delta_{\text{C}}$ (62.90 MHz; CDCl<sub>3</sub>) 25.1 (q), 50.6 (q), 80.8 (s), 126.77 (d), 126.74 (d), 127.9 (d) and 146.4 (s); *m/z* 212 (M<sup>+</sup>, 3%), 197 (100), 180 (19), 165 (32), 135 (53), 105(31), 91(6) and 77(53).

**1,1-Diphenylethane (30).**

Isolated yield: 10%, colourless oil;  $\nu_{\max}$ (film; NaCl)/cm<sup>-1</sup> 3061, 3026, 2967, 1600, 1493, 1450, 1026 and 699; <sup>1</sup>H NMR spectrum in accordance with published data:<sup>109</sup>  $\delta_{\text{H}}$ (250.13 MHz; CDCl<sub>3</sub>; Me<sub>4</sub>Si) 1.64 (3 H, d, *J* 7.3), 4.15 (1 H, q, *J* 7.3) and 7.13-7.31 (10 H, m);  $\delta_{\text{C}}$ (62.90 MHz; CDCl<sub>3</sub>) 21.8 (q), 44.7 (d), 126.0 (d), 127.6 (d), 128.3 (d) and 146.3 (s); *m/z* 182 (M<sup>+</sup>, 35%), 167 (100) and 165 (31).

**3.5.6 Irradiation of 1,4-dicyanobenzene (2), biphenyl (6), and 1-methoxy-2,2-diphenylethane (29) in methanol.**

A solution of 1,4-dicyanobenzene (**2**, 0.02 mol dm<sup>-3</sup>), biphenyl (**6**, 0.05 mol dm<sup>-3</sup>), and 1-methoxy-2,2-diphenylethane (**29**, 0.05 mol dm<sup>-3</sup>) in methanol (10 cm<sup>3</sup>) was irradiated for 10 h. Calibrated GC-FID analysis of the final photolysate revealed that 92% of the starting alkene (**29**) was consumed while 100% of **2** and 79% of **6** remained unreacted. Products observed included 1,1-dimethoxy-2,2-diphenylethane (**31**, 85%) and 1,2-dimethoxy-1,1-diphenylethane (**32**, 2%).

A pure sample of **31** was isolated from a large-scale photoreaction (30 cm<sup>3</sup>) identical in composition to the above, while a pure sample of **32** was obtained from an alternative photoreaction (*vide infra*).

**1,1-Dimethoxy-2,2-diphenylethane (31)**

Isolated yield: 56%, colourless oil; Spectral data in accordance with literature report:<sup>110</sup>  $\nu_{\max}$ (film; NaCl)/ $\text{cm}^{-1}$  3030, 2930, 1601, 1495, 1450, 1120, 1062, 750 and 700;  $\delta_{\text{H}}$ (250.13 MHz;  $\text{CDCl}_3$ ;  $\text{Me}_4\text{Si}$ ) 3.31 (6 H, s), 4.23 (1 H, d,  $J$  7.6), 5.00 (1 H, d,  $J$  7.6) and 7.18-7.33 (10 H, m);  $\delta_{\text{C}}$ (62.90 MHz;  $\text{CDCl}_3$ ) 54.0 (q), 54.5 (d), 106.4 (d), 126.4 (d), 128.3 (d), 128.7 (d) and 141.1 (s);  $m/z$  210 ( $\text{M}^+$ , 8%), 167 (12), 165 (14), 152 (6), 105 (6) and 75 (100).

**3.5.7 Irradiation of 1-methoxy-2,2-diphenylethene (29) in methanol.**

A solution of 1-methoxy-2,2-diphenylethene (**29**, 0.05 mol  $\text{dm}^{-3}$ ) in methanol (10  $\text{cm}^3$ ) was irradiated for 300 h. Calibrated GC-FID analysis of the photolysate indicated that 86% of the starting material (**29**) was consumed, yielding 1,1-dimethoxy-2,2-diphenylethene (**31**, 40%) and 1,2-dimethoxy-1,1-diphenylethene (**32**, 23%).

A pure sample of **32** was obtained from a large-scale photoreaction (60  $\text{cm}^3$ ) of identical composition to the above.

**1,2-Dimethoxy-1,1-diphenylethane (32)**

Isolated yield: 7%, colourless oil;  $\nu_{\max}$ (film; NaCl)/ $\text{cm}^{-1}$  3059, 3027, 2981, 2931, 2891, 1493, 1448, 1191, 1130, 1102, 1078, 756 and 700;  $\delta_{\text{H}}$ (250.13 MHz;  $\text{CDCl}_3$ ;  $\text{Me}_4\text{Si}$ ) 3.23 (3 H, s), 3.33 (3 H, s), 4.11 (2 H, s) and 7.23-7.38 (10 H, m);  $\delta_{\text{C}}$ (62.90 MHz;  $\text{CDCl}_3$ ) 51.6 (q), 59.6 (q), 76.3 (t), 82.2 (s), 127.1 (d), 127.3 (d), 128.0 (d) and 143.1 (s);  $m/z$  210 ( $\text{M}^+$ , 6%), 197 (100), 105 (71) and 77 (69).

**3.5.8 Irradiation of 4-fluorobenzonitrile (22a) in methanol.**

A solution of 4-fluorobenzonitrile (**22a**, 0.05 mol  $\text{dm}^{-3}$ ) in methanol (10  $\text{cm}^3$ ) was irradiated for 50 h. Calibrated GC-FID analysis of the final photolysate revealed no product formation together with 100% recovery of **22a**. Similar irradiation behind Quartz ( $\lambda > 190$  nm) furnished identical results.

### 3.5.9 Irradiation of 4-fluorobenzonitrile (**22a**) and 1,1-diphenylethene (**26**) in methanol.

A solution of 4-fluorobenzonitrile (**22a**, 0.05 mol dm<sup>-3</sup>) and 1,1-diphenylethene (**26**, 0.10 mol dm<sup>-3</sup>) in methanol (10 cm<sup>3</sup>) was irradiated for 75 h. Calibrated GC–FID analysis of the final photolysate revealed that 67% of **26** had been consumed while **22a** showed a 100% recovery. The products observed included 1-methoxy-2,2-diphenylethane (**27**, 21%), 1-methoxy-1,1-diphenylethane (**28**, 10%), and 1,1-diphenylethane (**30**, 2%).

SIM-MS of an identical photoreaction in methanol-*O*-d indicated 47% deuterium incorporation at the bisbenzylic position (C-2) of **27**.

### 3.5.10 Irradiation of 4-chlorobenzonitrile (**23a**) in methanol.

A solution of 4-chlorobenzonitrile (**23a**, 0.05 mol dm<sup>-3</sup>) in methanol (10 cm<sup>3</sup>) was irradiated for 50 h. Calibrated GC–FID analysis of the final photolysate revealed no product formation together with 100% recovery of **23a**.

### 3.5.11 Irradiation of 4-chlorobenzonitrile (**23a**) and 1,1-diphenylethene (**26**) in methanol.

A solution of 4-chlorobenzonitrile (**23a**, 0.05 mol dm<sup>-3</sup>) and 1,1-diphenylethene (**26**, 0.10 mol dm<sup>-3</sup>) in methanol (10 cm<sup>3</sup>) was irradiated for 75 h. Calibrated GC–FID analysis of the final photolysate revealed that 78% of **26** and 46% of **23a** had been consumed. The products observed included 1-methoxy-2,2-diphenylethane (**27**, 26%), 1-methoxy-1,1-diphenylethane (**28**, 2%), 1-methoxy-2,2-diphenylethane (**29**, 7%), 1,1-diphenylethane (**30**, <2%), 1,1-dimethoxy-2,2-diphenylethane (**31**, 6%), 1,2-dimethoxy-1,1-diphenylethane (**32**, 2%), 1-(4-cyanophenyl)-2,2-diphenylethane (**33a**, 3%), 1-(4-cyanophenyl)-2,2-diphenylethane (**34a**, 12%), and 1-(4-cyanophenyl)-2-methoxy-2,2-diphenylethane (**35a**, 17%).

Pure samples of **34a** and **35a** were obtained from a large-scale photoreaction (60 cm<sup>3</sup>) having an identical composition to the above. A pure sample of **33a** was obtained from an alternative photoreaction (*vide infra*).



SIM-MS of an identical photoreaction in methanol-*O*-d indicated 75% deuterium incorporation at the bisbenzylic position (C-2) of **27** and 64% deuterium incorporation at the bisbenzylic position (C-2) of **34a**.

*1-(4-Cyanophenyl)-2,2-diphenylethane (34a)*

Isolated yield: 2%, colourless oil;  $\delta_{\text{H}}$ (250.13 MHz; CDCl<sub>3</sub>; Me<sub>4</sub>Si) 3.41 (2 H, d, *J* 7.8), 4.19 (1 H, t, *J* 7.8), 7.07 (2 H, half AA'BB'), 7.16-7.25 (10 H, m) and 7.44 (2 H, half AA'BB');  $\delta_{\text{C}}$ (62.90 MHz; CDCl<sub>3</sub>) 42.2 (t), 51.5 (d), 119.0 (s), 122.8(s), 126.5 (d), 127.9 (d), 128.5 (d), 129.8 (d), 131.9 (d), 143.5(s) and 145.9 (s); *m/z* 167 (M<sup>+</sup>, 100%), 165 (30), 152 (17) and 116 (3) (M<sup>+</sup>, 283.1371. C<sub>21</sub>H<sub>17</sub>N requires *M*, 283.1361).

*1-(4-Cyanophenyl)-2-methoxy-2,2-diphenylethane (35a)*

Isolated yield: 3%, colourless crystals, mp 147.1-148.3°C (from methanol) (Found C, 84.0; H, 6.1; N, 4.4. C<sub>22</sub>H<sub>19</sub>NO requires C, 84.3; H, 6.1, N, 4.5%); obtained C 84.04%, H 6.06%, N 4.37%;  $\nu_{\text{max}}$ (film; NaCl)/cm<sup>-1</sup> 3054, 3027, 2934, 2826, 2221, 1606, 1490, 1446, 1192, 1079, 826, 775, 751 and 698;  $\delta_{\text{H}}$ (250.13 MHz; CDCl<sub>3</sub>; Me<sub>4</sub>Si) 3.15 (3 H, s), 3.63 (2 H, s), 6.83 (2 H, half AA'BB'), 7.18-7.29 (10 H, m) and 7.34 (2 H, half AA'BB');  $\delta_{\text{C}}$ (62.90 MHz; CDCl<sub>3</sub>) 42.0 (t), 51.0 (q), 83.4 (s), 109.8 (s), 119.2 (s), 127.1 (d), 127.5 (d), 127.9 (d), 131.1 (d), 131.2 (d), 142.8 (s) and 143.8 (s); *m/z* 281 (M<sup>+</sup>, 5%), 197 (100), 105 (34) and 77 (28).

**3.5.12 Irradiation of 4-bromobenzonitrile (24a) in methanol.**

A solution of 4-bromobenzonitrile (**24a**, 0.05 mol dm<sup>-3</sup>) in methanol (10 cm<sup>3</sup>) was irradiated for 50 h. Calibrated GC-FID analysis of the final photolysate revealed 100% **24a** consumption and the formation of benzonitrile (**35a**) in 71% yield. Benzonitrile (**35a**) was identified by comparison with a commercial sample.

### 3.5.13 Irradiation of 4-bromobenzonitrile (24a) and 1,1-diphenylethene (26) in methanol.

A solution of 4-bromobenzonitrile (**24a**, 0.05 mol dm<sup>-3</sup>) and 1,1-diphenylethene (**26**, 0.10 mol dm<sup>-3</sup>) in methanol (10 cm<sup>3</sup>) was irradiated for 75 h. Calibrated GC–FID analysis of the final photolysate revealed that 90% of **26** and 54% of **24a** had been consumed. The products observed included 1-methoxy-2,2-diphenylethane (**27**, 17%), 1-methoxy-1,1-diphenylethane (**28**, 2%), 1-methoxy-2,2-diphenylethene (**29**, 4%), 1,1-diphenylethane (**30**; <2%), 1,1-dimethoxy-2,2-diphenylethane (**31**, 5%), 1,2-dimethoxy-1,1-diphenylethane (**32**, <2%), 1-(4-cyanophenyl)-2,2-diphenylethane (**33a**, 5%), 1-(4-cyanophenyl)-2,2-diphenylethane (**34a**, 8%), 1-(4-cyanophenyl)-2-methoxy-2,2-diphenylethane (**35a**, 11%), benzonitrile (**36a**, 13%), and 3-cyano-9-phenylphenanthrene (**37a**, 4%).

A pure sample of **37a** was obtained from an alternative photoreaction (*vide infra*).

SIM-MS of an identical photoreaction in methanol-*O*-d indicated 77% deuterium incorporation at the bisbenzylic position (C-2) of **27** and 50% deuterium incorporation at the bisbenzylic position (C-2) of **34a**.

### 3.5.14 Irradiation of 4-iodobenzonitrile (25a) in methanol.

A solution of 4-iodobenzonitrile (**25a**, 0.05 mol dm<sup>-3</sup>) in methanol (10 cm<sup>3</sup>) was irradiated for 50 h. Calibrated GC–FID analysis of the final photolysate revealed 89% **25a** consumption and the formation of benzonitrile (**36a**) in 85% yield.

### 3.5.15 Irradiation of 4-iodobenzonitrile (25a) and 1,1-diphenylethene (26) in methanol.

A solution of 4-iodobenzonitrile (**25a**, 0.05 mol dm<sup>-3</sup>) and 1,1-diphenylethene (**26**, 0.10 mol dm<sup>-3</sup>) in methanol (10 cm<sup>3</sup>) was irradiated for 75 h. Calibrated GC–FID analysis of the final photolysate revealed that 88% of **26** and 100% of **25a** had been consumed. The products observed 1-methoxy-2,2-

diphenylethane (**27**, 12%), included 1-methoxy-1,1-diphenylethane (**28**, 2%), 1-methoxy-2,2-diphenylethane (**29**, 11%), 1,1-diphenylethane (**30**, <2%), 1,1-dimethoxy-2,2-diphenylethane (**31**, 19%), 1,2-dimethoxy-1,1-diphenylethane (**32**, <2%), 1-(4-cyanophenyl)-2,2-diphenylethane (**33a**, 38%), 1-(4-cyanophenyl)-2,2-diphenylethane (**34a**, 5%), 1-(4-cyanophenyl)-2-methoxy-2,2-diphenylethane (**35a**, 5%), benzonitrile (**36a**, 23%), and 3-cyano-9-phenylphenanthrene (**37a**, 21%).

Pure samples of **33a** and **37a** were obtained from a large-scale photoreaction (60 cm<sup>3</sup>) identical in composition to the above.

SIM-MS of an identical photoreaction in methanol-*O*-d indicated 86% deuterium incorporation at the bisbenzylic position (C-2) of **27** and 41% deuterium incorporation at the bisbenzylic position (C-2) of **34a**.

#### *1-(4-Cyanophenyl)-2,2-diphenylethane (33a)*

Isolated yield: 36%, colourless needles, mp 116.5-117.1°C (from hexanes), lit. mp 107-9°C;<sup>111</sup>  $\nu_{\max}$ (film; NaCl)/cm<sup>-1</sup> 3057, 3026, 2225, 1601, 1499, 1444, 827, 765, 737, 698 and 626;  $\delta_{\text{H}}$ (250.13 MHz; CDCl<sub>3</sub>; Me<sub>4</sub>Si) 6.94 (1 H, s) and 7.06-7.41 (14 H, m);  $\delta_{\text{C}}$ (62.90 MHz; CDCl<sub>3</sub>) 109.7 (s), 119.0 (s), 126.1 (d), 127.8 (d), 128.1 (d), 128.3(d), 128.4(d), 218.9 (d), 129.9 (d), 130.1 (d), 131.7 (d), 139.4 (s), 142.1 (s), 142.5 (s) and 146.2 (s); *m/z* 281 (M<sup>+</sup>, 100%), 266 (16), 203 (29) and 178(10).

#### *3-Cyano-9-phenylphenanthrene (37a)*

Isolated yield: 20%, colourless needles, mp 136.0-136.6°C (from hexanes);  $\nu_{\max}$ (film; NaCl)/cm<sup>-1</sup> 3062, 3025, 2225, 1616, 1517, 1494, 1443, 1431, 1413, 889, 813, 770, 725 and 702;  $\delta_{\text{H}}$ (250.13 MHz; CDCl<sub>3</sub>; Me<sub>4</sub>Si) 7.48-7.55 (10 H, m), 7.62 (1 H, app. td), 7.69 (1 H, s), 7.76 (1 H, app. td), 7.77 (1 H, dd, *J* 8.2, 1.5), 7.95 (1 H, d, *J* 8.2), 8.71 (1 H, d, *J* 8.2) and 9.04 (1 H, s);  $\delta_{\text{C}}$ (62.90 MHz; CDCl<sub>3</sub>) 109.6 (s), 119.6 (s), 122.8 (d), 126.6 (d), 127.3 (d), 127.6 (d), 127.7 (d), 127.9 (d), 128.1 (d), 128.2 (d), 128.5 (d), 129.5 (d), 129.6 (s), 129.7 (s), 129.8 (d), 131.4 (s), 133.8 (s), 139.8 (s) and 142.3 (s); *m/z* 279 (M<sup>+</sup>, 100%) and 125 (19).

Crystal Data:<sup>§</sup> C<sub>31</sub>H<sub>13</sub>N, *M* = 279.34, monoclinic, *a* = 7.817(4), *b* = 9.224(5), *c* = 20.638(6) Å, *β* = 99.43(4)°, *V* = 1468(1) Å<sup>3</sup>, *T* = 296K, space group P2<sub>1</sub>/a (no. 14), *Z* = 4, *μ* (Mo-Kα) = 0.73 cm<sup>-1</sup>, 2487 reflections measured, 2277 unique (*R*<sub>int</sub> = 0.143). The final *R* and *R*<sub>w</sub> were 0.059 and 0.068 respectively and are based on 512 observed reflections (*I* > 3.00σ(*I*)) and 117 parameters. All data was corrected for Lorentz and polarization effects. An empirical absorption correction (*ψ* scan) was also applied. Some non-hydrogen atoms were refined anisotropically, while the rest were refined isotropically; the phenyl group was refined as a rigid body. All calculations were performed using the teXsan crystallographic software package.<sup>60</sup>

### 3.5.16 Irradiation of 1-(4-cyanophenyl)-2,2-diphenylethene (**33a**) in methanol.

A solution of 1-(4-cyanophenyl)-2,2-diphenylethene (**33a**, 0.025 mol dm<sup>-3</sup>) in methanol (2 cm<sup>3</sup>) was irradiated for 6 h. No consumption of the starting material was observed. Similarly, a solution of **33a** (0.025 mol dm<sup>-3</sup>) and 4-chlorobenzonitrile (**23a**, 0.025 mol dm<sup>-3</sup>) in methanol (2 cm<sup>3</sup>) did not result in any consumption of starting materials after 6 h of irradiation. Conversely, a solution of **33a** (0.025 mol dm<sup>-3</sup>) and 4-iodobenzonitrile (**25a**, 0.025 mol dm<sup>-3</sup>) in methanol (2 cm<sup>3</sup>) resulted in 98% **33a** and 72% **25a** consumption after 6 h irradiation. Also observed was the formation of benzonitrile (**36a**, 80%) and 3-cyano-9-phenylphenanthrene (**37a**, 98%).

---

<sup>§</sup> Crystallographic data has been deposited as supplementary material and may be purchased from: The Depository of Unpublished Data, Document Delivery, CISTI, National Research Council Canada, Ottawa, Canada, K1A 0S2. Details of data collection, structure analysis and refinement, and tables of interatomic distances and bond angles have also been deposited with the Cambridge Crystallographic Data Centre and can be obtained upon request from: The Director, Cambridge Crystallographic Data Centre, University Chemical Laboratory, 12 Union Road, Cambridge, CB2 1EZ, U.K.

### 3.5.17 Irradiation of 4-chloroanisole (**23b**) in methanol.

A solution of 4-chloroanisole (**23b**, 0.05 mol dm<sup>-3</sup>) in methanol (10 cm<sup>3</sup>) was irradiated for 75 h. Calibrated GC–FID analysis revealed 88% **23b** consumption together with the formation of anisole (**36b**, 56%) and 1,4-dimethoxybenzene (**38**, 12%). Anisole (**36b**) and 1,4-dimethoxybenzene (**38**) were identified by comparison with commercial samples.

### 3.5.18 Irradiation of 4-chloroanisole (**23b**) and 1,1-diphenylethene (**26**) in methanol.

A solution of 4-chloroanisole (**23b**, 0.05 mol dm<sup>-3</sup>) and 1,1-diphenylethene (**26**, 0.10 mol dm<sup>-3</sup>) in methanol (10 cm<sup>3</sup>) was irradiated for 75 h. Calibrated GC–FID analysis revealed 78% consumption of **26** and 79% consumption of **23b** together with the formation of 1-methoxy-2,2-diphenylethane (**27**, 5%), 1-methoxy-1,1-diphenylethane (**28**, 5%), 1,1-diphenylethane (**30**, 2%), 1-(4-methoxyphenyl)-2,2-diphenylethane (**33b**, 40%), 1-(4-methoxyphenyl)-2,2-diphenylethane (**34b**, < 2%), 1-methoxy-2-(4-methoxyphenyl)-1,1-diphenylethane (**35b**, 4%), anisole (**36b**, 14%), 3-methoxy-9-phenylphenanthrene (**37b**, 8%), and 1,4-dimethoxybenzene (**38**, < 2%).

A pure sample of **33b** was obtained by an alternative synthesis method involving the dehydration of 2-(4-methoxyphenyl)-1,1-diphenylethanol, which was synthesized via a Grignard reaction between 4-methoxybenzylmagnesium chloride and benzophenone. The Grignard reagent was prepared according to a reported procedure.<sup>112</sup> The intermediate alcohol was subsequently dehydrated by refluxing with toluenesulphonic acid in benzene.

#### *1-(4-Methoxyphenyl)-2,2-diphenylethene (33b)*

Isolated yield: 73%, colourless crystals, mp 83.1-83.6°C (from ethanol), lit. mp 83-84°C.<sup>113</sup>  $\nu_{\max}$ (film; NaCl)/cm<sup>-1</sup> 3055, 3025, 2834, 1605, 1509, 1253, 1178, 1034 and 699;  $\delta_{\text{H}}$ (250.13 MHz; CDCl<sub>3</sub>; Me<sub>4</sub>Si) 3.75 (3 H, s), 6.65-6.93 (4 H, AA'BB'), 6.97 (1 H, s) and 7.20-7.35 (10 H, m);  $\delta_{\text{C}}$ (62.90 MHz; CDCl<sub>3</sub>) 55.2 (q), 113.4 (d), 127.2 (d), 127.3 (d), 127.4 (d), 127.7 (d), 128.2 (d), 128.7 (d), 130.1

(s), 130.4 (d), 130.8 (d), 140.58 (s), 140.63 (s), 143.6 (s) and 158.4 (s);  $m/z$  286 ( $M^{+}$ , 100%) and 165 (36).

A pure sample of **(35b)** was obtained by methylation of 2-(4-methoxyphenyl)-1,1-diphenylethanol synthesized above, according to a published procedure.<sup>114</sup>

***1-Methoxy-2-(4-methoxyphenyl)-1,1-diphenylethane (35b)***

Isolated yield: 30%, colourless plates, mp 102.8-103.7°C (from methanol), lit. mp 94-95°C.<sup>115</sup> Spectroscopic data in agreement with published results:<sup>115</sup>  $\nu_{\max}$ (film; NaCl)/ $\text{cm}^{-1}$  3057, 3024, 2936, 2831, 1611, 1513, 1245, 1179, 1077, 1036, 828, 755 and 701;  $\delta_{\text{H}}$ (250.13 MHz;  $\text{CDCl}_3$ ;  $\text{Me}_4\text{Si}$ ) 3.17 (3 H, s), 3.55 (2 H, s), 3.72 (3 H, s), 6.59-6.67 (4 H, AA'BB') and 7.17-7.27 (10 H, m);  $\delta_{\text{C}}$ (62.90 MHz;  $\text{CDCl}_3$ ) 40.5 (t), 50.8 (q), 55.0 (q), 83.4 (s), 112.8 (d), 126.7 (d), 127.6 (d), 127.7 (d), 128.7 (d), 131.3 (d), 144.8 (s) and 157.8 (s);  $m/z$  286 (1%), 197 (100), 105 (39) and 77 (31).

Compound **34b** was present in too small amounts to be isolated and was identified by GC-MS only.

***1-(4-methoxyphenyl)-2,2-diphenylethane (34b)***

$m/z$  288 ( $M^{+}$ , 3%), 167 (25), 165 (13) and 121 (100).

A pure sample of **37b** was obtained from an alternative photoreaction (*vide infra*).

**3.5.19 Irradiation of 4-bromoanisole (24b) in methanol.**

A solution of 4-bromoanisole (**24b**, 0.05 mol  $\text{dm}^{-3}$ ) in methanol (10  $\text{cm}^3$ ) was irradiated for 25 h. Calibrated GC-FID analysis revealed complete consumption of **24b** and the formation of 84% anisole (**36b**).

### 3.5.20 Irradiation of 4-bromoanisole (24b) and 1,1-diphenylethene (26) in methanol

A solution of 4-bromoanisole (**24b**, 0.05 mol dm<sup>-3</sup>) and 1,1-diphenylethene (**26**, 0.10 mol dm<sup>-3</sup>) in methanol (10 cm<sup>3</sup>) was irradiated for 75 h. Calibrated GC-FID analysis revealed 69% consumption of **26** and 100% consumption of **24b**, together with the formation of 1-methoxy-1,1-diphenylethane (**28**, 2%), 1-(4-methoxyphenyl)-2,2-diphenylethene (**33b**, 30%), 1-(4-methoxyphenyl)-2,2-diphenylethane (**35b**, < 2%), anisole (**36b**, 29%), and 3-methoxy-9-phenylphenanthrene (**37b**, 13%).

### 3.5.21 Irradiation of 4-iodoanisole (25b) in methanol.

A solution of 4-iodoanisole (**25b**, 0.05 mol dm<sup>-3</sup>) in methanol (10 cm<sup>3</sup>) was irradiated for 75 h. Calibrated GC-FID analysis revealed 64% **25b** consumption together with the formation of 87% anisole (**36b**). The reaction turned dark red upon photolysis.

### 3.5.22 Irradiation of 4-iodoanisole (4b) and 1,1-diphenylethene (5) in methanol.

A solution of 4-iodoanisole (**25b**, 0.05 mol dm<sup>-3</sup>) and 1,1-diphenylethene (**26**, 0.10 mol dm<sup>-3</sup>) in methanol (10 cm<sup>3</sup>) was irradiated for 75 h. Calibrated GC-FID analysis indicated that 49% of **26** and 100% of **25b** had been consumed. Products observed included 1-(4-methoxyphenyl)-2,2-diphenylethene (**33b**, 40%), 1-(4-methoxyphenyl)-2,2-diphenylethane (**34b**, < 2%), anisole (**36b**, 22%), and 3-methoxy-9-phenylphenanthrene (**37b**, 16%).

### 3.5.23 Irradiation of 1-(4-methoxyphenyl)-2,2-diphenylethene (33b) and 4-iodoanisole (25b) in methanol.

A solution of 1-(4-methoxyphenyl)-2,2-diphenylethene (**33b**, 0.025 mol dm<sup>-3</sup>) and 4-iodoanisole (**25b**, 0.025 mol dm<sup>-3</sup>) in methanol (2 cm<sup>3</sup>) resulted in 96% **33b** and 79% **25b** consumption after 6 h irradiation. Also observed was the

formation of anisole (**36b**, 80%) and 3-methoxy-9-phenylphenanthrene (**37b**, 94%).

A pure sample of **37b** was isolated from a large-scale photoreaction (30 cm<sup>3</sup>) of identical composition to the above.

#### *3-Methoxy-9-phenylphenanthrene (37b)*

Isolated yield: 60%, colourless oil; Spectroscopic data in agreement with published results: <sup>116</sup>ν<sub>max</sub>(film; NaCl)/cm<sup>-1</sup> 3057, 3022, 2932, 2833, 1621, 1598, 1503, 1439, 1429, 1253, 1221, 1177, 1036, 771 and 701; δ<sub>H</sub>(250.13 MHz; CDCl<sub>3</sub>; Me<sub>4</sub>Si) 4.02 (3 H, s), 7.25 (1 H, dd, *J* 8.5, 2.4), 7.43-7.63 (8 H, m), 7.80 (1 H, d, *J* 8.5), 7.91 (1 H, d, *J* 8.2), 8.07 (1 H, d, *J* 2.4) and 8.68 (1 H, d, *J* 7.6); δ<sub>C</sub>(62.90 MHz; CDCl<sub>3</sub>) 55.5 (q), 103.8 (d), 113.4 (d), 117.0 (d), 126.0 (d), 126.2 (s), 126.5 (d), 126.9 (d), 127.2 (d), 128.3 (d), 130.0 (s), 130.09 (d), 130.13 (d), 131.2 (s), 131.4 (s), 136.4 (s), 140.9 (s) and 158.5 (s); *m/z* 284 (M<sup>+</sup>, 100%), 269 (30) and 239 (42) (M<sup>+</sup>, 284.1196. C<sub>21</sub>H<sub>16</sub>O requires *M*, 284.1201).

#### **3.5.24 Thermal decomposition of 1-(4-cyanophenyl)-2-methoxy-2,2-diphenylethane (35a) and 1-methoxy-2-(4-methoxyphenyl)-1,1-diphenylethane (35b).**

A solution of 1-(4-cyanophenyl)-2-methoxy-2,2-diphenylethane (**35a**, 0.025 mol dm<sup>-3</sup>) in methanol (2 cm<sup>3</sup>) was left to stand in the dark for 5 days. GC-MS analysis indicated partial conversion to 1-(4-cyanophenyl)-2,2-diphenylethane (**33a**). Upon addition of a drop of hydrochloric acid, GC-MS indicated almost complete conversion of **35a** to **33a**. 1-Methoxy-2-(4-methoxyphenyl)-1,1-diphenylethane (**35b**) underwent conversion to 1-(4-methoxyphenyl)-2,2-diphenylethane (**33b**) under similar conditions.



# *Appendix*

---

<sup>1</sup>H NMR spectra of compounds **14**, **16-20**.

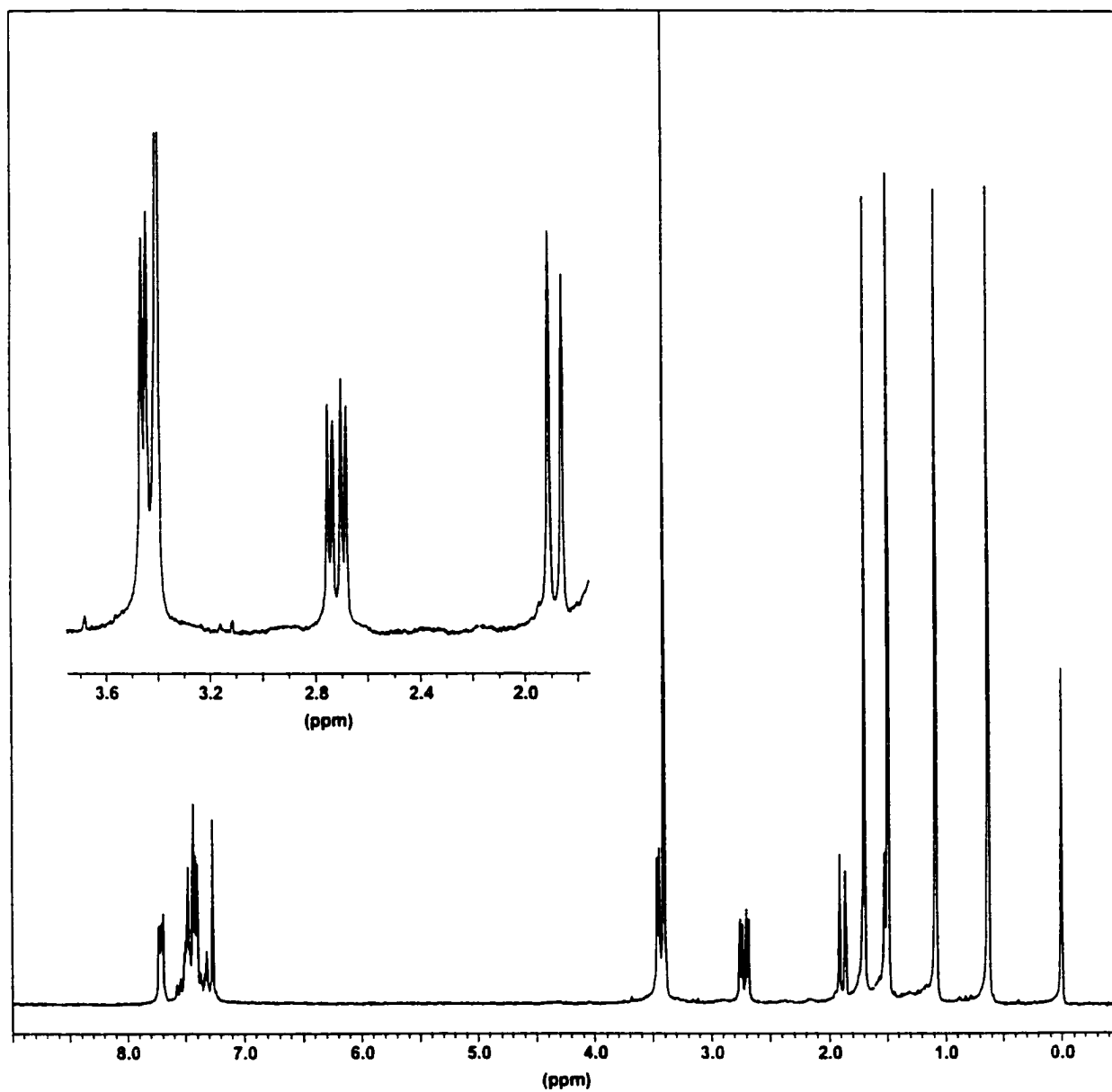


**Figure 14 :**  $^1\text{H}$  NMR spectrum of 1,5-dicyano-3-methoxy-2,2,4,4-tetramethyl-6,7-benzotricyclo[3.2.2.0<sup>3,8</sup>]nonane (14).

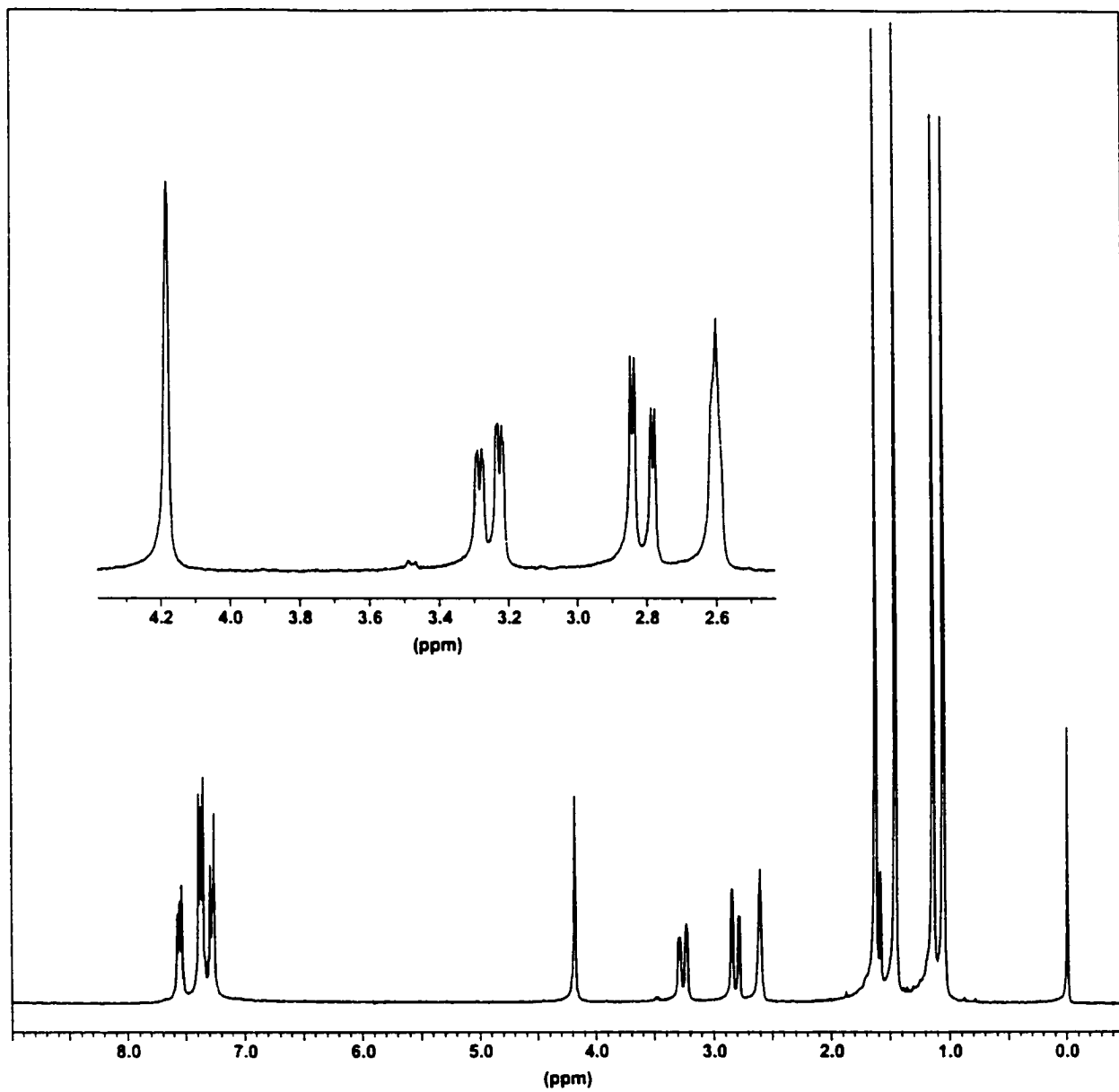


**Figure 15 :**  $^1\text{H}$  NMR spectrum of *cis*-1,4-dicyano-6,6,8,8-tetramethyl-7-oxo-2,3-benzo-*cis*-bicyclo[3.3.1]nonane (16).

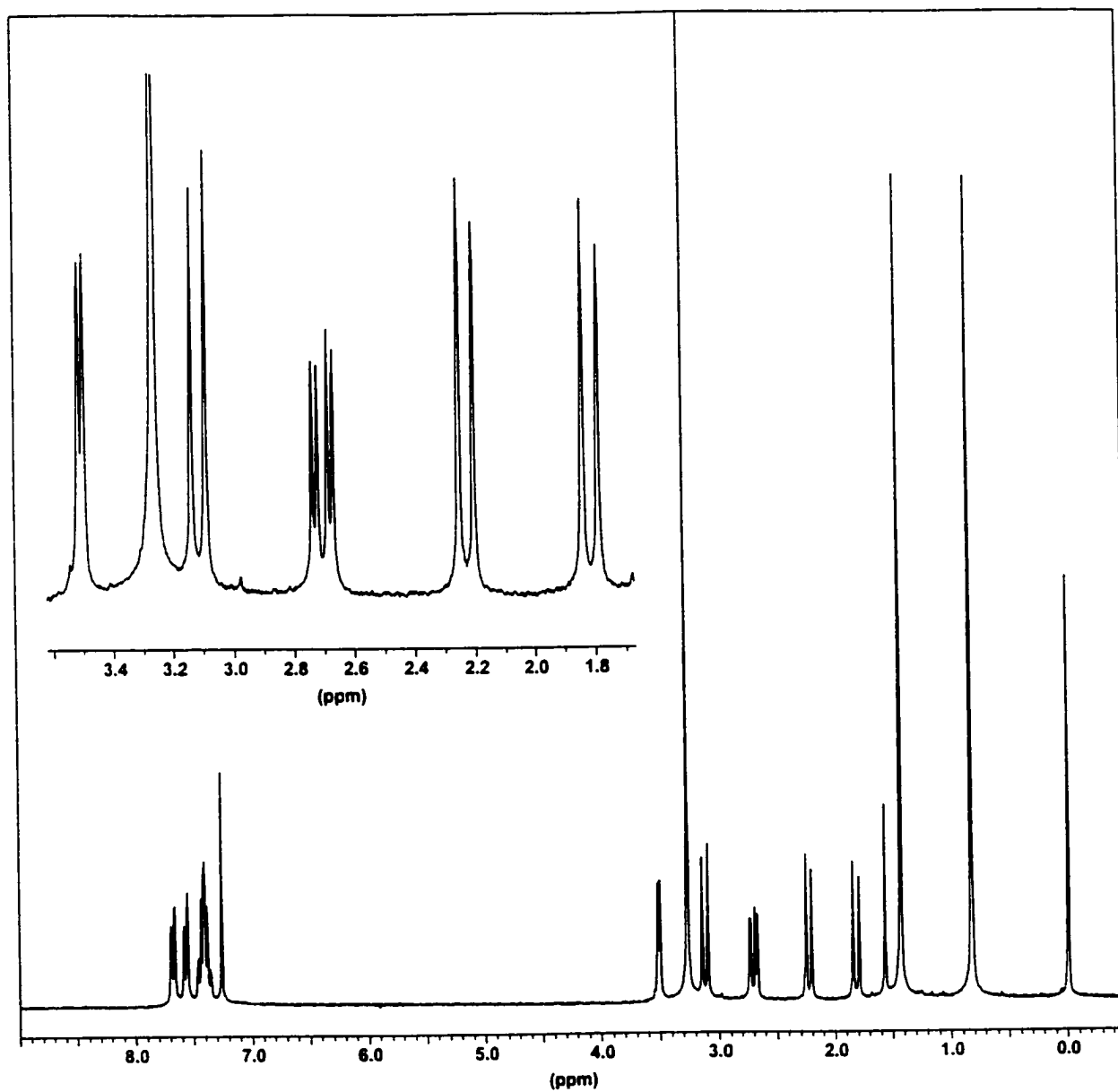


**Figure 16 :**  $^1\text{H}$  NMR spectrum of 1,5-dicyano-3-methoxy-4,4-dimethyl-6,7-benzotricyclo[3.2.2.0<sup>3,8</sup>]nonane (17).

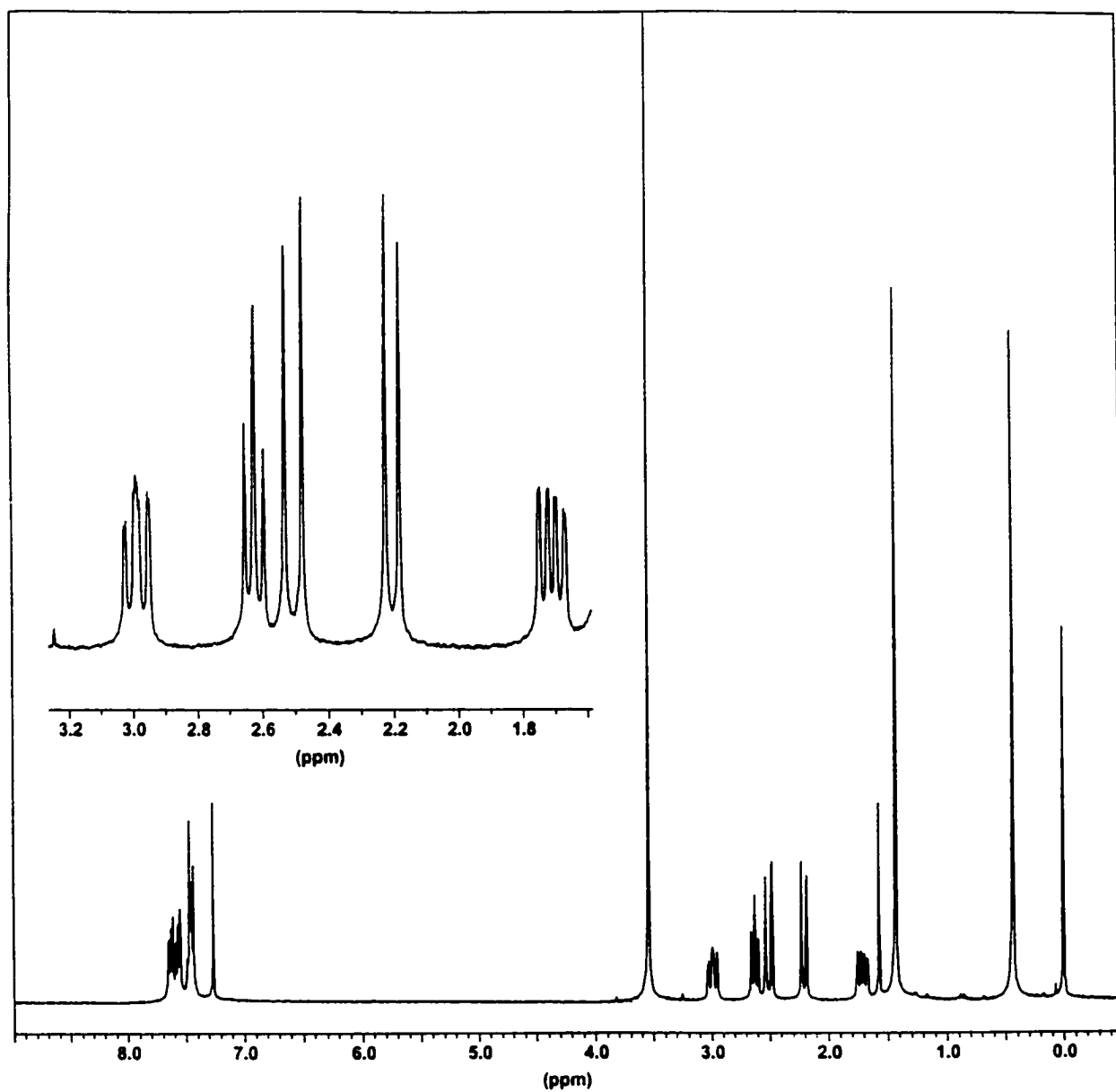


**Figure 17 :**  $^1\text{H}$  NMR spectrum of 2,5-dicyano-1-methoxy-9,9-dimethyl-3,4-benzotricyclo[3.3.1.0<sup>2,7</sup>]nonane (18).

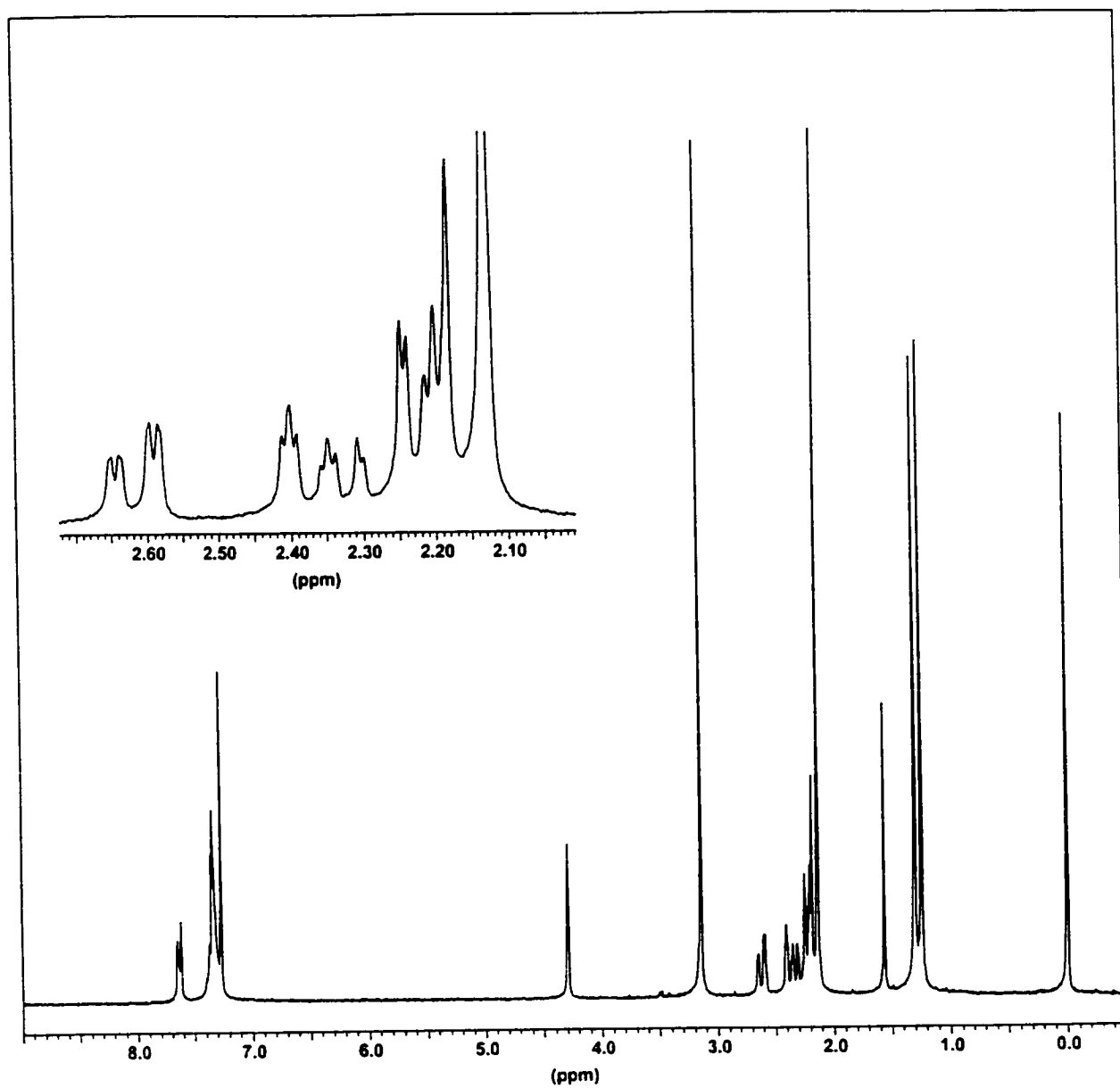


**Figure 18 :**  $^1\text{H}$  NMR spectrum of *cis*-1,4-dicyano-7,7-dimethoxy-6,6-dimethyl-2,3-benzo-*cis*-bicyclo[3.3.1]nonane (19).

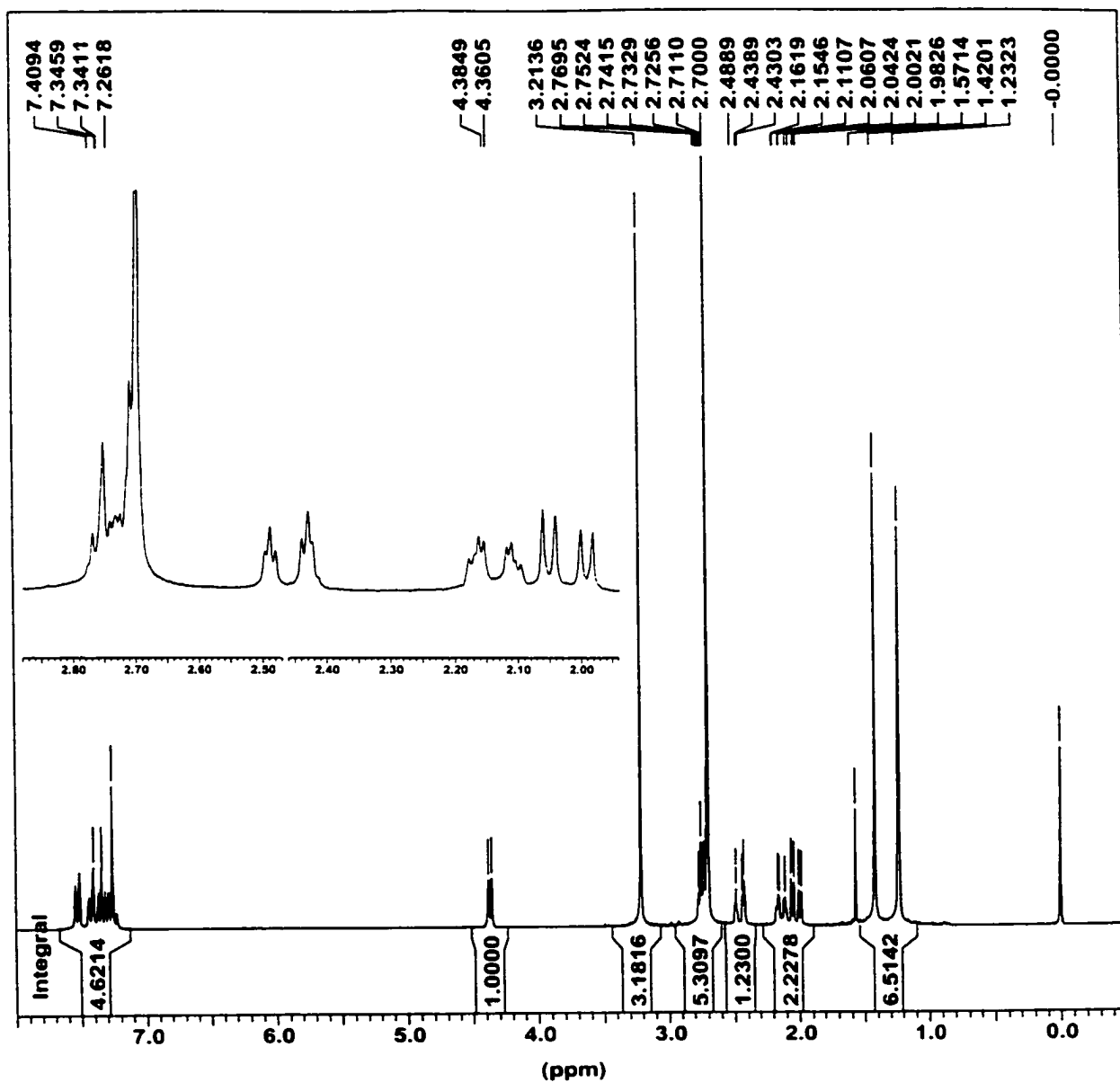


**Figure 19 :**  $^1\text{H}$  NMR spectrum of trans-1,4-dicyano-7,7-dimethoxy-8,8-dimethyl-2,3-benzo-cis-bicyclo[3.3.1]nonane (20).

## References

---

1. H. D. Roth, *Top. Curr. Chem.*, 1990, **136**, 1.
2. For collections of reviews on the various aspects of photoinduced electron transfer see, for example: (a) M. A. Fox and M. Chanon, eds., *Photoinduced Electron Transfer*, Parts A-D, Elsevier, Amsterdam, 1988; (b) J. Mattay, ed., *Top. Curr. Chem. Photoinduced Electron Transfer I-V*, 1990-1993, **156**, **158**, **159**, **163**, **168**; (c) W. H. Horspool and P. S. Song, eds., *CRC Handbook of Organic Photochemistry and Photobiology*, CRC Press, New York, 1995.
3. (a) M. Julliard and M. Chanon, *Chem. Rev.*, 1983, **83**, 425; (b) G. J. Kavarnos and N. J. Turro, *Chem. Rev.*, 1986, **86**, 401; (c) G. J. Kavarnos, *Top. Curr. Chem.*, 1990, **156**, 21.
4. (a) S. L. Mattes and S. Farid, in *Organic Photochemistry*, ed. A. Padwa, Marcel Dekker, New York, 1983, vol. 6, p. 233; (b) F. Muller and J. Mattay, *Chem. Rev.*, 1993, **93**, 99; (c) G. Pandey, *Top. Curr. Chem.*, 1993, **168**, 175; (d) A. Albini, M. Mella and M. Freccero, *Tetrahedron*, 1994, **50**, 575; (e) S. Hintz, A. Heidbreder and J. Mattay, *Top. Curr. Chem.*, 1996, **177**, 77.
5. (a) M. A. Fox and M. T. Dulay, *Chem. Rev.*, 1993, **93**, 341; (b) O. Legrini, E. Oliveros and A. M. Braun, *Chem. Rev.*, 1993, **93**, 671; (c) N. Getoff, *Proc. Indian Acad. Sci. (Chem. Sci.)*, 1993, **105**, 373.
6. M. R. Wasielewski, *Chem. Rev.*, 1992, **92**, 435.
7. (a) J. Moan, *Photochem. Photobiol.*, 1986, **43**, 681; (b) T. J. Dougherty, *Photochem. Photobiol.*, 1987, **45**, 879; (c) D. Dolphin, *Can. J. Chem.*, 1994, **72**, 1005; (d) R. Bonnett, *Chem. Soc. Rev.*, 1995, **24**, 19; (e) A. Harriman, in *CRC Handbook of Organic Photochemistry and Photobiology*, eds. W. H. Horspool and P. S. Song, CRC Press, New York, 1995, 1374.
8. J. Mattay and M. Vondenhof, *Top. Curr. Chem.*, 1991, **159**, 219.
9. (a) A. Weller, *Pure Appl. Chem.*, 1968, **6**, 155; (b) D. Rehm and A. Weller, *Isr. J. Chem.*, 1970, **8**, 259.



10. (a) J. R. Miller, J. V. Beitz and R. K. Huddleston, *J. Am. Chem. Soc.*, 1984, **106**, 5057; (b) I. R. Gould, D. Ege, S. L. Mattes and S. Farid, *J. Am. Chem. Soc.*, 1987, **109**, 3794; (c) I. R. Gould, J. E. Moser, D. Ege and S. Farid, *J. Am. Chem. Soc.*, 1988, **110**, 1991; (d) I. R. Gould, R. Moody and S. Farid, *J. Am. Chem. Soc.*, 1988, **110**, 7242; (e) I. R. Gould, J. E. Moser, B. Armitage, S. Farid, J. L. Goodman and M. S. Herman, *J. Am. Chem. Soc.*, 1989, **111**, 1917; (f) I. R. Gould, D. Ege, J. E. Moser and S. Farid, *J. Am. Chem. Soc.*, 1990, **112**, 4290; (g) F. D. Lewis, A. M. Bedell, R. E. Dykstra, J. E. Elbert, I. R. Gould and S. Farid, *J. Am. Chem. Soc.*, 1990, **112**, 8055; (h) I. R. Gould, R. H. Young, R. E. Moody and S. Farid, *J. Phys. Chem.*, 1991, **95**, 2068; (i) I. R. Gould and S. Farid, *J. Phys. Chem.*, 1993, **97**, 13067; (j) I. R. Gould, J. E. Moser, B. Armitage and S. Farid, *Res. Chem. Intermed.*, 1995, **21**, 793.
11. For some representative examples see: (a) T. Majima, C. Pac and H. Sakurai, *J. Chem. Soc., Perkin Trans. 1*, 1980, 2705; (b) D. S. Steichen and C. S. Foote, *J. Am. Chem. Soc.*, 1981, **103**, 1855; (c) A. P. Schaap, S. Siddiqui, S. D. Gagnon and L. Lopez, *J. Am. Chem. Soc.*, 1983, **105**, 5149; (d) S. C. Shim and J. S. Song, *J. Org. Chem.*, 1986, **51**, 2817; (e) Y. Kuriyama, T. Arai, H. Sakuragi and K. Tokumaru, *Chem. Lett.*, 1992, 879.
12. (a) R. M. Borg, D. R. Arnold and T. S. Cameron, *Can. J. Chem.*, 1984, **62**, 1785; (b) D. R. Arnold and M. S. Snow, *Can. J. Chem.*, 1988, **66**, 3012.
13. D. R. Arnold, M. S. W. Chan and K. A. McManus, *Can. J. Chem.*, 1996, **74**, 2143.
14. (a) D. R. Arnold, K. A. McManus and M. S. W. Chan, *Can. J. Chem.*, 1997, **75**, 1055; (b) M. S. W. Chan and D. R. Arnold, *Can. J. Chem.*, 1997, **75**, 1810.
15. H. J. P. de Lijser and D. R. Arnold, *J. Org. Chem.*, 1997, **62**, 8432.
16. K. A. McManus and D. R. Arnold, *Can. J. Chem.*, 1994, **72**, 2291.
17. (a) D. R. Arnold, K. A. McManus and X. Du, *Can. J. Chem.*, 1994, **72**, 415; (b) D. A. Connor, D. R. Arnold, P. K. Bakshi and T. S. Cameron, *Can. J. Chem.*, 1995, **73**, 762.
18. (a) K. A. McManus and D. R. Arnold, *Can. J. Chem.*, 1995, **73**, 2158; (b) H. Weng, C. Scarlata and H. D. Roth, *J. Am. Chem. Soc.*, 1996, **118**, 10947.
19. (a) J. E. Baldwin, *J. Chem. Soc., Chem. Commun.*, 1976, 734; (b) *J. Chem. Soc., Chem. Commun.*, 1976, 738; (c) A. L. J. Beckwith, *Tetrahedron*, 1981, **37**, 3073; (d) A. L. J. Beckwith and C. H. Schiesser, *Tetrahedron*, 1985, **41**, 3925.

20. (a) D. R. Arnold and X. Du, *J. Am. Chem. Soc.*, 1989, **111**, 7666; (b) D. R. Arnold and X. Du, *Can. J. Chem.*, 1994, **72**, 403; (c) D. R. Arnold, X. Du and H. J. P. de Lijser, *Can. J. Chem.*, 1995, **73**, 522; (d) T. Herbertz and H. D. Roth, *J. Am. Chem. Soc.*, 1996, **118**, 10954.
21. (a) R. A. Neunteufel and D. R. Arnold, *J. Am. Chem. Soc.*, 1973, **95**, 4080; (b) Y. Shigemitsu and D. R. Arnold, *J. Chem. Soc., Chem. Commun.*, 1975, 407; (c) A. J. Maroulis and D. R. Arnold, *Synthesis*, 1979, **10**, 819.
22. A. J. Maroulis, Y. Shigemitsu and D. R. Arnold, *J. Am. Chem. Soc.*, 1978, **100**, 535.
23. (a) S. L. Mattes and S. Farid, *J. Am. Chem. Soc.*, 1986, **108**, 7356; (b) L. J. Johnston and N. P. Schepp, *J. Am. Chem. Soc.*, 1993, **115**, 6564.
24. (a) D. R. Arnold, X. Du and K. M. Henseleit, *Can. J. Chem.*, 1991, **69**, 839; (b) D. R. Arnold, X. Du and J. Chen, *Can. J. Chem.*, 1995, **73**, 307.
25. (a) S. L. Mattes and S. Farid, *J. Am. Chem. Soc.*, 1983, **105**, 1386; (b) K. Mizuno, I. Nakanishi, M. Ichinose and Y. Otsuji, *Chem. Lett.*, 1989, 1095; (c) T. Hirano, S. Shiina and M. Ohashi, *J. Chem. Soc., Chem. Commun.*, 1992, 1544; (d) M. Kojima, A. Ishida, S. Takamuku, Y. Wada and S. Yanagida, *Chem. Lett.*, 1994, 1897; (e) S. Swansburg, K. Janz, G. Jocys, A. Pincock and J. Pincock, *Can. J. Chem.*, 1998, **76**, 35; (f) M. Kojima, A. Ishida, Y. Kuriyama, Y. Wada and H. Takeya, *Bull. Chem. Soc. Jpn.*, 1999, **72**, 1049.
26. (a) T. Yamashita, K. Shiomori, M. Yasuda and K. Shima, *Bull. Chem. Soc. Jpn.*, 1991, **64**, 366; (b) M. Yasuda, T. Isami, J. Kubo, M. Mizutani, T. Yamashita and K. Shima, *J. Org. Chem.*, 1992, **57**, 1351; (c) T. Yamashita, M. Yasuda, T. Isami, S. Nakano, K. Tanabe and K. Shima, *Tetrahedron Lett.*, 1993, **34**, 5131; (d) R. Kojima, T. Yamashita, K. Tanabe, T. Shiragami, M. Yasuda and K. Shima, *J. Chem. Soc., Perkin Trans. 1*, 1997, 217; (e) R. Kojima, T. Shiragami, K. Shima, M. Yasuda and T. Majima, *Chem. Lett.*, 1997, 1241; (f) M. Yasuda, R. Kojima, R. Ohira, T. Shiragami and K. Shima, *Bull. Chem. Soc. Jpn.*, 1998, **71**, 1655.
27. (a) Y. Inoue, T. Okano, N. Yamasaki and A. Tai, *J. Chem. Soc., Chem. Commun.*, 1993, 718; (b) S. Asaoka, T. Kitazawa, T. Wada and Y. Inoue, *J. Am. Chem. Soc.*, 1999, **121**, 8486.
28. (a) M. Yasuda, C. Pac and H. Sakurai, *Bull. Chem. Soc. Jpn.*, 1980, **53**, 502; (b) T. Majima, C. Pac, A. Nakasone and H. Sakurai, *J. Am. Chem. Soc.*, 1981, **103**, 4499.
29. (a) M. W. Klett and R. P. Johnson, *Tetrahedron Lett.*, 1983, **24**, 1107; (b) M. W. Klett and R. P. Johnson, *J. Am. Chem. Soc.*, 1985, **107**, 6615.

30. (a) Z. A. Jiang and C. S. Foote, *Tetrahedron Lett.*, 1983, **24**, 461; (b) K. Mizuno, T. Tamai, T. Nishiyama, K. Tani, M. Sawasaki and Y. Otsuji, *Angew. Chem. Int. Ed. Engl.*, 1994, **33**, 2113.
31. D. R. Arnold and A. J. Maroulis, *J. Am. Chem. Soc.*, 1977, **99**, 7355.
32. D. Mangion, D. R. Arnold, T. S. Cameron and K. N. Robertson, *J. Chem. Soc., Perkin Trans. 2*, 2001, 48.
33. (a) K. Somekawa, K. Haddaway, P. S. Mariano and J. A. Tossell, *J. Am. Chem. Soc.*, 1984, **106**, 3060; (b) K. Haddaway, K. Somekawa, P. Fleming, J. A. Tossell and P. S. Mariano, *J. Org. Chem.*, 1987, **52**, 4239.
34. (a) D. R. Arnold and A. H. Glick, *J. Chem. Soc., Chem. Commun.*, 1966, 813; (b) H. Gotthardt, R Steinmetz and G. S. Hammond, *J. Org. Chem.*, 1968, **33**, 2774; (c) H. J. T. Bos, C. Slagt and J. S. M. Boleij, *Recl. Trav. Chim. Pays-Bas*, 1970, **89**, 1170; (d) N. Ishibe and I. Tanigushi, *Tetrahedron*, 1971, **27**, 4883; (e) J. S. M. Boleij and H. J. T. Bos, *Tetrahedron Lett.*, 1971, 3201; (f) N. Ishibe, K. Hoshimoto and Y. Yamaguchi, *J. Chem. Soc., Perkin Trans. 1*, 1975, 318; (g) K. Ogino, T. Matsumoto, T. Kawai and S. Kozuka, *J. Org. Chem.*, 1979, **44**, 3352; (h) W. R. McKay, J. Ounsworth, P. E. Sum and L. Weiler, *Can. J. Chem.*, 1982, **60**, 872; (i) D. Becker, M. Nagler, Z. Harel and A. Gillon, *J. Org. Chem.*, 1983, **48**, 2584; (j) J. Kamphuis, P. D. J. Grootenhuis, A. P. Ruijter, R. G. Visser and H. J. T. Bos, *Isr. J. Chem.*, 1985, **26**, 120; (k) L. K. Sydnes and W. Stensen, *Acta Chem. Scand., Ser. B*, 1986, **40**, 657.
35. K. Maruyama and H. Imahori, *J. Org. Chem.*, 1989, **54**, 2692.
36. N. J. Turro and V. Ramamurthy, *Tetrahedron Lett.*, 1976, 2423.
37. J. Kamphuis, H. J. T. Bos, R. J. Visser, B. H. Huizer and C. A. G. O. Varma, *J. Chem. Soc., Perkin Trans. 2*, 1986, 1867.
38. (a) M. Karplus, *J. Am. Chem. Soc.*, 1963, **85**, 2870; (b) E. Breitmaier, *Structure Elucidation by NMR in Organic Chemistry*, Wiley, Chichester, UK, 1993, p. 43.
39. H. Friebolin, *Basic One- and Two-Dimensional NMR Spectroscopy*, VCH, New York, 1993, p. 91.
40. (a) D. D. M. Wayner, D. J. McPhee and D. Griller, *J. Am. Chem. Soc.*, 1988, **110**, 132; (b) B. A. Sim, P. H. Milne, D. Griller and D. D. M. Wayner, *J. Am. Chem. Soc.*, 1990, **112**, 6635.
41. (a) T. Asanuma, M. Yamamoto and Y. Nishijima, *J. Chem. Soc., Chem. Commun.*, 1975, 608; (b) H. Ikeda, T. Minegishi and T. Miyashi, *J. Chem. Soc., Chem. Commun.*, 1994, 297.

42. (a) M. Vanossi, M. Mella and A. Albini, *J. Am. Chem. Soc.*, 1994, **116**, 10070; (b) M. Mella, M. Freccero and A. Albini, *J. Org. Chem.*, 1994, **59**, 1047; (c) M. Mella, M. Fagnoni and A. Albini, *J. Org. Chem.*, 1994, **59**, 5614; (d) E. Fasani, D. Peverali and A. Albini, *Tetrahedron Lett.*, 1994, **35**, 9275; (e) M. Fagnoni, M. Mella and A. Albini, *Tetrahedron*, 1994, **50**, 6401; (f) M. Fagnoni, M. Mella and A. Albini, *Tetrahedron*, 1995, **51**, 859; (g) M. Mella, M. Freccero and A. Albini, *J. Chem. Soc., Chem. Commun.*, 1995, 41; (h) M. Fagnoni, M. Mella and A. Albini, *J. Am. Chem. Soc.*, 1995, **117**, 7877; (i) M. Fagnoni, M. Vanossi, M. Mella and A. Albini, *Tetrahedron*, 1996, **52**, 1785; (j) M. Mella, M. Freccero, T. Soldi, E. Fasani and A. Albini, *J. Org. Chem.*, 1996, **61**, 1413; (k) M. Mella, M. Fagnoni, M. Freccero, E. Fasani and A. Albini, *Chem. Soc. Rev.*, 1998, **27**, 81.
43. G. Ginzburg, B. Zinger and J. Y. Becker, *J. Electroanal. Chem.*, 1983, 57.
44. (a) R. S. Nicholson and I. Shain, *Anal. Chem.*, 1964, **36**, 706; (b) R. S. Nicholson and I. Shain, *Anal. Chem.*, 1965, **37**, 178.
45. (a) C. Pac, A. Nakasone and H. Sakurai, *J. Am. Chem. Soc.*, 1977, **99**, 5806; (b) T. Majima, C. Pac and H. Sakurai, *J. Chem. Soc., Perkin Trans. 1*, 1980, 2705; (c) T. Majima, C. Pac, A. Nakasone and H. Sakurai, *J. Am. Chem. Soc.*, 1981, **103**, 4499; (d) S.L. Mattes, H.R. Luss and S. Farid, *J. Phys. Chem.*, 1983, **87**, 4779; (e) T. Tamai, K. Mizuno, I Hashida and Y. Otsuji, *J. Org. Chem.*, 1992, **57**, 5338; (f) T. Yamashita, M. Yasuda, T. Isami, S. Nakano, K. Tanabe and K. Shima, *Tetrahedron Lett.*, 1993, **34**, 5131.
46. (a) K. Mizuno, K. Nakanishi and Y. Otsuji, *Chem. Lett.*, 1988, 1833; (b) M. Yasuda, T. Isami, J. Kubo, M. Mizutani, T. Yamashita and K. Shima, *J. Org. Chem.*, 1992, **57**, 1351; (c) K. Nakanishi, K. Mizuno and Y. Otsuji, *Bull. Chem. Soc. Jpn.*, 1993, **66**, 2371; (d) K. Mizuno, T. Tamai, T. Nishiyama, K. Tani, M. Sawasaki and Y. Otsuji, *Angew. Chem. Int. Ed. Engl.*, 1994, **33**, 2113.
47. J. J. McCullough, R. C. Miller and W. S. Wu, *Can. J. Chem.*, 1977, **55**, 2909.
48. D. R. Arnold, P. C. Wong, A. J. Maroulis and T. S. Cameron, *Pure Appl. Chem.*, 1980, **52**, 2609.
49. F. D. Lewis and R. J. DeVoe, *Tetrahedron*, 1982, **38**, 1069.
50. P. H. Mazzocchi and G. Fritz, *J. Am. Chem. Soc.*, 1986, **108**, 5362.
51. (a) P. S. Engel, D. J. Bishop and M. A. Page, *J. Am. Chem. Soc.*, 1978, **100**, 7009; (b) D. L. Baulch, P. K. Chown and D. C. Montague, *Int. J. Chem. Kinet.*, 1979, **11**, 1055.

52. K. Kokubo, T. Masaki and T. Oshima, *Org. Lett.*, 2000, **2**, 1979.
53. (a) F. D. Lewis, T. I. Ho and J. T. Simpson, *J. Am. Chem. Soc.*, 1982, **104**, 1924; (b) F. D. Lewis, *Acc. Chem. Res.*, 1986, **19**, 401.
54. (a) D. R. Arnold and S. A. Mines, *Can. J. Chem.*, 1987, **65**, 2312; (b) D. R. Arnold and S. A. Mines, *Can. J. Chem.*, 1989, **67**, 689; (c) D. Mangion, J. Kendall and D. R. Arnold, *Org. Lett.*, 2001, **3**, 45.
55. (a) A. Albin and S. Spreti, *Tetrahedron*, 1984, **40**, 2975; (b) Y. Kubo, K. Kiuchi and I. Inamura, *Bull. Chem. Soc. Jpn.*, 1999, **72**, 1101.
56. W. C. Neikam, G. R. Dimeler and M. M. Desmond, *J. Electrochem. Soc.*, 1964, **111**, 1190.
57. H. Freige and M. Klessinger, *J. Chem. Res. (S)*, 1977, 208.
58. G. Le Guillamton, Q. T. Do and J. Simonet, *Bull. Soc. Chim. Fr.*, 1990, **127**, 427.
59. W. C. Still, M. Kahn and A. Mitra, *J. Org. Chem.*, 1978, **43**, 2923.
60. Molecular Structure Corporation, teXsan for Windows, version 1.5, Crystal Structure Analysis Package, 1997-8.
61. G. M. Sheldrick, SHELX-97, Program for Crystal Structure Determinations, 1997.
62. A. Okamoto, M. S. Snow and D. R. Arnold, *Tetrahedron*, 1986, **42**, 6175.
63. D. Mangion and D. R. Arnold, *Can. J. Chem.*, 1999, **77**, 1655.
64. D. B. Denney, D. Z. Denney and S. P. Fenelli, *Tetrahedron*, 1996, **53**, 9835.
65. D. E. Bartak, K. J. Houser, B. C. Rudy and H. D. Hawley, *J. Am. Chem. Soc.*, 1972, **94**, 7526.
66. (a) J. Pinson and J. M. Savéant, *J. Chem. Soc., Chem. Commun.*, 1974, 933; (b) J. Pinson and J. M. Savéant, *J. Am. Chem. Soc.*, 1978, **100**, 1506; (c) C. P. Andrieux, C. Blocman, J. M. Dumas-Bouchiat and J. M. Savéant, *J. Am. Chem. Soc.*, 1979, **101**, 2431; (d) C. Amatore, J. Chaussard, J. Pinson, J. M. Savéant and A. Thiebault, *J. Am. Chem. Soc.*, 1979, **101**, 6012; (e) J. M. Savéant, *Acc. Chem. Res.*, 1980, **13**, 323; (f) F. M'Halla, J. Pinson and J. M. Savéant, *J. Am. Chem. Soc.*, 1980, **102**, 4120; (g) C. Amatore, J. Pinson, J. M. Savéant and A. Thiebault, *J. Am. Chem. Soc.*, 1981, **103**, 6930; (h) C. Amatore, J. Pinson, J. M. Savéant and A. Thiebault, *J. Am. Chem. Soc.*, 1982, **104**, 817; (i) D. Lexa and J. M.

- Savéant, *J. Am. Chem. Soc.*, 1982, **104**, 4503; (j) C. P. Andrieux, J. M. Savéant and D. Zann, *Nouv. J. Chim.*, 1984, **8**, 107; (k) C. Amatore, M. A. Oturan, J. Pinson, J. M. Savéant and A. Thiebault, *J. Am. Chem. Soc.*, 1985, **107**, 3451; (l) C. P. Andrieux, J. M. Savéant and K. Binh Su, *J. Phys. Chem.*, 1986, **90**, 3815; (m) M. A. Oturan, J. Pinson, J. M. Savéant and A. Thiebault, *Tetrahedron Lett.*, 1989, **30**, 1373; (n) J. M. Savéant, *Adv. Phys. Org. Chem.*, 1990, **26**, 1; (o) J. M. Savéant, *J. Phys. Chem.*, 1994, **98**, 3716; (p) Z. Chami, M. Gariel, J. Pinson, J. M. Savéant and A. Thiebault, *J. Org. Chem.*, 1991, **56**, 586; (q) J. M. Savéant, *Tetrahedron*, 1994, **50**, 10117; (r) C. P. Andrieux, M. Robert and J. M. Savéant, *J. Am. Chem. Soc.*, 1995, **117**, 9340; (s) C. P. Andrieux, J. M. Savéant and C. Tardy, *J. Am. Chem. Soc.*, 1997, **119**, 11546.
67. (a) C. Glidewell, *Chem. Scr.*, 1985, **25**, 142; (b) M. Moreno, I. Gallardo and J. Bertran, *J. Chem. Soc., Perkin Trans. 2*, 1989, 2017.
68. J. Casado, I. Gallardo and M. Moreno, *J. Electroanal. Chem.*, 1987, **219**, 197.
69. A. B. Pierini and J. S. Duca, *J. Chem. Soc., Perkin Trans. 2*, 1990, 1821.
70. (a) R. A. Rossi and J. F. Bunnett, *J. Org. Chem.*, 1973, **38**, 1407; (b) J. V. Hay, T. Hudlicky and J. F. Wolfe, *J. Am. Chem. Soc.*, 1975, **97**, 374; (c) J. F. Bunnett and J. E. Sundberg, *J. Org. Chem.*, 1976, **41**, 1702; (d) R. A. Rossi, R. H. Rossi and A. F. Lopez, *J. Org. Chem.*, 1976, **41**, 3371; (e) A. P. Komin and J. F. Wolfe, *J. Org. Chem.*, 1977, **42**, 2481; (f) S. Hoz and J. F. Bunnett, *J. Am. Chem. Soc.*, 1977, **99**, 4690; (g) J. F. Bunnett, *Acc. Chem. Soc.*, 1978, **11**, 413; (h) C. Galli and J. F. Bunnett, *J. Am. Chem. Soc.*, 1981, **103**, 7140.
71. M. A. Fox, J. Younathan and G. E. Fryxell, *J. Org. Chem.*, 1983, **48**, 3109.
72. R. Beugelmans, in *CRC Handbook of Organic Photochemistry and Photobiology*, eds. W. H. Horspool and P. S. Song, CRC Press, New York, 1995, p. 1200.
73. R. S. Davidson, J. W. Goodin and G. Kemp, *Advances in Physical Organic Chemistry*, Academic Press, London, 1984, p. 191.
74. N. J. Bunce, in *CRC Handbook of Organic Photochemistry and Photobiology*, eds. W. H. Horspool and P. S. Song, CRC Press, New York, 1995, p. 1181.
75. (a) W. Wolf and N. Kharasch, *J. Org. Chem.*, 1961, **26**, 283; (b) N. Kharasch and L. Gothlich, *Angew. Chem. Internat. Edit.*, 1962, **1**, 549; (c) J. A. Kampmeier and E. Hoppmeister, *J. Am. Chem. Soc.*, 1962, **84**, 3787; (d) W. Wolf and N. Kharasch, *J. Org. Chem.*, 1965, **30**, 2493; (e) T. Matsuura and K. Omura, *Bull. Chem. Soc. Jpn.*, 1966, **39**, 944; (f) N.

- Kharasch, R. K. Sharma and H. B. Lewis, *J. Chem. Soc., Chem. Commun.*, 1966, 418; (g) R. K. Sharma and N. Kharasch, *Angew. Chem. Internat. Edit.*, 1968, 7, 36; (h) R. Antonioletti, M. D'Auria, F. D'Onofrio, G. Piancatelli and A. Scettri, *J. Chem. Soc., Perkin Trans. 1*, 1986, 1755; (i) M. Nakada, C. Miura, H. Nishiyama, F. Higashi, T. Mori, M. Hirota and T. Ishii, *Bull. Chem. Soc. Jpn.*, 1989, 62, 3122; (j) M. D'Auria, E. De Luca, G. Mauriello and R. Racioppi, *J. Chem. Soc., Perkin Trans. 1*, 1998, 271.
76. (a) M. P. Cava and S. S. Libsch, *J. Org. Chem.*, 1974, 39, 577; (b) J. Grimshaw and A. P. de Silva, *Chem. Soc. Rev.*, 1981, 10, 181; (c) S. V. Kessar and A. K. Singh Mankotia, in *CRC Handbook of Organic Photochemistry and Photobiology*, eds. W. H. Horspool and P. S. Song, CRC Press, New York, 1995, p. 1218.
77. (a) N. J. Bunce, J. P. Bergsma, M. D. Bergsma, W. De Graff, Y. Kumar and L. Ravanal, *J. Org. Chem.*, 1980, 45, 370; (b) M. Nakada, S. Fukushi, H. Nishiyama, K. Okubo, K. Kume, H. Hirota and T. Ishii, *Bull. Chem. Soc. Jpn.*, 1983, 56, 2447; (c) G. G. Choudhry, A. A. M. Roof and O. Hutzinger, *Tetrahedron Lett.*, 1979, 2059; (d) P. K. Freeman, N. Ramnath and A. D. Richardson, *J. Org. Chem.*, 1991, 56, 3643; (e) P. K. Freeman, J.-S. Jang and N. Ramnath, *J. Org. Chem.*, 1991, 56, 6072.
78. M. A. Fox, W. C. Nichols and D. M. Lemal, *J. Am. Chem. Soc.*, 1973, 95, 8164.
79. D. R. Arnold and P. C. Wong, *J. Am. Chem. Soc.*, 1977, 99, 3361.
80. K. Gollnick, A. Schnatterer and G. Utschick, *J. Org. Chem.*, 1993, 58, 6049.
81. J. Woning, A. Oudenampsen and W. H. Laarhoven, *J. Chem. Soc., Perkin Trans. 2*, 1989, 2147.
82. G. Wittig and M. Schlosser, *Chem. Ber.*, 1961, 94, 1373.
83. H. M. Rosenberg and M. P. Serve, *J. Am. Chem. Soc.*, 1970, 92, 4746.
84. S. L. Murov, I. Carmichael and G. L. Hug, *Handbook of Photochemistry*, 2nd edn., Marcel Dekker, New York, 1993, p. 280.
85. (a) J. A. Marshall, *Acc. Chem. Res.*, 1969, 2, 33; (b) H. M. Rosenberg and M. P. Serve, *J. Org. Chem.*, 1972, 37, 141; (c) R. Bonneau, J. Jousset-Dubien, L. Salem and A. J. Yarwood, *J. Am. Chem. Soc.*, 1976, 98, 4329; (d) W. G. Dauben, H. C. H. A. von Riel, J. D. Robbins and G. J. Wagner, *J. Am. Chem. Soc.*, 1979, 101, 6383.
86. (a) P. Wan, S. Culshaw and K. Yates, *J. Am. Chem. Soc.*, 1982, 104, 2509; (b) J. McEwen and K. Yates, *J. Am. Chem. Soc.*, 1987, 109, 5800.

87. (a) D. R. Arnold and A. J. Maroulis, *J. Am. Chem. Soc.*, 1976, **98**, 5931; (b) D. R. Arnold, N. J. Fahie, L. J. Lamont, J. Wierzchowski and K. M. Young, *Can. J. Chem.*, 1987, **65**, 2734; (c) R. Popielarz and D. R. Arnold, *J. Am. Chem. Soc.*, 1990, **112**, 3068; (d) L. J. Lamont and D. R. Arnold, *Can. J. Chem.*, 1990, **68**, 390; (e) D. R. Arnold, L. J. Lamont and A. L. Perrott, *Can. J. Chem.*, 1991, **69**, 225.
88. G. M. Barrow, *Physical Chemistry*, 5th edn., McGraw-Hill, New York, 1988, p. 747.
89. J. A. Dean, *Lange's Handbook of Chemistry*, 14th edn., McGraw-Hill, New York, 1992.
90. Kevin McMahon, Ph.D. thesis, Dalhousie University, 1991.
91. T. P. Carsey, G. L. Findley and S. P. McGlynn, *J. Am. Chem. Soc.*, 1979, **101**, 4502.
92. P. J. Wagner and E. J. Siebert, *J. Am. Chem. Soc.*, 1981, **103**, 7329.
93. S. Niizuma, L. Kwan, and N. Hirota, *Mol. Phys.*, 1978, **35**, 1029.
94. H. Gerner, *J. Phys. Chem.*, 1986, **86**, 2028.
95. T. F. Palmer and S. S. Parmar, *J. Photochem.*, 1985, **31**, 273.
96. C. M. Previtali and T. W. Ebbesen, *J. Photochem.*, 1984, **27**, 9.
97. T. Ni, R. A. Caldwell and L. A. Melton, *J. Am. Chem. Soc.*, 1989, **111**, 457.
98. J. T. Pinhey and R. D. G. Rigby, *Tetrahedron Lett.*, 1969, 1271.
99. J. Eriksen, H. Lund and A. I. Nyvad, *Acta Chem. Scand. B*, 1983, **37**, 459.
100. (a) W. H. Laarhoven, *Trav. Chim. Pays-Bas*, 1983, **102**, 185; (b) W. H. Laarhoven, *Trav. Chim. Pays-Bas*, 1983, **102**, 241; (c) A. Gilbert, in *CRC Handbook of Organic Photochemistry and Photobiology*, eds. W. H. Horspool and P. S. Song, CRC Press, New York, 1995, p. 291.
101. (a) F. B. Mallory, C. S. Wood and J. T. Gordon, *J. Am. Chem. Soc.*, 1964, **86**, 3094; (b) G. S. Hammond, J. Saltiel, A. A. Lamola, N. J. Turro, J. S. Bradshaw, D. O. Cowan, R. C. Correll, V. Voet and C. Dalton, *J. Am. Chem. Soc.*, 1964, **86**, 3197.
102. C. S. Wood and F. B. Mallory, *J. Org. Chem.*, 1964, **29**, 3373.
103. K. A. Muszkat, *Top. Curr. Chem.*, 1980, **88**, 89.
104. M. Fagnoni, M. Mella and A. Albini, *Org. Lett.*, 1999, **1**, 1299.



105. (a) N. J. Bunce, *J. Org. Chem.*, 1982, **47**, 1948; (b) P. K. Freeman, R. Srinivasa, J.-A. Campbell and M. L. Deinzer, *J. Am. Chem. Soc.*, 1986, **108**, 5531.
106. (a) W. K. Smothers, K. S. Shanze and J. Saltiel, *J. Am. Chem. Soc.*, 1979, **101**, 1895; (b) N. J. Bunce and J. C. Gallacher, *J. Org. Chem.*, 1982, **47**, 1955.
107. W. A. Bonner and F. D. Mango, *J. Org. Chem.*, 1964, **29**, 430.
108. G. Wittig and M. Schlosser, *Chem. Ber.*, 1961, **94**, 1373.
109. F. Weinelt and H. J. Schneider, *J. Org. Chem.*, 1991, **56**, 5527.
110. T. Harada and T. Mukaiyama, *Bull. Chem. Soc. Jpn.*, 1993, **66**, 882.
111. W. Tadros, Y. Akhnookh and G. Aziz, *J. Chem. Soc.*, 1953, 186.
112. K. V. Baker, J. M. Brown, N. Hughes, A. J. Skarnulis and A. Sexton, *J. Org. Chem.*, 1991, **56**, 698.
113. M. Kamata, K. Murayama and T. Miyashi, *Tetrahedron Lett.*, 1989, **30**, 4129.
114. J. W. Hilborn, E. MacKnight, J. A. Pincock and P. J. Wedge, *J. Am. Chem. Soc.*, 1994, **116**, 3337.
115. M. Freccero, A. Pratt, A. Albin and C. Long, *J. Am. Chem. Soc.*, 1998, **120**, 284.
116. F. I. M. van Ginkel, J. Cornelisse and G. Lodder, *J. Am. Chem. Soc.*, 1991, **113**, 4261.